

**Investigation of molecular mechanisms of biofilm dispersal and attempts to
create an inducible gene expression system in *Campylobacter***

Amritha Ramesh

The thesis is being submitted in partial fulfilment of the requirements of the university for the
appropriate award

June 2020

Declaration

I declare that the work reported in this thesis is entirely my own and has been carried out at Kingston University, UK.

This thesis has not been submitted, in whole or in part, for any other degree at this or any other University.

Amritha Ramesh

Abstract

Campylobacter jejuni is the leading cause of bacterial foodborne diseases worldwide. *C. jejuni* and *Campylobacter coli* are the most predominant species of the genus that are responsible for gastrointestinal diseases in humans (Epps *et al.*, 2013). *C. jejuni* 11168H strain can form biofilms, whose cells are more resistant to antimicrobials and disinfectants, perhaps due to the fact that the bacterial cells are secured in an extra cellular polymeric matrix consisting of eDNA (extracellular DNA), proteins, and polysaccharides (Brown *et al.*, 2015b).

Bacterial dispersion takes place following the biofilm maturation step. The dispersed cells demonstrate greater colonizing properties than their sessile counterparts (Guilhen *et al.*, 2017). Therefore, studying the factors governing the dispersal process is vital as it would give a better understanding of the pathogen and may lead to the development of novel antimicrobial treatments, which in turn may help prevent future cases of campylobacteriosis.

In this study, dispersal of *C. jejuni* 11168H biofilms was observed. The role of the *cj0979* gene in biofilm formation was investigated and it was concluded that this gene alone was not responsible for the regulation of *C. jejuni* 11168H biofilm dispersal. Purified Cj0979 exhibited DNase activity and could degrade lambda DNA. In addition, purified Cj0979 reduced *C. jejuni* 11168H biofilm development, when added to the initial stages of biofilm formation. Importantly, these findings provide insights into the dispersal process of *C. jejuni* biofilms, which has not been reported elsewhere. A development and validation of an arabinose-inducible gene expression system was undertaken in this research to aid in the study of essential genes and nuclease encoding genes involved in biofilm dispersal. As a primary step, arabinose transporter genes *araE* and *lacYA177C* were introduced into *C. jejuni* since the transporters required for arabinose uptake are not present within these bacteria. Arabinose is essential for promoter function. The integration constructs carrying the arabinose transporter genes, were

verified by genome sequencing, confirming that they were free of deletions and point mutations. The gene cassettes carrying the *araE* and modified *lacY* genes were successfully integrated into the *C. jejuni* 11168H chromosome. Despite successful introduction of *araE* and modified *lacY* genes into *C. jejuni* 11168H induction of gene expression from P_{BAD} promoter could not be achieved. Possible reasons for this finding are discussed.

Acknowledgements

I would like to express my special thanks to my Director of Studies Prof Andrey Karlyshev, for his invaluable support, constructive guidance, and supervision provided during these four years. I would like to thank him once again for providing an opportunity to work on this project. His time and counsel throughout my study is greatly appreciated.

I would also like to thank my second supervisor Dr Caroline Kim for helping me in familiarising with the lab set up in my initial year of study. I would also like to express my gratitude to the staffs of Life Sciences department especially Michael and Gurm for their advises and help. I would like to extend my acknowledgement to my lab colleagues Dr Burhan Lehri and Dr Ana Vieira for their generous support.

I am very grateful to my family for being very understanding in helping me pursue this degree. Without their support and love, this journey would have not been possible.

Lastly, I am indebted to my mother and my partner for their support and encouragement. I would like to thank them for believing in me throughout and for being a huge part of my success.

Table of contents

Chapter 1: Introduction	1
1.1 The genus of <i>Campylobacter</i>	1
1.2 Epidemiology of <i>Campylobacter</i> infections	2
1.3 Prevalence of <i>Campylobacter</i> in the poultry and environment	4
1.4 Virulence properties	6
1.4.1 Motility and Chemotaxis	6
1.4.2 Adhesion	9
1.4.3 Invasion	10
1.4.4 Toxicity	11
1.5 Pathogenesis and clinical manifestations of <i>Campylobacter</i>	11
1.6 Factors affecting coccoid form formation	13
1.7 Viable but non-culturable state of <i>Campylobacter</i>	16
1.8 Inducible gene expression systems	17
1.9 Autocatalytic gene expression system	20
1.10 Bacterial biofilms	22
1.11 Formation of bacterial biofilms	23
1.11.1 Initiation step	24
1.11.1.1 Surface sensing and the role of flagella	24
1.11.1.2 Initial attachment	25
1.11.2 Proliferation step	26
1.11.3 Maturation step	26
1.11.4 Dispersal step	26
1.12 <i>C. jejuni</i> biofilms	27
1.12.1 Importance of Quorum sensing	30
1.12.2 Importance of extracellular DNA and the role of extracellular nucleases in biofilms	33
1.13 Aims and Objectives	37
Chapter 2: Materials and Methods	39
2.1 Bacterial strains and plasmids	39
2.2 Growth conditions and storage	39
2.3 Gram staining	40

2.4	Colony-forming units counting	41
2.5	Water	41
2.6	Construction of pRRBCD- <i>egfp-araE</i> and pRRBCD- <i>egfp-lacYA177C</i> plasmids	41
2.7	Biofilm growth assays and optimization	42
2.8	eDNA-B and eDNA-S purification	44
2.9	DNase activity assays	44
2.10	Proteinase K treatment	45
2.11	Removing media from supernatant	45
2.12	Trypsin treatment	45
2.13	Dextranase treatment	46
2.14	Plasmid DNA purification	46
2.15	Genomic DNA purification	46
2.16	Determining the quality of DNA	47
2.17	Agarose gel electrophoresis	47
2.18	Restriction analysis	47
2.19	DNA purification from agarose gel	48
2.20	Dephosphorylation	48
2.21	Polymerase chain reaction	48
2.22	Ligation	50
2.23	Preparation of electrocompetent cells of <i>C. jejuni</i>	50
2.24	Transformation experiments	50
2.24.1	Electroporation of <i>Campylobacter</i>	50
2.24.2	Transformation of <i>E. coli</i>	51
2.25	Supercoiled DNA and restriction analysis	51
2.26	Construction of <i>Campylobacter</i> mutants	52
2.26.1	11168H/ <i>cj1051</i> mutant	52
2.26.2	11168H/ <i>cj0979</i> mutant	52
2.26.3	RM1221/ <i>cje0256</i> mutant	53
2.27	Next Generation sequencing	54
2.28	Comparison of growth rates of the <i>C. jejuni</i> derivatives	54
2.29	Green Fluorescent Protein (GFP) expression studies	54
2.30	Protein expression	55
2.31	Protein purification	56

2.32	Protein analysis and detection techniques	56
2.32.1	Sodium dodecyl sulphate polyacrylamide gel electrophoresis	56
2.32.2	Coomassie staining	57
2.32.3	Western blotting	57
2.32.4	Bicinchoninic acid assay	58
2.32.5	Mass spectrometry	58
	Chapter 3: Results	59
3.1	Construction and verification of regulated gene expression systems in <i>C. jejuni</i>	59
3.1.1	Validation of pRRBCD- <i>egfp-araE</i> and pRRBCD- <i>egfp-lacYA177C</i> constructs	60
3.1.1.1	Verification of recombinant plasmids	60
3.1.1.2	Plasmid sequencing	63
3.1.1.3	Investigation of <i>gfp</i> induction using solid agar plates	65
3.1.2	Integration of the gene cassettes carrying the <i>araE</i> and <i>lacYA177C</i> genes into the chromosome of <i>C. jejuni</i> 11168H	66
3.1.2.1	Checking electroporation efficiencies of <i>C. jejuni</i> 11168H with control plasmids	66
3.1.2.2	Electroporation of pRRBCD- <i>egfp-araE</i> and pRRBCD- <i>egfp-lacYA177C</i> plasmids into <i>C. jejuni</i> chromosome	70
3.1.3	Troubleshooting electroporation issues with pRRBCD- <i>egfp-araE</i> plasmid	73
3.1.3.1	Construction of 11168H/ <i>cj1051</i> mutant	73
3.1.3.2	Comparison of electroporation efficiencies	78
3.1.3.3	Electroporation of pRRBCD- <i>egfp-araE</i> into 11168H/ <i>cj1051</i> mutant	80
3.1.4	Confirmation of integration of gene cassette carrying <i>araE</i> gene	82
3.1.4.1	Genome sequencing of derivative <i>C. jejuni</i> strains carrying <i>araE</i> and <i>lacYA177C</i>	82
3.1.4.2	Confirmation of gene cassette integration in the 11168H/ <i>cj1051</i> /pRRBCD- <i>araE</i> strain by polymerase chain reaction	83
3.1.5	Investigation of expression of <i>gfp</i> in <i>C. jejuni</i> derivative strains	84
3.1.5.1	Growth rates of derivative strains	85
3.1.5.2	GFP expression studies using solid agar plates	86
3.1.5.3	GFP expression studies using liquid cultures by fluorimeter	87
3.2	Investigation of the molecular mechanism of biofilm formation and dispersal in <i>C. jejuni</i> 11168H	90
3.2.1	Identification of the dispersal stage of <i>C. jejuni</i> 11168H and investigation of the composition of DNA complex in the culture supernatant	90

3.2.1.1	Identification of the dispersal stage of <i>C. jejuni</i> 11168H strain	91
3.2.1.2	DNase test assays of 11168H supernatant	92
3.2.1.3	Treatment of 11168H supernatant with trypsin	97
3.2.1.4	Identification of products of proteolytic digestion	99
3.2.1.5	Treatment of 11168H supernatant with dextranase	101
3.2.2	Investigation of the role of <i>cj0979</i> gene in biofilm formation of <i>C. jejuni</i> 11168H	103
3.2.2.1	Construction of 11168H/ <i>cj0979</i> mutant	103
3.2.2.2	Comparison of the biofilm formation and dispersal patterns between wild- type and mutant strains	109
3.2.3	Functional analysis of a putative nuclease Cj0979	110
3.2.3.1	Construction of the pBAD33- <i>cj0979</i> plasmid	111
3.2.3.2	Expression, purification, and detection of Cj0979	113
3.2.3.3	Western blotting	114
3.2.3.4	Construction of the pBAD33- <i>cj0979N</i> plasmid	116
3.2.3.5	Expression, purification, and detection of Cj0979N	119
3.2.3.6	Construction of pBAD33- <i>cj0979LP</i>	120
3.2.3.7	Expression, purification, and detection of Cj0979LP	124
3.2.3.8	Determining the concentration of Cj0979LP	126
3.2.3.9	DNase activity tests of Cj0979LP	126
3.2.3.10	Effect of purified Cj0979LP on <i>C. jejuni</i> 11168H biofilms	127
3.3	Investigation of the role of <i>cje0256</i> in biofilm forming ability of <i>C. jejuni</i> RM1221	129
3.3.1	Investigation of biofilm formation ability of <i>C. jejuni</i> RM1221	130
3.3.2	Construction of <i>C. jejuni</i> RM1221/ <i>cje0256</i> mutant	131
3.3.2.1	Construction and verification of pUC19- <i>cje0256</i> -kanR construct	131
3.3.2.2	Electroporation of pUC19- <i>cje0256</i> -kanR into <i>C. jejuni</i> RM1221 strain	135
3.3.2.3	Methylation of DNA	135
3.3.2.4	Restriction digestion of methylated DNA	135
3.3.3	Functional analysis of a putative nuclease Cje0256	139
3.3.3.1	Construction of pBAD33- <i>cje0256</i> and pBAD33- <i>cje0256LP</i>	139
3.3.3.2	Purification of Cje0256 and Cje0256LP	143
3.3.3.3	Western blotting	147
	Chapter 4: Discussion and future work	148

4.1	Construction and verification of systems for regulated gene expression in <i>C. jejuni</i>	148
4.2	Investigation of molecular mechanism of biofilm formation and dispersal in <i>C. jejuni</i> 11168H	153
4.3	Investigation of the role of <i>cje0256</i> in the biofilm-forming ability of <i>C. jejuni</i> RM1221	157
Chapter 5: Conclusion		161
Chapter 6: References		162
Appendix		196

List of Figures

Figure 1. The reservoirs and pathways involved in <i>C. jejuni</i> transmission	4
Figure 2. The most imperative routes of transmission of <i>Campylobacter</i> from animals to humans	6
Figure 3. The major proteins associated with the hook-basal body of <i>C. jejuni</i> flagella.....	8
Figure 4. Positive and negative regulation of the <i>ara</i> operon in <i>E. coli</i>	20
Figure 5. Schematic illustration of biofilm development.....	24
Figure 6. Schematic representation of QS.....	32
Figure 7. Schematic representation of biofilm dispersal.....	35
Figure 8. Verification of pRRBCD- <i>egfp-lacYA177C</i> by restriction analysis.....	61
Figure 9. Verification of pRRBCD- <i>egfp-araE</i> by restriction analysis.....	62
Figure 10. Plasmid maps showing the locations of the arabinose transporter genes, P _{BAD} promoter and AraC regulatory region, reporter gene <i>gfp</i> , and the chloramphenicol resistance gene cassette.....	64
Figure 11. Fluorescence images of <i>E. coli</i> strains carrying the arabinose transporter genes, in the presence of 0.1% final concentration arabinose.....	66
Figure 12. Restriction maps of control plasmids.....	67
Figure 13. Restriction analysis of control plasmids.....	68
Figure 14. Linear genetic map of plasmid pRRC and the three possible products of recombination of the plasmid with the different rRNA loci of the <i>C. jejuni</i> genome.....	69
Figure 15. Linear genetic map of plasmid pSpoT showing the location of <i>spoT</i> _for and <i>spoT</i> _rev primers on the plasmid.....	69
Figure 16. Verification of morphology of <i>C. jejuni</i> transformants by Gram staining	69
Figure 17. Confirmation of integration of <i>cam</i> ^r cassette into the chromosome of <i>C. jejuni</i> and inactivation of <i>spoT</i> gene in <i>C. jejuni</i> 11168H.....	70
Figure 18. Verification of morphology of <i>C. jejuni</i> 11168H/pRRBC- <i>egfp-lacYA177C</i> by Gram staining	71
Figure 19. Confirmation of integration of the gene cassette carrying <i>lacYA177C</i> gene into <i>C. jejuni</i> 11168H chromosome by PCR.....	72
Figure 20. Linear genetic map of <i>C. jejuni</i> 11168H/pRRBCD- <i>egfp-lacYA177C</i> showing the location of the PCR verification primers.....	72
Figure 21. Amplification of <i>cj1051</i> gene with flanking regions from <i>C. jejuni</i> 11168H chromosomal DNA using primers <i>cj1051</i> _for and <i>cj1051</i> _rev by PCR	74

Figure 22. Verification of an intermediate construct pGEM-T-1051 by restriction analysis ..	75
Figure 23. Verification of p1051-tetR by restriction analysis.....	76
Figure 24. Verification of the inactivation of <i>cj1051</i> gene in <i>C. jejuni</i> 11168H by PCR.....	78
Figure 25. PCR verification of <i>C. jejuni</i> 11168H and 11168H/ <i>cj1051</i> transformants from comparative electroporation experiment using control plasmids.....	80
Figure 26. Verification of morphology of <i>C. jejuni</i> 11168H/pRRBCD- <i>egfp-araE</i> by Gram staining	81
Figure 27. Linear genetic map of <i>C. jejuni</i> 11168H/pRRBCD- <i>egfp-araE</i> showing the location of the PCR verification primers	81
Figure 28. PCR amplification of region between 16S gene and chloramphenicol promoter site in 11168H/pRRBCD- <i>egfp-araE</i> transformant by PCR.....	82
Figure 29. Chromosomal region between the 16S and 28S rRNA genes containing the P _{BAD} promoter, <i>cam^r</i> , <i>gfp</i> , and <i>lacYA177C</i> genes	83
Figure 30. Chromosomal region between the 16S and 28S rRNA genes containing P _{BAD} promoter, <i>cam^r</i> , <i>gfp</i> , and <i>araE</i> genes	83
Figure 31. Confirmation of the integration of gene cassette carrying the <i>araE</i> gene into the chromosome of <i>C. jejuni</i> 11168H/ <i>cj1051</i> by PCR.....	84
Figure 32. Comparison of growth rates of the <i>C. jejuni</i> derivative strains to the wild-type strain	86
Figure 33. Fluorescence testing of bacterial samples in whole cell suspensions before and after induction	88
Figure 34. Fluorescence testing of bacterial samples in lysates before and after induction	89
Figure 35. Biofilm formation curve of <i>C. jejuni</i> 11168H in borosilicate test tubes over a 10 days period	92
Figure 36. Gel image showing the attempt to detect DNase activity in culture supernatant. ..	93
Figure 37. Gel electrophoresis of eDNA samples and culture supernatant.....	94
Figure 38. Investigation of possible effects of medium and DNase buffer on migration pattern of eDNA samples on a 1% agarose gel	95
Figure 39. DNase activity of Proteinase K treated culture supernatant	96
Figure 40. Gel electrophoresis of trypsin treated samples	99
Figure 41. BLASTp search result showing sequence alignment between uncharacterized protein and YdcH (<i>E. coli</i>).	101
Figure 42. Gel electrophoresis of dextranase treated samples.	103

Figure 43. Amplification of <i>cj0979</i> gene with flanking regions from 11168H chromosomal DNA using primers <i>cj0979_for</i> and <i>cj0979_rev</i> by PCR.....	105
Figure 44. Clone checker analysis of pGEM-T-0979 clones.	105
Figure 45. Verification of an intermediate construct pGEM-T-0979 by restriction analysis	106
Figure 46. Verification of p0979-kanR by restriction analysis.....	107
Figure 47. Verification of the inactivation of <i>cj0979</i> gene in <i>C. jejuni</i> 11168H by PCR using primers <i>cj0979_for</i> and <i>cj0979_rev</i>	109
Figure 48. Biofilm assay of <i>C. jejuni</i> 11168H/ <i>cj0979</i> in comparison to wild-type 11168H strain.	110
Figure 49. Amplification of <i>cj0979</i> gene from <i>C. jejuni</i> 11168H chromosomal DNA with primers <i>cj0979_expr_for</i> and <i>cj0979_expr_rev</i>	111
Figure 50. Verification of pBAD33- <i>cj0979</i> by restriction analysis.....	112
Figure 51. Analysis of fractions from <i>E. coli</i> /pBAD33- <i>cj0979</i> expression and purification experiment.....	114
Figure 52. Western blotting of fractions from <i>E. coli</i> /pBAD33- <i>cj0979</i> expression and purification experiments.....	116
Figure 53. Verification of pBAD33- <i>cj0979N</i> by restriction analysis.	118
Figure 54. Analysis of fractions from <i>E. coli</i> /pBAD33- <i>cj0979N</i> purification and supernatant samples from <i>E. coli</i> /pBAD33- <i>cj0979</i> expression experiments	120
Figure 55. Amplification of <i>cj0979LP</i> gene from <i>C. jejuni</i> 11168H chromosomal DNA with primers <i>cj0979_LP_for</i> and <i>cj0979_LP_rev</i>	122
Figure 56. Verification of pBAD33- <i>cj0979LP</i> by restriction analysis	123
Figure 57. Analysis of fractions from <i>E. coli</i> /pBAD33- <i>cj0979LP</i> expression and purification experiment.....	125
Figure 58. Analysis of fractions from <i>E. coli</i> /pBAD33- <i>cj0979LP</i> expression and purification experiment.....	126
Figure 59. DNase activity of purified Cj0979LP protein.....	127
Figure 60. Effects of purified Cj0979LP, DNase I and culture supernatant on biofilm formation	128
Figure 61. Biofilm assay of <i>C. jejuni</i> 11168H and RM1221	130
Figure 62. Amplification of <i>cje0256</i> gene with flanking regions from <i>C. jejuni</i> RM1221 chromosomal DNA using primers <i>cje0256f_mod</i> and <i>cje0256r_mod</i>	132
Figure 63. Verification of an intermediate construct pUC19- <i>cje0256</i> by restriction analysis	133

Figure 64. Verification of pUC19- <i>cje0256</i> -kanR by restriction analysis	134
Figure 65. Restriction analysis of methylated pUC19- <i>cje0256</i> -kanR with RsaI	137
Figure 66. Restriction analysis of re-methylated pUC19- <i>cje0256</i> -kanR with RsaI.....	138
Figure 67. Verification of pBAD33- <i>cje0256</i> by restriction analysis.	141
Figure 68. Verification of pBAD33- <i>cje0256</i> LP by restriction analysis.....	142
Figure 69. Analysis of fractions from <i>E. coli</i> /pBAD33- <i>cje0256</i> protein expression and purification experiment.	144
Figure 70. Analysis of fractions from <i>E. coli</i> /pBAD33- <i>cje0256</i> LP and <i>E. coli</i> /pBAD33- <i>cj0979</i> LP protein expression and purification experiment.....	145
Figure 71. Analysis of fractions from <i>E. coli</i> /pBAD33- <i>cje0256</i> , <i>E. coli</i> /pBAD33- <i>cje0256</i> LP, and <i>E. coli</i> /pBAD33- <i>cj0979</i> LP expression and purification experiments	146
Figure 72. Western blotting of Cj0979LP and eluates from <i>E. coli</i> /pBAD33- <i>cje0256</i> and <i>E.</i> <i>coli</i> /pBAD33- <i>cje0256</i> LP purification experiments.	147

List of Tables

Table 1: PCR conditions used with Promega GoTaq® Green Master Mix	49
Table 2: PCR conditions used with NEB Q5® High-Fidelity DNA Polymerase	49
Table 3: List of primers used in this study	49
Table 4: DNA concentration and purity of plasmids pRRBCD- <i>egfp-araE</i> and pRRBCD- <i>egfp-lacYA177C</i> using NanoVue Plus Spectrophotometer	63
Table 5: Comparison of electroporation efficiencies (CFU/μg DNA used) of <i>C. jejuni</i>	79
Table 6: NanoVue readings of purified eDNA samples.	94
Table 7: NanoVue readings of second purification of eDNA-B.	96
Table 8: DNA concentration and purity of supernatant sample before and after media exchange	97
Table 9: Estimation of protein and DNA content in samples	98
Table 10: List of the first 10 most abundant proteins detected by Mass spectrometry	100
Table 11: Analysis of supernatant samples after treatment with dextranase.	102

List of Abbreviations

AI-1	Autoinducer 1
AI-2	Autoinducer 2
BHI	Brain heart infusion
BLASTp	Basic local alignment search tool- Protein blast
BLASTn	Basic local alignment search tool- Nucleotide blast
bp	Base pair
BSA	Bovine serum albumin
CBA	Columbia blood agar
CCR	Carbon catabolite repression
CF	Coccoid form
CFF	Coccoid form formation
CFU	Colony forming unit
CLC GWB	CLC genomics workbench
CPS	Capsular polysaccharide
DNA	Deoxyribonucleic acid
DNase I	Deoxyribonuclease I
dNTP	Deoxyribonucleoside triphosphate
eDNA	Extracellular DNA
eDNA-B	Extracellular DNA from biofilm

eDNA-S	Extracellular DNA from culture supernatant
eDNase	Extracellular DNase
EDTA	Ethylenediaminetetraacetic acid
EPM	Extracellular polymeric matrix
GBS	Guillain-Barré syndrome
kb	Kilobase
kDa	Kilodalton
LB	Lennox broth
LOS	Lipooligosaccharide
MFS	Miller-Fisher syndrome
MH	Mueller Hinton
MS	Mass spectrometry
NCBI	National Center for Biotechnology Information
NETs	Neutrophil extracellular traps
Ni	Nickel
OD	Optical density
PBS	Phosphate buffered saline
PCR	Polymerase chain reaction
PG	Peptidoglycan
PVDF	Polyvinylidene difluoride

QS	Quorum sensing
SDS-PAGE	Sodium dodecyl sulphate polyacrylamide gel electrophoresis
SEM	Standard error of mean
SOC	Super optimal broth with catabolite repression
TBS	Tris-buffered saline
TBST	Tris-buffered saline tween 20
UV	Ultraviolet
VBNC	Viable but non-culturable
WT	Wild-type

Chapter 1: Introduction

1.1 The genus of *Campylobacter*

In 1886, Theodore Escherich released the first report on the world's leading foodborne pathogen, *Campylobacter*, after initially observing *Campylobacter*-resembling microorganisms in the colon of children with cholera infantum (Snelling *et al.*, 2005). Mc Fadyean and Stockman first isolated the pathogen in 1913 from bovine foetuses (Mc Fadyean and Stockman, 1913). Smith and Orcutt (1927) isolated a group of similar organisms from faeces of cattle with diarrhoea, naming it *Vibrio fetus*. In 1944, another group of microorganisms was isolated by Doyle (1944) and named *Vibrio coli*, as their shape was different from the previously isolated microorganisms by Smith and Orcutt (1927). Following this discovery, it was not until 1963 that the *Campylobacter* genus was first proposed by Sebald and Veron (1963), who identified fundamental differences between the discovered organisms and true *Vibrio* species (On, 2001; Véron and Chatelain, 1973).

In 1977, Skirrow developed a selective supplement for *Campylobacter* consisting of polymyxin B, vancomycin, and trimethoprim; this supplement eventually improved the isolation procedure for these bacteria (Skirrow, 1977). The genus belongs to the family of *Campylobacteraceae* under the order *Campylobacterales* of the class *Epsilonproteobacteria* and phylum *Proteobacteria* (Kaakoush *et al.*, 2015; Vandamme and Deley, 1991). Currently, the genus consists of 26 species and 9 sub-species, with *C. jejuni* being the most accountable species for gastrointestinal diseases followed by *C. coli* (Kaakoush *et al.*, 2015).

Campylobacter species are small, spiral, or rod-shaped microorganisms with AT-rich genomes (Bronowski *et al.*, 2014). They typically measure 0.2–0.8 µm in width and 0.5–5 µm in length, and contain a polar flagellum that aids in its corkscrew motility for attachment and colonization of host cells (Bolton, 2015; Frirdich *et al.*, 2017). The exceptions are *C. showae*,

which contains multiple flagella, and *C. gracilis*, a non-motile strain (Silva *et al.*, 2011).

1.2 Epidemiology of *Campylobacter* infections

C. jejuni is the leading contributor to gastrointestinal diseases worldwide, accounting for more than 80–90% of reported cases (Poelzler *et al.*, 2018). According to the Centers for Disease Control and Prevention in the US, approximately 1.3 million cases of campylobacteriosis are reported yearly (Centers for Disease Control and Prevention, 2017). The European Centre for Disease Prevention and Control confirmed in their annual epidemiological report that there were 250,161 cases of campylobacteriosis in 2017 within the EU/EEA region. They identified the UK, the Czech Republic and Germany as the major contributors to campylobacteriosis (European Centre for Disease Prevention and Control, 2017). In the past 10 years, the numbers of reported cases of campylobacteriosis have increased in Europe, the US and Australia. The total number of cases reported in other parts of the world, such as Africa, Asia and the Middle East, remains ambiguous, but the prevalence of *C. jejuni* infections has been confirmed in these regions (Kaakoush, 2015). In developing countries, the lack of national surveillance programmes leads to underestimation of the total number of reported cases (Giangaspero, 2018; Park, 2002). However, in both developed and developing countries, these infections are usually caused by environmental and food contamination. *Campylobacter* is prevalent in food-producing animals, wild animals and companion animals, but poultry has served as the largest reservoir for *Campylobacter* infections, contributing to more than 70% of all cases (Wagenaar *et al.*, 2013; Epps *et al.*, 2013). Poultry includes chickens, turkeys and ducks; contaminated chickens continue to represent the largest reserve of human campylobacteriosis. A report by the Food Standards Agency in the UK revealed that up to 72.9% of retail chickens surveyed between 2014 and 2015 tested positive for *Campylobacter* (Kaakoush *et al.*, 2015). Other key contributing risk factors include consumption of contaminated water, unpasteurized milk and international travel (Kaakoush *et al.*, 2015; Poelzler *et al.*, 2018). The risk associated with

international travel varies depending on the travel destination. A meta-analysis conducted in 2009 revealed that the chances of acquiring campylobacteriosis rose with holidaymakers travelling to South East Asia, South Asia, Africa and Latin America (Kaakoush *et al.*, 2015).

The rate of infection increases in infants, the elderly and people with underlying diseases (*Campylobacter*, 2018). Figure 1 shows a representation of all the major sources and risk factors involved in the transmission of *C. jejuni* from animals to humans. Quantifying the contribution of each animal reservoir to human campylobacteriosis is complicated because transmission can occur through more than one pathway. All the risk factors mentioned below are interconnected and collectively contribute to the overall burden of *C. jejuni* infections (Wagenaar *et al.*, 2013).

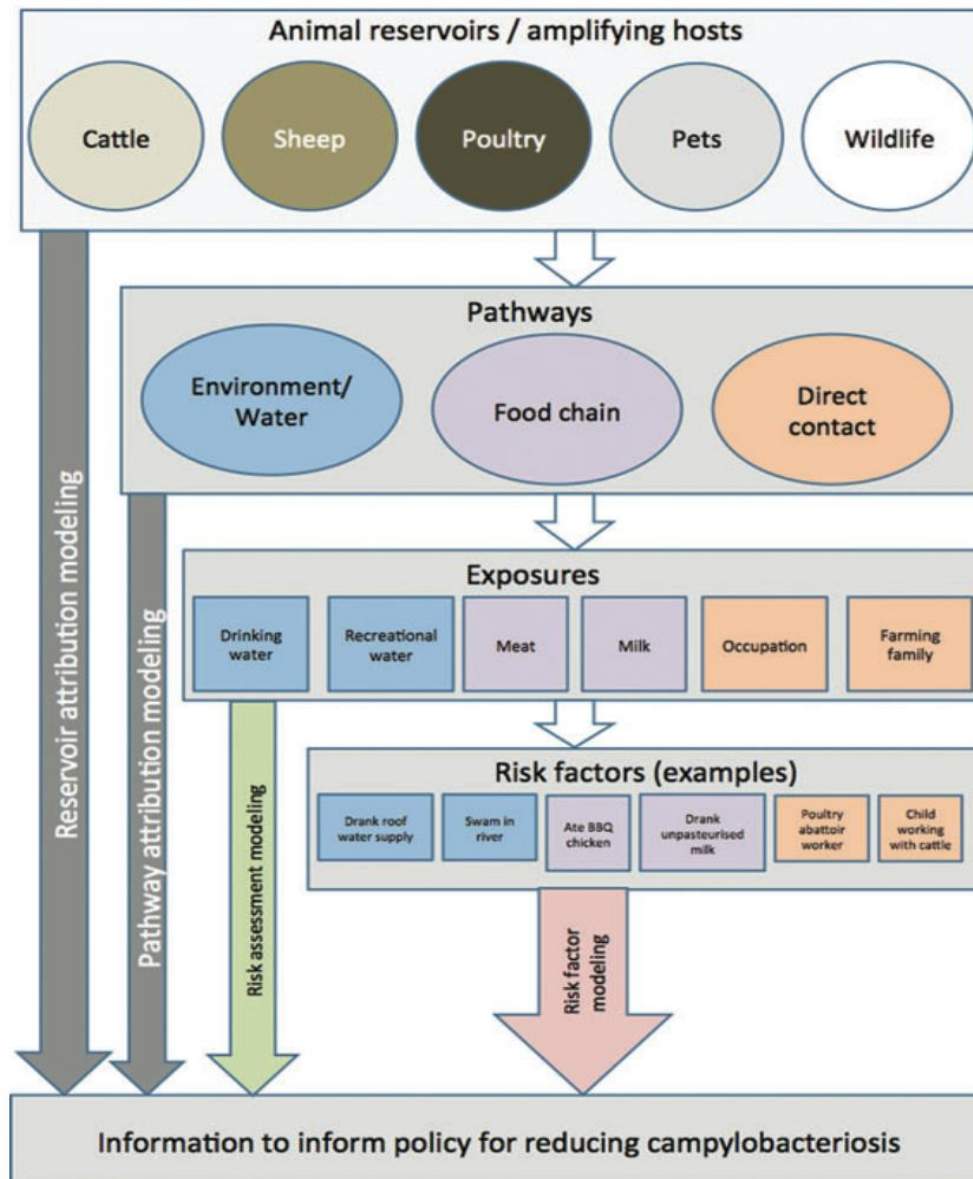


Figure 1. The reservoirs and pathways involved in *C. jejuni* transmission (Wagenaar *et al.*, 2013).

1.3 Prevalence of *Campylobacter* in the poultry and environment

The poultry industry is the predominant contributor to *C. jejuni* infections (Silva *et al.*, 2011). The infection can spread at any of the following stages: rearing; slaughtering; transporting; processing; handling; and consumption of the products (Skarp *et al.*, 2016). Poultry processing can lead to environmental contamination, such as contamination of surface water via cecal or fecal routes, which may then potentially cross-contaminate humans either by direct or indirect contact. Thermophilic *Campylobacter* causes most of the reported campylobacteriosis cases

(Gölz *et al.*, 2018). The ceca (intestinal tract) in chicks serve as the primary colonization site and usually contain around 10^6 to 10^8 CFU/g bacteria (Hermans *et al.*, 2011), with just about 35 CFU/g bacteria required for chick colonization (Stern *et al.*, 1988). Furthermore, flies, rodents, and wild birds often contaminate poultry flocks, as illustrated in Figure 2.

Colonization in chicks usually occurs within the first day of exposure, whereupon they become asymptomatic carriers of *C. jejuni* (Gölz *et al.*, 2018). Several studies have reported an increase in campylobacteriosis incidence in poultry flocks during the summer and autumn months due to the increased activity of flies during this period. In European countries such as Norway, Sweden, Iceland, and Finland, the prevalence is much lower due to shorter summers (Wagenaar *et al.*, 2013). Vertical transmission of infection occurs very rarely in the poultry industry; therefore, each broiler cycle in the farms starts *Campylobacter*-free (Wagenaar *et al.*, 2013). The degree of colonization generally depends on the following factors: flock size; population thinning; lack of biosecurity; and the production type (Gölz *et al.*, 2018; Wagenaar *et al.*, 2013).

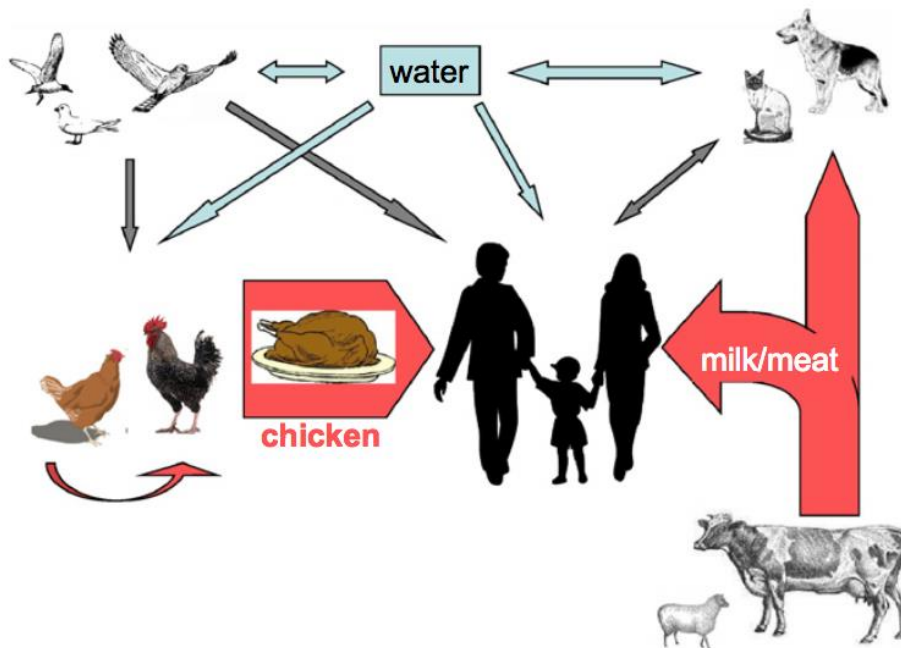


Figure 2. The most imperative routes of transmission of *Campylobacter* from animals to humans (Dasti *et al.*, 2010).

1.4 Virulence properties

The degree of infection in humans largely depends on the virulence of a strain and the immune response of each individual. Motility, adhesion, invasion, and toxin production have been identified as the major virulence factors required to cause gastrointestinal tract infections (Silva *et al.*, 2011).

1.4.1 Motility and Chemotaxis

Motility is important in *Campylobacter*'s survival in the challenging environment of the gastrointestinal tract. *C. jejuni* possess one or two polar flagella consisting of O-linked glycosylation flagellin and has a helical shape, which assists in movement through the niches present inside the body (Hermans *et al.*, 2011). The flagellum consists of a hook-basal body and a flagella filament. The flagella filament is composed of multimers of proteins such as FlaA (major flagellin protein) and FlaB (minor flagellin protein) and is attached to a hook, which is connected to a base situated in the cytoplasm and the inner membrane (Silva *et al.*,

2011). The hook-basal body comprises several different proteins, as shown in Figure 3 below. The regulation of *flaA* is under the control of the σ^{28} promoter. The σ^{54} promoter regulates the transcription of *flaB* and other genes in the hook-basal body (Silva *et al.*, 2011). Expression of σ^{54} genes is regulated by a two-component regulatory system containing the response regulator FlgR and the sensor kinase FlgS. The *flaA* and *flaB* are independently expressed where the σ^{28} and σ^{54} promoter activity depends on the chemotactic and environmental stimuli (Hermans *et al.*, 2011).

Previous mutation studies have suggested that the presence of *flaA* is more essential for the colonization of chickens than *flaB* (Bolton, 2015; Wassenaar *et al.*, 1993). The importance of motility in virulence has been confirmed, as non-flagellated mutants displayed colonization impairment *in vitro* (Dasti *et al.*, 2010; Guerry *et al.*, 1992; Yao *et al.*, 1994). Other studies have shown that a mutation in the *maf5* gene (motility accessory factor 5) in *C. jejuni* hindered colonization (Karlyshev *et al.*, 2002; Jones *et al.*, 2004; Hermans *et al.*, 2011). In addition, flagellin O-linked glycosylation was demonstrated to be vital for flagella assembly, motility, and chick colonization through mutational studies of the genes *cj1321-1325/6* (Bolton, 2015; Champion *et al.*, 2005). This finding was further confirmed in a study conducted by Howard *et al.* (2009), in which one gene in particular, *cj1324*, was found to be vital for chick colonization.

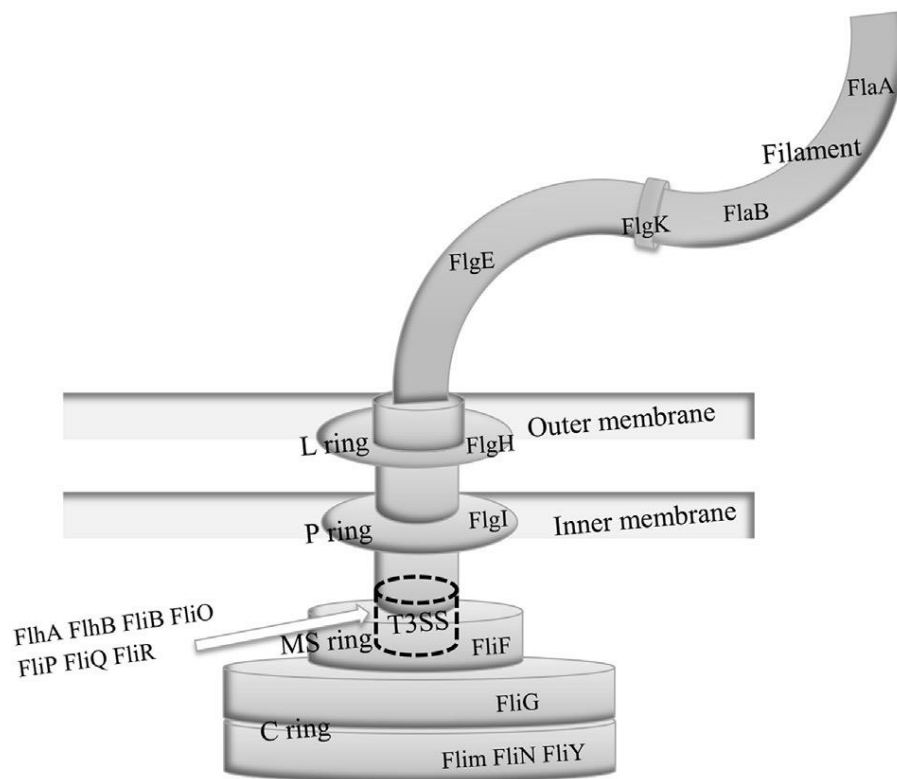


Figure 3. The major proteins associated with the hook-basal body of *C. jejuni* flagella (Bolton, 2015).

Chemotaxis is a process in which bacteria sense favourable chemical environments and move accordingly in an attempt to survive an unfavourable environment and induce colonization of intestinal mucosa (Hermans *et al.*, 2011; Hamer *et al.*, 2010). Glycoproteins and mucins (components of the mucus) have been identified as primary chemoattractants. Other chemoattractants include metabolic substrates and some organic acids (Marchant *et al.*, 2002 Bolton, 2015). From an analysis of the *C. jejuni* genome, Hendrixson and DiRita (2004) identified the following chemotaxis proteins: CheA; CheB; CheR; CheW; CheY; CheV; and methyl-accepting chemotaxis proteins (MCP). The MCP, which linked to CheA via CheW or CheV, senses any fluctuations in the concentration of the chemoattractant. CheW and CheV are both adapter proteins, which are required for chemotaxis. Upon activation of the monomer CheA, a phosphoryl group is transferred to either CheY or CheB, which then binds to FliM in the flagellar motor, promoting directional changes of the bacteria by changing the motor

rotation movement from anti-clockwise to clockwise (Hamer *et al.*, 2010). This change causes the bacteria to shift from a smooth to a tumbling motion (Hamer *et al.*, 2010). From an analysis of the *C. jejuni* genome sequence, Marchant *et al.* (2002) identified 10 MCPs (labelled as transducer-like proteins). Vegge *et al.* (2009) demonstrated that mutation in the *tlp1*, *tlp4*, and *tlp10* genes exhibited reduced levels of chick colonization in *C. jejuni*, further establishing the significance of chemotaxis in virulence. In another work by Hermans *et al.* (2011), a mutation in the *luxS* gene, which produces autoinducer-2 (AI-2) molecules, exhibited reduced levels of chemotaxis and thereby reduced levels of chick colonization.

1.4.2 Adhesion

The severity of infection depends on the adhesion of *C. jejuni* to the intestinal epithelial cells. Several adhesins present on the surface of *Campylobacter*, such as the fibronectin-binding outer-membrane protein CadF, the autotransporter CapA, the periplasmic-binding protein PEB1, and the surface-exposed lipoprotein JlpA, usually facilitate this adhesion (Dasti *et al.*, 2010). Konkel *et al.* (1997) found the CadF protein binds to fibronectin, a glycoprotein located in the extracellular matrix of the gastrointestinal tract that plays a chief role in internalization of the bacteria. Ziprin *et al.* (1999) deduced that a *cadF* knockout mutant failed to colonize the cecum of chicks due to its lack of adhesive ability, indicating the significance of *cadF* adhesion for successful chick colonization. Through mutational studies, Jin *et al.* (2001) suggested the *jlpA* that encodes a 42 kDa lipoprotein plays a role in mediating the adhesion of *C. jejuni* with their host cells. Furthermore, Ashgar *et al.* (2007) identified CapA as an auto-transporter protein, which is involved in the adhesion of *C. jejuni* to human epithelial cells *in vitro* and colonization of chick intestines *in vivo*. An insertional mutation in the *capA* gene displayed a reduction in colonization of the chicks and a reduced adhesion to Caco-2 cells (Ashgar *et al.*, 2007). Similarly, Pei and Blaser (1993) identified PEB1 as well-conserved in most *C. jejuni* and *C. coli*, finding it plays a vital role in the adhesion of *Campylobacter* to HeLa cells and

thereby heavily influences the virulence of the strain and the colonization of the host.

1.4.3 Invasion

The invasion ability of *Campylobacter* varies from strain to strain, which makes the elucidation of factors responsible for this mechanism difficult. Until now, researchers have reported microtubule-dependent and actin-filament-dependent invasion mechanisms in *Campylobacter* (Hermans *et al.*, 2011; Dasti *et al.*, 2010). The flagella also serve a secondary function as an export apparatus, aiding in the secretion of non-flagella proteins during *C. jejuni* invasion. Konkel *et al.* (2004) established that the flagella assist the transport of *Campylobacter* invasion antigens into the cell and thus play an important biological role in colonization. The full function of these *Campylobacter* invasion antigens remains unclear; however, a mutation in the *ciaB* gene resulted in a reduced invasion ability of epithelial cells, suggesting that this gene plays an important role in colonization. Other bacterial factors that are important in invasion are capsular polysaccharide (CPS), lipooligosaccharide (LOS) and O- and N-linked glycan structures present in *Campylobacter* (Hermans *et al.*, 2011). CPS surrounds the surface of *C. jejuni*, facilitating in the survival and colonization of the host (Hermans *et al.*, 2011). A mutation in *kpsM* (CPS transporter gene) in *C. jejuni* 11168H led to a significant reduction in colonising ability of the strain (Jones *et al.*, 2004). A study by Louwen *et al.* (2008), demonstrated that the sialylation of the outer core of LOS resulted in increased epithelial invasion by several *C. jejuni* strains. The *pgl* multi-gene locus encodes the N-linked glycosylation system that controls the posttranslational modification of several proteins including the flagellin. On the contrary, the O-linked glycosylation pathway is only responsible for the modification of flagellar subunits (Karlyshev *et al.*, 2005b). Karlyshev *et al.* (2004) demonstrated that a mutation in the *pglH* gene has resulted in a reduction in the ability of two *C. jejuni* strains to invade the human epithelial cells.

1.4.4 Toxicity

Cytolethal-distending toxin (CDT) is produced by *Campylobacter* and is a well-characterised toxin. This toxin was widely studied in many Gram-negative bacteria (Bolton, 2015). CDT leads to cell-cycle arrest and cytoplasmic distension and, in turn, chromatin fragmentation and eventually cell death (Lara-Tejero and Galan, 2000). Three genes encode the CDT: *cdtA*; *cdtB*; and *cdtC*. For CDT to be fully functional all three-gene products are required; Lara-Tejero and Galan (2001) demonstrated that there was no toxicity when each gene product was individually tested. The CDT tripartite holotoxin is composed of CdtA and CdtC, which are the heterodimeric subunits, and CdtB, which is the enzymatically active subunit (Lara-Tejero and Galan, 2001). This CDT is functionally and biologically similar to the mammalian DNase I enzyme (Elwell and Dreyfus, 2000). It has been deduced that in *cdtB* mutants with single amino acid substitution in residues responsible for catalysis and magnesium activity, the mutations did not cause cell-cycle arrest or distension in *Campylobacter* (Lara-Tejero and Galan, 2000). The CDT causes cell-cycle arrest during the G2/M phase by blocking the CDC2 kinase, necessary for mitosis (Pickett and Whitehouse, 1999). Following this, cell division ceases, but the cytoplasm grows to five times its original size, which eventually results in cell death (Lara-Tejero and Galan, 2000). Purdy *et al.* (2000) investigated *C. jejuni* NCTC 11168 *cdtB* and 81176 *cdtB* mutants, observing no cytotoxicity in 11168 and very low levels of toxicity unrelated to CDT action in 81176. These findings suggest that CDT is still the principle toxin produced by *Campylobacter* strains, although some strains may produce more than one toxin. Other putative toxins, such as enterotoxins and hepatotoxins, have been experimentally identified in *Campylobacter*, but only CDT has been studied in detail and confirmed from genome sequences (Purdy *et al.*, 2000; Janssen *et al.*, 2008).

1.5 Pathogenesis and clinical manifestations of *Campylobacter*

To establish an infection, *Campylobacter* must counteract the immune response of the host

cells. In humans, upon oral exposure to *Campylobacter*, the virulence characteristics enable the bacteria to pass through the mucus layer, which is the first line of defence, and reach the underlying epithelial cells, where an infection is generally established (Young *et al.*, 2007). Upon bacterial invasion of the human epithelial cells and release of toxins, the innate immune response of the individual is activated followed by the adaptive immune response. Invading bacteria are usually detected by Toll-like receptors; this stimulation induces the production of an early cytokine (IL-8). This response further activates the employment of macrophages, neutrophils, and dendritic cells to fight off the invading *Campylobacter*. These interactions collectively trigger a massive pro-inflammatory response followed by the production of cytokines, thus resulting in inflammation of the epithelial cells and infections in humans (Young *et al.*, 2007; Schnee and Petri, 2017). Symptoms associated with campylobacteriosis can generally be classified as mild but can lead to severe complications in occasional cases. The general clinical symptoms include watery or bloody diarrhoea, abdominal cramps, headache, and nausea (Janssen *et al.*, 2008). These symptoms usually persist for no more than a week. The infections are typically self-limiting and produce mainly gastro-enteric symptoms, but in rare cases can lead to post-infectious complications such as Guillain-Barré syndrome (GBS) and Miller-Fisher syndrome (MFS) (Allos, 2001). MFS is a subvariant and a milder form of GBS, but both are neuromuscular disorders, which can cause weaknesses and respiratory insufficiencies leading to paralysis (Rees *et al.*, 1995). In addition, an estimated 25–40% of patients diagnosed with GBS worldwide report suffering from campylobacteriosis a few weeks prior to the diagnosis (Nyati and Nyati, 2013). However, post-infection complications are uncommon; only 0.1% of the *C. jejuni* infections lead to extraintestinal complications (Mori *et al.*, 2014).

Researchers have demonstrated two different dosages of *C. jejuni* cells (500 CFU and 800 CFU) have caused infections in studies of humans (Robinson, 1981; Black *et al.*, 1993). In

chickens they are present in very large numbers up to 10^8 as commensal bacteria, until it was shown to cause symptoms in chickens in a recent study by Humphrey *et al.* (2014). The difference in body temperature in the two hosts (chickens 41–45°C, humans 37°C) may account for most of the variation in infection mechanism between humans and chickens (Young *et al.*, 2007). A study by Bras *et al.* (1999) illustrated a change in the differential transcriptional profile as well as the membrane structure upon the increase of temperature from 37°C to 42°C due to the upregulation of genes involved in transport, binding proteins, and cell wall components. *C. jejuni* is known to induce an innate immune response by the production of cytokines in both humans and chickens, and thus possesses the capability to induce a pro-inflammatory response in both hosts (Smith *et al.*, 2008). In addition, while studies have demonstrated the production of pro-inflammatory cytokines such as IL-1 β , IL-6 and the inflammatory chemokines CXCLi1 and CXCLi2 in chicken cells, they have failed to establish subsequent infections (Smith *et al.*, 2008; Kaiser *et al.*, 2005). However, in a recent study by Humphrey *et al.* (2014), the authors observed an innate response leading to intestinal inflammation and diarrhoea in chickens. *C. jejuni* were detected by Toll-like receptors in the chicken's gut. These receptors activated an innate response that employed heterophils to fight off the invading *C. jejuni*, resulting in a pro-inflammatory response then leading to infection (Humphrey *et al.*, 2014).

1.6 Factors affecting coccoid form formation

Campylobacter species undergo a change in morphology and transform into coccoid form (CF) when exposed to stressful environmental conditions (Koike, 1982). The helical shape is generally observed during the exponential growth phase, while the CF is noted during the stationary growth phase of these bacteria. Temperature stress, oxidative stress, pH stress, and nutrient limitations all contribute to this morphological transition (Harvey and Leach, 1998). In addition, a few studies have suggested that the coccoid form formation (CFF) involves

partial degradation of the peptidoglycan (PG) of the cells (Moran and Upton, 1986; Amano and Shibata, 1992).

Campylobacter species grow optimally at temperatures between 37°C and 42°C under microaerobic conditions (5% O₂, 10% CO₂, and 85% N₂). Experiments have revealed significant retardation in the growth of cells at temperatures below 30°C (Doyle and Roman, 1981; Hazeleger *et al.*, 1998; Tangwatcharin *et al.*, 2006). Hudock *et al.* (2005) compared CFF rates of two *C. jejuni* strains at 37°C, 25°C, and 4°C, respectively. The authors demonstrated that the most of the cells transformed into CF within 96 h at temperatures of 25°C and 37°C, while only 7.1% of cells became coccoidal after 14 days' incubation at 4°C.

Campylobacter species are typically microaerophilic microorganisms and exposure to oxygen levels and reactive oxygen species (ROS) such as superoxides and hydrogen peroxides increases the rate of CFF. A study by Lee *et al.* (2005) demonstrated the morphological transition of two *C. jejuni* strains into CFF when exposed to aerobic conditions for 48 h. Harvey and Leech (1998) deduced similar results in their research. In general, bacteria should be able to neutralize these ROS species with the help of enzymes, which aid in inactivation of these toxic compounds (Bronowski *et al.*, 2014; Harvey and Leach, 1998). On another note, *C. jejuni* have the capability to grow under aerobic conditions due to the inclusion of an oxygen scavenger such as blood to the growth media. These compounds counteract the effects of oxygen toxic products (Hazeleger *et al.*, 1998; Humphrey, 1990).

C. jejuni cultures grow optimally between pH 6.5 and 7.5, although growth is observed even at pH 5.5 and pH 8.0 (Doyle and Roman, 1981). *Campylobacter* species are exposed to different pH ranging from pH 2 to pH 6 during colonization of a human host, when exposed to inorganic acids in the stomach to organic acids in the small intestine (Rao *et al.*, 2004; Birk *et al.*, 2012). *Campylobacter* species are more sensitive to acidic stress when compared to other

Gram-negative bacteria, perhaps due to the absence of acid resistance systems and global stress regulators otherwise found in other bacteria (Birk *et al.*, 2012).

Campylobacter cells enter a stationary or starvation state when the availability of nutrients becomes limited. As the cells transition from the exponential growth stage to the stationary stage, morphological transition into CF where the cells exist as viable but non-culturable (VBNC) forms, occurs (Ng *et al.*, 1985). The cells in the VBNC forms have slower rates of growth with low metabolic activity and possess the ability to produce degradative enzymes (Klancnik *et al.*, 2006; Klancnik *et al.*, 2009).

The bacterial cell wall, which maintains the integrity and shape of the cell, serves as the cell's most important structural part. It comprises a macromolecular structure generally known as PG or murein (Schleifer and Kandler, 1972). PG is a heteropolymer consisting of glycan strands and short peptide molecules cross-linked within the structure (Ikeda and Karlyshev, 2012). Ng *et al.* (1985) studied the spiral form and CF of *C. jejuni* under an electron microscope and discovered that cells within the same colony possessed different shapes. They observed a new ring-like or doughnut shape, presumed to be the intermediate stage before CF. In addition, cells in the centre appeared to transition into CF when compared to the cells on the periphery. The authors concluded that the lower level of nutrients available in the centre could be responsible for this observed difference. Overall, the cell wall gradually degenerates during the transition process, thus implying PG degradation. In the study by Amano and Shibata (1992), the authors reported isolation of more PG from active spiral forms than in CF. In summary, evidence from previous studies suggests that the cell wall gradually degrades during the transition process, thus potentially indicating the role of PG in CF.

In the closely related bacterium *Helicobacter pylori*, *amiA* was identified as the first genetic determinant responsible for the morphological transition. *amiA* encodes a putative PG

hydrolase (Chaput *et al.*, 2006). Costa *et al.* (1999) revealed that a considerable change in the muropeptide composition occurred during the morphological transition process in *H. pylori*. Chaput *et al.* (2006) demonstrated an accumulation of N-acetyl-D- glucosaminyl (1,4)-N-acetylmuramoyl-L-Ala–D-Glu, also known as GM-dipeptide, during the transition, which led to the formation of a looser macromolecule due to the lack of PG transpeptidation. Chaput *et al.* (2006) proposed that *amiA* mutant weakened GM-dipeptide motif accumulation; thereby hindering the formation of CF. The authors concluded that morphological transition from bacillary to CF resulted from a partial degradation of PG, which is regulated by *amiA*. Due to the genetic and biochemical similarities between *H. pylori* and *Campylobacter*, an attempt to inactivate this gene in *Campylobacter* was carried out in a previous study (Ikeda, 2014). The attempt was rendered unsuccessful due to the presence of just one copy of an *amiA*-like gene in *C. jejuni* in contrast to *H. pylori*, indicating its role as an essential gene. For this purpose, a gene expression system in *Campylobacter* is necessary, which would permit the construction of conditionally lethal mutants. The P_{BAD} promoter of the arabinose operon, which has also been recognized as an efficient system in the study of essential genes, provides tight regulation of a cloned gene (Guzman *et al.*, 1999). In this study, the utilization of the P_{BAD} promoter will be studied in *Campylobacter* for the first time. The results of the study will benefit researchers who are interested in developing novel molecular biology tools and antimicrobial agents to fight resistant bacteria.

1.7 Viable but non-culturable state of *Campylobacter*

The VBNC state of *C. jejuni* cells was first discovered by Rollins and Cowell (1986). VBNC cells retain metabolic activity but cannot be cultured on laboratory media (Rollins and Colwell, 1986). The cells undergo major metabolic changes such as reduction in ATP synthesis, nutrients transport, and macromolecular synthesis (Oliver, 2005). Studies examining the resuscitation of the VBNC cells into culturable and thus infectious forms sometimes contradict

each other. A few studies have demonstrated colonization in mice and chicks by *C. jejuni* VBNC cells (Jones *et al.*, 1991; Cappelier *et al.*, 1999; Stern *et al.*, 1994; Pearson *et al.*, 1993), whereas the authors of other studies have failed to report similar findings (Beumer *et al.*, 1992; Medema *et al.*, 1992).

The variation in results could occur due to difference in the strains, varying environmental conditions used to induce VBNC cells, and methods used to analyse non-culturability. In addition, researchers have demonstrated that the *C. jejuni* VBNC cells can be resuscitated into culturable forms with acid treatment (Cappelier *et al.*, 2000; Chaveerach *et al.*, 2003). Wolf and Oliver (1992) demonstrated that *V. vulnificus* could be resuscitated into culturable forms *in vitro*, *in vivo*, and *in situ*, by simply by increasing the temperature. Similarly, another study indicated that VBNC *V. vulnificus* cells administered to mice led to their death (Oliver, 2005). In addition, *Enterococcus faecalis* VBNC cells displayed the ability to adhere to the cultured heart and epithelial cells of the urinary tract (Pruzzo *et al.*, 2002).

1.8 Inducible gene expression systems

In molecular biology, a regulated system is required for the investigation of essential genes, as it permits the study of conditionally lethal mutants. In addition, such systems also provide flexibility in the rapid turn off and on of the cloned gene (Huang *et al.*, 2011). Uncontrollable expression of genes can sometimes become toxic, leading to undesirable effects such as cell death and growth inhibition (Sukchawalit *et al.*, 1999). Regulated expression can also address issues such as inclusion body formation and outgrowth of segregants that may otherwise occur with uncontrollable expression (Baig *et al.*, 2014; Baneyx and Mujacic, 2004; Beisel and Afroz, 2016; Hartley and Kane, 1991; Marschall *et al.*, 2016). An efficient regulatable expression system should comprise a non-toxic, cheap, and exogenous inducer and offer a wide range of gene regulation with little to no basal expression (Zhang *et al.*, 2015; Zhang *et al.*,

2012).

Several studies exist examining different regulatable expression systems consisting of the following promoters: P_{LAC} (Yanisch-Perron *et al.*, 1985); P_{TAC} (Deboer *et al.*, 1983); P_L and P_R (Elvin *et al.*, 1990); and P_{TRC} (Brosius *et al.*, 1985). The most widely known and extensively used inducible gene expression systems are the lactose-inducible *lac* system, studied by Novick and Weiner (1957), and the arabinose-inducible *ara* system developed by Guzman *et al.* (1995). Both systems display the ‘all or nothing’ or ‘autocatalytic’ induction phenomenon at subsaturating levels of inducer concentrations (Fritz *et al.*, 2014).

The arabinose-inducible system is widely used in *Escherichia coli* and many other bacteria (Newman and Fuqua, 1999; Zhang *et al.*, 2012). The *ara* system is favoured over the *lac* system, because repression is often incomplete in the latter due to leaky promoters and the absence of secondary operators to maintain a full range of regulation. Conversely, the *ara* system efficiently provides a switch-like mechanism where a cloned gene can be efficiently turned on or off simply by changing the sugars in the medium (Siegele and Hu, 1997). The *ara* system provides tight regulation of the cloned gene under study, with a very low level of background expression in the absence of an inducer and high levels of expression in the presence of an inducer (Guzman *et al.*, 1995).

The *ara* system comprises the AraC protein, *araBAD* catabolic genes (Englesberg *et al.*, 1969), *araJ*, initiator and operator sites. The function of *araJ* remains unknown (Reeder and Schleif, 1991). The *araBAD* genes encode proteins that convert arabinose into D-xylose-5-phosphate, which is the final product that enters the pentose phosphate pathway (Schleif, 2010). The AraC protein acts as a positive and negative regulator, which represses its own synthesis and positively regulates the expression of the downstream genes in the presence of arabinose (Khlebnikov *et al.*, 2000). The *ara* operon undergoes carbon catabolic repression (CCR), and

this process largely depends on the type of sugar present in the medium. In the presence of glucose, reduced levels of expression are obtained as glucose lowers the cyclic AMP in the medium, which is required for RNA polymerase binding (Guzman *et al.*, 1995; Ogden *et al.*, 1980).

In the *ara* operon, arabinose is the true inducer, which does not require the activation of other enzymes in the catabolic pathway for induction to take place, unlike the *lac* operon (Englesberg *et al.*, 1969; Schleif, 2010). When the concentration of arabinose reaches above a certain threshold, arabinose-AraC complex binds to the initiator half sites (*araI*₁ and *araI*₂), followed by the binding of the CRP-cAMP complex to its binding site adjacent to the initiator site. This binding allows RNA polymerase to bind to the promoter site and initiate transcription of the transporter and the catabolism genes (Figure 4b) (Megerle *et al.*, 2008). Under normal conditions, arabinose is transported into the cells by arabinose permeases, which are encoded by the high-affinity transporter *araFGH* and the low-affinity transporter *araE* (Khlebnikov *et al.*, 2001; Megerle *et al.*, 2008). AraE is located on the inner membrane and transports arabinose into the cells by diffusion, and *araFGH* codes for a high-affinity ABC transporter (Lee *et al.*, 1981; Schleif, 2010). Daruwalla *et al.* (1981) suggested that AraE is the more prevalent transporter, as the growth rates and arabinose carbon cell yields obtained were lower in AraE⁻ than AraF⁻ strains. On the other hand, in the absence of arabinose, the AraC protein tends to bind to the initiator half site (*araI*₁) and also the operator site (*araO*₂) upstream of the P_{BAD} promoter region, leading to the formation of a DNA loop, preventing the binding of RNA polymerase and resulting in the repression of the *ara* genes (Figure 4a) (Newman and Fuqua, 1999; Schleif, 2010).

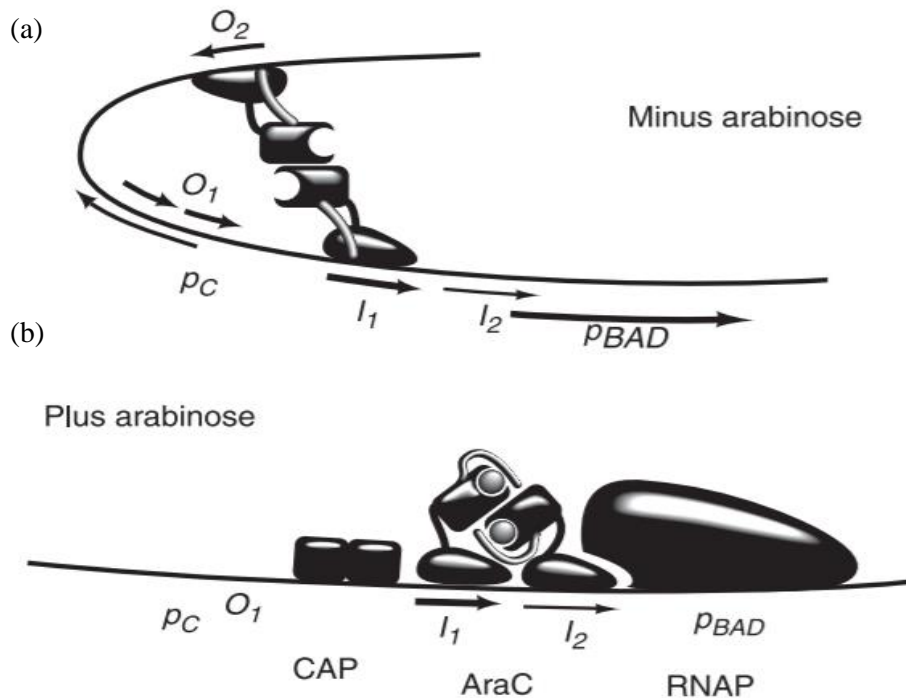


Figure 4. Positive and negative regulation of the *ara* operon in *E. coli* (Schleif, 2010).

(a) Negative regulation. In the absence of arabinose, it is not energetically favourable for AraC to bind to the initiator half sites *araI*₁ and *araI*₂. Therefore, each arm of the dimeric AraC binds to the non-adjacent half-sites *araI*₁ and *araO*₂, resulting in the formation of a DNA loop. The DNA loop provides steric hindrance for the binding of RNA polymerase, thereby suppressing transcription from the P_{BAD} promoter.

(b) Positive regulation. In the presence of arabinose, AraC undergoes conformational change and arabinose binds to the dimerization domain of the protein. AraC-arabinose complex binds to the initiator half-sites (*araI*₁ and *araI*₂), as it is the energetically favourable state; subsequently, the CRP-cAMP complex binds to its site, resulting in linear DNA in which RNA polymerase binds to the promoter site, thereby driving transcription from the P_{BAD} promoter site (Schleif, 2010).

1.9 Autocatalytic gene expression system

Autocatalytic gene expression occurs when the gene encoding the inducer transporter is controlled by the concentration of the inducer molecules present inside the cell itself. This phenomenon in the *ara* operon was established and confirmed by Siegele and Hu (1997), who studied population distributions at subsaturating levels of the inducer. Autocatalytic gene

expression was also observed in a few other noted works, where the authors deduced that at subsaturating concentrations of the inducer, the cells displayed heterogeneous expression where some cells were fully induced, while the remainder were uninduced or had little induction. During this time, the rate of induction was also reported to be directly proportional to the amount of inducer molecules present inside the cells (Khlebnikov *et al.*, 2000; Megerle *et al.*, 2008). Additionally, further induction occurs when the cells with sufficient inducer molecules are induced at the time of induction, which in turn activates the production of more inducer molecules, allowing for increased arabinose transportation (Morgan-Kiss *et al.*, 2002). Studies have revealed that the all-or-nothing response could also occur due to the depletion of arabinose, as a result of the metabolism of the already induced cells (Megerle *et al.*, 2008).

Several studies that describe the utilization of the arabinose-inducible system in other bacteria have been conducted, but an investigation of the system in *Campylobacter* does not exist, mainly due to the lack of arabinose transportation in these bacteria. The genes that encode arabinose transporters are not present within the *C. jejuni* genome. Unlike *E. coli*, the preferable source of energy is not glucose and other carbohydrates; instead, *C. jejuni* utilizes amino acids and other small organic acids as a source of carbon and energy (Line *et al.*, 2010; Parkhill *et al.*, 2000; Weingarten *et al.*, 2009). As mentioned above, arabinose in *E. coli* is transported via arabinose permeases via an autocatalytic induction process. Khlebnikov *et al.* (2000) were the first to provide a breakthrough study that could overcome the issues associated with the autocatalytic process in the *ara* operon. In their study, the *araE* gene was placed under the control of a different promoter independent of the arabinose concentration in the medium. The system was coupled and validated using a reporter gene (*gfp*) placed under the control of a P_{BAD} promoter (arabinose-dependent), while the expression of the transporter gene was independent of the expression of the reporter gene in *E. coli* (Khlebnikov *et al.*, 2000; Khlebnikov *et al.*, 2001). In another study, Morgan-Kiss *et al.* (2002) demonstrated the utilization of another

transporter for arabinose uptake in *E. coli*. They concluded that arabinose was transported into *E. coli* with the help of a modified *lacY* gene and the authors reported homogenous expression of the reporter *gfp* gene (Morgan-Kiss *et al.*, 2002).

1.10 Bacterial biofilms

Bacteria exist in the natural environment as multicellular communities known as biofilms; over 99% of bacteria can form biofilms (Houry *et al.*, 2010; Liaqat *et al.*, 2018). Bacterial biofilm formation takes place either as a defense mechanism or when the bacteria sense a favourable habitat (Jefferson, 2004). Biofilms are classified as mono-species or multi-species consortia of bacterial cells that attach to one another in a self-produced polymeric matrix and adhere to inert or living surfaces (Li *et al.*, 2017). Multi-species biofilms often tend to possess larger amounts of extracellular polymeric substances than mono-species biofilms (Feng *et al.*, 2016). Biofilm formation depends on several factors, such as nutrient availability, pH, temperature, oxygen availability, osmotic pressure, surface topography, the presence of organic and inorganic compounds, and the presence of antimicrobials (Rossi *et al.*, 2017). Biofilms can usually form on different types of surfaces, such as glass (Brown *et al.*, 2015a; Brown *et al.*, 2015b; Dykes *et al.*, 2003), stainless steel (Gunther *et al.*, 2009; Hanning *et al.*, 2008; Sanders *et al.*, 2007), plastics (Lim and Kim, 2017; Reeser *et al.*, 2007), and nitrocellulose membranes (Kalmokoff *et al.*, 2006). Biofilms that form on food contact surfaces in food-processing environments are regarded as a significant risk factor (Li *et al.*, 2017). Biofilms can result in economic loss in the food industries due to food spoilage, bio-corrosion on equipment used in food production, and loss of operating time (Rossi *et al.*, 2017). In addition, biofilm formation on the surfaces of heat exchangers leads to biofouling, which can cost many industries, such as paper, oil and gas, and polymer production, financially (Liaqat *et al.*, 2018). Infections due to biofilms that form on medical equipment such as catheters, cardiac pacemakers, contact lenses, dentures, and prosthetic heart valves are responsible for over 50% of nosocomial infections (Roy *et al.*,

2018).

The chief component of biofilms is the extracellular polymeric matrix (EPM), which ensures cohesion between the cells, maintains the shape of the overall biofilm structure, and protects the cells from external factors (Brown *et al.*, 2014; Steichen *et al.*, 2011). The EPM mainly comprises polysaccharides, nucleic acids, lipids, and proteins (Brown *et al.*, 2014; Brown *et al.*, 2015b; Feng *et al.*, 2016). Bacteria existing in biofilms exhibit improved survival ability; protection against phagocytosis (host defence system); and resistance to antimicrobial treatment, metal toxicity, acids, fluid shear (blood flow and action of saliva), and cleaning procedures (Costerton *et al.*, 1999; Kim *et al.*, 2015; Teh *et al.*, 2014). In addition, gene transfer between different species in a biofilm can occur, increasing the risk of more virulent strains (Satpathy *et al.*, 2016; Lewis, 2001). Cells in a biofilm matrix are more than 1000 times more resistant to antimicrobials and disinfectants (Fux *et al.*, 2005; Reuter *et al.*, 2010).

1.11 Formation of bacterial biofilms

Biofilm formation involves four steps: initiation; proliferation; maturation; and dispersion (Figure 5) (Li *et al.*, 2017; Sulaeman *et al.*, 2010).

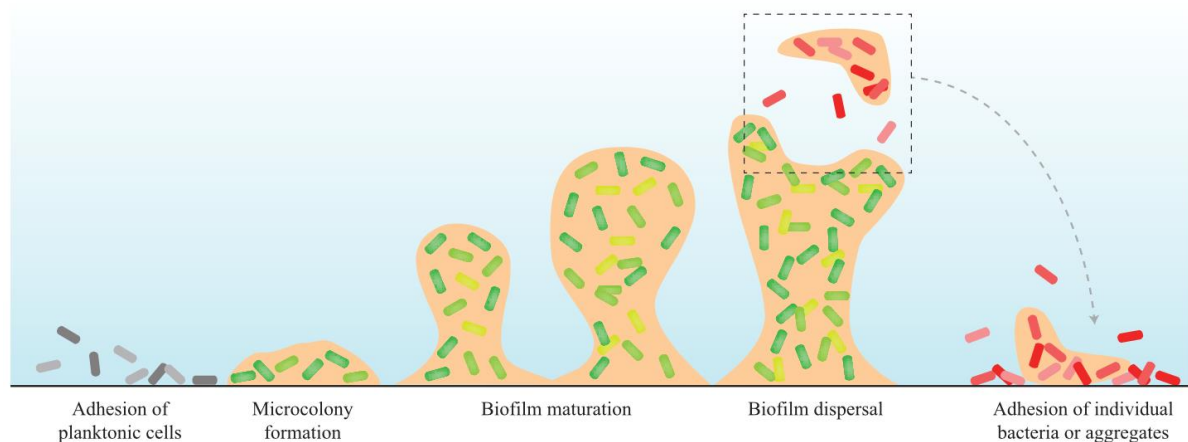


Figure 5. Schematic illustration of biofilm development (Guilhen *et al.*, 2017).

The figure depicts the stages involved in biofilm formation; initial attachment of planktonic cells to the surface, formation of sessile cells, followed by the formation of a mature biofilm structure, and then finally dispersion of the cells from the biofilm matrix.

1.11.1 Initiation step

1.11.1.1 Surface sensing and the role of flagella

Bacteria move via passive transport (assisted by flow of media), diffusive transport (assisted by Brownian motion), or active transport (assisted by flagella) (Lejeune, 2003). Surface sensing is an important mechanism responsible for motility. Motility allows the bacteria to reach their target surface or organ with the aid of surface appendages such as flagella. Surface sensing by bacteria is mediated by chemotaxis (Cheng *et al.*, 2019); organic substrates such as blood, urine, and saliva, which usually constitute the conditioning film layering the substratum surface, act as chemoattractants (Bos *et al.*, 1999; Garrett *et al.*, 2008). Flagella-mediated motility via the chemotaxis pathway is dependent on the varying gradients of chemoattractants/chemorepellants, and determines the direction of the flagella rotation (Suchanek, 2017). The cells swim in a clockwise (forward) or anti-clockwise motion (tumbles) towards a surface in response to these stimuli. The movement of motile cells in response to chemotaxis can result in the establishment of a new biofilm on a surface or provide planktonic

cells to an already established biofilm (Suchanek, 2017). Flagella are several times the length of the cell and can enter the gaps and crevices in difficult surfaces (Haiko and Westerlund-Wikström, 2013; Houry *et al.*, 2010). In addition to motility, flagella aid in overcoming the repulsive forces between the surface and the bacteria in preparation for adhesion (Garrett *et al.*, 2008; Liaquat *et al.*, 2018).

1.11.1.2 Initial attachment

The initiation step is the first stage of biofilm formation and is expected to occur within the first few hours (Sulaeman *et al.*, 2010). The initial attachment of the bacterial cells to the surface is a reversible step, which is generally facilitated by the pili or flagella of the bacteria (Armbruster *et al.*, 2018; Pratt and Kolter, 1998). In motile strains, the flagellum consists of thousands of subunits (flagellins) arranged in a filament with a flagella cap protein at the end (Freitag *et al.*, 2016). This cap adheres to the surface and helps in overcoming the electrostatic barrier (Tuson and Weibel, 2013). Furthermore, during the initial attachment stage, the attraction between the surface and the adhering bacteria increases further when the surface-attached flagella collapses, thereby ensuring a larger contact area is available for adhesion (Carniello *et al.*, 2018; McClaine and Ford, 2002). This initial attachment is mainly governed by weak Van der Waals forces, hydrophobic interactions, and electrostatic forces, so the cells can be easily removed by cleaning procedures during this stage (Kumar *et al.*, 2017; Rossi *et al.*, 2017). Conversely, non-motile bacteria also possess the ability to form biofilms at low- and medium-fluid velocities. At high-fluid velocities, the cells do not attach as they are transported with the flow (Tuson and Weibel, 2013). In non-motile strains, other surface structures, such as CPS and type IV pili, aid in the initial attachment process of biofilm formation (Brooks and Mias, 2018). During the subsequent irreversible stage, the attachment is strengthened due to the production of exopolymers, adhesins, and extracellular DNA by the adhered cells. During this stage, stronger bonds exist, such as hydrogen, covalent, and dipole-dipole interactions

(Rossi *et al.*, 2017).

1.11.2 Proliferation step

The proliferation stage involves the formation of microcolonies following stable attachment of the cells to the surface. During this stage, quorum sensing (QS) is activated and communication between cells in the bacterial community occurs through chemical signalling, which in turn promotes the formation of sessile cells (Rossi *et al.*, 2017).

1.11.3 Maturation step

During the maturation stage, the microbial cells are encased in a more structured matrix with greater cell density, and the cells communicate through cell-to-cell signalling (Jamal *et al.*, 2018; Srey *et al.*, 2013). QS between the colonies of the bacterial biofilm induces the expression of genes that favour the production of extracellular polymeric substances. In a study describing DNA microarray analysis of mature *Pseudomonas* biofilms, nearly 70 genes with varying functions showed differential expression during this stage (Whiteley *et al.*, 2001). The communication between the microbial cells is crucial, as it triggers the exchange of substrates, transportation of metabolic products, and excretion of metabolic end products (Srey *et al.*, 2013; Rossi *et al.*, 2017). The EPM consists of open water channels, which aid in the circulation of nutrients to the sessile cells and the removal of waste products.

1.11.4 Dispersal step

The dispersal step is an important phase of the biofilm process, as it involves the release of cells from the original site of infection into the environment or host (Guilhen *et al.*, 2017). Dispersion can occur as a result of cell death, increased shear forces, enzymatic production, nutrient availability, predator grazing, or other stress-inducing factors (Kaplan and Fine, 2002; Kostakioti *et al.*, 2013; Sauer *et al.*, 2004). In comparison to their sessile counterparts, the dispersed cells that exit the biofilm matrix either die or possess increased metabolism (Pettigrew

et al., 2014). These cells also possess greater colonising traits, such as increased ability to invade epithelial cells (Marks *et al.*, 2013) and to escape phagocytosis (Chua *et al.*, 2014; Guilhen *et al.*, 2017). Previous studies have deduced that dispersed cells have a different transcriptome and virulence profiles than sessile or planktonic cells. Guilhen *et al.* (2016) demonstrated that dispersed cells of *Klebsiella pneumonia* overexpressed genes (such as *truB*, *yebE*, *pspB*, *pspA*, *cusA*, *envR*, and *ytdD*) involved in translation, implying that these cells were more metabolically active than the cells within the biofilm. Similarly, subsequent studies have observed an overexpression of genes involved in virulence. Marks *et al.* (2013) demonstrated that dispersed cells of *Streptococcus pneumonia* possessed a greater capacity to invade epithelial cells as a result of overexpression of virulence genes than did either planktonic or sessile cells. In another study, the authors established that dispersed *Pneumococcal* cells caused bacteremia in murine models, whereas sessile and planktonic cells failed, demonstrating the virulence and pathogenicity of the dispersed cells (Pettigrew *et al.*, 2014).

1.12 *C. jejuni* biofilms

Biofilm-related infections contribute to more than 75% of microbial diseases in humans (Guilhen *et al.*, 2017). *C. jejuni* biofilms are generally found in food-processing plants and equipment (mainly poultry processing), water supply, and plumbing systems at animal husbandry facilities (Teh *et al.*, 2014; Feng *et al.*, 2016; Hermans *et al.*, 2011; Siringan *et al.*, 2011; Trachoo *et al.*, 2002). A recent study by Balogu *et al.* (2014) discovered that the frequent human–carcass interactions during packaging and relatively poor sanitary conditions in the chicken-processing industries often promote biofilm formation and the subsequent persistence of these bacteria. This study also found *C. jejuni* appeared most frequently in the packaging line and dressing table in poultry facilities. The continual presence of organic substances such as proteins, which increase the chances of *C. jejuni* survival and attachment to food contact surfaces due to increased nutrient availability, poses a major problem in the chicken-processing

industries (Rossi *et al.*, 2017; Melo *et al.*, 2017). In addition, researchers have confirmed the persistence of *C. jejuni* in environmental water, such as ground, river, and drinking water (Ica *et al.*, 2012; Culotti and Packman, 2015). Contamination of environmental water could occur for several reasons: wastewater from poultry industries; defecation of farm animals; and the subsequent spread of these bacteria by flies and rodents (Bronowski *et al.*, 2014).

Campylobacter species are microaerophiles capable of surviving the harsh stress conditions often present in the environment (Bronnec *et al.*, 2016; Sulaeman *et al.*, 2010). Although how *C. jejuni* survives in these challenging environments is unknown, the formation of biofilms might serve as an adaption method to prolong survival (Bronnec *et al.*, 2016; Sulaeman *et al.*, 2010; Teh *et al.*, 2014). In addition, the ability of *C. jejuni* to form mono-species biofilms and co-exist with other bacterial biofilms may explain the prevalence of these bacteria in the environment as well as their ability to cause infections in humans (Teh *et al.*, 2019; Bronnec *et al.*, 2016).

Ica *et al.* (2012) investigated the survival capability of *C. jejuni* in mono- and mixed-species biofilms and deduced that these bacteria possessed greater survival and biofilm-forming capabilities in multi-species biofilms in the presence of *Pseudomonas aeruginosa* than mono-species biofilms. *P. aeruginosa* creates favourable conditions for the survival of *C. jejuni*, resulting in a comparatively robust biofilm. Through LIVE/DEAD staining, researchers have demonstrated that *C. jejuni* cells in multi-species biofilm maintain culturability for longer periods of time than the cells in the mono-species biofilm that transition into VBNC forms more quickly (Bronowski *et al.*, 2014; Ica *et al.*, 2012). Culotti and Packman (2015) reported similar conclusions, finding a reduction of dissolved oxygen from 9 mg/L to 0.6 mg/L by *P. aeruginosa*, which generated a more suitable environment for *C. jejuni*'s survival. *P. aeruginosa* are present everywhere in the environment and are regarded as excellent biofilm

formers. They have the ability to readily form mono-species biofilms on any carbon surface and are followed by the production of a strong EPM, which acts as a recruiter of other bacteria, eventually leading to a multi-species biofilm structure (Bronowski *et al.*, 2014; Ica *et al.*, 2012; Trachoo *et al.*, 2002; Sanders *et al.*, 2007). In addition, multi-species biofilms provide *C. jejuni* with greater availability of nutrients and secondary metabolites for longer survival. Other factors such as higher temperatures and longer contact times increase the degree of initial attachment and decrease the probability of detachment in *Campylobacter* biofilms (Nguyen *et al.*, 2012; Nguyen *et al.*, 2010).

In *Campylobacter*, the initial adhesion process is mediated by flagella in conjunction with other adhesins (Svensson *et al.*, 2014). Previous studies investigating the role of flagella in *E. coli*, *Clostridium* and *P. aeruginosa* have all demonstrated that flagella play a vital role in biofilm initiation by providing movement as well as acting as an attachment factor (Ren *et al.*, 2018; Freitag *et al.*, 2016). Similarly, some studies examining *Campylobacter* have revealed a similar function of the flagella with respect to surface interactions (Bridier *et al.*, 2015). Over 50 flagella-related genes with diverse functions are present in *Campylobacter* (Ren *et al.*, 2018). Ren *et al.* (2018) investigated the effects of inactivating the *flhF* gene (encoding the flagellar biosynthesis regulator) on the colonizing properties of *C. jejuni*. The mutation revealed decreased colonizing ability due to reduced adhesive and invasive capabilities. A study by Freitag *et al.* (2016) investigated the flagella cap protein FliD for its adhesive capabilities. This study indicated that the protein acts as an adhesin and binds to host-cell glycosaminoglycans, confirming its importance in the initial attachment of the *C. jejuni* cells. Furthermore, Joshua *et al.* (2006) have demonstrated that *maf5* (flagella) mutant exhibited reduced levels of attachment during the early stages of *C. jejuni* biofilm formation. Kim *et al.* (2015) demonstrated *flgA* is involved in the flagellar biosynthesis as well as biofilm formation in *C. jejuni*. In another study, Lim and Kim (2017) posited that the absence of the *eptC* gene (flagellar

biosynthesis) altered the initial adherence pattern of *C. jejuni* biofilms, suggesting that the gene plays a role in the biofilm initiation process. In addition, Reuter *et al.* (2010) demonstrated that the motile variant of *C. jejuni* NCTC 11168 formed 50% more effective biofilms than the non-motile or the *flaAB* mutant strains under microaerobic conditions.

C. jejuni can form three types of biofilm in a liquid culture: (1) flocs-cell aggregates suspended in the liquid; (2) cells attached to an inert surface; and (3) pellicles-cell aggregates formed at the air-liquid interface (Bronnec *et al.*, 2016; Joshua *et al.*, 2006). *C. jejuni* biofilms are extremely resistant to antimicrobial treatment and cleaning procedures. The *C. jejuni* cells in a biofilm are able to withstand oxygen and lower-temperature stress twice as well as their planktonic cells and also exist as VBNC forms (Magajna and Schraft, 2015).

1.12.1 Importance of Quorum sensing

QS is a mechanism adapted by many bacteria for cell communication through small, diffusible signalling molecules known as autoinducers (Vendeville *et al.*, 2005). These molecules enable cell-density-dependent gene regulation (Gözl *et al.*, 2012). Autoinducer molecules are utilized and recognized by both Gram-negative and Gram-positive bacteria for gene regulation involved in survival and pathogenesis. Autoinducer-1 (AI-1) molecules mediate intraspecies-specific communication in Gram-negative bacteria, while small oligopeptides are responsible for these communications in Gram-positive bacteria. AI-2 molecules mediate intra- and interspecies communication in both Gram-negative and Gram-positive bacteria (Gözl *et al.*, 2012). The most typical AI-1 molecule in Gram-negative bacteria is acyl homoserine lactones (HSL) (Moorhead and Griffiths, 2011). These molecules are produced by the LuxI enzyme and can freely diffuse into the cytoplasm. As the cell density increases, the concentration of AI-1 increases. After a certain threshold of intracellular concentration is achieved, the molecules bind to LuxR, thereby activating the LuxR/AI-1 cellular transcriptional-activator system for

the expression of other genes (Plummer, 2012; Gözl *et al.*, 2012). Similar orthologues of *luxI/luxR* genes are identified in about 70 Gram-negative species, such as *P. aeruginosa*, *Salmonella*, and *Agrobacterium tumefaciens*, although not *H. pylori* (Gözl *et al.*, 2012). Genome sequence analysis of *C. jejuni* does not reveal any obvious homologues of genes encoding an AI-1 synthase (Parkhill *et al.*, 2000). However, Moorhead and Griffiths (2011) have identified an N-(3-hydroxy-butanoyl)-L-HSL in cell-free extracts of *C. jejuni* 81-176 and cj11, labelling this HSL mimic as CjA. They reported that this HSL mimic increased IL-8 production, inhibited biofilm formation, and regulated virulence gene expression.

The production of AI-2 was first discovered in *Vibrio harveyi* using bioluminescence assays. In brief, the LuxS enzyme produces AI-2 molecules that in turn bind to the LuxP protein after reaching a certain threshold, activating the LuxQ inner-membrane protein. This event triggers the dephosphorylation of the response regulator LuxO, which in turn alters gene expression (Plummer, 2012; Gözl *et al.*, 2012). In other bacteria, such as *Salmonella* and *E. coli*, AI-2 molecules bind to LsrB, which belongs to the ABC transporter; the molecules are transported through the same system into the cell wall, where they undergo phosphorylation and regulate gene expression of other target genes through the LsrR transcriptional-repressor (Plummer, 2012; Gözl *et al.*, 2012). A simple illustration of gene expression via QS is shown in Figure 6.

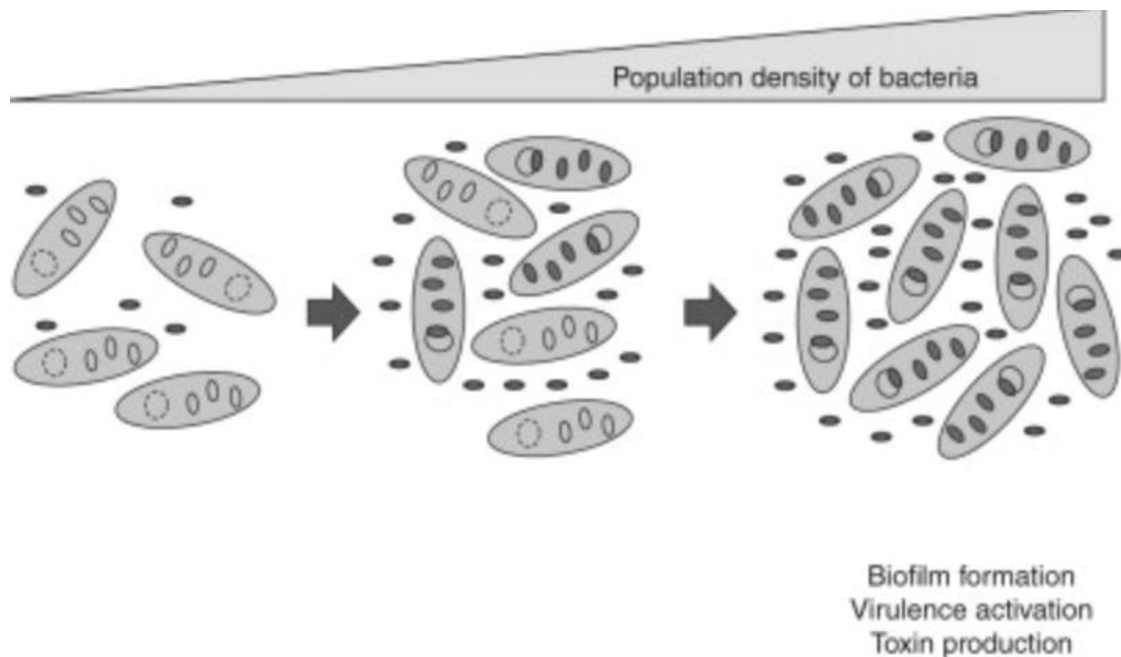


Figure 6. Schematic representation of QS (Goulden *et al.*, 2013).

The concentration of autoinducer molecules is lesser at low cell densities for the activation of the receptor protein and induction of QS regulated gene expression. As the cell density increases (as shown from left to right), the number of autoinducer molecules increases, which then binds to receptors triggering an up-regulation of genes involved in virulence, biofilm formation, and toxin production.

Elvers and Park (2002) analysed the sequence of *C. jejuni* NCTC 11168, becoming the first to identify the protein Cj1198, which shares over 70% sequence identity with LuxS from *V. harveyi*, *E. coli*, and *Haemophilus influenzae*. They demonstrated that *C. jejuni* produces AI-2, using bioluminescence assays conducted on cell-free extracts with *V. harveyi* as a positive control. In addition, the authors showed that the *cj1198* mutant had lower motility than the wild-type strain, suggesting that QS is essential for motility. Furthermore, Quinones *et al.* (2009) demonstrated that AI-2 molecules were produced in *Campylobacter* during the late exponential phase, observing slow degradation during the early stationary phase. The uptake or sensing mechanism of AI-2 by *Campylobacter* is not fully understood yet, since comparative genomic studies have revealed the absence of Lsr homologs (Plummer, 2012).

Furthermore, researchers have investigated the role of the *luxS* gene in adhesion and invasion. Quinones *et al.* (2009) demonstrated that the *C. jejuni* 81176/*luxS* mutant possessed less

adhesive and invasive ability than the wild-type strain. In the same study, the authors showed that the mutant displayed lower chemotactic response to organic acids and increased response in the presence of amino acids. In addition, the role of *luxS* and QS in cytotoxin production has also been investigated. Jeon *et al.* (2005) revealed that fewer cells were affected during the G2/M phase, and a 39% decrease in *cdt* gene expression with the mutant was observed. Similarly, QS also plays a major role in *C. jejuni* biofilms and is known to govern biofilm processes such as sessile cells formation, expression of virulent genes, and animal colonization (Plummer, 2012; Rossi *et al.*, 2017; Lamas *et al.*, 2018). The QS mechanism enables cell-to-cell communication between species and regulates biofilm formation through the alteration of specific gene expression. These communications enable bacterial cells to produce thicker and stronger biofilms in the exponential stage (Plummer, 2012). A study by Reeser *et al.* (2007) revealed a reduction in biofilm formation of *C. jejuni* M129 as compared with the wild-type strain, due to a mutation in the *luxS* gene. The studies mentioned above provide sufficient evidence to suggest that QS via *luxS* in *Campylobacter* plays a vital role in *C. jejuni* virulence and survival mechanisms.

1.12.2 Importance of extracellular DNA and the role of extracellular nucleases in biofilm

eDNA serves as a nutrient source and aids in horizontal gene transfer between bacterial cells in a biofilm (Ibáñez de Aldecoa *et al.*, 2017). It is secreted by live cells or enters the medium by lysed cells (Hamilton *et al.*, 2005; Tetz *et al.*, 2009; Wu and Xi, 2009). A mutation in *gelE*, gene encoding a secreted protease (responsible for autolysis) led to reduced accumulation of biofilms in *E. faecalis* due to the lack of eDNA release, which is a key component of the EPM (Thomas *et al.*, 2008). In a similar study by Qin *et al.* (2007), a mutation in *AtlE* (an autolysin) inhibited biofilm formation in *Staphylococcus epidermis* due to the lack of eDNA accumulation required for biofilm formation. In *Campylobacter* biofilms, eDNA release occurs in a process

called autolysis (Svensson *et al.*, 2014; Ibáñez de Aldecoa *et al.*, 2017). In most bacterial biofilms, QS regulates eDNA synthesis and release (Ibáñez de Aldecoa *et al.*, 2017).

Furthermore, eDNA is considered as an integral component in *C. jejuni* biofilms, as it provides structural strength to the biofilm matrix (Brown *et al.*, 2015b). It also plays a similar structural role in other bacteria, such as *P. aeruginosa*, *E. coli*, and *Staphylococcus aureus* (Chiang *et al.*, 2013; Mann *et al.*, 2009; Zhao *et al.*, 2013). The link between eDNA and the structure of the bacterial biofilms was first studied in *P. aeruginosa* by Whitchurch *et al.* (2002). The authors demonstrated complete disintegration of the biofilm consisting of eDNA in the presence of the DNase I enzyme, confirming the necessity of eDNA in maintaining the biofilm structure. Svensson *et al.* (2014) revealed that eDNA is vital for biofilm formation and maintenance in *C. jejuni* 81-176. Brown *et al.* (2015a) demonstrated that eDNA plays an important role during all stages of biofilm maturation in *C. jejuni* strains NCTC 11168 and 81116. In the same study, the authors also established that pre-treating surfaces with this enzyme prevented biofilm formation. DNases play a vital role in biofilm dispersion as they are responsible for breaking down eDNA. Dispersal of biofilms can be achieved by either exogenous addition of extracellular DNase (eDNases) to biofilms or the upregulation of the production of eDNases. Many bacteria produce eDNases, which in turn regulates the dispersal of biofilms (Jakubovics *et al.*, 2013). A schematic illustration of the main components of the EPM matrix and the factors that regulate dispersion is shown in Figure 7. Extracellular nucleases are also responsible for the degradation of DNA from Neutrophil extracellular traps (NETs) (Binnenkade *et al.*, 2018). Evidence of DNA degradation in NETs by extracellular nucleases has been observed with other bacteria such as *Vibrio cholerae*, *Streptococcus*, and *S. aureus* (Buchanan *et al.*, 2006; Seper *et al.*, 2013; Berends *et al.*, 2010).

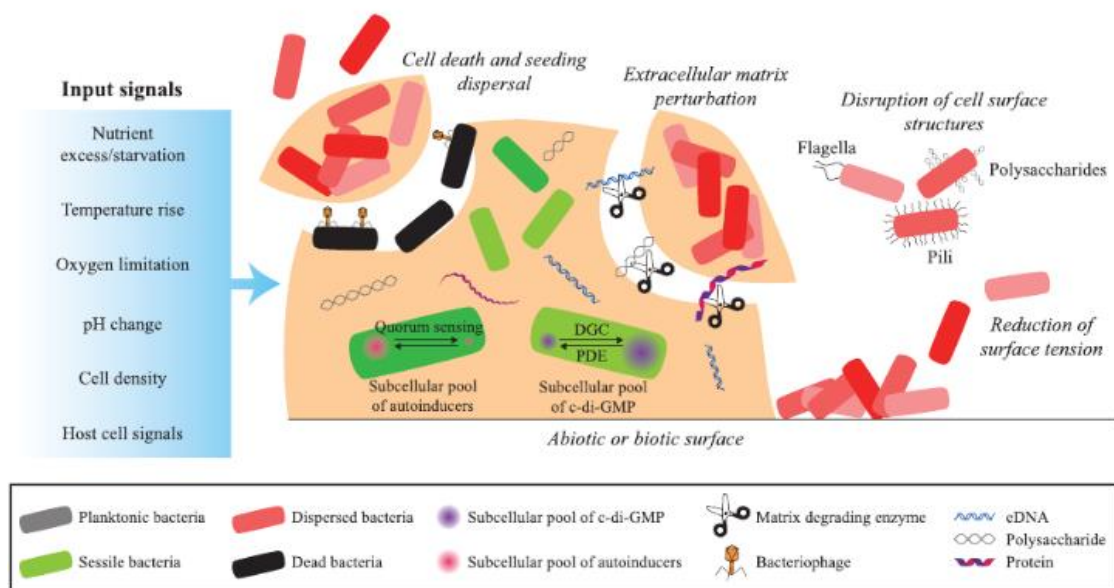


Figure 7. Schematic representation of biofilm dispersal (Guilhen *et al.*, 2017). Biofilm process is mediated via QS with the aid of autoinducer molecules. Proteins, eDNA, and polysaccharides shown above are constituents of EPM. Dispersion is facilitated by nucleases which degrade eDNA and cause perturbation of the EPM. The cells that leave a biofilm matrix can either colonise new host/environment or dead (Reuter *et al.*, 2010).

Recent studies by Kierdowski *et al.* (2014) identified two thermonucleases (*nuc1* and *nuc2*) present in *S. aureus*. These nucleases serve as biofilm regulators, and both were suggested to be identical and exhibiting similar ability to degrade eDNA, thereby causing a reduction in biofilm formation (Kiedrowski *et al.*, 2011; Kiedrowski *et al.*, 2014; Tang *et al.*, 2008). In another study, Beenken *et al.* (2012) demonstrated that inactivation of one or both thermonucleases (*nuc1* and *nuc 2*) in *S. aureus* caused an increase in biofilm formation *in vitro*. In another study, a secreted nuclease NucB was discovered in the supernatant of marine isolates of *Bacillus licheniformis* and was confirmed to disperse established mono- and multi-species biofilms (Nijland *et al.*, 2010). Similarly, Steichen *et al.* (2011) demonstrated a similar Nuc nuclease in *Neisseria gonorrhoeae*, and also revealed an increase in biofilm formation in the absence of the *nuc* gene. A study conducted by Seper *et al.* (2011) revealed that two other nucleases in *V. cholerae* demonstrated similar enzymatic properties and effect on biofilms.

However, the addition of DNase to existing or new biofilms does not always cause eDNA degradation resulting in reduction of biofilm. A few studies have noted exceptions, such as in *Burkholderia cenocepacia* and *H. pylori*. Thicker biofilm formation was observed in *B. cenocepacia* biofilms upon treatment with DNase (Pulmoenzyme) (Novotny *et al.*, 2013). In the closely related bacterium *H. pylori*, no significant difference in biofilm formation was noted when DNase I was added to new and existing biofilms (Grande *et al.*, 2011).

Similar studies of *Campylobacter*, however, are limited. The understanding of the molecular mechanism and the genes involved in the process of biofilm formation to dispersion is still in its infancy (Lim and Kim, 2017). Brown *et al.*'s study (2015b) remains the only work in this field emphasizing the identification of the genetic determinant of an extracellular nuclease and its role in biofilm formation in *Campylobacter*. The authors demonstrated that the mutation of the *cje1441* gene encoding a DNase resulted in increased biofilm formation, thus confirming the role of this particular gene in the biofilm properties of *C. jejuni* RM1221. They also demonstrated that co-incubation of *C. jejuni* RM1221 with other biofilm-forming strains such as 11168 and 81116 resulted in dispersion of pre-formed biofilms. In another study, a *dns* (*cje0256*) gene was shown to inhibit natural competence in a subset of *C. jejuni* strains including RM1221 due to nuclease activity (Gaasbeek *et al.*, 2009). In a subsequent study by Gaasbeek *et al.* (2010), the authors identified two more nucleases (Cje0566 and Cje1441) that inhibited natural transformation in another subset of *C. jejuni* strains that lacked the *cje0256* gene.

1.13 Aims and Objectives

C. jejuni biofilms offer greater resistance to antimicrobial treatment and disinfection procedures. In addition to this, cells in a biofilm existing in VBNC forms have been demonstrated to maintain viability for up to several months, which poses a serious challenge to the healthcare. These VBNC cells are generally accompanied by a morphological transition into CF in *C. jejuni*. Therefore, deducing the genetic factor responsible for the morphological transition and understanding the molecular mechanism involved in biofilm dispersal of these bacteria, may aid in the development of new intervention strategies to reduce the rate of infections caused by *Campylobacter*. The recent increase in multidrug-resistant forms of these bacteria has led to decreased efficacy of antimicrobials against biofilms, thus illustrating the need for such a study.

This study aims to develop an inducible gene expression system in *Campylobacter* that employs the widely used P_{BAD} promoter. The development of this system will assist in the study of the role of *amiA* in CFF in *C. jejuni* with the aid of conditional lethal mutants. Another proposed utilization of this system is to study the regulated expression of nuclease gene in *C. jejuni* and its effects on the biofilm dispersal phenotype.

The objectives of this study are as follows (i) Integration of gene cassettes carrying arabinose transporter genes (*araE* and *lacYA177C*) into *C. jejuni* 11168H chromosome (ii) Expression of the transporter genes in *Campylobacter* in the presence of arabinose (iii) Upon successful induction of the reporter gene in *C. jejuni*, use the regulated system to study the effects of *amiA* mutant on CFF (iv) Identification of the dispersal stage of *C. jejuni* 11168H biofilms (v) Investigation of the role of *cj0979* in *C. jejuni* biofilm formation (vi) Investigation of the enzymatic properties of Cj0979 (vii) Investigation of the effects over expression of *cj0979* on *C. jejuni* 11168H biofilm formation/dispersal (viii) Investigation of the role of *cje0256* in *C.*

jejuni RM1221 biofilms (ix) Study the effects of overproduction of Cje0256 on *C. jejuni* RM1221 biofilms.

Chapter 2: Materials and Methods

2.1 Bacterial strains and plasmids

The *C. jejuni* strains used in this study were 11168H, 81-176, and RM1221. *C. jejuni* 11168H is a hyper-motile derivative of strain NCTC 11168 (Karlyshev *et al.*, 2002). *C. jejuni* 81-176 was isolated from raw milk during an outbreak of diarrhoea (Gaynor *et al.*, 2004). *C. jejuni* RM1221 was isolated from retail chickens (Hao *et al.*, 2016).

Competent cells of *E. coli* used for cloning and transformation experiments were purchased from New England Biolabs (NEB) and Stratagene. The XL1 cells were purchased from Stratagene for blue-white screening. The cells C2523L, C2566L, and C3037L were purchased from NEB and used for other transformations depending on the antibiotic selection required for the specific experiment.

Plasmids pRRC and pSpOT were employed as controls for *C. jejuni* electroporation experiments (Karlyshev and Wren, 2005a; Ikeda and Karlyshev, 2012). Plasmid pRRT was used as a source of tetracycline resistance gene cassette (*tet^r*) (Karlyshev, unpublished). Plasmid pJMK30 served as a source of kanamycin resistance gene cassette (*kan^r*) (Trieu-Cuot *et al.*, 1985). Plasmids pBAD33 (Guzman *et al.*, 1995), pGEM-T Easy vector (Promega), and pUC19 (NEB) were also used for cloning experiments.

The other plasmid derivatives employed in this study were pRRBCD-*egfp-lacYA177C* and pRRBCD-*egfp-araE*. Both plasmids were constructed during previous PhD studies conducted in the supervisor's lab (Ikeda, 2014; Rubinchik, 2014).

2.2 Growth conditions and storage

All media used in this study were sterilized by autoclaving at 121°C for 15 min prior to use. All laboratory strains were stored at -80°C as suspensions in suitable media (LB for *E. coli* or

MH for *C. jejuni*) supplemented with 15% glycerol. MH broth, LB broth, PBS, and 100% glycerol were purchased from Fisher Scientific. *C. jejuni* strains were grown on Columbia blood agar (CBA) (Fisher Scientific) plates supplemented with 2% *Campylobacter* selective Skirrow supplement (Fisher Scientific) and 5% defibrinated horse blood (Fisher Scientific) for 48 h under microaerobic conditions (5% O₂, 10% CO₂ and 85% N₂) in a controlled atmosphere incubator (Don Whitley Scientific) at 37°C. Alternatively, the cultures were grown in gas jars containing CampyGen gas generating sachets (Oxoid) at 37°C. For liquid cultures, cells from CBA plates were harvested and re-suspended in BHI broth (Fisher Scientific) and grown in a shaking incubator at 250 rpm at 37°C. *E. coli* strains were grown on LB agar plates (Fisher Scientific) under aerobic conditions at 37°C. LB broth was used as growth media for liquid cultures, which were grown in a shaking incubator at 120 rpm.

The agar plates and broth cultures were supplemented with selective antibiotics whenever required. The following final concentrations were used: kanamycin (50 µg/mL); tetracycline (1 µg/mL); chloramphenicol (10 µg/mL); and ampicillin (100 µg/mL). All stock solutions of these antibiotics were purchased from Sigma Aldrich.

2.3 Gram staining

A tiny amount of bacteria was collected with a sterile 1 µL loop and smeared on a microscope glass slide containing 10 µL of PBS. The slide was washed with crystal violet (CV) for 30 s, which then was followed by the addition of iodine for 30 s. Ethanol was added to the slide to remove excess stain. As a final step, the slide was flooded with carbol fuchsin for 30 s, washed again with distilled water, and dried. Gram staining reagents were purchased from Prolabs Diagnostics.

The slide was then observed using a light microscope (Fisher brand™ AX-500 Series Compound Research Microscope). As a common practice, the 4× zoom lens was used to

visualize the stained area. Once zoomed, oil was added to the slide to provide a better focus with a 100× immersion lens. Motic Image software was used to capture live images.

2.4 Colony-forming units counting

Colony-forming units (CFU) counting was calculated with bacterial growth from a one-day CBA plate. An inoculum of *Campylobacter* suspended in BHI broth with an initial optical density (OD₆₀₀) of 0.5 was prepared. 100 μL of this suspension was added to 900 μL of PBS to prepare 1:10 serial dilutions. 50 μL of 10⁻⁶ and 10⁻⁵ serial dilutions were then plated on a CBA plate. The plates were incubated under microaerobic conditions for two to three days. Single colonies were counted using a colony counter from which CFU/mL was calculated.

2.5 Water

For all molecular biology experiments, highest-grade water (18.2 mΩ) was obtained from a Millipore Direct-Q UV purification system. For all other experiments, pure double-distilled water (10-15 mΩ) obtained from ELGA DV35 purification system was used.

2.6 Construction of pRRBCD-*egfp-araE* and pRRBCD-*egfp-lacYA177C* plasmids

Plasmids pRRBCD-*egfp-araE* and pRRBCD-*egfp-lacYA177C* contained a reporter gene *gfp* under the control of the inducible arabinose promoter P_{BAD} and *araE*/modified *lacY* gene under the control of a chloramphenicol promoter.

The ClaI/SalI fragment of pBAD33 containing a regulatory region and an inducible promoter was cloned into the pRR XbaI site (after blunt-ending with T4 DNA polymerase) to produce pRRB. The orientation of the cloned fragment was verified by restriction digestion with EcoRV. The *cam'* gene cassette, isolated from pAV35 (van Vliet *et al.*, 1998) by digestion with KpnI, was blunt-ended and inserted into the blunt-ended XbaI site of pRRB to produce pRRBC. The orientation of the insert was determined by double digestion with SphI and ClaI. The

pRRBC construct was verified by primer walking sequencing to ensure that there were no mutations. An XbaI fragment of pEGFP (BD Biosciences Clontech, Palo Alto, CA) containing a *gfp* gene was blunt-ended and cloned into the blunt-ended KpnI site of the pRRBC to produce pRRBC-*egfp*. The correct orientation of this construct was determined by digestion with StyI (Ikeda, 2014).

A DNA fragment with *E. coli* K12 *araE* gene (1.5 kb) was amplified using Phusion High Fidelity DNA Polymerase (NEB) and primers *araE_for* and *araE_rev* containing SalI restriction site. After cloning into pGEM-T vector and verification by sequencing, the SalI fragment with *araE* was cloned into the SalI site of pRRBCD-*egfp*. A derivative with the correct orientation of the fragment was designated, and pRRBCD-*egfp-araE* was constructed (Rubinchik, 2014).

A 1.3 kb DNA fragment with the *E. coli* K12 *lacY* gene was amplified with primers *lacY_for* and *lacY_rev* and cloned into the pGEM-T Easy vector to produce pGEM-T-*lacY*. The latter was then used as a template for another polymerase chain reaction (PCR) with primers *lacYA177C_for* and *lacYA177C_rev* primers to change codon GCA for TGT, leading to a replacement of alanine at position 177 for cysteine. This was carried out by using Q5[®] High-Fidelity DNA Polymerase to prevent other unintended mutations. The resulting construct was verified by sequencing and was designated pGEM-T-*lacYA177C*. SalI fragment with gene *lacYA177C* was cloned into the SalI site of pRRBCD-*egfp* in the correct orientation (verified by restriction analysis) and the designated pRRBCD-*egfp-lacYA177C* was constructed (Ikeda, 2014).

2.7 Biofilm growth assays and optimization

C. jejuni biofilm assays were conducted in borosilicate glass test tubes (Fisher Scientific) (Brown *et al.*, 2015b) and non-treated 96-well polystyrene microtiter plates (Corning) (Reeser *et al.*, 2007). Cells from a two-day-old plate were used to prepare the inoculum. Cells were

harvested and resuspended in BHI broth to an initial OD₆₀₀ of 0.5. Generally, a maximum of 2 mL of the bacterial suspension was added to test tubes and 200 µL was added to microtiter plates. Where culture supernatant was not required for further DNase testing, only 1 mL of culture was added to the test tubes. The test tubes/plates were incubated under static conditions in a microaerobic incubator at 37°C for a maximum period of 10 days. For the staining procedure, the supernatant was removed from tubes/plates, and the surface was rinsed carefully twice with distilled water. The tubes/plates were left to dry at 45°C for 30 min. 1% CV was used to stain the biofilm. For test tubes, 2 mL/1mL of the CV solution was added, and for microtiter plates, 200 µL was used. The tubes/plates were incubated in a shaking platform (30 oscillations/min) for 30 min at room temperature. The CV solution was then removed, and the tubes/plates were washed twice with distilled water to remove any excess non-bound CV. For biofilm quantification, a 20% acetone and 80% ethanol solution was used to dissolve the CV stained biofilm from the tubes/plates (Brown *et al.*, 2015b; Reeser *et al.*, 2007). Both solvents were purchased from Fisher Scientific. In the case of test tubes containing 2mL bacterial suspension, excess background CV staining was removed with a two-step dissolving technique. For the first step, 1 mL of the acetone-ethanol solution was added for about 15 min, and the solution was removed and discarded. For the second step, 2 mL of acetone-ethanol solution was added to the already treated test tubes. For test tubes containing 1 mL of bacterial suspension, the two-step dissolving procedure was not implemented due to the lower culture volume. 1mL of the acetone-ethanol solution was added to the test tubes to dissolve the biofilm for quantification. For the plates, 200 µL of the acetone-ethanol solution was used to dissolve the biofilm. The tubes/plates were left on a shaking platform (30 oscillations/min) for 30 min. 200 µL of the dissolved biofilm was transferred onto a clean microtiter plate, and absorbance was read at a wavelength of 595 nm using a plate reader (Tecan M220).

2.8 eDNA-B and eDNA-S purification

Monarch PCR and DNA clean-up kit (NEB) was employed for the purification of eDNA-B from biofilms and eDNA-S from culture supernatant. For eDNA-B purification, the cell suspension was removed from the test tubes. 150 μL of 1 \times Tris EDTA (TE) buffer (10 mM Tris-HCl, 1 mM disodium EDTA, pH 8.0) from Sigma Aldrich was added to each test tube and the attached biofilm was removed with the help of a sterile swab (Fisher Scientific). The bacterial suspension in TE was pipetted up and down vigorously to break the biofilm, and the entire suspension was used for eDNA-B purification. 300 μL of binding buffer was added to the suspension and loaded onto a spin column and subsequently centrifuged. The spin column was then washed twice with 200 μL of wash buffer. No cell lysis step was incorporated, and the buffers used did not contain any detergents that would cause cell lysis for the release of intracellular DNA. The eDNA-B was eluted from the column to a final volume of 10 μL . For the purification of eDNA-S, 10 μL of culture supernatant was mixed with 20 μL of binding buffer and loaded onto a spin column and centrifuged. The spin column was rinsed twice with 200 μL of wash buffer. 10 μL of elution buffer was added to the column to elute eDNA-S. The purified DNA was checked for concentration and purity using a NanoVue spectrophotometer (Thermo Fisher Scientific).

2.9 DNase activity assays

For the DNase activity assays, the substrate DNA was either lambda DNA (NEB) or eDNA-B. A final concentration of 1 \times NEB DNase reaction buffer (10 mM Tris-HCl, 2.5 mM MgCl_2 , 0.5 mM CaCl_2) was added to each sample. The NEB DNase I enzyme served as a positive control in this experiment. Samples were incubated at 37°C for 1 to 4 h. The samples were analyzed using gel electrophoresis.

2.10 Proteinase K treatment

The supernatant from the test tube was collected and spun down at 13,000g (Labnet Prism R Refrigerated Microcentrifuge) for 5 min. The cell pellet was discarded. For the sterilisation of culture supernatant, the sample was filter-sterilized using a 0.22 μm Millipore filter and stored at -20°C . The filter sterilized supernatant sample was treated with proteinase K to check for the presence of proteins bound to the DNA complex. 10 μL of culture supernatant was incubated with 1 μL of proteinase K (20 mg/mL), obtained from an Invitrogen Genomic DNA kit, at 55°C for 1 h.

2.11 Removing media from supernatant

For removing low molecular weight compounds, 500 μL of filter-sterilized culture supernatant was added to Corning Spin-X UF spin concentrator (cut-off value of 5 kDa) and spun down at 14,500 g for 15 min. After the initial spin cycle, the flowthrough was discarded and the buffer in the column was exchanged with a $1\times$ TE buffer (final concentration). 200 μL of TE buffer was added to the fraction in the column and then centrifuged for a further 15 min. The buffer exchange step was repeated thrice. After the final centrifugation step, the retentate (supernatant after media exchange) was collected for further testing and the flowthrough was discarded.

2.12 Trypsin treatment

Trypsin (Thermo Fisher Scientific) was added to the supernatant sample after media exchange at 1:50 w/w ratio following manufacturer's recommendation. In this experiment, 2.4 μg of trypsin (2.4 μL of 1 $\mu\text{g}/\mu\text{L}$) was added to 120 μg of the supernatant sample and incubated at 37°C for 4 h. After incubation, the sample was loaded onto Corning Spin-X UF spin concentrators (cut-off value of 10 kDa) and spun down at 13,000 g for 2 min. The flowthrough fraction (F1) was collected and saved for further analysis. $1\times\text{TE}$ buffer was added to the retentate sample to make up to a volume of 100 μL and centrifugation for another 2 min was repeated. After centrifugation, flowthrough fraction (F2) and F1 from the first centrifugation

step were sent for mass spectrometry analysis. All three fractions were analysed using bicinchoninic acid (BCA) assay to determine the concentrations of the proteins present. The fractions were also analysed by NanoVue to obtain the corresponding purity compositions.

2.13 Dextranase treatment

Dextranase was added to cleave any dextrans, which may be bound to DNA complex in the supernatant sample after media exchange. 2.6 μL of dextranase (1 unit/mL) (Sigma Aldrich) was added to 50 μL supernatant sample after media exchange by following the manufacturer's protocol and incubated at 37°C for 4 h. After incubation, the sample was loaded onto Corning Spin-X UF spin concentrators (cut-off value of 10 kDa) and spun at 13,000 g for 2 min. The flowthrough fraction (F1) was collected and saved for further analysis. 1xTE buffer was added to the retentate sample to make up to a volume of 100 μL , and centrifugation was repeated for another 2 min. After centrifugation, the retentate, flow-through fraction (F2), and F1 were analysed using NanoVue spectrophotometer.

2.14 Plasmid DNA purification

E. coli strains carrying the plasmids of interest were grown on LB plates supplemented with an antibiotic. About half a loop of cells was collected from a plate following an overnight incubation and used for plasmid DNA purification. QIAprep Spin Miniprep Kit (Qiagen) was used for the purification following the manufacturer's guidelines.

2.15 Genomic DNA purification

A Genra Puregene Yeast/Bact. kit from Qiagen was used for the extraction of chromosomal DNA. Bacterial growth from a one-day culture plate was used for *Campylobacter* genomic DNA purifications.

2.16 Determining the quality of DNA

A NanoVue Plus Spectrophotometer was used to analyse the purity (denoted by A260/A280 and A260/A230 ratios) and concentration of DNA samples under study. The testing was carried out following the manufacturer's guidelines. DNA elution buffer was used as a reference for DNA samples. 1xTE buffer was used as a reference for supernatant, trypsin-treated, and dextranase-treated samples.

2.17 Agarose gel electrophoresis

A 1% agarose gel was used for gel electrophoresis. The gel was prepared by mixing agarose powder in Tris borate buffer (TBE) purchased from Fisher Scientific. The mixture was heated in a microwave for 2 min and let to cool. Once cooled, 0.5 µg/mL of ethidium bromide (Fisher Scientific) was added to the mixture and subsequently allowed to set in a gel cassette. Samples were loaded onto the gel with bromophenol blue-based loading buffer (NEB). The NEB Quick-Load[®] Purple 2-Log DNA Ladder (0.1–10.0 kb) was used as a standard control to compare and estimate the size of the test DNA fragments. A run time of 1 h at 150 V was used unless longer or shorter times were required for specific experiments. The gel was visualized using G Box (Syngene) employing GeneSnap software, while the estimation of the obtained band sizes and their corresponding DNA amounts were analysed using GelAnalyzer and DNA ladder as a control.

2.18 Restriction analysis

All enzymes and reaction buffers were purchased from NEB. The restriction digestion reactions were conducted following the manufacturer's guidelines. The incubation times varied according to the enzyme selection ranging from 15 min to a maximum of 1 h. Where necessary, the restriction enzymes were deactivated by incubating them at 65°C for 20 min. The expected fragment sizes were determined using the NEB cutter V2 program. The circular and linear genetic maps of the plasmids used in this study were generated using SnapGene Viewer.

2.19 DNA purification from agarose gel

The sample to be gel extracted was run on 1% agarose gel at 150 V for 1 h. After the run was completed, the gel was viewed under a 'long wavelength' setting in a transilluminator, and the band of interest was carefully cut out using a clean scalpel. The DNA from the band was extracted using a Monarch Gel purification kit (NEB) following the manufacturer's instructions.

2.20 Dephosphorylation

Dephosphorylation of the vector was carried out prior to cloning experiments. Antarctic phosphatase enzyme from NEB was used for this purpose, and the experiment was carried out following the manufacturer's guidelines.

2.21 Polymerase chain reaction

Primers for PCR were designed, and the sequences were sent to Sigma Aldrich for synthesis. The lyophilized primers were then mixed with Milli-Q water to obtain a stock concentration of 100 μ M and stored at -20°C as instructed in the technical sheet provided by the manufacturer. GoTaq[®] Green Master Mix (Promega) and Q5[®] High-Fidelity DNA Polymerase (NEB) were used in this study. For GoTaq[®] Green Master Mix, the following components were added in the following order: reaction buffer; forward primer (2 μ M); reverse primer (2 μ M); DNA (0.5 μ g); and Milli-Q water. For Q5[®] High-Fidelity DNA Polymerase, the following components were added in the following order: reaction buffer; forward primer (2 μ M); reverse primer (2 μ M); dNTP (10 mM) (Fisher Scientific); polymerase (0.25-0.5 μ L); DNA (0.5 μ g); and Milli-Q water. The PCR conditions (Table 1 and 2) were established following the manufacturer's protocol. Table 3 below includes the list of primers used in this study

Table 1. PCR conditions used with Promega GoTaq® Green Master Mix

PCR step	Temperature	Duration of step	Number of cycles
Initial denaturation	95 °C	2 min	1
Denaturation	95 °C	30 s	25
Annealing	55 °C	30 s	
Extension	72 °C	1 min per kb	
Final extension	72 °C	5 min	1

Table 2. PCR conditions used with NEB Q5® High-Fidelity DNA Polymerase

PCR step	Temperature	Duration of step	Number of cycles
Initial denaturation	98 °C	30 s	1
Denaturation	98 °C	10 s	25
Annealing	45 °C	30 s	
Extension	72 °C	30 s per kb	
Final extension	72 °C	2 min	1

Table 3. List of primers used in this study

Primer	Sequence 5'→3'
ak233	GCAAGAGTTTTGCTTATGTTAGCAC
ak234	GAAATGGGCAGAGTGTATTCTCCG
ak235	GTGCGGATAATGTTGTTTCTG
ak237	TCCTGAACTCTTCATGTCGATTG
spoT_for	TTGAAACCAATCGATGAAGAATTATTGC
spoT_rev	TTAACTTCTTTATAAGCATCATTAAAGATG
cj1051_for	AGTGTGTTAATTTCAAACCTCATAGCTAATAATC
cj1051_rev	GTAATTTTCTCTCCTAAGAATTCTTTCATAGC
pBAD_for	GATTAGCGGATCCTACCTGAC
pBAD_up	GCCGTCAAGTTGTCATAATTGGTAACG
pRR1	GTAATCGTAGATCAGCCATGCTACG
lacY_for	GTCGACAAGGAAATCCATTATGTACTATTTAAAAAAC
lacY_rev	GTCGACTTAAGCGACTTCATTCACCTGACGACGCAG
araE_for	GTCGAC AGGAGGAAAAA ATGGTACTATC
araE_rev	GTCGACTCAGACGCCGATATTTCTCAAC
cj0979_for	CTCCGCCTTCAAAGAAATGATTTCTCCTTC
cj0979_rev	GAAGAATATGCACAACCTTGAAGAATACGCATC
cj0979_LP_for	AAAATCTAGAAAGAAGGAGATATACCATGCAAAATTC TAGTTTTGAAG GAAAAGTAGTTAGA
cj0979_LP_rev	TTCCGCATGCTTAGTGATGATGATGATGATGGAATTTA TTGTGTTTTTCCATTTATAAG
cj0979_N_expr_for	AAAATCTAGAAGGAGGTATAACCATGCACCATCACCATC ACCATAGAAT AAATTATAAAAAAATATTTAATCTG

cj0979_N_expr_rev	TTCCGCATGCTTAGAATTTATTGTGTTTTCTCCATTTATAAG
cje0256f_mod	TCAGAAATCTAGAGTGCTAGAAATGAATATAGTGCCGTAATAGC
cje0256r_mod	AAACACGAATTCTTTAAAAAAGCACTTAATTAATAATCATTCATAC
cje0256_LP_for_mod	ATAATCTAGAAAGAAGGAGATATACCATGAAAAGTTT TGAAGAAAGCA A
cje0256_LP_rev_mod	AGAAGCATGCTTAGTGATGATGATGATGATGGAGTAATGCTCTAATTC TTTTTTC
cje0256_for	ATAATCTAGAAAGAAGGAGATATACCATGAAAAAATAATAAGCGTTT TAATACT
cje0256_rev	AGAAGCATGCTTAGTGATGATGATGATGATGGAGTAATGCTCTAATTC TTTTTTCTTC

2.22 Ligation

T4 ligase (Promega) and Quick ligase (NEB) were used in this study for ligation experiments. A 3:1 (insert: vector) molar ratio was used with both kits. The ligation reactions were set up following the manufacturer's guidelines, and 5 μ L of the ligated product was used for each transformation experiment.

2.23 Preparation of electrocompetent cells of *C. jejuni*

Bacterial cultures from a fresh one-day culture plate, grown under microaerobic conditions, were harvested and re-suspended in 1 mL of MH broth (Fisher Scientific). The suspension was centrifuged at 10,000 rpm at 4°C for 5 min. The bacterial pellet was then resuspended in 1 mL of pre-made ice-cold wash buffer (272 mM sucrose (Sigma Aldrich) and 15% glycerol) and subsequently centrifuged under the same conditions. This step was repeated thrice. The cells were finally resuspended in 500 μ L of wash buffer, and 50 μ L aliquots were prepared for immediate use for electroporation experiments or for storage at -80°C.

2.24 Transformation experiments

2.24.1 Electroporation of *Campylobacter*

For *C. jejuni* experiments, 50 μ L aliquots of the electrocompetent cells were used for each electroporation. Electroporation cuvettes 0.22 mm (Molecular Bioproducts) were left on ice

for 10 min prior to electroporation. 1 μg of DNA was added to the cells and slowly suspended by pipetting up and down. The electroporation mixture was transferred into ice-cold cuvettes, and the cuvette was transferred to an electroporation pod. Electroporation was carried out in a Gene Pulser X-cell electroporator (Biorad) at 2.5 kV, 200 Ω , and 25 μF with a time constant of approximately 5 ms. 100 μL of Super Optimal broth with Catabolite repression medium (SOC) (Invitrogen) was added to the cuvettes, and the electroporated mixture was plated onto a non-selective plate and left for incubation under microaerobic conditions at 37°C. The growth from the non-selective plate was re-streaked onto a selective antibiotic plate the following day, and the plate was incubated under optimal conditions for a further two to three days.

2.24.2 Transformation of *E. coli*

For *E. coli* transformation experiments, 50 μL of commercial chemically competent cells were used for each experiment. The cells were thawed on ice until the last crystal disappeared. DNA was added to the cells and further incubated on ice for 30 min. The tubes containing the cells were then transferred to a water bath at 42°C. The duration of heat shock varied depending on the batch of cells. The following heat shock times were carried out with the respective cell types: 10 s for C2566L; 20 s for C2523L; and 45 s for XL1. Following heat shock, the cells were incubated on ice for further 2–5 min depending on the cell type used. 950 μL of SOC medium was added to the competent cells, and 100 μL of cell suspension was spread onto an LB agar plate (containing the relevant antibiotic) using an L-shaped spreader and incubated for a day.

2.25 Supercoiled DNA and restriction analysis

CloneChecker kit from Invitrogen was used for supercoiled DNA and initial restriction analysis. Bacteria was suspended in 6 μL of LB broth. For restriction analysis, 3 μL of the suspension was added to 8 μL of the green solution and heated at 100°C for 30 s. After the mixture cooled down, 1 μL of 10 \times restriction enzyme buffer and 1 μL of restriction enzyme

were added and further incubated for 30 min. Then, 2 μ L of loading dye was added, and the entire mixture was analysed using gel electrophoresis. For supercoiled DNA analysis, 3 μ L of the bacterial suspension was added to 5 μ L of the red solution and pipetted up and down for approximately three times. 5 μ L of the yellow solution was added to the mixture and vortexed for 15 s. Then, 4 μ L of loading dye was added, and the entire mixture was analysed using gel electrophoresis.

2.26 Construction of *Campylobacter* mutants

2.26.1 11168H/*cj1051* mutant

A *cj1051* gene of *C. jejuni* 11168H was PCR amplified using *cj1051_for* and *cj1051_rev* primers using GoTaq[®] Green Master Mix (Promega) with an extension time of 3 min. The amplified PCR product was ligated into cloning vector pGEM-T Easy vector (Promega) and transformed into *E. coli* C2523L competent cells. The transformants were screened using CloneChecker and restriction analysis. The pGEM-T-1051 clones containing the insert were chosen for further cloning experiments. Plasmid pRRT was used as a source of tetracycline cassette (*tet'*). The pRRT plasmid was digested with NheI and XbaI to produce compatible ends for cloning, and the resulting 2.8 kb band was gel-purified. The excised fragment was then inserted into the XbaI site of the pGEM-T-1051 to create p1051-tetR. The cloned product was then transformed into *E. coli* C2523L cells, and the transformants were screened using CloneChecker and restriction analysis for the isolation of clones carrying the insert and the gene cassette. Clones with the insert and the *tet'* gene in the correct orientation were selected for insertional mutagenesis in *C. jejuni* 11168H to create 11168H/*cj1051* strain.

2.26.2 11168H/*cj0979* mutant

A *cj0979* gene of *C. jejuni* 11168H was amplified using *cj0979_for* and *cj0979_rev* primers using GoTaq[®] Green Master Mix (Promega) with an extension time of 3 min. The amplified PCR product was ligated into cloning vector pGEM-T Easy vector (Promega) and transformed

into *E. coli* C2523L competent cells. The transformants were screened using CloneChecker and restriction analysis. The pGEM-T-0979 clones with the insert were chosen for further cloning experiments. Plasmid pJMK30 served as a source of kanamycin resistance cassette (*kan^r*). The pJMK30 plasmid was digested with SmaI to produce a blunt-ended fragment. The gel-purified fragment was then inserted into the blunt-ended ClaI site of the pGEM-T-0979 to create p0979-kanR. The cloned product was then transformed into *E. coli* C2523L cells, and the transformants were screened using CloneChecker and restriction analysis. Clones with the insert and the *kan^r* in the correct orientation were selected for insertional mutagenesis in *C. jejuni* 11168H to create 11168H/*cj0979* strain.

2.26.3 RM1221/*cje0256* mutant

A *cje0256* gene of *C. jejuni* RM1221 was PCR amplified using primers *cje0256f_mod* and *cje0256r_mod* using Q5[®] High-Fidelity DNA Polymerase with an extension time of 3 min. The amplified 2.2 kb PCR product was digested with EcoRI and XbaI to produce sticky ends. The pUC19 plasmid was digested with the same enzymes and run on the gel; the larger fragment was gel-purified and used for ligation with the EcoRI/XbaI digested *cje0256* PCR fragment. 5 µL of the ligated mixture was transformed into *E. coli* XL1 Blue competent cells for blue-white screening. The white colonies were screened using CloneChecker and restriction analysis. The pUC19-*cje0256* clones with the insert were chosen for further cloning experiments. Plasmid pJMK30 was employed as a source of the kanamycin resistance cassette (*kan^r*). The pJMK30 plasmid was digested with SmaI to produce a blunt-ended fragment. The gel-purified fragment was then inserted into the Eco53KI site of the pUC19-*cje0256* to create pUC19-*cje0256*-kanR. The cloned product was then introduced into *E. coli* XL1 blue competent cells, and the transformants were again screened using CloneChecker and restriction analysis. Clones with the insert and the *kan^r* gene in the correct orientation were selected for insertional mutagenesis in *C. jejuni* RM1221 to create RM1221/*cje0256*.

2.27 Next Generation sequencing

Verification of *C. jejuni* integration constructs and transformants was carried out by genome sequencing. The genome sequencing libraries were constructed using NEB Next® Fast DNA Fragmentation and Library Prep kit for Ion Torrent (NEB). Adapters were attached to both ends of the fragmented DNA by following manufacturer's instructions. Size selection on a 2% E-gel in accordance with the DNA size required for the Ion Torrent sequencing kit was carried out. Subsequently, Bioanalyzer 2100 was employed to precisely determine the size and the concentration of the DNA fragments. Emulsion PCR was carried out using Ion One Touch 2 system. During this process, the adapter-ligated DNA underwent denaturation and was fixed to the ion spherical particles (ISP), after which the DNA attached to the ISP was amplified. One end of the fragment contains an adapter sequence, where the polymerase attaches, and the other end attaches to the beads. Enrichment process was implemented to remove particles that did not contain DNA. The enriched sample was then transferred onto a 316v2 chip (Life technologies), resulting in an overall good loading. The genome sequencing was conducted using Ion Torrent PGM (Life Technologies).

2.28 Comparison of growth rates of the *C. jejuni* derivatives

To compare growth rates, the wild-type and derivative *C. jejuni* strains were suspended in BHI broth with a starting OD₆₀₀ of 0.1 and incubated on a shaker at 250 rpm at 37°C under microaerobic conditions. For induction experiments, 0.2% final concentration arabinose was added to the liquid culture after 6 h and incubated for a further 21 h. Optical density measurements were taken at the required time intervals.

2.29 Green Fluorescent Protein (GFP) expression studies

Expression of *gfp* in the *E. coli* and *C. jejuni* derivatives carrying the *araE* and *lacYA177C* genes was tested using a fluorescence microscope (Nikon 80i Eclipse) with bacterial cultures grown on solid media with and without arabinose.

For fluorimetry, 150 μ L of *E. coli*/pRRBCD-*egfp-lacYA177C* in LB broth with an initial OD₆₀₀ of 0.5 was incubated in wells of a 96-well, non-treated polystyrene microtiter plate (Corning). The culture was incubated for 2 h in an aerobic incubator at 37°C with shaking at 120 rpm. For induction, 0.1% final concentration arabinose was added and further incubated for 2 h. Similarly, *C. jejuni* strains were suspended in BHI broth with an initial OD₆₀₀ of 0.5 and incubated on a shaking platform at 250 rpm under microaerobic conditions at 37°C for 2 h. After the initial incubation, 0.2% final concentration arabinose was added and additional incubation for 2 h was carried out. After completing the induction cycle, the cells were centrifuged at 4,000 g for 30 min, resuspended in PBS, and fluorescence readings of the whole cells were recorded. Similarly, the fluorescence of the lysed cells of *E. coli* and *C. jejuni* were measured after resuspending the cells in a lysis mixture (Buffering Salts, 550 mM KOAc, and 2.5% Triton X-100) in the presence of EDTA (5 mM) and protease inhibitor cocktail (Sigma Aldrich, p8849). Fluorescence intensity was measured using BMG Labtech FLUOstar at excitation wavelength 485 nm and emission wavelength 520 nm.

2.30 Protein expression

The *E. coli* strain harbouring the pBAD33 plasmid carrying the gene of interest was grown on LB agar plates containing chloramphenicol. A tiny amount of bacteria was collected from a one-day plate and inoculated into 5 mL of LB broth containing chloramphenicol and incubated overnight on a shaking platform at 120 rpm at 37°C. The 5 mL overnight culture was transferred into fresh 25 mL LB broth, and the initial OD₆₀₀ was recorded. The culture was incubated in the same shaking incubator at 120 rpm until it reached an OD₆₀₀ of 0.6. At this point, the bacterial suspension was divided into two bottles, and 0.1% final concentration arabinose was added to one of them. The other bottle served as a control for the protein purification experiment. The bottles were further incubated for 2 h. Optical density was again measured at the end of the induction cycle.

2.31 Protein purification

Following the 2 h induction period, a 1 mL sample of induced and uninduced culture was collected, spun down at 10,000 g for 2 min, and used for protein purification employing the MagneHis™ Protein purification system (Promega). After centrifugation, the LB broth was replaced by 100 µL of 1× lysis buffer and 1 µL of DNase I enzyme and incubated for 20 min on a rocker at room temperature. The Nickel particles (Ni) particles were thoroughly vortexed before use. 30 µL of Ni particles were added to the lysate and properly mixed by inverting the tubes approximately 10 times. 500 mM of NaCl (Sigma Aldrich) was added to the mixture before the addition of Ni particles to improve protein binding. The tubes were then left to stand in a magnetic holder for about 30 s. The clear lysate buffer was removed, and the Ni particles were then washed with wash buffer and NaCl thrice. The protein was eluted with 100 µL of elution buffer. The purified protein was stored at 4°C.

2.32 Protein analysis and detection techniques

2.32.1 Sodium dodecyl sulphate polyacrylamide gel electrophoresis

For the sodium dodecyl sulphate polyacrylamide gel electrophoresis (SDS-PAGE) gels, NuPAGE Novex 4–12% Bis-Tris gel (Invitrogen), NuPage 3-(N-morpholino) propanesulfonic acid (MOPS), or 2-(N-morpholino) ethanesulfonic acid (MES) running buffer was employed. The stock solutions of the running buffers were 20×, and they were used at a working concentration of 1× by diluting with distilled water. MOPS running buffer was used with higher-sized proteins and MES running buffer was used with smaller-sized proteins. The protein samples were mixed with 2× NuPage LDS sample buffer and heated at 70°C for 10 min prior to gel loading. The SDS-PAGE gel was run at 150 V for 90 min. PageRuler Plus Prestained Protein ladder (Thermo Fisher Scientific) was used as a standard for comparison.

2.32.2 Coomassie staining

The SDS-PAGE gel was carefully removed from the gel rig and washed with distilled water for 5 min. This step was repeated thrice. The gel was then stained with Invitrogen Safe Blue stain for 1 h, followed by a de-staining step (1 h to overnight) on a gentle rocker (10 oscillations/min). Following this step, the gel was washed again with distilled water for 1 h. The gel was read using the 'lower white' setting of the GeneSnap software. Gel Analyzer was used to analyse the protein sizes on the gel.

2.32.3 Western blotting

The gel from SDS-PAGE run was separated from the cassette and submerged in 50 mL of transfer buffer (48 mM Tris, 39 mM glycine, 1.3 mM SDS, 20% methanol) for approximately 15 min. In parallel, the PVDF membrane (Immobilon-P 0.45 μ M polyvinylidene difluoride) was activated in the presence of 100% methanol for 15 s and washed twice with Milli-Q water for 2 min per wash. The membrane was then soaked in transfer buffer for 5 min before it was transferred to the trans blotter. Simultaneously, eight filter papers were soaked in transfer buffer for 15 min. The membrane and the gel were assembled on the cathode in the following order: four filter papers; gel; membrane; and finally four filter papers. A semi-dry transfer run was conducted at 15 V for 90 min. After the transfer was complete, the membrane was washed twice with 1 \times Tris- buffered saline (TBS) buffer for 10 min per wash. The membrane was treated with blocking buffer (3% w/v BSA in 1 \times TBS) for 1 h at room temperature. After blocking was completed, the membrane was washed twice with TBST buffer containing 0.1% Tween 20 (Sigma Aldrich) for 10 min followed by a single wash of 10 min with TBS buffer. A 1:1,000 working dilution of the 6xHis Epitope tag monoclonal antibody (Invitrogen) solution in blocking buffer was freshly prepared and added to the membrane. The membrane was incubated with the primary antibody for 1 h at room temperature. After incubation was complete, the membrane was washed twice with TBST buffer for 10 min per wash followed by

a single wash of 10 min with TBS buffer. Following the wash, the membrane was incubated with anti-mouse IgG, HRP-linked secondary antibody (Cell signalling technologies) diluted to 1:1,000 in 10 mL 1×TBS and 10% non-fat dried milk powder (Marvel Original). After 1 h, the membrane was washed four times with 1× TBST buffer for 10 min per wash. For chemiluminescent detection, SuperSignal West Pico Chemiluminescent substrate (Thermo Fisher Scientific) was added to the gel following the manufacturer's guidelines just before imaging the membrane. GeneSys software was used to capture the membrane image.

2.32.4 Bicinchoninic acid assay

Protein concentration was determined using a Pierce BCA protein assay kit (Thermo Fisher Scientific). The bovine serum albumin (BSA) standard provided with the kit was diluted to known concentrations with varying amounts of elution buffer or 1× TE buffer. These diluted samples were employed as standards for comparison. Elution buffer was used as the diluent for purified protein samples. TE buffer was used as the diluent for trypsin treated samples. The experiment was executed according to the manufacturer's guidelines. The absorbance was read at 562 nm using a Tecan plate reader.

2.32.5 Mass spectrometry

The mass spectrometer analysis was performed by Cambridge Centre for Proteomics, University of Cambridge, Cambridgeshire using LC MS/MS ESI-ORBITRAP-HCD. The list of proteins and their abundance ratios were analysed using Scaffold and MHT files. The 10 most abundant proteins were selected and further studied using NCBI BLASTp and UniProtKB.

Chapter 3: Results

3.1 Construction and verification of regulated gene expression systems in *C. jejuni*

This section will describe an attempt to develop an inducible gene expression system in *Campylobacter* employing the arabinose inducible P_{BAD} promoter in conjunction with the pRR plasmid system. Many other researchers have examined the use of this arabinose-inducible regulatable promoter system in gene regulation studies with other bacteria, as previously described in the introduction; however, the system has not been utilized with *Campylobacter*, perhaps because these bacteria do not contain any arabinose transporter genes. The pRR plasmid system is based on the principle of homologous recombination, and the selected gene is expressed through the introduction of a gene cassette into a non-coding spacer region of an rRNA gene cluster of the *C. jejuni* chromosome. *Campylobacter* research employs the practice of delivering exogenous genes using the pRR plasmid system in these bacteria (Karlyshev and Wren, 2005a).

Therefore, this section will discuss the testing of the regulatable gene expression systems pRRBCD-*egfp-araE* and pRRBCD-*egfp-lacYA177C*, utilizing both the P_{BAD} promoter and the pRR plasmid system, in *Campylobacter*. The arabinose transporter genes (*araE* and *lacYA177C*) placed under the control of a constitutive promoter were introduced into *C. jejuni*. Upon successful transportation of arabinose, this system would be used to study the role of the *amiA* gene in CFF in *Campylobacter*. Previous studies have identified this gene as an important genetic determinant governing the morphological transition in a similar bacteria *H. pylori*, where *amiA* mutant displayed a reduction in CF transition (Chaput *et al.*, 2006). In contrast to *H. pylori*, *amiA* is only present as a single copy in *Campylobacter* and was suggested to be an essential gene (Ikeda, 2014). Thus, for the investigation of the function of this gene, a system that allows the construction of conditionally lethal mutants would be required.

3.1.1 Validation of pRRBCD-*egfp-araE* and pRRBCD-*egfp-lacYA177C* constructs

The expression plasmids pRRBCD-*egfp-araE* and pRRBCD-*egfp-lacYA177C* were verified by restriction analysis and genome sequencing to ensure there were no mutations. In addition, the functionality of the P_{BAD} promoter was verified in *E. coli* with the aid of a reporter gene (*gfp*). Fluorescence microscopy was used to demonstrate the induction of GFP protein.

3.1.1.1 Verification of recombinant plasmids

The plasmids carrying the arabinose transporter genes *araE* and *lacYA177C* were purified from *E. coli* strains. The strains were recovered after one-day growth on LB agar supplemented with 10 µg/mL chloramphenicol. Plasmid DNA purification yielded high concentration DNA. The concentrations of purified pRRBCD-*egfp-araE* and pRRBCD-*egfp-lacYA177C* plasmids were 790 ng/µL and 453 ng/µL, respectively. The plasmids were verified by restriction analysis. The restriction enzyme Sall was chosen for pRRBCD-*egfp-lacYA177C*, while the enzymes NdeI and BsaBI were designated for the analysis of pRRBCD-*egfp-araE*. The restriction digestions produced 6.2 kb and 1.2 kb fragments for pRRBCD-*egfp-lacYA177C* and 4.9 kb, 1.8 kb, and 1.4 kb fragments for pRRBCD-*egfp-araE*, as expected, thus confirming the plasmids (Figures 8 and 9).

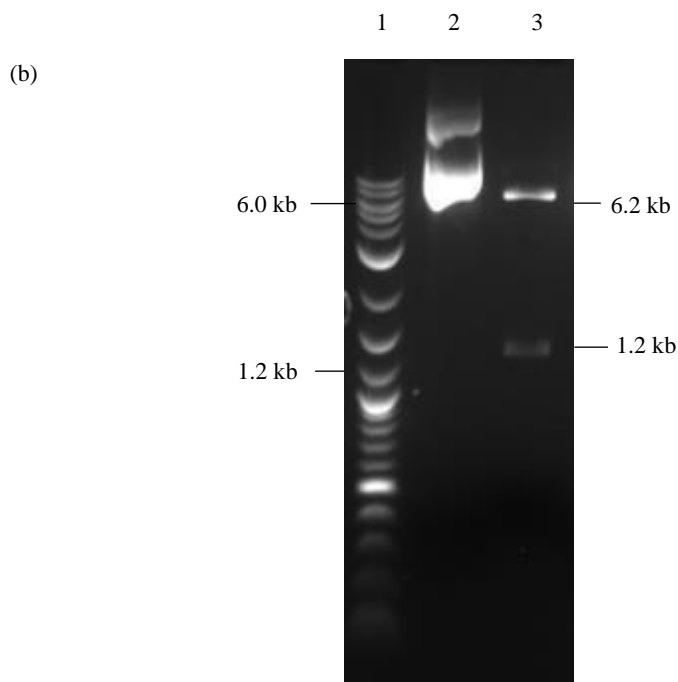
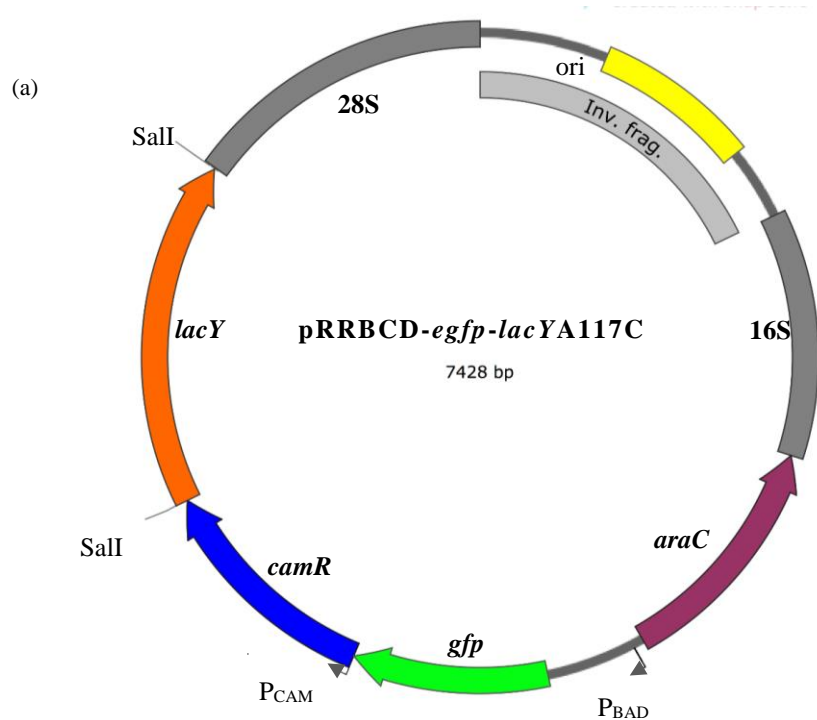


Figure 8. Verification of pRRBCD-*egfp-lacYA117C* by restriction analysis.
 (a) Restriction map of the plasmid indicating the SalI restriction sites.
 (b) Gel image showing uncut and digested pRRBCD-*egfp-lacYA117C* with SalI.
 Expected fragment sizes: 6.2 kb and 1.2 kb.
 Samples: 1, 2-Log DNA ladder; 2, pRRBCD-*egfp-lacYA117C*;
 3, pRRBCD-*egfp-lacYA117C* SalI

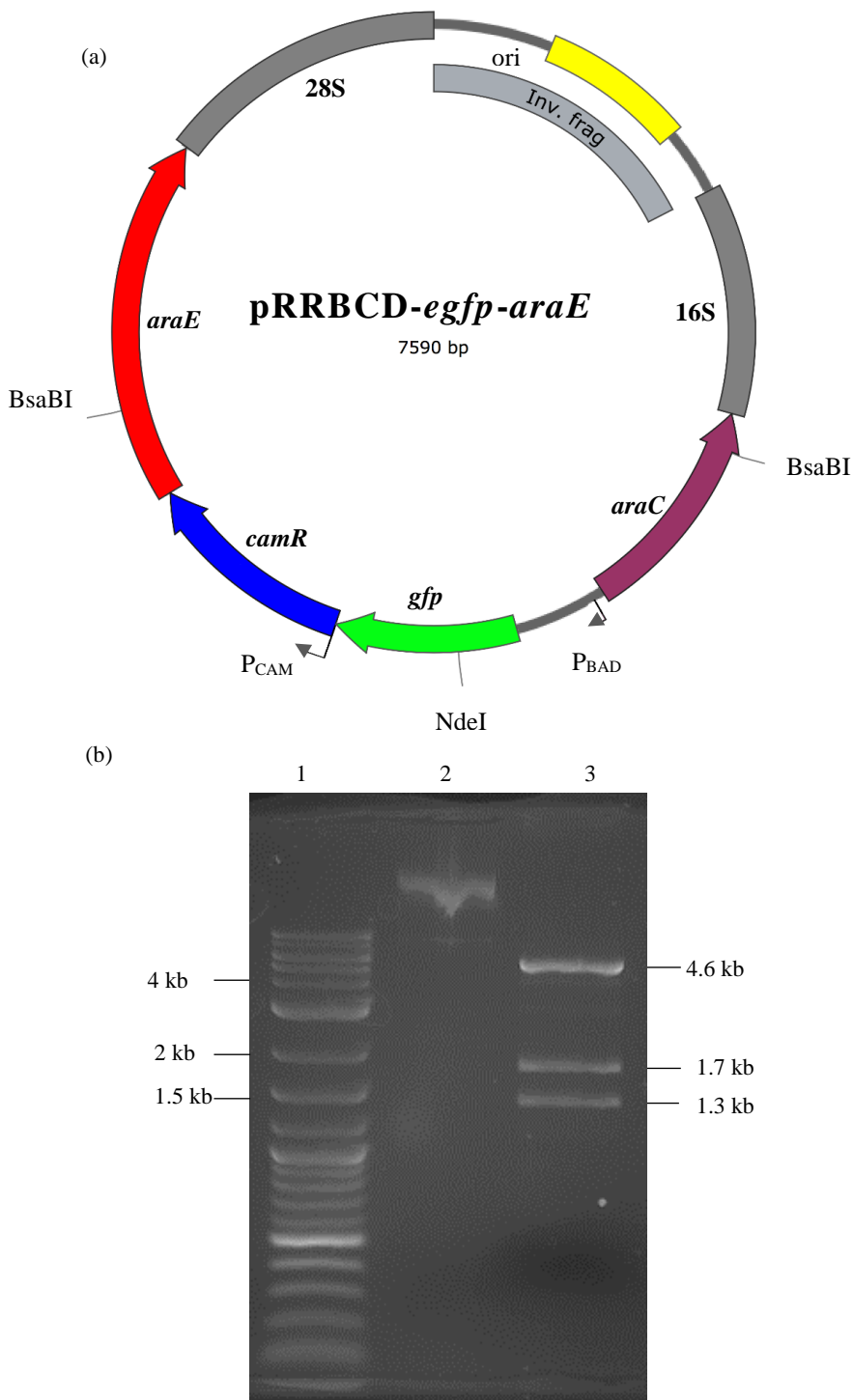


Figure 9. Verification of pRRBCD-*egfp-araE* by restriction analysis.

(a) Restriction map of the plasmid indicating *NdeI* and *BsaBI* restriction sites.

(b) Gel image showing uncut and digested pRRBCD-*egfp-araE* with *NdeI* and *BsaBI*.

Expected fragment sizes: 4.6 kb; 1.7 kb; and 1.3 kb.

Samples: 1, 2-Log DNA ladder; 2, pRRBCD-*egfp-araE*; 3, pRRBCD-*egfp-araE* *NdeI/BsaBI*

3.1.1.2 Plasmid sequencing

The plasmids carrying the *araE* and *lacYA177C* genes were analysed using next generation sequencing in order to verify these constructs and check for possible spontaneous mutations (including indels). The plasmids were first checked using NanoVue spectrophotometer to determine the concentration and purity (Table 4), which may affect sequencing data quality.

Table 4. DNA concentration and purity of plasmids pRRBCD-*egfp-araE* and pRRBCD-*egfp-lacYA177C* using NanoVue Plus Spectrophotometer. Elution buffer was used as a reference for NanoVue readings.

pRRBCD- <i>egfp-araE</i>		pRRBCD- <i>egfp-lacYA177C</i>	
Conc. ng/ μ L	453	Conc. ng/ μ L	790
A260/A280	1.808	A260/A280	1.849
A260/A230	2.266	A260/A230	2.107

The ratios obtained were confirmed to be within the accepted range (A260/A280~1.8-2; A260/A230~2-2.2), confirming high purity of the DNA samples. The reads obtained from the Torrent Server were analysed and assembled using *de novo* assemblers. CLC Genomics software was used for read mapping and to check for any mutations/abnormalities in the output sequence. The analysis of the verified consensus of both plasmids revealed lack of mutations or deletions throughout the entire sequence. However, a fragment of size 1.3 kb at the start of the insert appeared to be inverted (shown in Figure 10) in both constructs. The inversion arose due to a cloning artefact and it was away from the pBAD regulatory region or the insert, therefore had no impact on gene expression or transformation. Figure 10 represents the plasmid maps for each plasmid generated by SnapGene Viewer using the verified consensus.

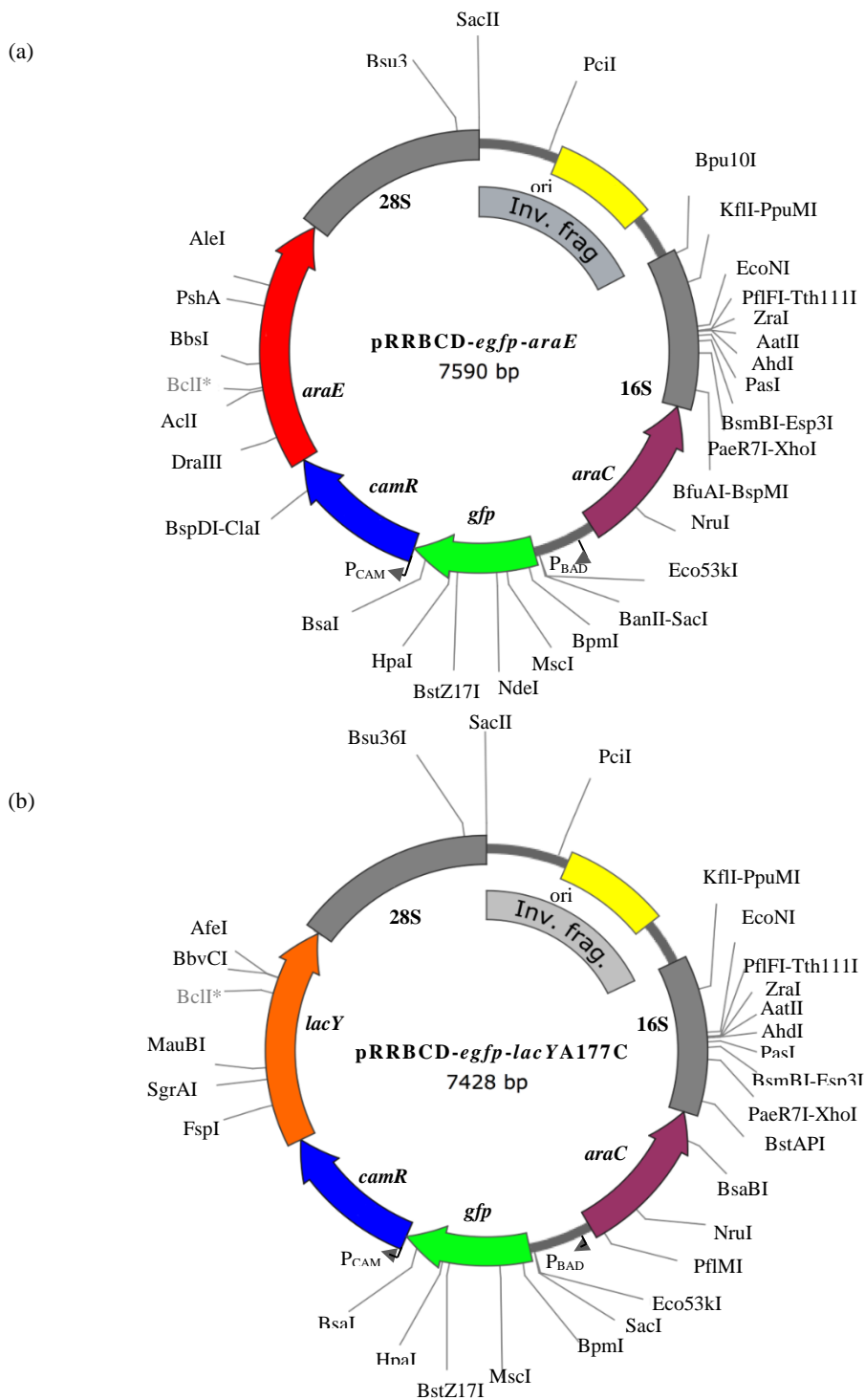


Figure 10. Plasmid maps showing the locations of the arabinose transporter genes, P_{BAD} promoter and AraC regulatory region, reporter gene *gfp*, and the chloramphenicol resistance gene cassette. Images were generated using SnapGene using sequences obtained from Ion Torrent PGM. The region highlighted in grey represents the inverted region upstream of the P_{BAD} regulatory region. (a) pRRBCD-*egfp-araE* (b) pRRBCD-*egfp-lacYA177C*.

3.1.1.3 Investigation of *gfp* induction using solid agar plates

The verified plasmids were first validated in *E. coli* for the induction of GFP, which was placed under the control of an inducible P_{BAD} promoter so as to test its functionality. For this purpose, fluorescence testing was conducted on single colonies of the *E. coli* strains carrying the plasmids. *E. coli*/pRRBCD-*egfp-lacYA177C* and *E. coli*/pRRBCD-*egfp-araE* strains were grown on LB agar plates supplemented with 10 µg/mL chloramphenicol and final concentration of 0.1% arabinose. A fixed concentration of arabinose was used, as this experiment focused solely on checking for the presence of GFP induction. Control plates were tested in parallel without arabinose present in the medium. The bacterial cultures were re-streaked to single colonies; these were tested using bright field and fluorescence microscopy after one day of growth. Both confluent and single colonies displayed high-intensity fluorescence. Figure 11 illustrates a single colony of each strain and its relevant fluorescence intensity with and without arabinose present in the medium. The results suggested that the P_{BAD} promoter in the plasmids were functional in *E. coli*, allowing transcription of the downstream *gfp* gene in the presence of arabinose.

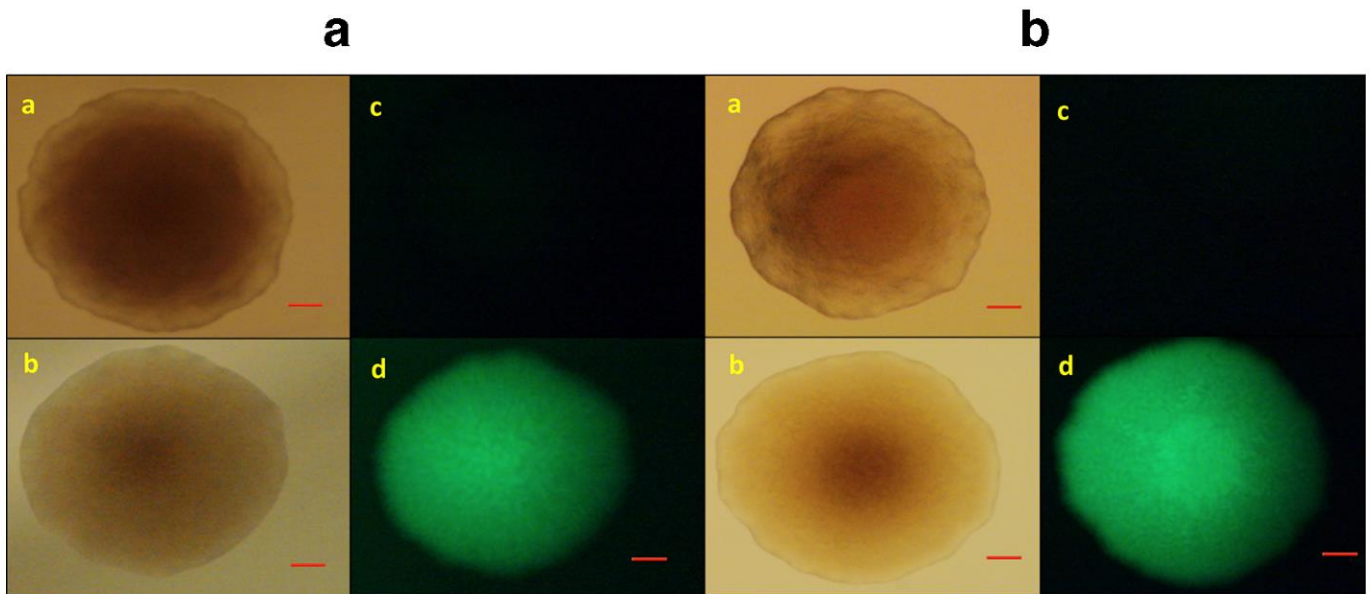


Figure 11. Fluorescence images of *E. coli* strains carrying the arabinose transporter genes, in the presence of 0.1% final concentration arabinose (Ramesh *et al.*, 2019). The same imaging settings were used for the test cultures and the negative control. The red scale bar denotes 100 μ M.

(a) *E. coli*/pRRBCD-*egfp-araE* (b) *E. coli*/pRRBCD-*egfp-lacYA177C*. a,b- under ambient light, c,d- fluorescence, a,c-without arabinose, b,d- with arabinose

3.1.2 Integration of the gene cassettes carrying the *araE* and *lacYA177C* genes into the chromosome of *C. jejuni* 11168H

The validated expression plasmids were subsequently tested in *Campylobacter*. The gene cassettes carrying the *araE* and mutant *lacY* were introduced into *C. jejuni* via electroporation. The integration of the gene cassettes was confirmed by PCR, using the forward primers (ak233, ak234, and ak235), as they correspond to the three rRNA loci present in the *C. jejuni* chromosome.

3.1.2.1 Checking electroporation efficiencies of *C. jejuni* 11168H with control plasmids

The pRRC and pSpoT plasmids were used as controls for electroporation experiments. Previous studies with various *C. jejuni* strains confirmed the efficiency of both plasmids (Ikeda and Karlyshev, 2012; Karlyshev and Wren, 2005a). The pRRC and pSpoT plasmids were

purified from their respective *E. coli*/pRRC and *E. coli*/pSpoT strains and confirmed by restriction analysis. Figures 12 and 13 illustrate the expected fragments obtained with restriction analysis.

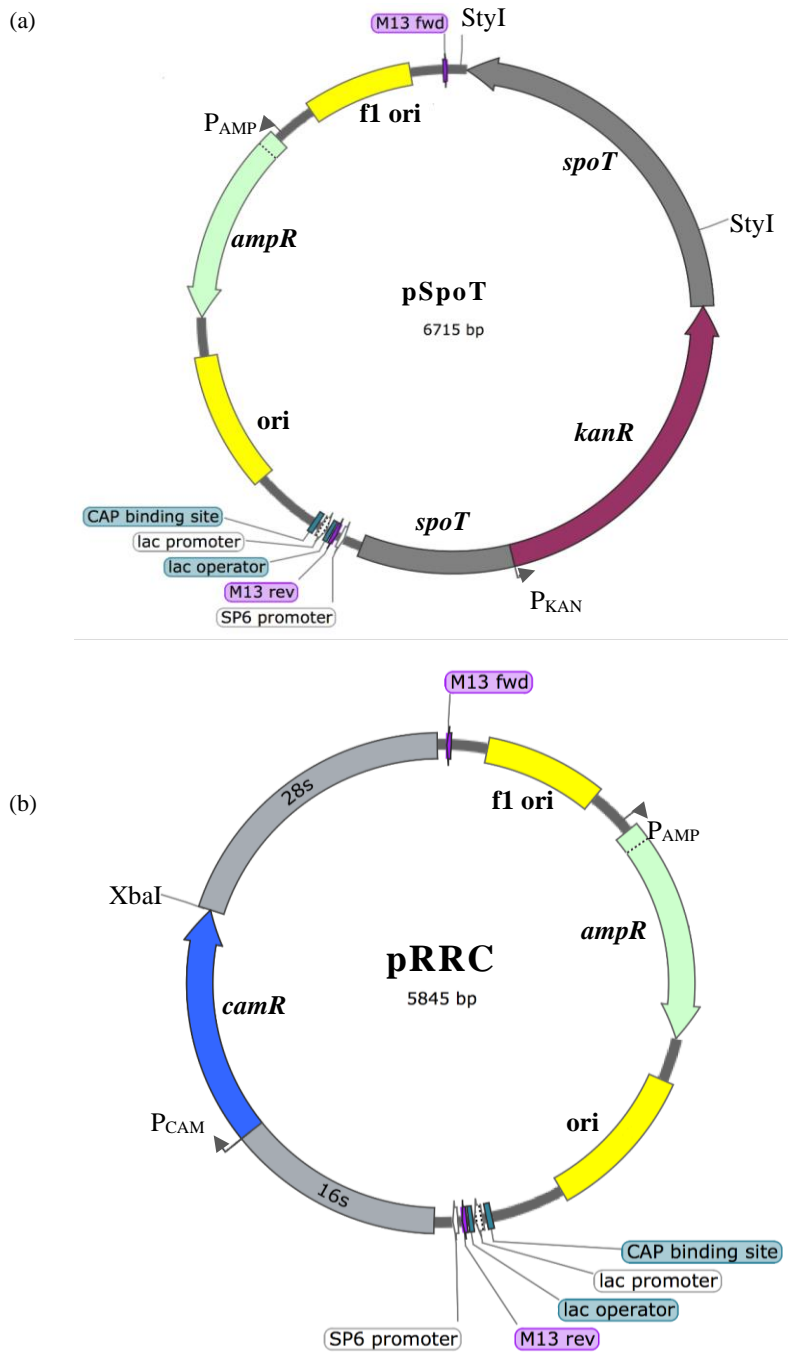


Figure 12. Restriction maps of control plasmids.
 (a) pSpoT (b) pRRC

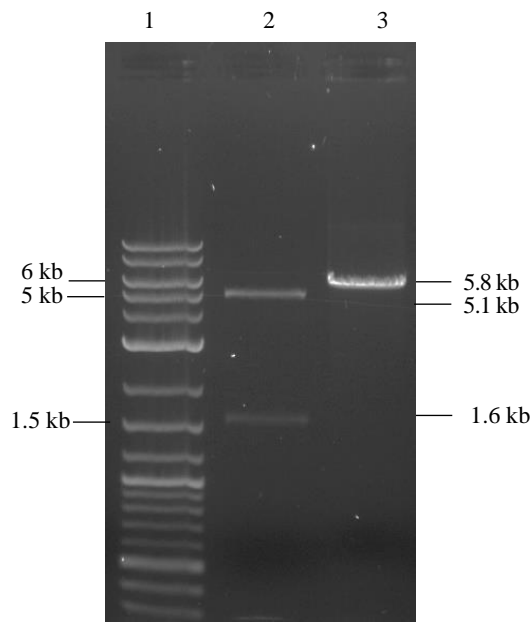


Figure 13. Restriction analysis of control plasmids.

Gel image showing digested pSpoT and pRRC. Plasmid pSpoT was digested with StyI. Plasmid pRRC was digested with XbaI. Expected fragment sizes: pSpoT with StyI- 5.1 kb and 1.6 kb; pRRC with XbaI- 5.8 kb.

Samples: 1, 2-Log DNA ladder; 2, pSpoT StyI; 3, pRRC XbaI.

1 μg of each control DNA was used for electroporation, and a time constant between 5.0–5.3 ms was obtained. The electroporation efficiencies for 11168H/pRRC ranged between 452 CFU/ μg DNA to 572 CFU/ μg DNA, while the efficiencies for 11168H/pSpoT ranged between 80 CFU/ μg DNA to 152 CFU/ μg DNA. The resulting transformants were then re-streaked for verification by PCR. For 11168H/pSpoT transformants, *spoT_for* and *spoT_rev* primers specific to the *spoT* gene were chosen. For 11168H/pRRC, the forward primers (ak233-ak235) corresponding to the three different 16S rRNA loci and reverse primer ak237 corresponding to the *cam^r* resistance cassette were used. The locations of these primers in their respective plasmids is illustrated in Figures 14 and 15. The transformants were also confirmed to be *Campylobacter* by Gram staining, as illustrated in Figure 16. Figure 17 indicates the PCR verification results. The expected size of 2.4 kb was obtained with 11168H/pRRC transformant. The result also confirms that the chloramphenicol gene cassette was inserted at the chromosomal site where primer ak233 is located. The expected size of 3.7 kb with

11168H/pSpoT transformants was obtained, and the presence of the *kan^r* resistance cassette was confirmed.

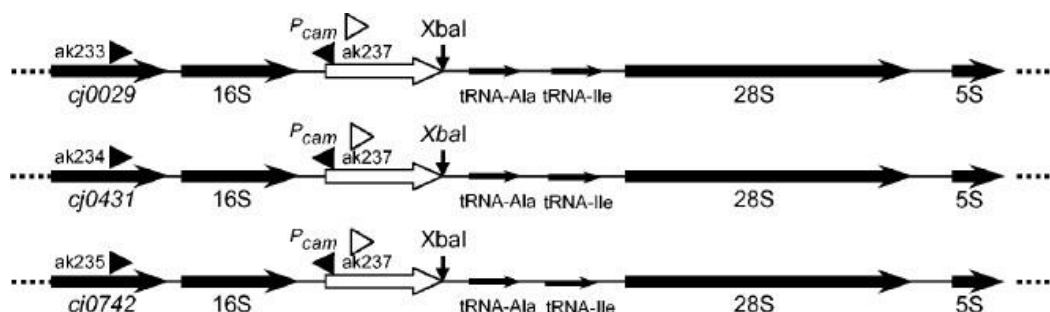


Figure 14. Linear genetic map of plasmid pRRC and the three possible products of recombination of the plasmid with the different rRNA loci of the *C. jejuni* genome (Karlyshev and Wren, 2005a). Regions corresponding to primers ak233-ak235 are as shown.

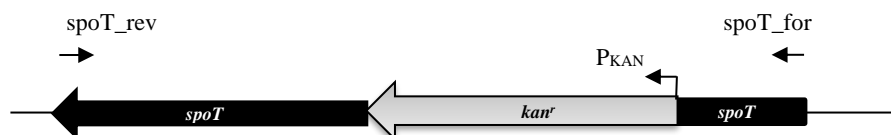


Figure 15. Linear genetic map of plasmid pSpoT showing the location of spoT_for and spoT_rev primers on the plasmid.

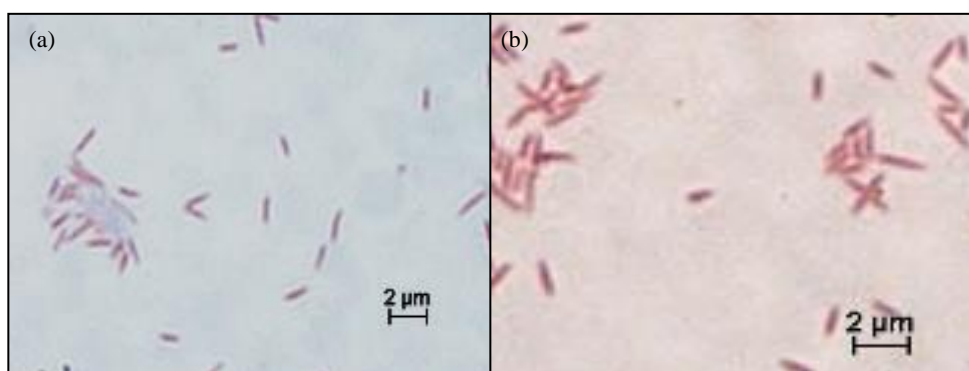


Figure 16. Verification of morphology of *C. jejuni* transformants by Gram staining. *C. jejuni* cultures were grown under microaerobic conditions at 37°C for 24 h, Gram stained, and visualized using a light microscope.

(a) 11168H/pRRC (b) 11168H/pSpoT

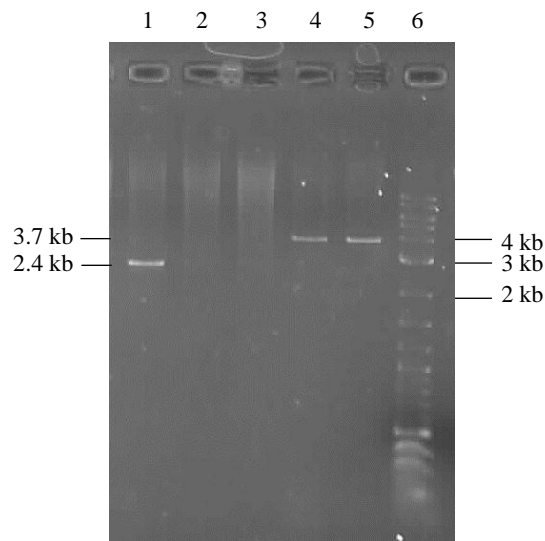


Figure 17. Confirmation of integration of *cam^r* cassette into the chromosome of *C. jejuni* and inactivation of *spoT* gene in *C. jejuni* 11168H. Genomic DNA was used as template DNA. GoTaq[®] Green Master Mix was used. Expected sizes: 11168H/pRRC-2.4 kb; 11168H/pSpoT-3.7 kb.

Samples: 1, 11168H/pRRC with primers ak233/ak237; 2, 11168H/pRRC with primers ak234/ak237; 3, 11168H/pRRC with primers ak235/237; 4, 11168H/pSpoT clone 1 with primers spoT_for and spoT_rev; 5, 11168H/pSpoT clone 2 with primers spoT_for and spoT_rev; 6, 2-Log DNA ladder.

3.1.2.2 Electroporation of pRRBCD-*egfp-araE* and pRRBCD-*egfp-lacYA177C* plasmids into *C. jejuni* chromosome

C. jejuni 11168H competent cells were confirmed to be efficient when tested with the control plasmids. The same batches of cells were used for the electroporation of the plasmids carrying the arabinose transporter genes. 1 μ g of pRRBCD-*egfp-araE* and pRRBCD-*egfp-lacYA177C* plasmids were electroporated into *C. jejuni* 11168H electrocompetent cells with a time constant ranging between 5.0 ms and 5.1 ms. Control plasmid pRRC was electroporated in parallel. A few colonies were obtained with the 11168H/pRRBCD-*egfp-lacYA177C* with an electroporation efficiency of 52 CFU/ μ g DNA, whereas no colonies were obtained with the 11168H/pRRBCD-*egfp-araE* after four days of incubation. Electroporation efficiency of 582 CFU/ μ g DNA was obtained with the control electroporation experiment.

The re-streaked transformants (11168H/pRRBCD-*egfp-lacYA177C*) were tested by Gram

staining and confirmed to be *Campylobacter* (Figure 18). The integration of the gene cassette carrying the *lacYA177C* was verified using PCR. GoTaq[®] Green Master Mix was used for the amplification experiment. PCR amplification confirmed that the integration of the gene cassette carrying the *lacYA177C* was inserted into the integration site where primer ak235 sequence is located (Figure 19). Two sets of primer pairs were employed for the verification. One set consisted of the same forward primers (ak233-ak235) as used with pRRC transformants, and the reverse primer pBAD_up sequence was located near the P_{BAD} promoter itself, which amplified the 2.4 kb region between the chromosomal site and the P_{BAD} promoter (Figure 20). The second set of primers (pBAD_for and ak237) were positioned within the plasmid, which produced a fragment size of 1.1 kb, amplifying the internal region between P_{BAD} promoter and chloramphenicol promoter region (Figure 20). However, several repeats of electroporation of pRRBCD-*egfp-araE* into *C. jejuni* 11168H cells were carried out and all the attempts resulted in no colonies.



Figure 18. Verification of morphology of *C. jejuni* 11168H/pRRBC-*egfp-lacYA177C* by Gram staining. *C. jejuni* culture was grown under microaerobic conditions at 37°C for 24 h, Gram stained, and visualized using a light microscope.

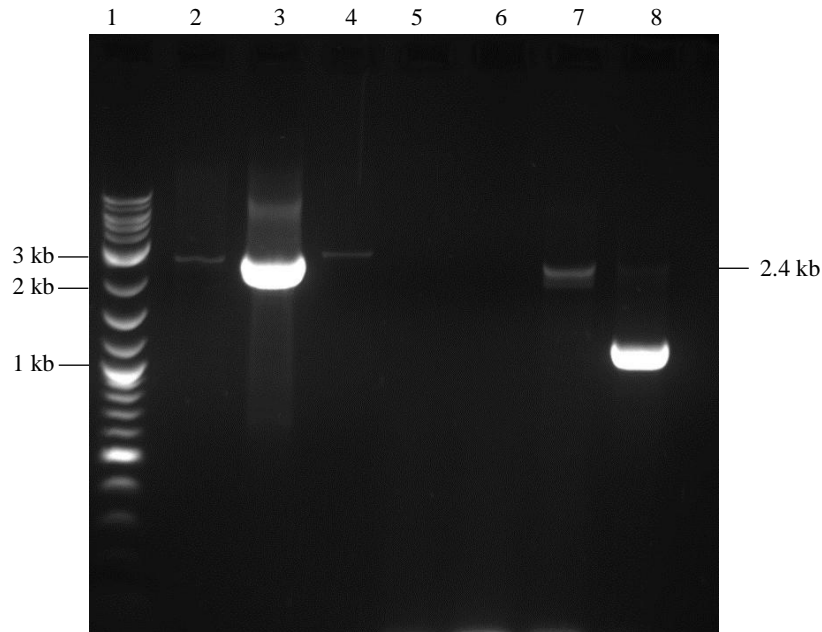


Figure 19. Confirmation of integration of the gene cassette carrying *lacYA177C* gene into *C. jejuni* 11168H chromosome by PCR. Genomic DNA was used as template DNA. GoTaq[®] Green Master Mix was used. Expected sizes: 11168H/pRRC with primers ak233-ak235/ak237- 2.4 kb; 11168H/pRRBCD-*egfp-lacYA177C* and ak233-ak235/pBAD_up-2.4 kb; 11168H/pRRBCD-*egfp-lacYA177C* and pBAD_for/ak237- 1.1 kb. Samples: 1, 2-Log DNA ladder; 2, 11168H/pRRC with primers ak233/ak237; 3, 11168H/pRRC with primers ak234/ak237; 4, 11168H/pRRC with primers ak235/237; 5, 11168H/pRRBCD-*egfp-lacYA177C* with primers ak233/pBAD_up; 6, 11168H/pRRBCD-*egfp-lacYA177C* with primers ak234/pBAD_up; 7, 11168H/pRRBCD-*egfp-lacYA177C* with primers ak235/pBAD_up; 8, 11168H/pRRBCD-*egfp-lacYA177C* with primers pBAD_for/ak237.

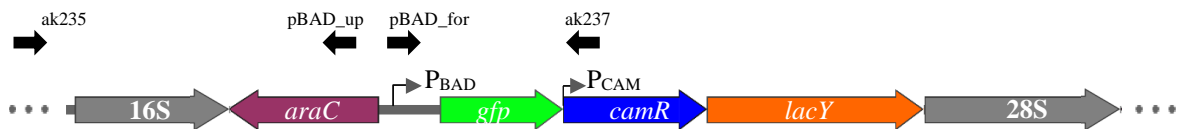


Figure 20. Linear genetic map of *C. jejuni* 11168H/pRRBCD-*egfp-lacYA177C* showing the location of the PCR verification primers. Location of primer 235 corresponds to the RNA locus present in the *C. jejuni* genome. Location of pBAD_up and pBAD_for primers corresponds to the pBAD regulatory region. Location of primer ak237 corresponds to the *cam^r* cassette.

3.1.3 Troubleshooting electroporation issues with pRRBCD-*egfp-araE* plasmid

To troubleshoot electroporation experiments of the *araE* construct in *C. jejuni*, the 11168H/*cj1051* mutant was constructed. This gene encodes a restriction endonuclease. Holt *et al.* (2012) suggested that the absence of this gene resulted in an increase in electroporation efficiency of wild-type *C. jejuni* NCTC 11168. In this part of the study, the 11168H/*cj1051* mutant was constructed via insertional mutagenesis using *kan^r* cassette. This strain was then utilized for the electroporation with pRRBCD-*egfp-araE* plasmid.

3.1.3.1 Construction of 11168H/*cj1051* mutant

Primers *cj1051_for* and *cj1051_rev* were designed and utilized to PCR amplify the *cj1051* gene (≈ 1.96 kb) with flanking regions from the *C. jejuni* 11168H genome, as illustrated in Figure 21. The steps involved in the construction of this plasmid are shown in Figure S1 in the Appendix. The gene fragment was cloned into the pGEM-T Easy vector, and the intermediate recombinant plasmid pGEM-T-1051 was verified by restriction analysis using enzymes *SwaI* and *SalI*. The digestion produced the expected fragments of sizes 3.4 kb and 1.6 kb, as illustrated in Figure 22. Plasmid pRRT was digested with *XbaI* and *NheI*, and the fragment containing the *tet^r* resistance cassette was gel-purified and used for cloning. The *tet^r* resistance cassette was inserted into the *XbaI* site of the intermediate construct (Figure 22a). The resulting recombinant p1051-*tetR* clone was then verified by restriction analysis using *SwaI*. The digestion produced expected fragments of sizes 5 kb and 2.8 kb, confirming that the gene and the *tet^r* were in the same orientation, as illustrated in Figure 23.

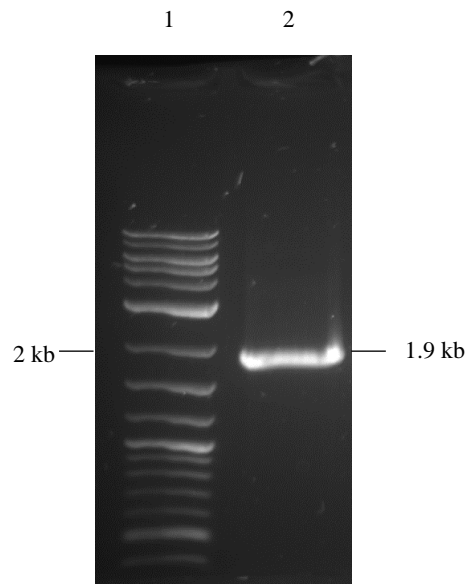


Figure 21. Amplification of *cj1051* gene with flanking regions from *C. jejuni* 11168H chromosomal DNA using primers *cj1051_for* and *cj1051_rev* by PCR. GoTaq[®] Green Master Mix was used. Expected size is approximately 1.96 kb. Samples: 1, 2-Log DNA ladder; 2, *cj1051*.

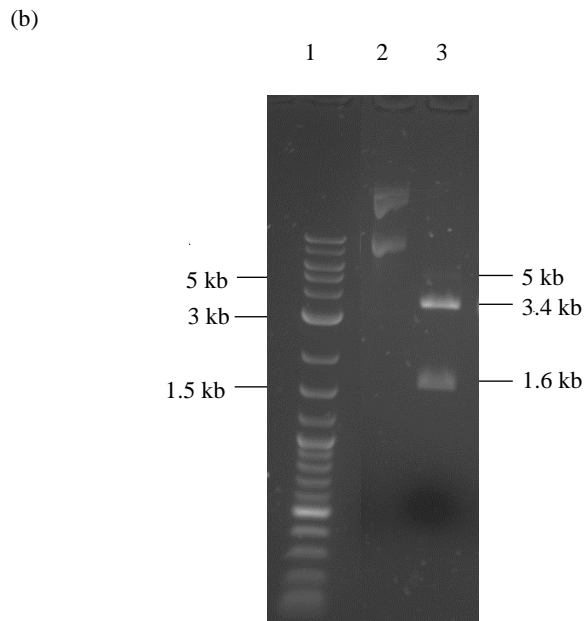
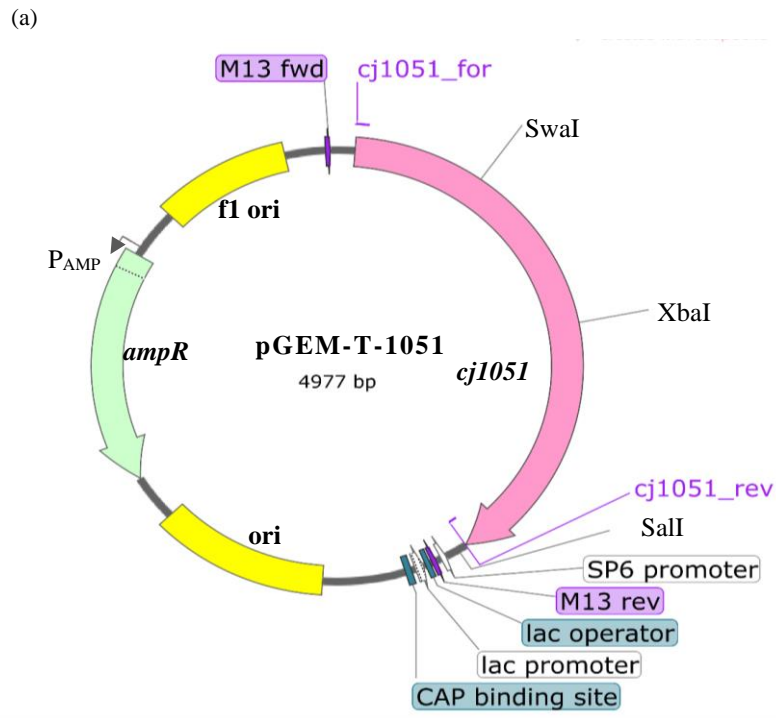


Figure 22. Verification of an intermediate construct pGEM-T-1051 by restriction analysis.

(a) Restriction map of the plasmid indicating the *SwaI* and *SalI* sites used in restriction analysis, and *XbaI* insertional site used in cloning experiment.

(b) Gel image showing uncut (lane 2) and digested pGEM-T-1051 with *SwaI* and *SalI* (lane 3). Expected fragment sizes: 3.4 kb and 1.6 kb.

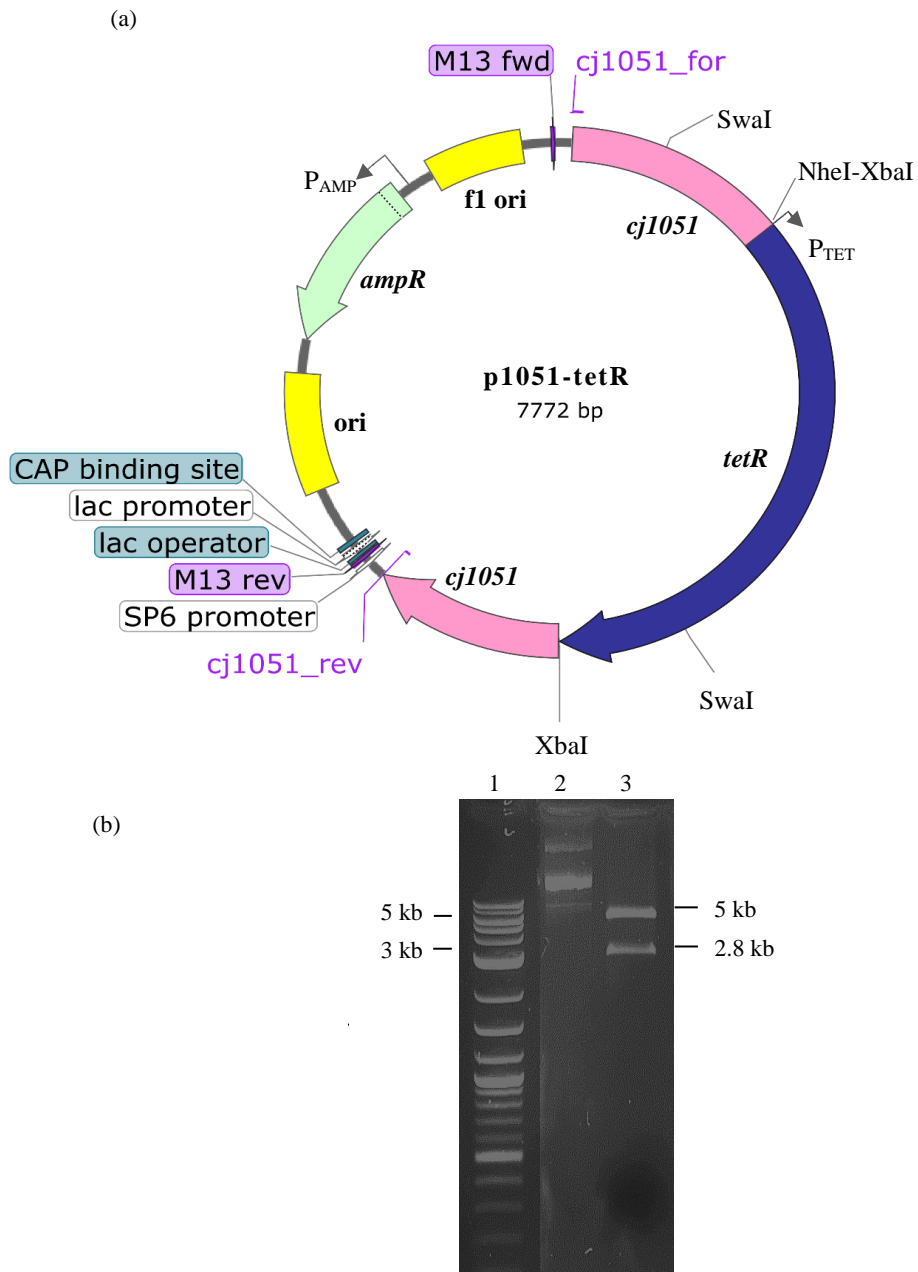


Figure 23. Verification of p1051-tetR by restriction analysis.

(a) Restriction map of the plasmid indicating the *Swa*I sites used in restriction analysis, and *Xba*I and *Xba*I/*Nhe*I integration sites after the insertion of the *tet*^r cassette.

(b) Gel image showing uncut and digested p1051-tetR with *Swa*I.

Expected fragment sizes: 5.0 kb and 2.8 kb.

Samples: 1, 2-Log DNA ladder; 2, p1051-tetR; 3, p1051-tetR *Swa*I

The verified p1051-tetR clone was then electroporated into *C. jejuni* 11168H cells to create the mutant *C. jejuni* 11168H/*cj1051*. 1 µg of p1051-tetR DNA was electroporated, with a time constant of 5 ms. The entire electroporated volume was placed on a non-selective plate and incubated for 10 h under standard conditions. Several studies in the past have varied initial incubation times ranging from 4 h to overnight (Miller *et al.*, 1988; Davis *et al.*, 2008; Hansen *et al.*, 2007; Holt *et al.*, 2012). This study employed an incubation period of 10 h after initial attempts with overnight as well as 5 h incubation resulted in poor or no transformants. The growth was then re-streaked onto a tetracycline selective plate and incubated for a further three days until tetracycline-resistant colonies appeared producing an electroporation efficiency of 30 CFU/µg DNA.

The transformants were confirmed by Gram staining as *Campylobacter*. The mutation was further confirmed by PCR employing *cj1051* gene-specific primers. An expected PCR product of size 4.9 kb was obtained, and the result confirmed that the *tet^r* cassette has disrupted the *cj1051*, thereby creating the knockout mutant 11168H/*cj1051* (Figure 24).

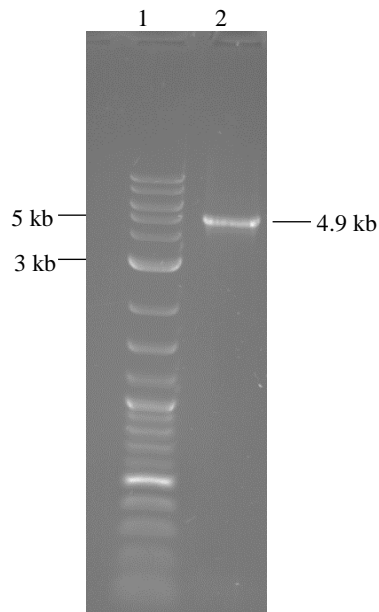


Figure 24. Verification of the inactivation of *cj1051* gene in *C. jejuni* 11168H by PCR. Primers *cj1051_for* and *cj1051_rev* were used. Genomic DNA was used as template DNA. GoTaq[®] Green Master Mix was used. Expected PCR product size: 4.9 kb.

Samples: 1, 2-Log DNA ladder; 2, 11168H/*cj1051*

3.1.3.2 Comparison of electroporation efficiencies

Electroporation efficiencies of the *C. jejuni* wild-type 11168H and the 11168H/*cj1051* mutant strains were compared. Competent cells of both strains were prepared in parallel, and 1 μ g of pRRC and pSpoT plasmids were electroporated into both. The non-selective plates were incubated for the same length of time, approximately 10 h. After the initial incubation period, pRRC transformants were re-streaked onto chloramphenicol (10 μ g/mL) selective plates and pSpoT transformants were re-streaked onto kanamycin (50 μ g/mL) selective plates, respectively. The selective plates were incubated for a further two to three days. The experiment was repeated thrice in a conventional incubator, and the results are summarized in Table 5.

Table 5. Comparison of electroporation efficiencies (CFU/ μ g DNA) of *C. jejuni* 11168H and 11168H/*cj1051* electroporation experiments. Values are an average from three biological replicates.

	pRRC		pSpoT	
	11168H	11168H/ <i>cj1051</i>	11168H	11168H/ <i>cj1051</i>
Electroporation efficiency CFU/ μ g	545	818	29	230
<i>p</i> -value	0.009		0.015	
Standard deviation	58.95	80.01	4.35	85.29

A few clones from each electroporation plate were selected and analysed by Gram staining and verified by PCR by using pRRC integration and *spoT* gene specific primers. PCR produced expected band sizes with both pRRC and pSpoT transformants, as illustrated in Figure 25. After three repeats of electroporation of both strains with pRRC and pSpoT, the efficiency was observed to be higher for the mutant with both control plasmids as anticipated; as reflected by the *p*-values shown in Table 5.

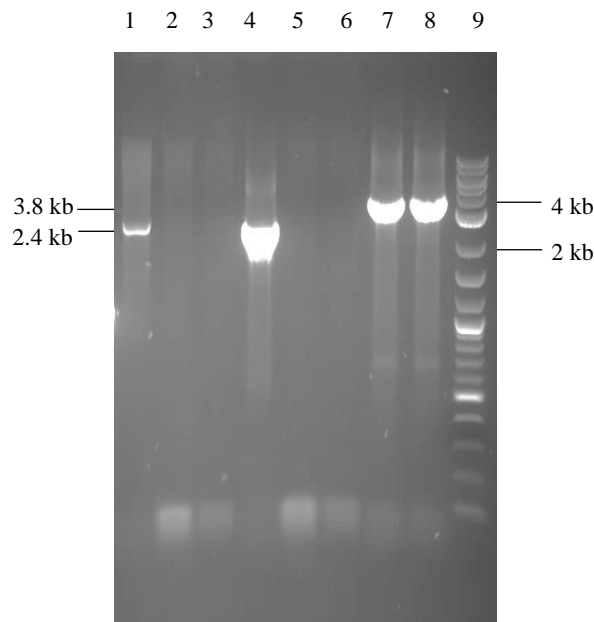


Figure 25. PCR verification of *C. jejuni* 11168H and 11168H/*cj1051* transformants from comparative electroporation experiment using control plasmids. Genomic DNA was used as template DNA. GoTaq[®] Green Master Mix was used. Expected sizes: pRRC transformants-2.4 kb; pSpoT transformants-3.8 kb.

Samples: 1, 11168H/pRRC with primer ak233/ak237; 2, 11168H/pRRC with primer ak234/ak237; 3, 11168H/pRRC with primer ak235/ak237; 4, 11168H/*cj1051*/pRRC with primer ak233/ak237; 5, 11168H/*cj1051*/pRRC with primer ak234/ak237; 6, 11168H/*cj1051*/pRRC with primer ak235/ak237; 7, 11168H/pSpoT with primers spoT_for and spoT_rev; 8, 11168H/*cj1051*/pSpoT with primers spoT_for and spoT_rev; 9, 2-Log DNA ladder.

3.1.3.3 Electroporation of pRRBCD-*egfp-araE* into 11168H/*cj1051* mutant

The 11168H/*cj1051* mutant was used as a recipient strain for the electroporation of pRRBCD-*egfp-araE* construct. 1 μ g of DNA was electroporated into freshly prepared mutant electrocompetent cells. The time constant was 5.1 ms with electroporation efficiency of approximately 80 CFU/ μ g DNA. The transformant was re-streaked for further analysis by Gram staining and PCR verification. Gram staining revealed the culture to be pure *C. jejuni*, as illustrated in Figure 26. For PCR verification, the same set of primers (ak233-ak235/pbad_up) used for the confirmation of 11168H/pRRBCD-*egfp-lacYA177C* was employed. GoTaq[®] Green Master Mix was used for the PCR amplification experiment. The internal primer pair (pRR1/ak237), as illustrated in Figure 27, amplified the region from the 16S rRNA gene to the

chloramphenicol promoter site (Figure 28). Conversely, no amplification was observed with the external primers corresponding to the chromosomal sites (ak233- ak235). The lack of amplification could therefore be due to a technical error in analysis.



Figure 26. Verification of morphology of *C. jejuni* 11168H/pRRBCD-*egfp-araE* by Gram staining. *C. jejuni* culture was grown under microaerobic conditions at 37°C for 24 h, Gram stained, and visualized using a light microscope.

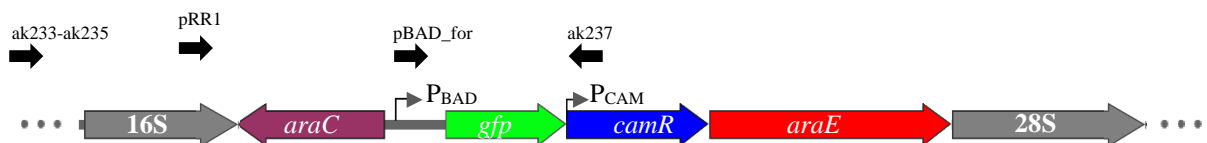


Figure 27. Linear genetic map of *C. jejuni* 11168H/pRRBCD-*egfp-araE* showing the location of the PCR verification primers. Location of primers ak233-235 corresponds to the three different RNA loci present in the *C. jejuni* genome. Location of primer ak237 corresponds to the *cam^r* cassette. Location of primer pBAD_for corresponds to the pBAD regulatory region. Location of primer pRR1 corresponds to the region downstream of the 16S rRNA gene.

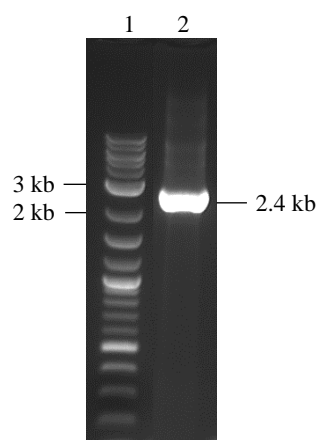


Figure 28. PCR amplification of region between 16S gene and chloramphenicol promoter site in 11168H/pRRBCD-*egfp-araE* transformant by PCR. Genomic DNA was used as template DNA. GoTaq[®] Green Master Mix was used. Primers pRR1/ak237 were used for verification. Expected PCR product size: 2.4 kb. Samples: 1, 2-Log DNA ladder; 2, 11168H/*cj1051*/pRRBCD-*egfp-araE*

3.1.4 Confirmation of integration of gene cassette carrying *araE* gene

In this section, sequencing of *C. jejuni* 11168H/*cj1051*/pRRBCD-*egfp-araE* and 11168H/pRRBCD-*egfp-lacYA177C* were carried out. The sequencing was conducted to ensure no point mutations in and near the respective genes existed and no deletions or possible insertions had occurred.

3.1.4.1 Genome sequencing of derivative *C. jejuni* strains carrying *araE* and *lacYA177C* genes

The genome sequencing was carried out as described in Materials and Methods. CLC Genomics Workbench software mapped the reads onto the reference genome sequence of *C. jejuni* strain NCTC 11168 (1,641,481 nt, accession number GCA_000009085.1) and then the consensus sequences were extracted. The contigs generated by Torrent server SPAdes *de novo* assembly plug-in (version 5.0.0.0.0) were used to close the gaps between the consensus sequences. Following this, the generation of contiguous sequences was further verified by read mapping. The sizes of the genomes of the *C. jejuni* derivatives were as follows: 1,647,847 nt (102× coverage) (11168H/*cj1051*/pRRCBD-*egfp-araE*) and 1,645,651 nt (152× coverage)

(11168H/pRRBCD-*egfp-lacYA177C*).

Figures 29 and 30 illustrate the results from the assembled sequences, confirming that the gene cassettes carrying the *araE* and modified *lacY* had been integrated between the rRNA gene clusters as anticipated. The sequencing results revealed no point mutations or indels had occurred and confirmed the derivatives were free of errors. In addition, full functionality of P_{BAD} , *gfp*, *araE/lacYA177C* and regulatory regions required for expression was confirmed. The genome sequences are available in the NCBI GenBank database under the accession numbers CP022439.1 (11168H/pRRBCD-*egfp-lacYA177C*) and CP022559.1 (11168H/*cj1051/pRRBCD-egfp-araE*). The insertional inactivation of the *cj1051* gene in *C. jejuni* 11168H/*cj1051/pRRBCD-egfp-araE* was also confirmed.

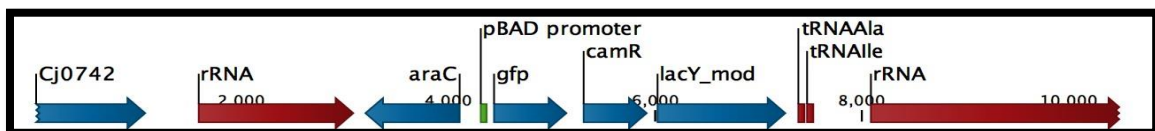


Figure 29. Chromosomal region between the 16S and 28S rRNA genes containing the P_{BAD} promoter, *cam^r*, *gfp*, and *lacYA177C* genes (CLC Genomics Workbench software) (Ramesh *et al.*, 2019).

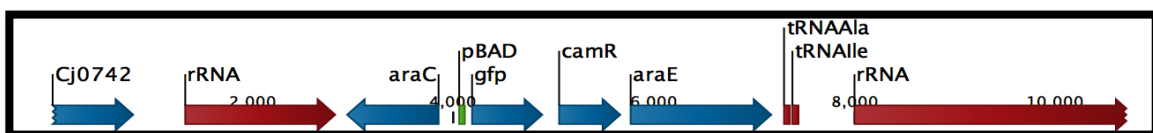


Figure 30. Chromosomal region between the 16S and 28S rRNA genes containing P_{BAD} promoter, *cam^r*, *gfp*, and *araE* genes (CLC Genomics Workbench software) (Ramesh *et al.*, 2019).

3.1.4.2 Confirmation of gene cassette integration in the 11168H/*cj1051/pRRBCD-egfp-araE* strain by polymerase chain reaction

The genome sequencing convincingly indicated, that the derivative strain 11168H/*cj1051/pRRBCD-egfp-araE* did not possess any deletions and the gene cassette was

indeed integrated correctly into the rRNA gene cluster. To troubleshoot any potential issues with PCR, another type of polymerase (NEB Q5[®] High-Fidelity DNA Polymerase) with higher proofreading properties was purchased and checked with the same clone with external primers. The expected fragment of 4.6 kb was obtained with this polymerase, as illustrated in Figure 31, further confirming that the gene cassette carrying the *araE* gene was successfully integrated into the integration site (corresponding to primer ak235) of the *C. jejuni* chromosome.

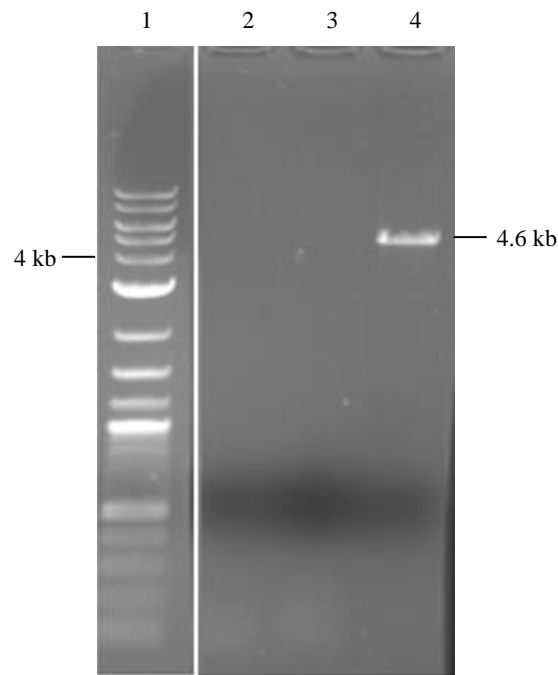


Figure 31. Confirmation of the integration of gene cassette carrying the *araE* gene into the chromosome of *C. jejuni* 11168H/*cj1051* by PCR (Ramesh *et al.*, 2019). Genomic DNA was used as template DNA. NEB Q5[®] High-Fidelity DNA Polymerase was used for PCR. Expected PCR product size: 4.6 kb. Samples: 1, 2-Log DNA ladder; 2, 11168H/*cj1051*/pRRBCD-*egfp-araE* with primers ak233/ak237; 3, 11168H/*cj1051*/pRRBCD-*egfp-araE* with primers ak234/ak237; 4, 11168H/*cj1051*/pRRBCD-*egfp-araE* with primers ak235/ak237.

3.1.5 Investigation of expression of *gfp* in *C. jejuni* derivative strains

The expression study of the reporter gene *gfp* in both the *C. jejuni* derivative strains will be carried out in this section. GFP induction in the presence of varying concentrations of arabinose will be monitored in solid culture by fluorescence microscopy and in liquid culture using

fluorimetry. Induction studies of GFP were conducted to investigate the function of the inserted arabinose transporter genes and to confirm the functionality of P_{BAD} promoter in *C. jejuni*.

3.1.5.1 Growth rates of derivative strains

To determine the growth rates of the *C. jejuni* derivative strains in comparison to the wild-type 11168H, OD₆₀₀ was measured using shaking cultures. The effect of arabinose addition was also investigated in these assays, using a final arabinose concentration of 0.2%. The OD₆₀₀ of the initial inoculum was adjusted to 0.1, and readings were taken every 1.5 h up to 6 h. Arabinose was added after 6 h, and the cultures were incubated on a shaker at 250 rpm overnight. During the initial 6 h, the growth rates were comparable between the two derivative strains, as well as among the induced and uninduced cultures of all three strains. Final OD₆₀₀ measurements were taken after 21 h (which included overnight incubation). Figure 32 illustrates that the wild-type uninduced culture grew faster than the uninduced derivative cultures. In addition, a significant difference in OD₆₀₀ readings was obtained between induced and un-induced cultures of 11168H, *lacYA177C* and *araE* derivative strains, indicating the addition of arabinose caused retardation of growth in all three strains.

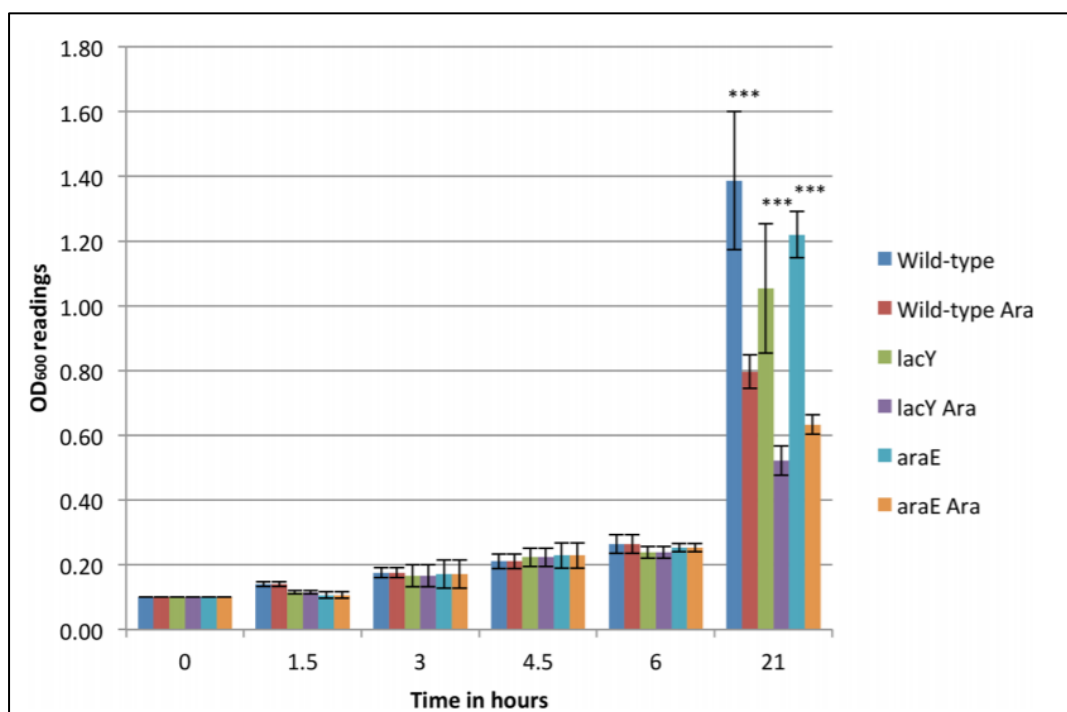


Figure 32. Comparison of growth rates of the *C. jejuni* derivative strains to the wild-type strain (Ramesh *et al.*, 2019). Wild-type, 11168H uninduced; Wild-type Ara, 11168H induced; *lacY*, 11168H/pRRBCD-*egfp-lacYA177C* uninduced; *lacY* Ara, 11168H/pRRBCD-*egfp-lacYA177C* induced; *araE*, 11168H/*cj1051/pRRBCD-egfp-araE* uninduced; *araE* Ara, 11168H/*cj1051/pRRBCD-egfp-araE* induced. The graph is a representation of three biological experiments with three technical replicates. *** $p \leq 0.001$. *P* values to show the effect of arabinose on the growth rate of each strain when compared to uninduced cells (11168H, $p < 0.0001$; 11168H/pRRBCD-*egfp-lacYA177C*, $p < 0.0001$; 11168H/*cj1051/pRRBCD-egfp-araE*, $p < 0.0001$). *P* values to show the difference in growth rate between wild-type and derivative strains at the end of 21 h (11168H and pRRBCD-*egfp-lacYA177C*, p , 0.8; 11168H and 11168H/*cj1051/pRRBCD-egfp-araE*, p , 0.9).

3.1.5.2 GFP expression studies using solid agar plates

The *gfp* induction in the derivative strains was studied using solid agar plates as was done when testing *E. coli*. The CBA plates for *C. jejuni* growth contained 0.02% and 0.2% final concentrations of arabinose, as well as 10 $\mu\text{g/mL}$ of chloramphenicol. The strains were incubated for two to three days until single colonies appeared. The single colonies were then visualized using brightfield and fluorescence microscopy, but no fluorescence was detected. The positive control plate *E. coli/pRRBCD-egfp-lacYA177C* indicated good-intensity

fluorescence of single colonies under the same microscope settings.

3.1.5.3 GFP expression studies using liquid cultures by fluorimeter

The *C. jejuni* derivative strains were further tested in liquid cultures for the induction of the reporter gene *gfp*. *E. coli*/pRRBCD-*egfp-lacYA177C* was tested alongside as a control for the fluorimeter experiment. Testing in liquid cultures was carried out, as the sensitivity for GFP fluorescence signal is greater when compared to fluorescence microscopy. After incubation of test cultures with arabinose for 2 h, fluorescence signals from the whole cell suspensions and lysates were measured. Figures 33 and 34 revealed highly significant differences in induction signals between the induced and uninduced cultures of the *E. coli* control strain. Conversely, a somewhat noticeable difference was obtained between induced and uninduced cultures of the 11168H/*cj1051*/pRRBCD-*egfp-araE* in whole cell suspensions only (Figure 33). In addition, whole suspensions of 11168H/pRRBCD-*egfp-lacYA177C* demonstrated no difference in signals, as reflected by the very high *p*-value. Similarly, the variation between the induced and uninduced cultures of the lysates of both derivative strains was not statistically significant, as shown in Figure 34.

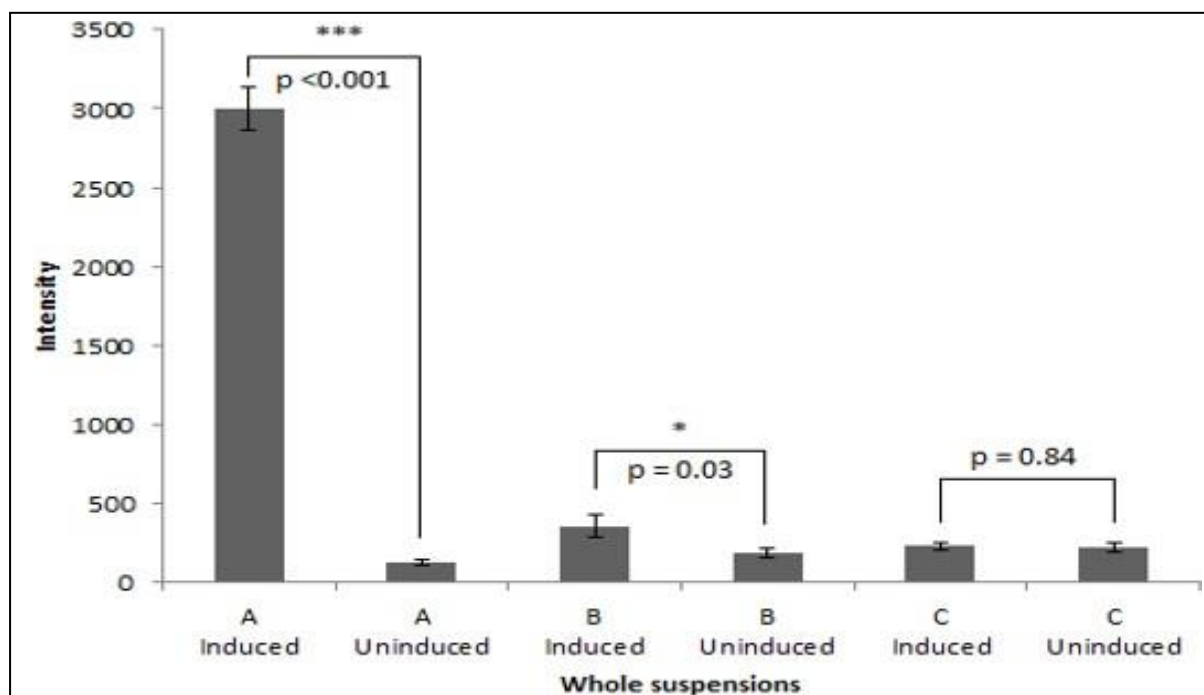


Figure 33. Fluorescence testing of bacterial samples in whole cell suspensions before and after induction (Ramesh *et al.*, 2019). The graph is a representation of three independent experiments consisting of three technical replicates. Standard error mean values were used to represent error bars. * $0.01 < p \leq 0.05$, *** $p \leq 0.001$. (A) *E. coli*/pRRBCD-*egfp-lacYA177C*, (B) 11168H/*cj1051*/pRRBCD-*egfp-araE*, (C) 11168H/pRRBCD-*egfp-lacYA177C*.

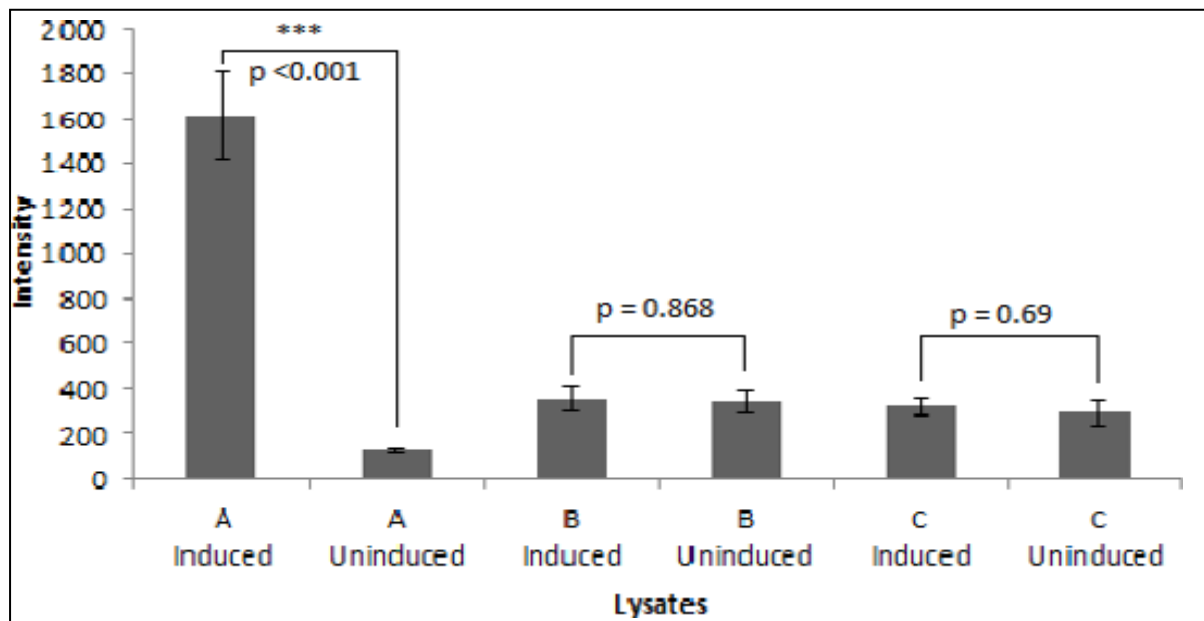


Figure 34. Fluorescence testing of bacterial samples in lysates before and after induction (Ramesh *et al.*, 2019). The graph is a representation of three independent experiments consisting of three technical replicates. Standard error mean values were used to represent error bars. *** $p \leq 0.001$.

(A) *E. coli*/pRRBCD-*egfp-lacYA177C*. (B) 11168H//*cj1051*/pRRBCD-*egfp-araE*. (C) 11168H/pRRBCD-*egfp-lacYA177C*.

3.2 Investigation of the molecular mechanism of biofilm formation and dispersal in *C. jejuni* 11168H

This section describes the investigation of a possible role of a nuclease gene in the dispersal mechanism of *C. jejuni* 11168H biofilms. Gene *cj0979* annotated as a putative nuclease in *C. jejuni* strain NCTC 11168 was further studied in this section. This gene is conserved in other *Campylobacter* genomes; however, its function has not yet been studied. An 11168H/*cj0979* knockout mutant was constructed and the effects of the mutation on the biofilm formation were studied. In addition, the enzymatic properties of purified Cj0979 were investigated. The protein was purified utilising an inducible promoter of the pBAD33 plasmid, following a previous study by Guzman *et al.* (1995). The function of extracellular nucleases in association with biofilm formation is widely studied in other bacteria such as *S. aureus* and *V. cholerae* (Kierdowski *et al.*, 2011; Seper *et al.*, 2013). Brown *et al.* (2015b) investigated the role of nucleases in *C. jejuni* RM1221 biofilms. This study is the only published work associated with *Campylobacter*. Thus, in this section, investigation of a possible role of a putative nuclease Cj0979 in *Campylobacter* 11168H biofilm dispersion was studied, as it has not been reported elsewhere.

3.2.1 Identification of the dispersal stage of *C. jejuni* 11168H and investigation of composition of DNA complex in the culture supernatant

The biofilm-forming pattern of the wild-type *C. jejuni* 11168H was investigated in this work. Biofilm formation was quantified using CV assay. In addition, the detection of nuclease activity in the culture supernatant was also attempted. DNase assays of the supernatant samples were conducted to detect any potential activity of a secreted nuclease possibly present in the medium. Furthermore, mass spectrometry analysis was employed in an attempt to determine the composition of DNA complex present in the culture supernatant.

3.2.1.1 Identification of the dispersal stage of *C. jejuni* 11168H strain

This section primarily focuses on the investigation of the biofilm formation pattern of the widely studied *C. jejuni* 11168H strain. Initially, biofilm formation was optimized after comparing its growth on different surfaces, such as widely used test tubes and microtiter plates. Both types of surfaces were employed in previous studies with *Campylobacter* (Brown *et al.*, 2015b; Reeser *et al.*, 2007; Joshua *et al.*, 2006). Preliminary results obtained with test tubes and microtiter plates suggested that the ring-like structure formed at the air-liquid interface was thicker in test tubes. Therefore, test tubes were chosen as the growth surface for further biofilm testing of *C. jejuni* 11168H strain.

For biofilm assays, *C. jejuni* strain 11168H was grown in BHI broth with an initial OD₆₀₀ of 0.5. The cultures were grown in test tubes under static, microaerobic conditions at 37°C. Cultures were tested for biofilm formation every 24 h for a period of 10 days. A good amount of biofilm was observed after Day 4 with the highest formation on Day 8, after which reduction in the absorbance signals of the stained biofilm occurred, thus confirming dispersal. The test tube assays included a two-step washing process to remove excess background staining that had occurred at the base of the tubes. The results in Figure 35 represent three assays. The difference in absorbance values between Day 8 and Day 9 was statistically significant, therefore confirming the dispersal phenomenon shown in the Figure 35. The error bars were quite high, possibly because each test tube in the technical replicates was separately manually handled, introducing potential variations in the experiment.

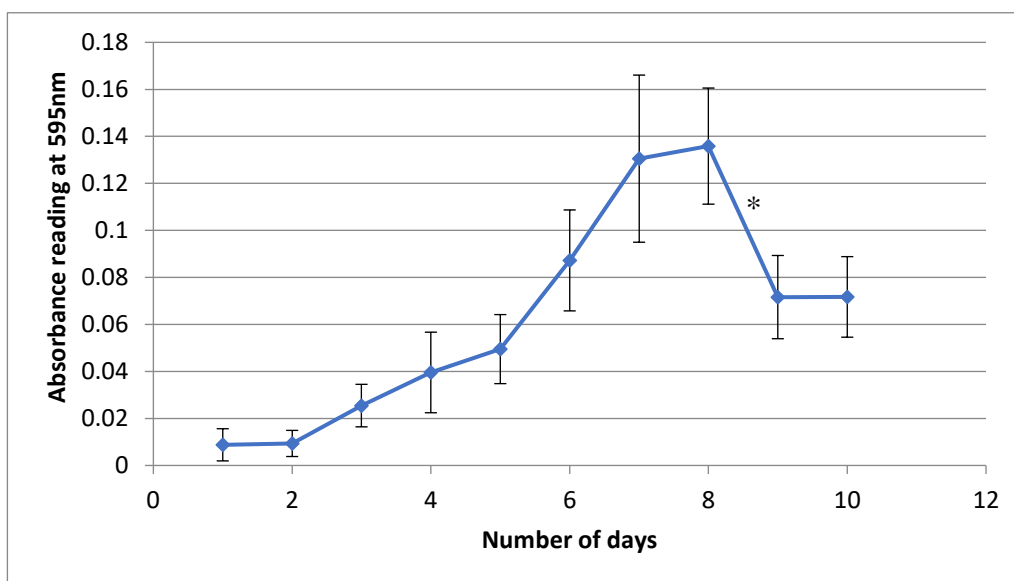


Figure 35. Biofilm formation curve of *C. jejuni* 11168H in borosilicate test tubes over a 10 days period. Absorbance of CV staining was measured at 595 nm. The graph is a representation of three independent experiments comprising of three technical replicates. * $0.01 < p \leq 0.05$. p value – comparison of absorbance values between day 8 and 9. Standard error of mean values was used to represent error bars.

3.2.1.2 DNase test assays of 11168H supernatant

Since biofilm dispersion was observed after Day 8, the bacterial culture was then spun down and the supernatant was tested for DNase activity. The bacterial pellet was discarded. The culture supernatant was sterilized by passing through a millipore filter and employed for DNase testing with eDNA-B as substrate. The eDNA-B was purified from biofilm on day 8. The eDNA-B was incubated with sterile culture supernatant to check for any possible nuclease activity. After incubation for 1 h at 37°C, the samples were run on an agarose gel. Figure 36 illustrates the results of this analysis and the bands appeared very faint on the gel as the concentration of eDNA-B was very low, approximately 8 ng/μL. This gel did not conclusively indicate whether there was any DNase activity; on one hand, the band for eDNA-B was not visible in lanes 3-5, but on the other hand, the bands in these lanes have appeared higher than the control lane 2.

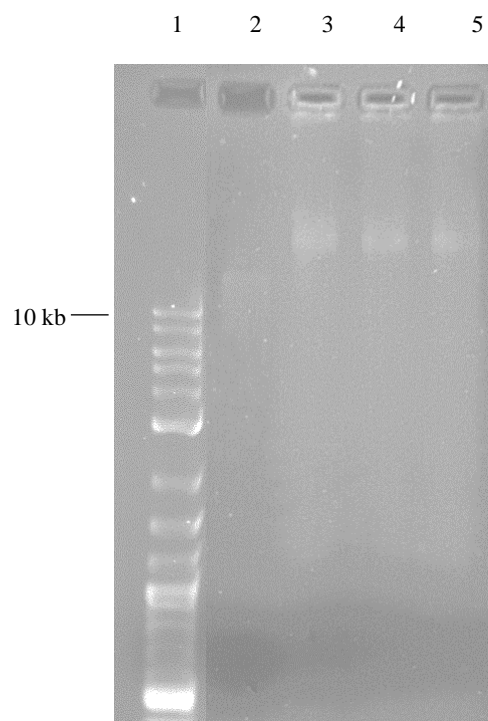


Figure 36. Gel image showing the attempt to detect DNase activity in culture supernatant. Equal amounts of DNA are present in lanes 2-5. Sample in lane 2 was run alongside as a positive control.

Samples: 1, 2-Log DNA ladder; 2, eDNA-B; 3- 5, eDNA-B, 1x DNase buffer, and 10 μ L supernatant.

To determine whether any residual eDNA in the supernatant remained, 10 μ L of the sample was purified and labelled eDNA-S. The product was run alongside eDNA-B and the culture supernatant for comparison, revealing that the purified product contained eDNA, as seen in Figure 37. Table 6 represents the concentrations and purity obtained with the eDNA samples in comparison with a diluted pSpOT plasmid with TE buffer (control). The very low values of A260/A230 of the eDNA samples may suggest carryover of sugars from the biofilm matrix itself. This experiment confirmed the presence of eDNA in the supernatant sample but the mystery regarding slow mobility remained. Since sample in lane 4 without the addition of eDNA-B has moved slower on the gel, a suspicion was that the observed retardation could be due to the interactions of the salts present in the culture media.

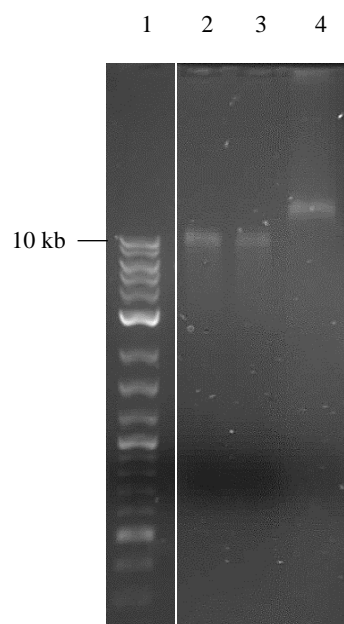


Figure 37. Gel electrophoresis of eDNA samples and culture supernatant. Equal amounts of eDNA was applied in lanes 2 and 3.

Samples: 1, 2-Log DNA ladder; 2, eDNA-B; 3, eDNA-S; 4, 10 μ L culture supernatant.

Table 6. NanoVue readings of purified eDNA samples. Diluted pSpoT was used a positive control for the NanoVue readings due to low concentration test samples. Elution buffer was used as a reference. Table shows average values of three readings.

Samples	Concentration(ng/ μ L)	A260/A280	A260/A230
pSpoT	8.67	1.64	1.88
eDNA-B	12.33	1.47	0.68
eDNA-S	6.67	1.51	0.86

To exclude the effects of medium and DNase buffer on the difference in mobility, eDNA-B was incubated with just pure BHI broth and the DNase buffer at 37°C. The results confirmed that the medium and DNase buffer do not affect the mobility, as all samples ran at the same level on the gel (Figure 38).

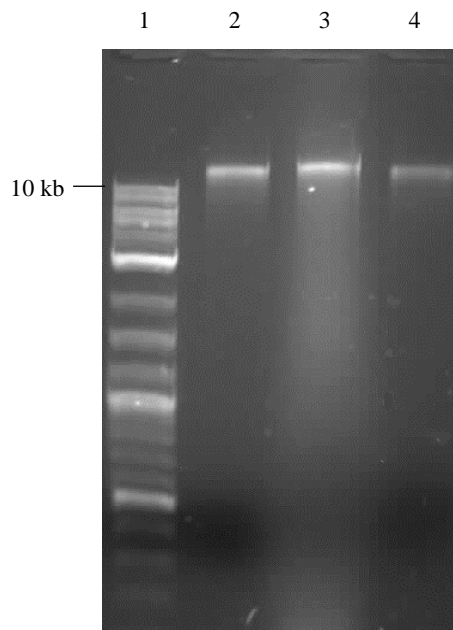


Figure 38. Investigation of possible effects of medium and DNase buffer on migration pattern of eDNA samples on a 1% agarose gel. Equal amounts of DNA were added (lanes 2-4). 10 μ L of BHI broth was used. 2 μ L of 10 \times NEB DNase buffer was used.

Samples: 1, 2-Log DNA ladder; 2, eDNA-B; 3, eDNA-B and BHI broth; 4, eDNA-B and 1 \times NEB DNase buffer.

The DNase assays with eDNA-B were repeated for reproducibility. The effect of proteinase K on the culture supernatant was also tested. Table 7 provides the NanoVue readings of the eDNA samples from the new purification which was used in the following test. The samples were treated with proteinase K to obtain DNA from bound proteins in the supernatant sample. All the samples were incubated under the same conditions. The results seen in Figure 39 correspond to the results seen on previous gels (Figures 36, 37, and 38).

There was no effect of the medium or the buffer on the mobility. In all the cases with supernatant and eDNA samples, the band migrated slower. Proteinase K-treated samples ran faster than culture supernatant samples, suggesting that proteinase K had an effect in breaking down contaminants present in the DNA complex in culture supernatant sample. Therefore, this led to the deduction that there may be DNA binding proteins present in the supernatant sample.

Table 7. NanoVue readings of second purification of eDNA-B. Diluted pSpoT plasmid was used as control for low concentration test samples. Elution buffer was used as a reference for NanoVue readings. Table shows average values of three readings

Samples	Concentration (ng/ μ L)	A260/A280	A260/A230
pSpoT (Control)	8.67	1.640	1.879
eDNA-B	15.67	1.382	0.962

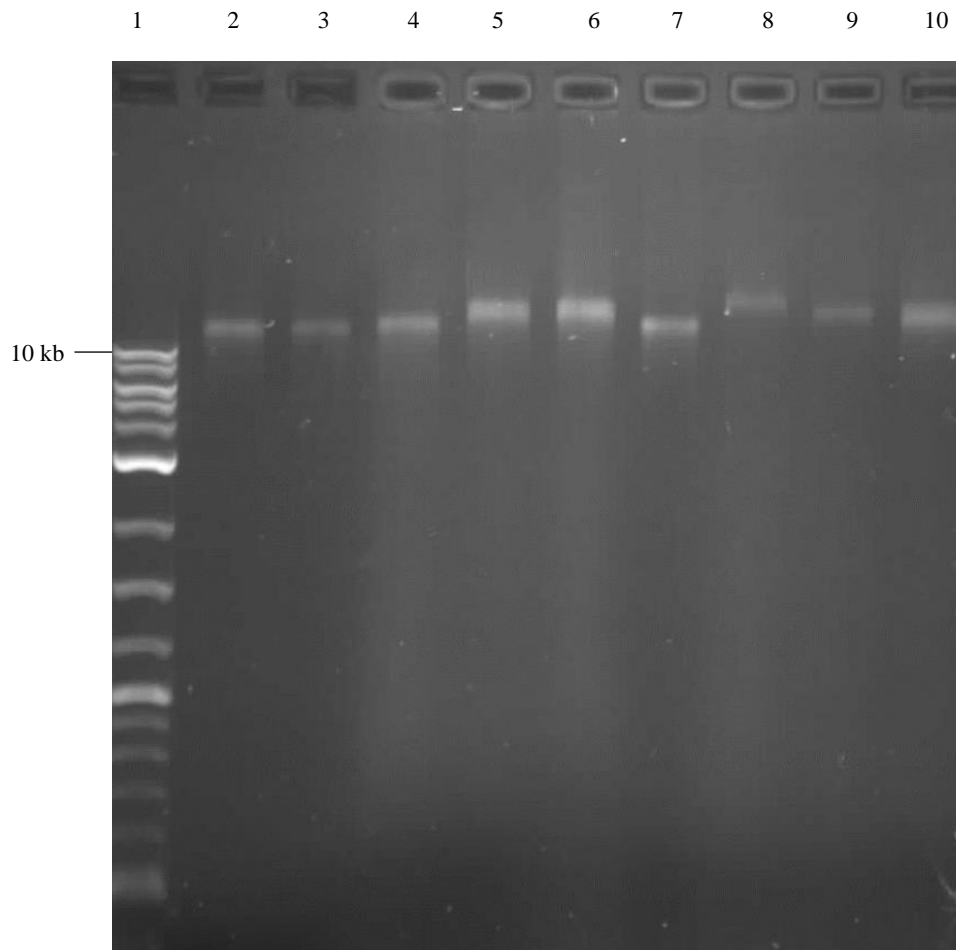


Figure 39. DNase activity of Proteinase K treated culture supernatant. Equal amounts of 55 ng of eDNA-B was used. 10 μ L of culture supernatant was used. 2 μ L of 10 \times DNase buffer was used. 10 μ L of BHI broth was used.

Samples: 1, 2-Log DNA ladder; 2, eDNA-B; 3, eDNA-S; 4, eDNA-B and BHI broth; 5, eDNA-B and supernatant; 6, eDNA-B, supernatant, and DNase buffer; 7, eDNA-B and DNase buffer; 8, culture supernatant; 9, Proteinase K treated supernatant; 10, Proteinase K treated supernatant and eDNA-B.

3.2.1.3 Treatment of 11168H supernatant with trypsin

This section focused on the elimination of all low molecular weight proteins and sugars and smaller DNA/RNA fragments from the culture supernatant sample. The supernatant sample was buffer exchanged with 1x TE buffer producing a fold change of 2500, using spin concentrators (5 kDa cut-off value). The supernatant sample after media exchange was tested for A260/A280 and A260/A230 ratios using NanoVue spectrophotometer (Table 8). The values were compared with the culture supernatant sample, which served as a control.

Table 8. DNA concentration and purity of supernatant sample before and after media exchange. TE buffer was used as a reference for NanoVue readings. Table shows average values from three repeats. Comparison of the purities between two samples is denoted by *p* values

Samples	Nucleic acids (μg)	A260/A280	<i>p</i> -value	A260/A230	<i>p</i> -value
Supernatant sample after media exchange	5.2	1.291	< 0.002	0.206	< 0.002
Culture supernatant	6.8	1.380		0.388	

Results in Table 8 showed a slight decrease in A260/A280 ratio of the supernatant sample after buffer exchange, which indicated a change in the composition of the protein-DNA complex, potentially due to the removal of oligonucleotides smaller than 5 kDa. In addition, a reduction observed in the A260/A230 ratio suggests the presence of a larger fraction of carbohydrates after the buffer exchange process. The change in both ratios was statistically significant ($p < 0.002$) when compared to the culture supernatant.

Trypsin was chosen as the enzyme to cleave proteins into smaller peptides in the supernatant sample after media exchange. After the trypsin treatment, the sample was further passed through a spin concentrator (cut-off value of 10 kDa) to remove cleaved off peptides. BCA assay was used to determine protein concentrations of the retentate and flowthrough fractions; the amounts present in each fraction are as represented in Table 9. The amount of protein

content was greater in the flowthrough fraction 1 when compared to the retentate fraction, as expected. In addition, the amount of nucleic acids in the retentate sample compared to flowthrough fractions also confirmed that the majority of the nucleic acids was retained (as retentate) in the column itself, as anticipated. All three trypsin-treated fractions were run on a gel, and a visible band was obtained with only the retentate fraction (Figure 40). This suggests that the flowthrough fractions contained DNA fragments smaller than 10 kDa. These fragments cannot be detected on a 1% agarose gel.

Table 9. Estimation of protein and DNA content in samples. NanoVue spectrophotometer was used to determine the amount of nucleic acids in each fraction. BCA assay was used to determine the amount of protein in each fraction. Table represents average values from three readings.

Samples	Nucleic acids (μg)	Protein (μg)
Supernatant sample after media exchange	9.2	124
Retentate	4.7	18.8
Flowthrough 1	1.9	23.4
Flowthrough 2	1.8	18.2

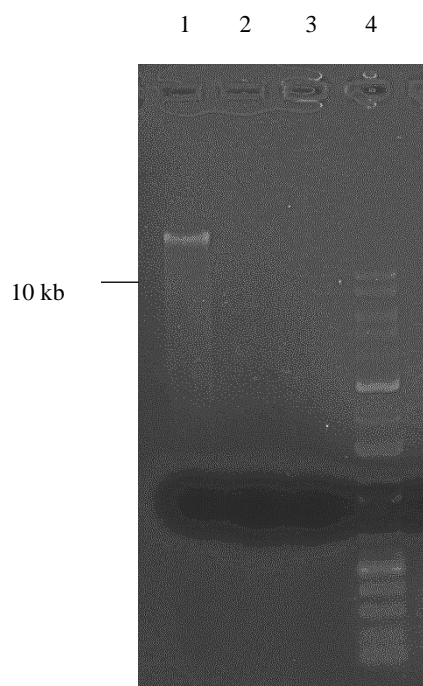


Figure 40. Gel electrophoresis of trypsin treated samples. The three fractions (retentate and flowthrough fractions) were run on a 1% agarose gel. 0.3 μ g of DNA was applied to lanes 1-3.

Samples: 1, Retentate; 2, flowthrough 1; 3, flowthrough 2; 4, 2-Log DNA ladder.

3.2.1.4 Identification of products of proteolytic digestion

Mass spectrometry analysis was carried out to explore the composition of proteins in the DNA complex. Flowthrough fraction 1, containing cleaved off peptides, was sent for mass spectrometry analysis to the Cambridge Centre for Proteomics. The data was received in an MHT file format where the proteins were listed according to their abundance index (emPAI) values. The resulting file had more than 300 hits; therefore, to simplify data analysis, the first 10 most abundant proteins were shortlisted and further investigated (Table 10).

Table 10. List of the first 10 most abundant proteins detected by Mass spectrometry

GenBank accession code	Name	Function	Sample	
			emPAI	Percentage(%)
sp Q9PI64 ACP_CAMJE	Acyl carrier protein	Involved in fatty acid biosynthesis and lipid biosynthesis	13.92	6.3
sp Q9PHM9 IPYR_CAMJE	Inorganic pyrophosphatase	Functions as a hydrolase and involved in hydrolysis of pyrophosphate	10.37	4.7
tr Q0PC22 Q0PC22_CAMJE	Peptidyl-prolyl cis-trans isomerase	Functions as an isomerase and rotamase	8.99	4.5
sp Q9PPE0 TPX_CAMJE	Thiol peroxidase	Converts organic hydroperoxides and hydrogen peroxide to water and alcohols. Involved in oxidative stress protection of the cells.	8.62	3.9
tr Q0PB64 Q0PB64_CAMJE*	Uncharacterized protein		7.93	3.6
sp O69303 EFTU_CAMJE	Elongation factor Tu	Involved in GTP-dependent binding during protein biosynthesis	7.9	3.5
tr Q0PAY5 Q0PAY5_CAMJE	Isocitrate dehydrogenase	Involved in metal ion binding.	5.39	2.4
sp Q9PHY1 SUCC_CAMJE	Succinate-CoA ligase	Plays a functional role in the citric acid cycle (TCA). Involved in the synthesis of either ATP or GTP.	5.19	2.4
sp O69289 CH60_CAMJE	60 kDa chaperonin	Involved in protein refolding and prevents misfolding	4.65	2.1
sp O69298 DNAK_CAMJE*	Chaperone protein DnaK	Involved in ATP binding, protein folding and unfolded protein binding	4.47	2

The function and origin of each protein was studied and summarized in the Table above, and it was concluded that the majority of the proteins listed serve general housekeeping functions excluding one uncharacterized protein with an unknown function. The sequence of this protein was obtained from UniProtKB and used for BLASTp analysis against the Swiss-Prot database to identify similar proteins. The search resulted in one hit with a 43% match to a protein called from YdcH from *E. coli* (Figure 41). Unfortunately, no studies for this protein exist yet.

BLASTp result for uncharacterized protein

Amino acid sequence for uncharacterized protein (Cj0449c)

> Cj0449c (Query sequence)

```
MLHEYRELMSELKGDHAFDKLFDRHNELDLDDMIKDAEEGRTSLSSMEISTLKKEKLVKDELSQYLANYKK
```

>RecName: Full, Uncharacterized protein YdcH (Subject sequence)

Score	Expect	Method	Identities	Positives	Gaps
50.1 bits(118)	7e-09	Compositional matrix adjust.	29/68(43%)	44/68(64%)	4/68(5%)
Query 1	MLHEYRELMSELKGDHAFDKLFDRHNELDLDDMI--KDAEEGRTSLSSMEISTLKKEKLVH	58			
	M EYR+L+S LK ++ F LFD+HN+LD I K+ +GR + E+ +KK+KL +				
<u>Sbjct</u> 1	MFPEYRDLISRLKNENPRFMSLFDKHNKLDHEIARKEGSDGRG--YNAEVVRMKKQKLQL	58			
Query 59	KDELSQYL 66				
	KDE+ + L				
<u>Sbjct</u> 59	KDEMLKIL 66				

Figure 41. BLASTp search result showing sequence alignment between uncharacterized protein and YdcH (*E. coli*).

3.2.1.5 Treatment of 11168H supernatant with dextranase

The A260/A230 ratio of the supernatant sample after media exchange was low suggesting the presence of sugar or sugar-containing compounds (Table 8). To determine whether the presence of dextran-like polysaccharides caused the low ratios, the sample was treated with dextranase, an enzyme that digests dextrans, as in a previous study (Jowiya *et al.*, 2015). The treatment with dextranase was conducted following the protocol provided by the manufacturer. The samples were passed through a spin concentrator (cut-off value of 10 kDa) following treatment. The retentate and flowthrough fractions were checked using gel electrophoresis (Figure 42) and a visible band was obtained only with the retentate sample. However, the flowthrough fractions contained nucleic acids as shown in Table 11. The reason for the lack of detection on the gel could be that the DNA fragments present in these fractions were below 10 kDa and cannot be viewed on a 1% agarose gel. NanoVue readings (Table 11) revealed an increase in the A260/A230 ratio in the retentate fraction; the difference was highly significant when compared to the supernatant sample after media exchange, as denoted by the *p*-value. Despite the difference, there was no substantial increase in the values as was expected following dextranase

treatment. Conversely, the low A260/A230 ratios of the flowthrough fractions confirmed the lack of oligosaccharides in these samples. Table 11 also revealed that pure oligonucleotides with size below 10 kDa were present in the flowthrough fractions, especially flowthrough 2. This was also confirmed by the highly significant difference in the A260/A280 ratios of the flowthrough fractions when compared to the supernatant sample after media exchange. However, the A260/A280 ratio of the retentate fraction also shows a significant increase after the treatment, which was a slight contradiction. In summary, the results suggest that the supernatant sample does not contain any dextran-like polysaccharides neither in the bound nor free forms. The low A260/A230 ratio could suggest the presence of other types of polysaccharides in the supernatant sample that are not cleavable by dextranase.

Table 11. Analysis of supernatant samples after treatment with dextranase. TE buffer was used as a reference for NanoVue readings. Table shows average values with three repeats.

Samples	Nucleic acids (μg)	A260/A280	<i>p</i> values in comparison to supernatant after media exchange	A260/A230	<i>p</i> values in comparison to supernatant after media exchange
Supernatant after media exchange	9.2	1.291		0.206	
Retentate	3.0	1.34	0.001	0.25	<0.0001
Flowthrough 1	1.9	1.82	<0.0001	0.21	0.04
Flowthrough 2	3.9	1.68	<0.0001	0.23	0.05

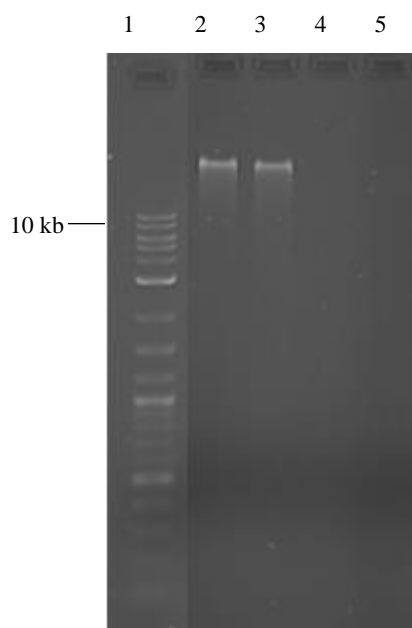


Figure 42. Gel electrophoresis of dextranase treated samples. The final three fractions (retentate and flowthrough fractions) were run on a 1% agarose gel. 0.3 μ g of DNA was applied to lanes 2-5. Sample in lane 2 was applied as a control. Samples in lanes 3-5 are treated with dextranase. Samples: 1, 2-Log DNA ladder; 2, supernatant after media exchange; 3, retentate; 4, flowthrough 1; 5, flowthrough 2.

3.2.2 Investigation of the role of *cj0979* gene in biofilm formation of *C. jejuni* 11168H

This section reports the investigation of a role of *cj0979* gene in *C. jejuni* 11168H biofilms. The *cj0979* was annotated as a probable nuclease-encoding gene in *C. jejuni* NCTC 11168 genome, according to GenBank (taxid: 19222). A possible role of this particular gene was studied with the aid of site-directed mutagenesis. A *kan^r* resistance gene cassette was used to disrupt the *cj0979* gene in 11168H strain to create *C. jejuni* 11168H/*cj0979* mutant. Biofilm formation study was conducted to determine the phenotype of the mutant.

3.2.2.1 Construction of 11168H/*cj0979* mutant

Primers *cj0979_for* and *cj0979_rev* were designed to PCR amplify *cj0979* (\approx 1.99 kb) with flanking regions from the 11168H chromosomal DNA. GoTaq[®] Green Master Mix was used for the PCR amplification. The expected fragment size was obtained, as indicated in Figure 43.

The schematic representation of the plasmid construction is illustrated in Figure S2 in the Appendix. The gene was cloned into a pGEM-T Easy vector, and ampicillin-resistant clones were screened using CloneChecker analysis (Figure 44). Clones with higher molecular weight band were selected for restriction analysis with ClaI and PstI. The digestion yielded two fragments of expected sizes (4.1 kb and 0.7 kb), confirming the intermediate recombinant plasmid pGEM-T-0979 (Figure 45). For the site-directed mutagenesis, a kanamycin resistance cassette was isolated from plasmid pJMK30. The pJMK30 plasmid was digested with SmaI and the blunt-ended fragment *kan^r* was ligated into the blunt ended ClaI site of the pGEM-T-0979 (blunt-ended using T4 DNA polymerase) construct to create p0979-kanR (Figure 45a). CloneChecker was used for screening of the final recombinant plasmid p0979-kanR. Clone with higher molecular weight band was chosen and confirmed using restriction analysis with Sall, which yielded the expected fragments with sizes 5.6 kb and 0.9 kb, confirming the gene and the inserted *kan^r* were in the same orientation (Figure 46).

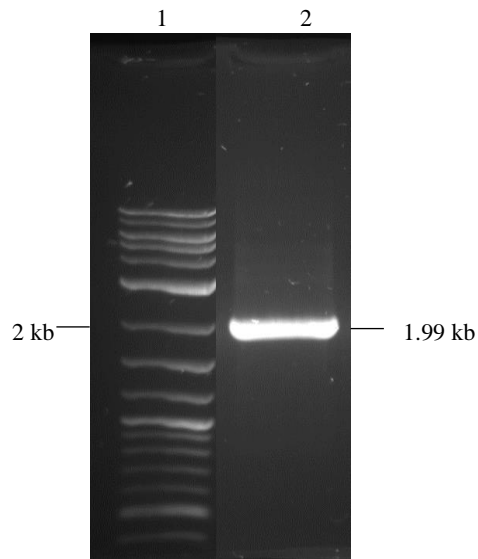


Figure 43. Amplification of *cj0979* gene with flanking regions from 11168H chromosomal DNA using primers *cj0979_for* and *cj0979_rev* by PCR. GoTaq[®] Green Master Mix was used. Expected size is approximately 1.99 kb. Samples: 1, 2-Log DNA ladder; 2, *cj0979*

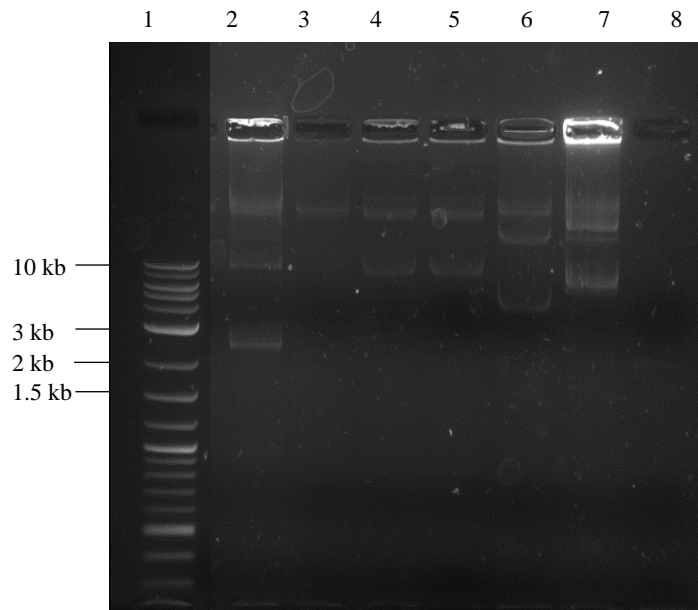


Figure 44. Clone checker analysis of pGEM-T-0979 clones. Cell lysates were used for the analysis.

Samples: 1, 2-Log DNA Ladder; 2, pGEM-T-0979 clone 1; 3, pGEM-T-0979 clone 2; 4, pGEM-T-0979 clone 3; 5, pGEM-T-0979 clone 4; 6, pGEM-T-0979 clone 5; 7, pGEM-T-0979 clone 6; 8, pGEM-T empty vector.

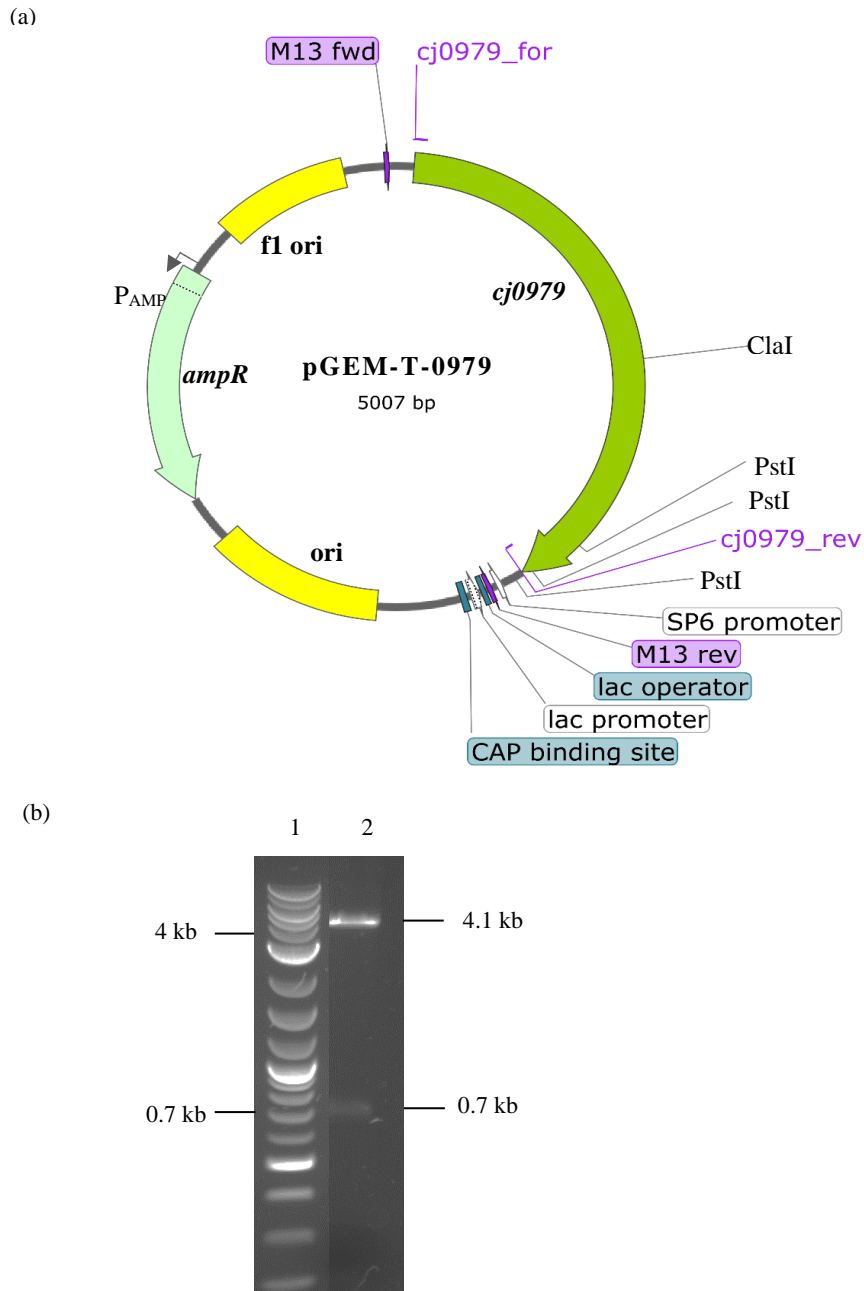


Figure 45. Verification of an intermediate construct pGEM-T-0979 by restriction analysis.

(a) Restriction map of the plasmid indicating the ClaI and PstI sites used in restriction analysis, and ClaI insertional site used in cloning experiment.

(b) Gel image showing digested pGEM-T-0979 with ClaI and PstI. Expected fragment sizes: 4.1 kb; 0.7 kb; 0.1 kb; and 0.06 kb.

Samples: 1, 2-Log DNA ladder; 2, pGEM-T-0979 ClaI/PstI

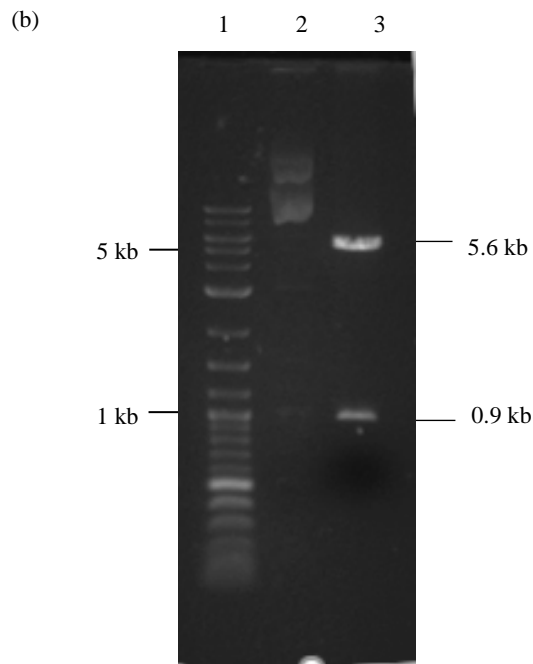
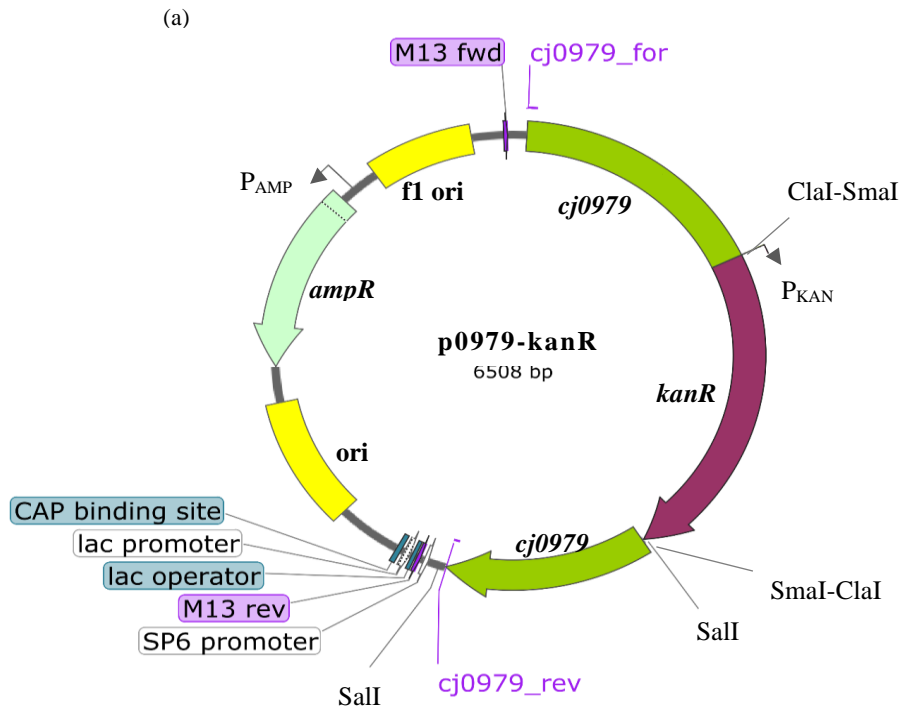


Figure 46. Verification of p0979-kanR by restriction analysis.
 (a) Restriction map of the plasmid indicating the SalI sites used in restriction analysis, and ClaI/SmaI insertional sites after the insertion of the *kan^r* cassette.
 (b) Gel image showing uncut and digested p0979-kanR with SalI. Expected fragment sizes: 5.6 kb and 0.9 kb.
 Samples: 1, 2-Log DNA ladder; 2, p0979-kanR; 3, p0979-kanR SalI.

The verified construct was then used for electroporation into *C. jejuni* 11168H competent cells. Plasmid pRRC was employed as a control for the electroporation experiment. 1 µg of DNA was utilized for electroporation, and a time constant of 5.1 ms was achieved with both electroporation experiments. The electroporated 11168H/pRRC and 11168H/p0979-kanR cells were then plated on non-selective plates and incubated for 10 h, after which the former was re-plated on a selective chloramphenicol plate and the latter was plated on kanamycin plate. The selective plates were then incubated for two more days. Three kanamycin-resistant clones from 11168H/*cj0979* plate and one clone from the control plate were re-streaked for further analysis by Gram staining and PCR verification. For PCR verification of 11168H/*cj0979*, gene specific primers (*cj0979_for* and *cj0979_rev*) were used (Figure 46a). An expected PCR product of 3.5 kb was obtained, which encompassed an increase of 1.5 kb corresponding to the size of the *kan^r* cassette, confirming the insertional inactivation of *cj0979* (Figure 47).

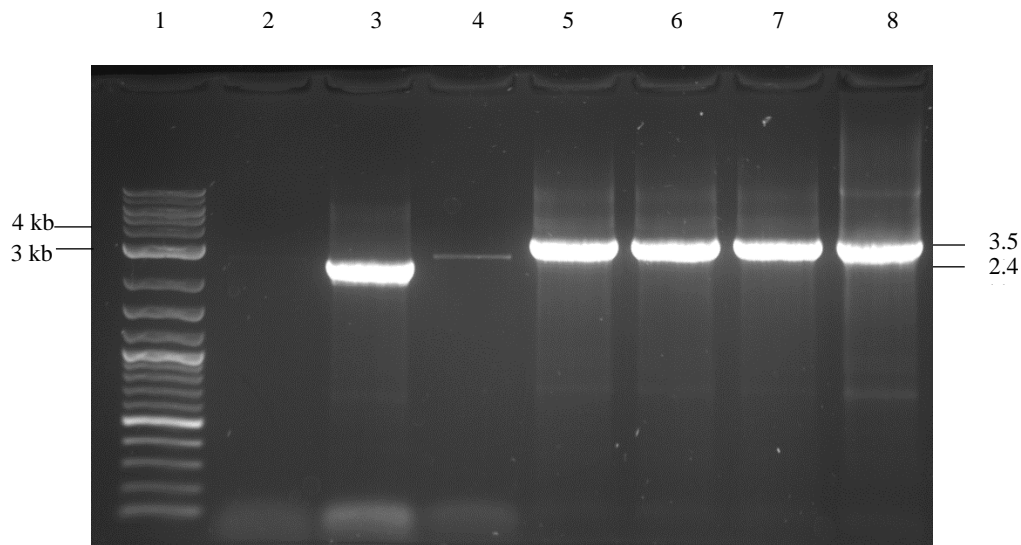


Figure 47. Verification of the inactivation of *cj0979* gene in *C. jejuni* 11168H by PCR using primers *cj0979_for* and *cj0979_rev*. Genomic DNA was used as template DNA for the transformants. GoTaq[®] Green Master Mix was used. Expected PCR product sizes: 11168H/pRRC-2.4 kb; 11168H/*cj0979*-3.5 kb. Samples: 1, 2-Log ladder; 2, 11168H/pRRC with ak233/ak237; 3, 11168H/pRRC with ak234/ak237; 4, 11168H/pRRC with ak235/ak237; 5, 11168H/*cj0979* clone 1; 6, 11168H/*cj0979* clone 2; 7, 11168H/*cj0979* clone 3; 8, p0979-kanR plasmid.

3.2.2.2 Comparison of the biofilm formation and dispersal patterns between wild-type and mutant strains

The biofilm-forming ability of the mutant was tested in this section. The 11168H/*cj0979* strain was expected to form denser biofilms than the wild-type strain due to the absence of the extracellular DNase gene. In other bacteria, similar nuclease genes were responsible for the breakdown of eDNA present in the biofilm matrix (Kiedrowski *et al.*, 2011; Steichen *et al.*, 2011). Many studies have revealed that the addition of DNase I caused a degradation of the eDNA of the EPM. This causes a looser macromolecular structure, leading to dispersal of cells into the culture medium (Brown *et al.*, 2015a).

The starting OD₆₀₀ for both cultures (11168H and 11168H/*cj0979*) was set to 0.5 in BHI broth. The assays were conducted in test tubes and 2 mL of inoculum was incubated under microaerobic conditions for ten days. The tubes were washed with CV on Days 4, 5, 6 and 10.

Background staining was removed in a two-step wash procedure, as performed in the wild-type biofilm assay. The graph (Figure 48) of absorbance of CV stain versus number of days, represents biofilm formation of the mutant in comparison to the wild-type. The *p*-values between the two strains for all time points (days 4, 5, 6 and 10) were above 0.1, thus indicating that the difference observed was not statistically significant.

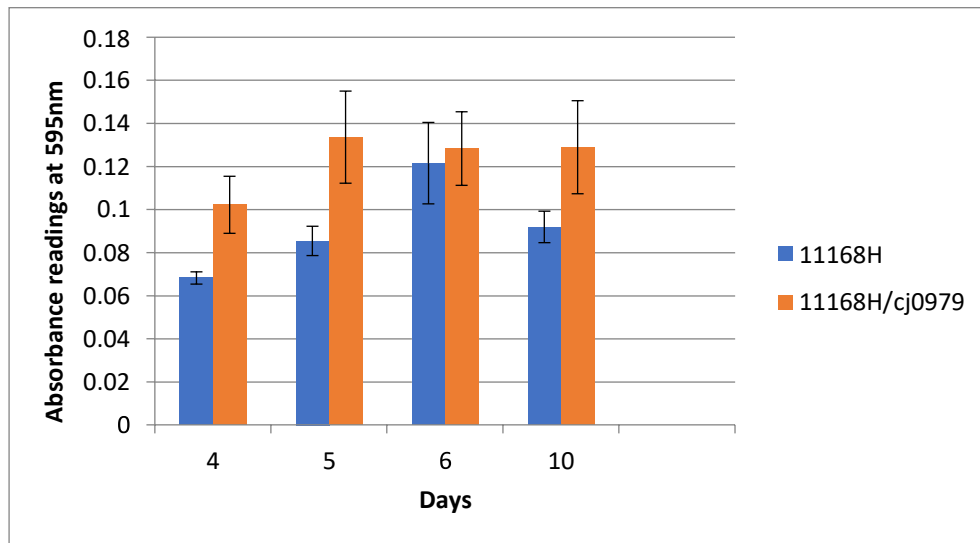


Figure 48. Biofilm assay of *C. jejuni* 11168H/*cj0979* in comparison to wild-type 11168H strain. Absorbance of CV staining was measured at 595 nm. The graph is a representation of three biological and technical replicates. Standard error of mean values were used to represent error bars.

3.2.3 Functional analysis of a putative nuclease Cj0979

This section describes the analysis of the enzymatic properties of purified Cj0979. The pBAD33 plasmid was employed for the construction of the expression vector carrying the *cj0979* gene. The expression plasmid carrying the nuclease gene was introduced into *E. coli*. The *E. coli* culture was induced in the presence of arabinose and the protein was purified from cell lysates. In order to purify Cj0979, three different approaches were undertaken: 6xHis tag attached to C-terminal of Cj0979; 6xHis tag attached to N-terminal of Cj0979; and removal of leader peptide from Cj0979.

3.2.3.1 Construction of the pBAD33-*cj0979* plasmid

Primers *cj0979_expr_for* and *cj0979_expr_rev* were designed for the PCR amplification of gene *cj0979* from *C. jejuni* 11168H chromosomal DNA using Q5[®] High-Fidelity DNA Polymerase (Figure 49). A 6×His tag was attached to the C-terminal of Cj0979. The expected PCR product is as shown in Figure S3 in the Appendix.

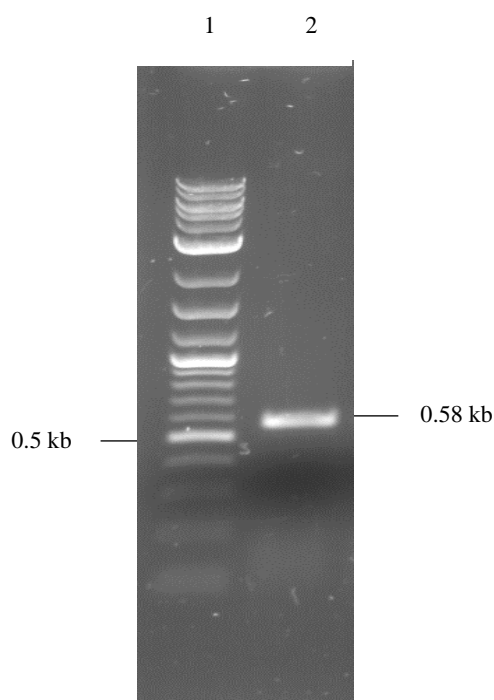


Figure 49. Amplification of *cj0979* gene from *C. jejuni* 11168H chromosomal DNA with primers *cj0979_expr_for* and *cj0979_expr_rev*. Q5[®] High-Fidelity DNA Polymerase was used. Expected PCR product size: 0.58 kb.

Samples: 1, 2-Log DNA Ladder; 2, *cj0979*

Plasmid pBAD33 was confirmed by restriction analysis with EcoRI. The PCR fragment was ligated into the pBAD33 vector using XbaI and SphI enzymes. The ligation mixture was then transformed into *E. coli* C25661 competent cells, and chloramphenicol-resistant clones were isolated for further analysis. ClaI enzyme was used for restriction analysis and the digestion produced 4.2 kb and 1.7 kb fragments, as expected (Figure 50), confirming the recombinant plasmid. The resulting plasmid pBAD33-*cj0979* was sent for Sanger sequencing with vector-derived primers (pBAD_for and pBAD_rev) corresponding to the flanking regions on either

side of the insert. The data was analysed using Chromas and BLASTn programs, and the output result revealed a 100% identity.

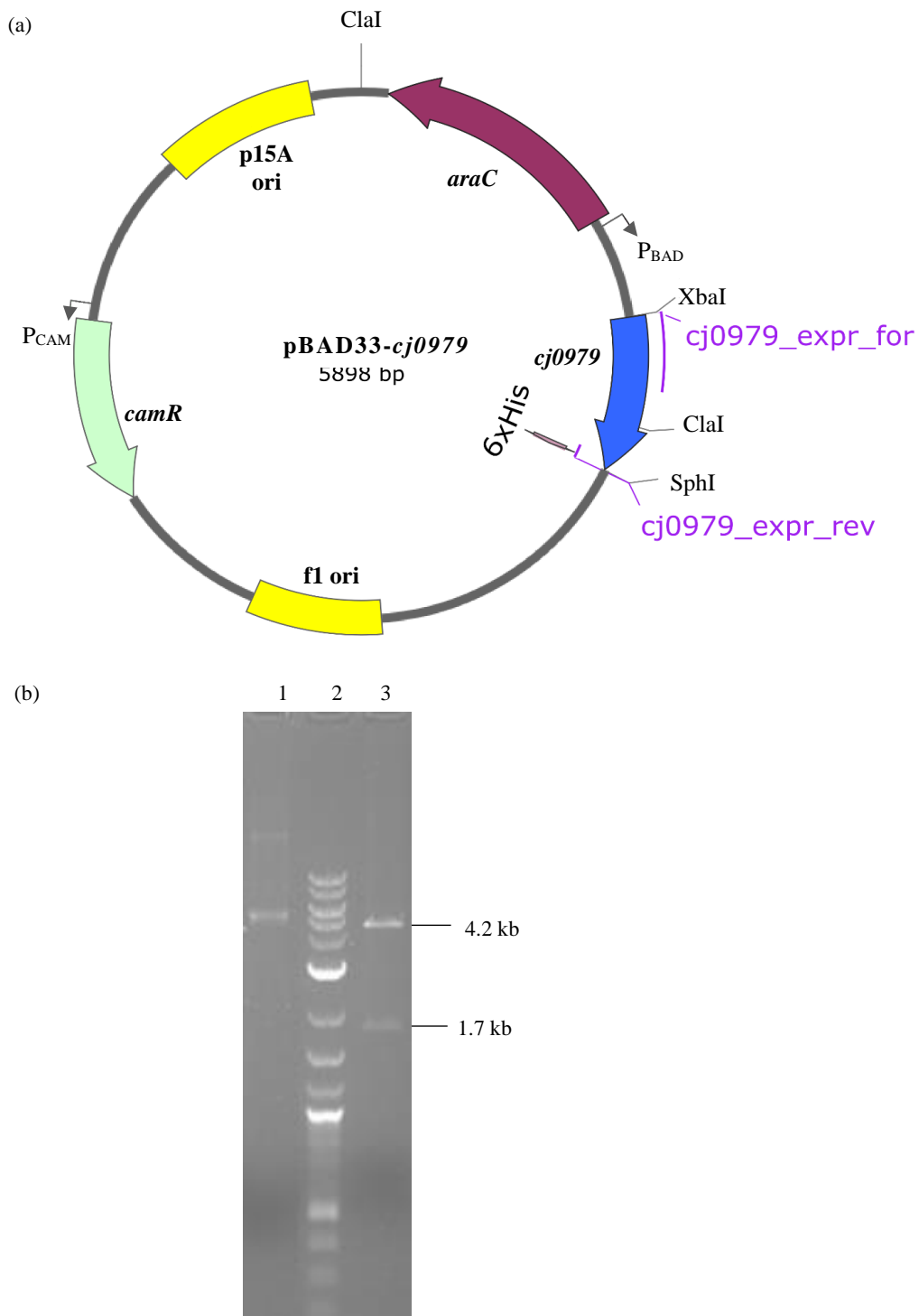


Figure 50. Verification of pBAD33-cj0979 by restriction analysis.

(a) Restriction map of the plasmid indicating ClaI restriction sites used in restriction analysis, and XbaI/SphI cloning sites.

(b) Gel image showing uncut and digested pBAD33-cj0979 with ClaI. Expected sizes: 4.2 kb and 1.7 kb.

Samples: 1, pBAD33-cj0979; 2, 2-Log DNA ladder; 3, pBAD33-cj0979 ClaI

3.2.3.2 Expression, purification, and detection of Cj0979

The Cj0979 protein was expressed in *E. coli* in the presence of arabinose in the attempt to purify the protein for DNase studies. Large-scale and small-scale purification of the protein was carried out. A 0.1% final concentration of arabinose was used for induction and the purification was initially conducted using Qiagen Ni-NTA kit. The culture was induced at an OD₆₀₀ of 0.6 and incubated for 3 h, after which the cells were collected from the induced culture for protein purification. Whole cell suspensions, lysates, wash fractions, and eluted protein fractions were run on an 12% SDS-PAGE gel and analysed using Coomassie staining. The stained gel failed to reveal the presence of the protein.

Therefore, the purification was repeated with induction time of 2 h to exclude a possibility of protein degradation, which could otherwise occur with longer incubation times. As a negative control, protein purification from the uninduced culture was conducted. For the repeat, small-scale protein purification using MagneHis kit was carried out. Similar to the first purification, all four fractions were analysed on an SDS-PAGE gel, with the application of equivalent amounts of samples in all lanes (Figure 51). The bands that appeared in the lanes containing all induced and uninduced fractions looked similar in appearance, except for the uninduced wash fraction lane, which appeared to be quite faint due to some product loss during gel loading. Neither of the lanes carrying the uninduced and induced eluates revealed the expected protein band near 21.3 kDa.

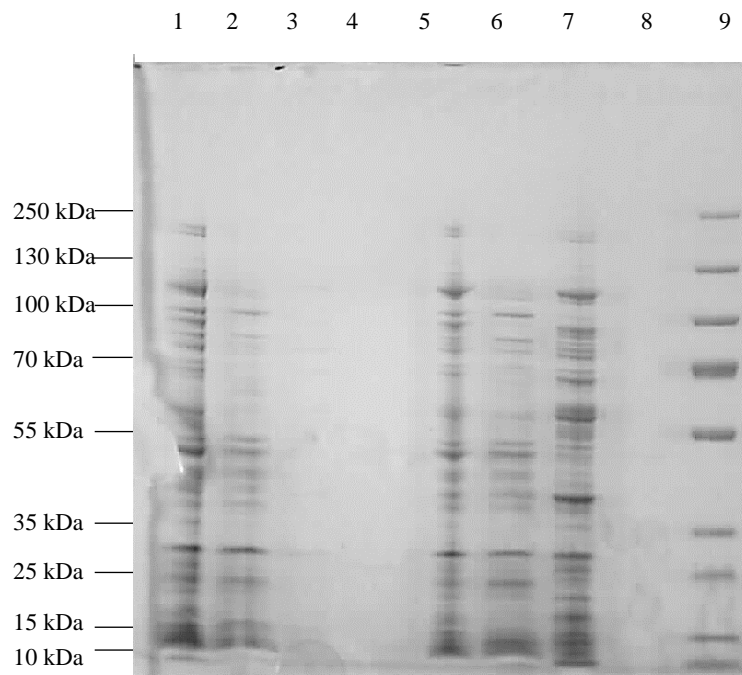


Figure 51. Analysis of fractions from *E. coli*/pBAD33-*cj0979* expression and purification experiment.

Lanes 1-4, uninduced fractions; lanes 5-8, induced fractions. Expected size of Cj0979: 21.3 kDa.

Samples: 1, Whole cell suspensions; 2, Lysate; 3, Wash fractions 1, 2 and 3; 4, Eluate; 5, Whole cell suspensions; 6, Lysate; 7, Wash fractions 1, 2 and 3; 8, Eluate; 9, Pre-stained ladder.

3.2.3.3 Western blotting

The purified samples from the first and second purifications were tested by Western blotting, since Coomassie staining did not reveal the expected Cj0979. Western blotting was carried out due to its greater sensitivity for protein detection when compared to Coomassie staining.

The Western blotting results were more promising, as a band corresponding to the 21.3 kDa Cj0979 protein was detected. No bands were seen in the uninduced fractions (lanes 1–4), as expected (Figure 52). The band corresponding to the Cj0979 protein was detected in the induced whole cell suspension, induced lysate, and the induced purified protein lane. The band was not seen in the induced wash fraction lane.

Furthermore, a band corresponding to the Cj0979 protein was also observed in the lane corresponding to whole cell suspension from the induced sample from the first purification (lane 11), confirming the protein was indeed expressed but with low yield for detection using Coomassie staining. The sizes were estimated using Gel Analyzer. However, lane 12 showed no product, suggesting that the protein underwent degradation due to storage at 4°C for approximately two weeks. The whole cell suspension and the purified protein were stored at different temperatures; the whole cell suspensions were stored at -20°C to inhibit any bacterial growth, while the purified protein was stored at 4°C for two weeks.

Overall, the detection of Cj0979 protein was successful, as illustrated in Figure 52. However, the protein could be detected only with a higher-sensitivity assay, such as Western blotting, suggesting the protein had very low yield, and thus confirming its unsuitability for downstream DNase testing experiments.

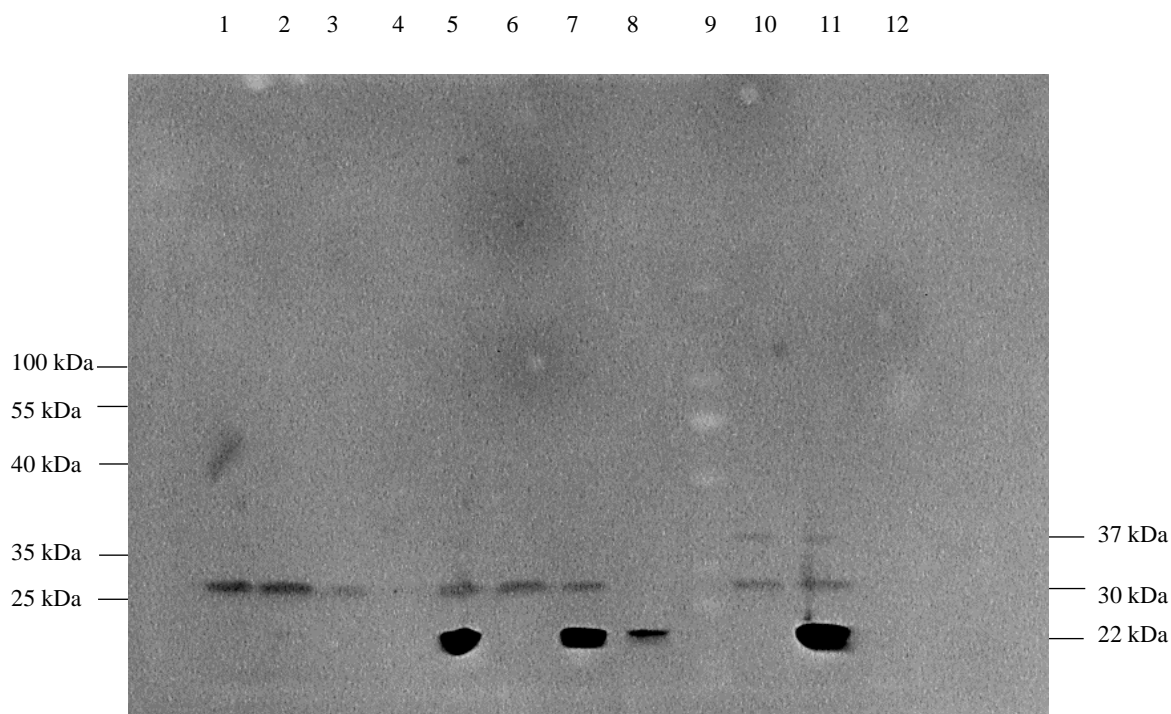


Figure 52. Western blotting of fractions from *E. coli*/pBAD33-*cj0979* expression and purification experiments.

Lanes 1-4, uninduced fractions; lanes 5-8, induced fractions; lanes 1-8, samples from second purification experiment; lanes 10-12, samples from first purification experiment. Expected size of Cj0979: 21.3 kDa.

Samples: 1, Whole cell suspensions; 2, Lysate; 3, Wash fractions 1,2, 3; 4, Protein; 5, Whole cell suspensions; 6, Wash fractions 1,2, 3; 7, Lysate; 8, Protein; 9, Pre-stained ladder; 10, Uninduced whole cell suspension; 11, Induced whole cell suspension; 12, Protein from induced sample.

3.2.3.4 Construction of the pBAD33-*cj0979*N plasmid

As an alternative approach, a slight modification in the construction of the pBAD33 expression construct carrying the *cj0979* gene was undertaken, as in a previous study, in order to purify protein with a better yield (Atas *et al.*, 2016). The 6×His tag was attached to the N-terminal of Cj0979 (Figure 53a). The N-terminal 6×His tag will prevent the signal peptide from being cleaved off during expression, thereby preventing the protein from being secreted. The expression vector was constructed following the same protocol as for pBAD33-*cj0979*. Primers *cj0979_N_expr_for* and *cj0979_N_expr_rev* were designed to amplify the gene. The expected PCR product is as shown in Figure S4 in the Appendix. The PCR fragment was digested with

XbaI and SphI and ligated with XbaI and SphI digested pBAD33. The ligation mixture was transformed into *E. coli* C2523L competent cells. The chloramphenicol-resistant clone was selected for ClaI restriction verification, and the digestion produced fragments of 4.2 kb and 1.7 kb (Figure 53). The same recombinant plasmid pBAD33-*cj0979N* was sent for Sanger sequencing with vector-derived primers (pBAD_for and pBAD_rev) corresponding to the flanking regions on either side of the insert. The sequencing results were analysed using BLASTn and Chromas programs, and the results revealed no errors.

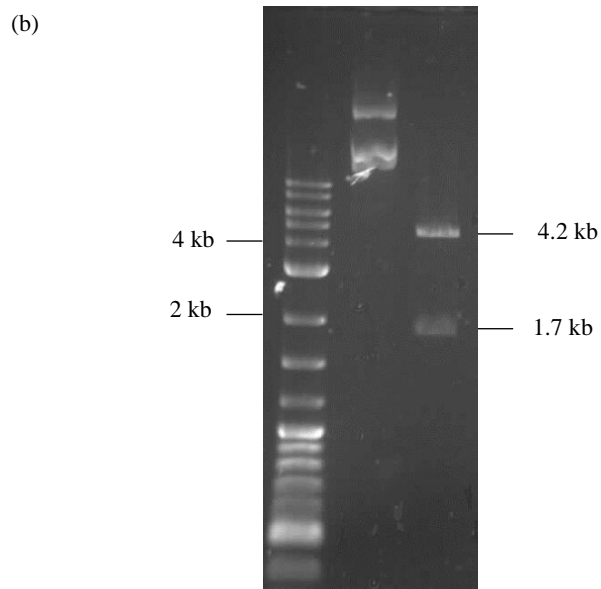
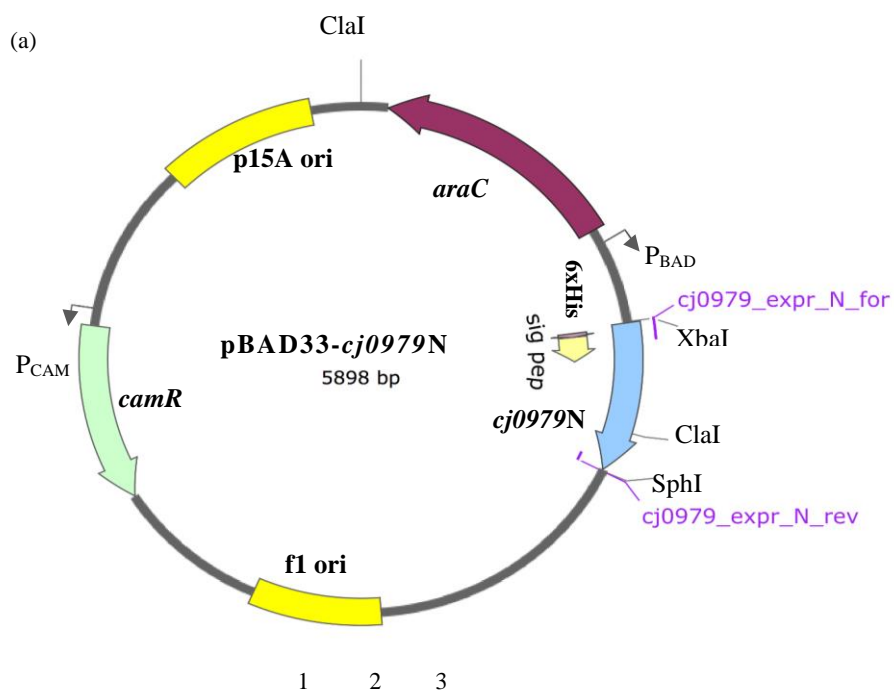


Figure 53. Verification of pBAD33-*cj0979N* by restriction analysis.

(a) Restriction map of the plasmid indicating *ClaI* restriction sites used in restriction analysis, and *XbaI*/*SphI* cloning sites.

(b) Gel image showing uncut and digested pBAD33-*cj0979N* with *ClaI*. Expected sizes: 4.2 kb and 1.7 kb.

Samples: 1, 2-Log DNA ladder; 2, pBAD33-*cj0979N*; 3, pBAD33-*cj0979N* *ClaI*.

3.2.3.5 Expression, purification, and detection of Cj0979N

The verified construct was then used for protein expression and purification using MagneHis kit. To increase the stability of the protein during the purification process, protease inhibitor was added prior to the lysis step. The effect was compared with culture without the addition of protease inhibitor. The cultures were induced with a 0.1% final concentration of arabinose at an OD₆₀₀ 0.6 and incubated for 2 h, at which point the cells were collected for protein purification.

The samples were run with equivalent amounts on a 12% SDS-PAGE gel. Since protein from *E. coli*/pBAD33-*cj0979* revealed signs of degradation, these purified samples were tested on the day of purification and after two days of storage at 4°C. The results indicated no significant difference between the induced and uninduced purified samples under both conditions (with and without protease inhibitor). The target protein was not detected in any of the lanes (Figure 54). Although it may have been possible to detect the protein with western blotting due to its higher sensitivity for low yield proteins (as with Cj0979), this detection would not aid in its downstream experiments. Therefore, these samples were not analysed using Western blotting.

Additionally, supernatant samples from the expression of *E. coli*/pBAD33-*cj0979* were tested alongside. These were analysed in parallel to confirm that no protein secretion into the culture supernatant during expression had occurred. The culture supernatant was collected at the end of incubation period (i.e., 2 h with arabinose) and spun down and subsequently filter-sterilized, and a 5 µL aliquot was tested using gel electrophoresis followed by Coomassie staining. The gel picture revealed that protein could not be detected in the supernatant (Figure 54).

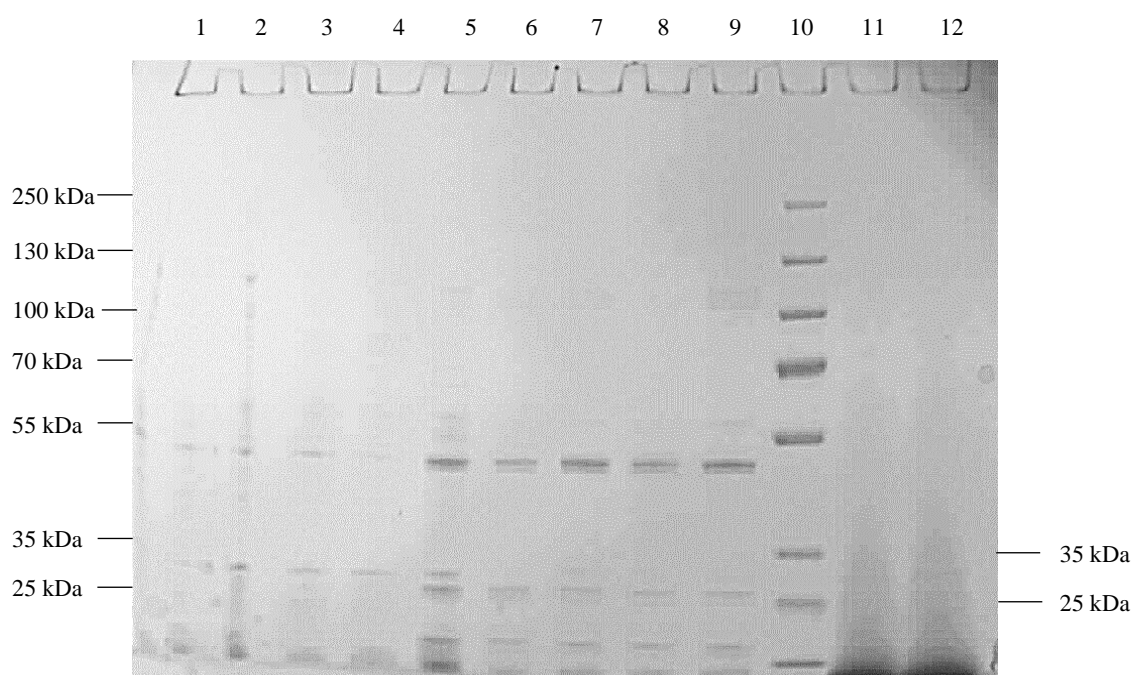


Figure 54. Analysis of fractions from *E. coli*/pBAD33-*cj0979N* purification and supernatant samples from *E. coli*/pBAD33-*cj0979* expression experiments. Samples in lanes 11 and 12 are supernatant samples from an independent experiment (*E. coli*/pBAD33-*cj0979*). Expected size of Cj0979N: 21.3 kDa. Samples: 1, Uninduced whole cell suspension; 2, Induced whole cell suspension; 3, Uninduced wash fractions 1,2 and 3; 4, Induced wash fractions 1,2 and 3 with protease inhibitor; 5, Eluate from uninduced sample at the time of purification; 6, Eluate from induced sample at the time of purification; 7, Eluate from induced sample with protease inhibitor at the time of purification; 8, Eluate from induced sample after two days storage at 4°C; 9, Eluate from induced sample with protease inhibitor after two days storage at 4°C; 10, Pre-stained ladder; 11, Supernatant sample from uninduced *E. coli*/pBAD33-*cj0979* expression; 12, Supernatant sample from induced *E. coli*/pBAD33-*cj0979* expression.

3.2.3.6 Construction of pBAD33-*cj0979*LP

The elimination of the leader peptide was carried out to troubleshoot issues with low-yield protein purification and to confirm if Cj0979 was a secretory protein. SignalP 3.0 program was used for the prediction of the signal peptide sequence in Cj0979. The software predicted the signal sequence to be between 1 and 39 amino acids. In addition, the predicted leader sequence in Cj0979 was compared to similar thermonucleases in *Staphylococcus* (Kiedrowski *et al.*, 2011; Kiedrowski *et al.*, 2014), using Clustal Omega analysis (Figure S5 in the Appendix). The

amino acids sequences were aligned showing sequence similarity indicating cleavage site near 39 position amino acid. Therefore, the first 117 bases were removed from the *cj0979* gene sequence and the remaining sequence was labelled *cj0979LP* as shown in Figure S6 in the Appendix.

Primers *cj0979_LP_for* and *cj0979_LP_rev* were designed for the amplification of the *cj0979LP* gene. The expected PCR product is as shown in Figure S7 in the Appendix. The cloning principle employed was the same as for the pBAD33-*cj0979* expression construct. The primers were used to PCR amplify the 0.45 kb gene fragment from the 11168H chromosomal DNA (Figure 55). The fragment was then digested with XbaI and SphI and used for ligation with the pBAD33, digested with the same enzyme pair. The ligation mixture was transformed into *E. coli* C2566L competent cells. Chloramphenicol-resistant clones were selected for further analysis. ClaI enzyme was used for restriction digestion confirmation. The enzyme cut the plasmid in two places, yielding the expected fragment sizes of 4.2 kb and 1.6 kb (Figure 56). The verified pBAD33-*cj0979LP* plasmid was sent for Sanger sequencing with vector-derived primers (*pBAD_for* and *pBAD_rev*) to ensure no mutations occurred in the insert or the flanking regions. The output sequence derived from Chromas produced a 100% identity when checked with BLASTn.

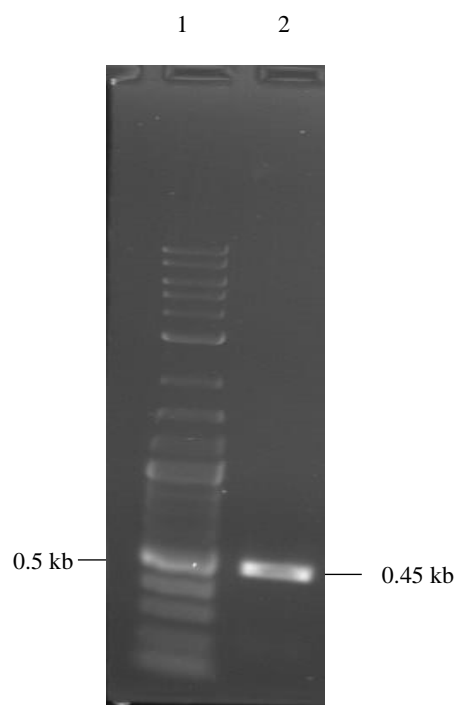


Figure 55. Amplification of *cj0979LP* gene from *C. jejuni* 11168H chromosomal DNA with primers *cj0979_LP_for* and *cj0979_LP_rev*. Q5[®] High-Fidelity DNA Polymerase was used. Expected PCR product size: 0.45 kb. Samples: 1, 2-Log DNA ladder; 2, *cj0979LP*.

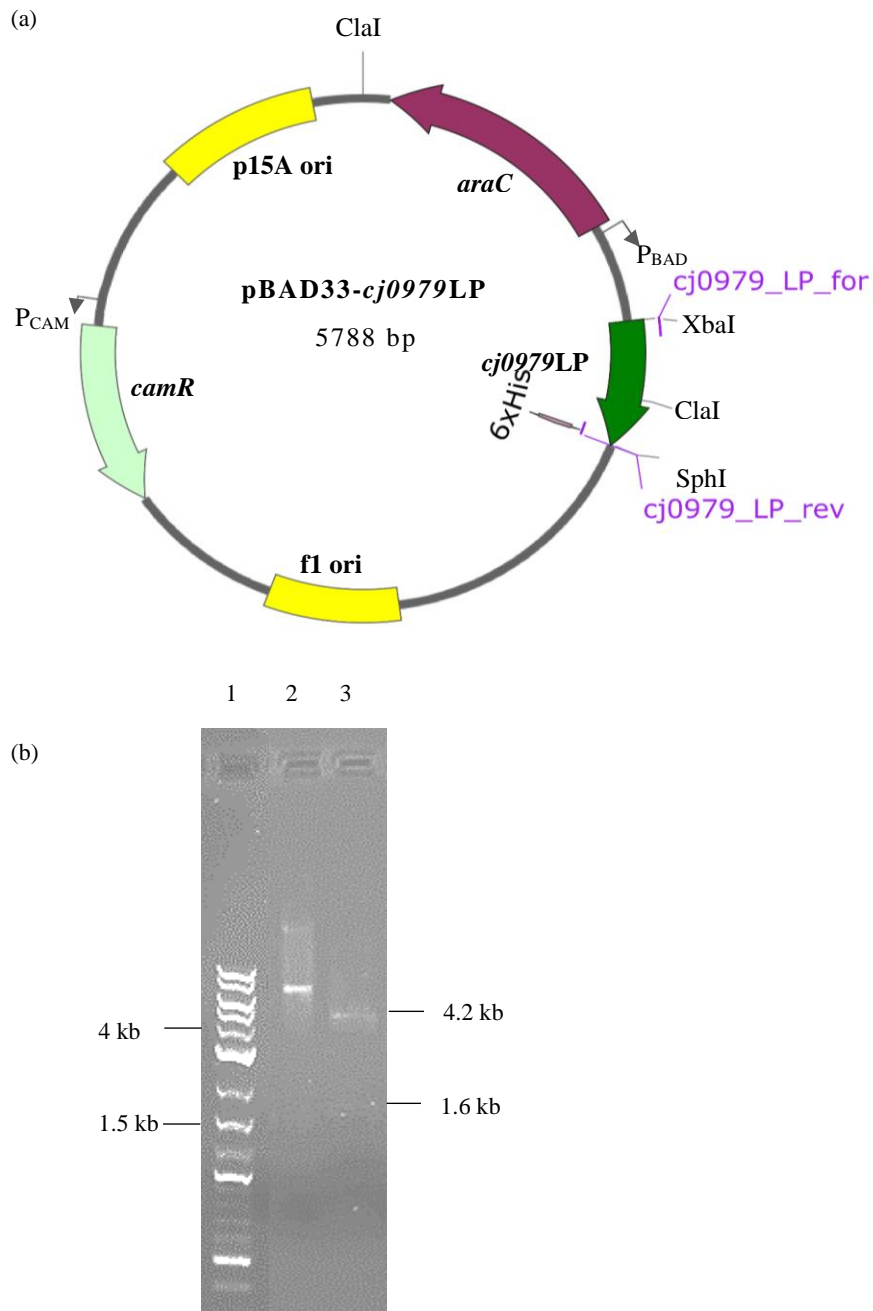


Figure 56. Verification of pBAD33-cj0979LP by restriction analysis.
 (a) Restriction map of the plasmid indicating ClaI restriction sites used in restriction analysis and XbaI/SphI cloning sites.
 (b) Gel image showing uncut and digested pBAD33-cj0979LP with ClaI. Expected sizes: 4.2 kb and 1.6 kb.
 Samples: 1, 2-Log DNA ladder; 2, pBAD33-cj0979LP; 3, pBAD33-cj0979LP ClaI

3.2.3.7 Expression, purification, and detection of Cj0979LP

An *E. coli* strain carrying the pBAD33-*cj0979LP* was set up for protein expression. Arabinose 0.1% final concentration was added at an OD₆₀₀ of 0.6, as before, and induction time of 2 h was employed. Samples were collected at the end of the 2 h, and purification was conducted from induced and uninduced cultures using a MagneHis purification kit. Whole cell suspensions, lysates, wash fractions, and purified samples were all run on an SDS-PAGE gel with equivalent amounts of cells in each lane. The first gel run was conducted with the usual MOPS buffer, as with previous gels, but since the expected protein size was small (i.e., 16.8 kDa), the band separation of the protein marker was not satisfactory for comparison. Therefore, a more suitable buffer like the MES buffer, which provides better separation for low molecular weight proteins was selected for further protein analysis.

The protein gels with MOPS and MES buffers revealed bands for the expected Cj0979LP protein in the induced lanes only of all three different fractions (whole cell suspension, lysate, and purified protein) as expected. In the first gel with MOPS buffer, two time points were tested (the same day of purification and after three days of storage at 4°C). The bands in the induced protein lanes 9 and 11 in Figure 57 revealed that storage at 4°C did not cause degradation as similar intensity bands were obtained. Figure 58 revealed that a clear separation of bands of the pre-stained ladder occurred after the use of the MES buffer. The band corresponding to the target protein Cj0979LP was evidenced at 16.8 kDa in the lanes containing the induced fractions. The sizes were estimated using Gel Analyzer.

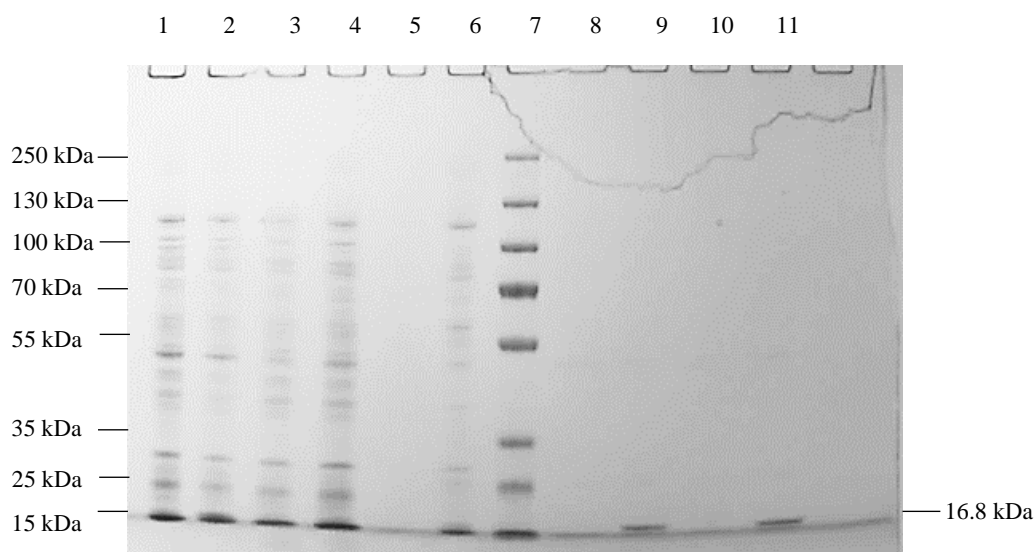


Figure 57. Analysis of fractions from *E. coli*/pBAD33-*cj0979LP* expression and purification experiment. SDS-PAGE gel was run using MOPS buffer. Expected size of Cj0979LP: 16.8 kDa.

Samples: 1, Uninduced whole cell suspension; 2, Induced whole cell suspension; 3, Uninduced lysate; 4, Induced lysate; 5, Uninduced wash fractions 1,2,3; 6, Induced wash fractions 1,2,3; 7, Pre-stained ladder; 8, Purified protein from uninduced sample same day as purification; 9, Purified protein from induced sample same day as purification; 10, Purified protein from uninduced sample after storage at 4°C for three days; 11, Purified protein from induced sample after storage at 4°C for three days.

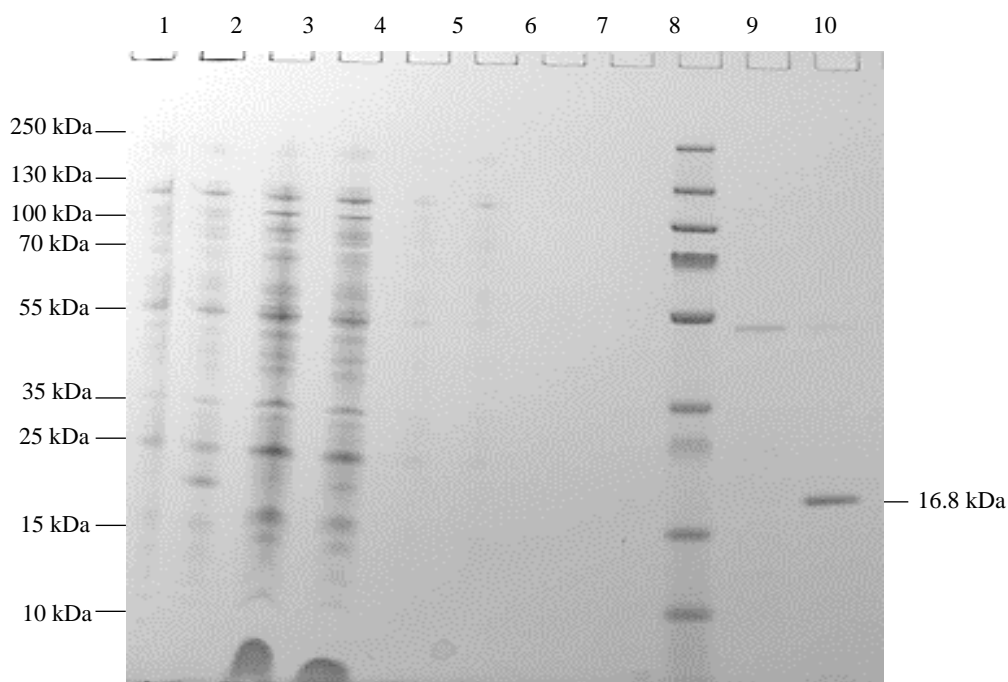


Figure 58. Analysis of fractions from *E. coli*/pBAD33-*cj0979LP* expression and purification experiment. SDS-PAGE gel was run using MES buffer. Expected size of Cj0979LP: 16.8 kDa.

Samples: 1, Uninduced whole cell suspension; 2, Induced whole cell suspension; 3, Uninduced lysate; 4, Induced lysate; 5, Uninduced wash fraction 1; 6, Induced wash fraction 1; 7, Uninduced wash fractions 2 and 3; 8, Induced wash fractions 2 and 3; 9, Pre-stained ladder; 10, Purified protein from uninduced sample; 11, Purified protein from induced sample.

3.2.3.8 Determining the concentration of Cj0979LP

The concentration of the purified protein was determined using the BCA assay. Each well in the assay used 10 μ L of the protein sample. The BSA standard was prepared using the elution buffer. The BCA assay was conducted following the manufacturer's protocol, and a standard calibration curve of absorbance of each dilution of BSA standard versus concentration was plotted. Concentration was determined using the best-fit linear equation generated from the calibration curve. In this instance, the concentration of Cj0979 was approximately 125 μ g/mL.

3.2.3.9 DNase activity tests of Cj0979LP

The purified protein was tested for DNase activity using lambda DNA as the substrate. Lambda DNA was incubated with purified protein for 1 h at 37°C, and the samples were then analysed

on the gel. DNase I enzyme was used as positive control. Lambda DNA with only the buffer was used as negative control.

As seen on the gel in Figure 59, the band corresponding to the negative control remained as expected. The positive control succeeded (lane 4); the band corresponding to the lambda DNA has disappeared, suggesting that DNA degradation occurred. Interestingly, similar results were obtained with the test protein (lanes 5-7), where complete degradation was seen with the purified induced proteins.

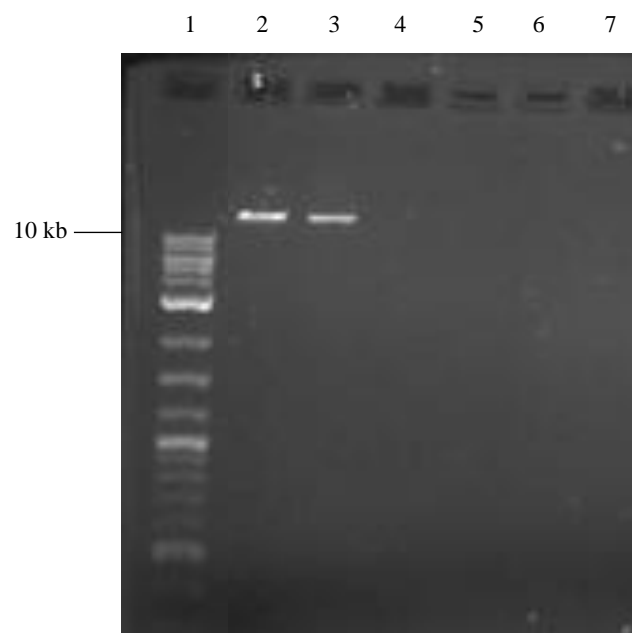


Figure 59. DNase activity of purified Cj0979LP protein. Lambda DNA was used as a substrate. Equal amounts of DNA were applied to each well.

Samples: 1, 2-Log DNA ladder; 2, Lambda DNA; 3, Lambda DNA and DNase buffer; 4, Lambda DNA, buffer, and DNase I; 5- 7, Lambda DNA, buffer, and induced protein.

3.2.3.10 Effect of purified Cj0979LP on *C. jejuni* 11168H biofilms

The activity of purified Cj0979LP protein was tested through its addition to existing *C. jejuni* 11168H biofilms to determine any potential influence on the growth or dispersal pattern. As seen from the previous result, good biofilm formation occurs beginning on Day 4. The inoculum was set at OD₆₀₀ 0.5 in BHI broth. 1 mL of inoculum was added to test tubes and

incubated under microaerobic conditions. No background washing step was carried out as the absorbance readings of the BHI only control tubes were simply subtracted since the culture volume used was lesser in this instance. 0.5 μg of Cj0979LP protein, along with a final concentration of $1\times$ DNase buffer, were added to the existing *C. jejuni* biofilm test tubes on Day 4. DNase I was added along with a DNase buffer, which served as a positive control. Additionally, another set of tubes was treated with 200 μL of sterile 11168H supernatant with the buffer to determine whether there was DNase activity in the supernatant. After the addition, the tubes were further incubated for one day, after which the biofilm was CV-stained. Figure 60 illustrates the results, indicating that the addition of Cj0979LP and 11168H supernatant indeed caused a reduction in biofilm growth. The absorbance readings obtained with the treated tubes were much lower than those from the 11168H tubes alone. In addition, the difference obtained was also statistically significant, as reflected by the p -values.

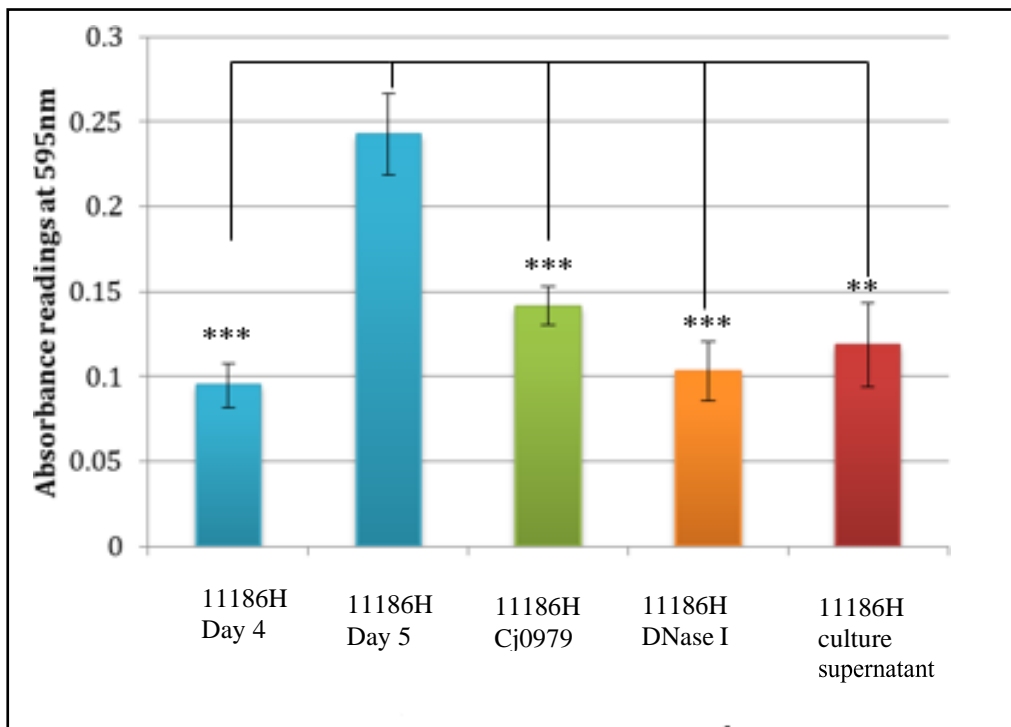


Figure 60. Effects of purified Cj0979LP, DNase I and culture supernatant on biofilm formation. Assays were set up with initial OD_{600} 0.5. Biofilm was stained on day 4 and day 5. ** $0.001 < p \leq 0.01$, *** $p \leq 0.001$. The graph is a representation of three independent experiments consisting of three technical replicates. Standard error of mean values was used to represent error bars.

3.3 Investigation of the role of *cje0256* in biofilm forming ability of *C. jejuni* RM1221

In this section, the biofilm-forming ability of *C. jejuni* RM1221 was compared to that of the *C. jejuni* 11168H strain. This work was intended to examine the role of *cje0256* (gene encoding an extracellular nuclease) in the biofilm formation of *C. jejuni* RM1221. The strain RM1221 also contains two other DNase encoding genes, *cje1441* and *cje0566* (Gaasbeek *et al.*, 2009; Gaasbeek *et al.*, 2010). According to previous studies, *C. jejuni* RM1221 does not form strong biofilms and is considered to be a poor biofilm former (Brown *et al.*, 2015b).

The presence of homologues of Cje1441, Cje0256, and Cje0566 in *C. jejuni* NCTC 11168 was checked using BLASTp. The amino acid sequences of all three proteins were used as the input for this analysis. Homologues of Cje1441 and Cje0566 were present in *C. jejuni* 11168 (Figure S8 in the Appendix), but no match was obtained with Cje0256. The CDS (coding sequence) region in Figure S8 corresponded to the same protein, Cj0594c, which is annotated as putative DNA/RNA non-specific endonuclease and whose function has not been confirmed experimentally. In addition, the protein Cj0979 from 11168H was compared with the three DNases in RM1221 using BLASTp (Figure S9). The query coverage was poor in all three results. In conclusion, the results confirmed that *C. jejuni* 11168H does not contain homologues of *cje0256* gene. As 11168H lacks only this DNase gene when compared to RM1221, yet forms stronger biofilms, the evidence suggests that *cje0256* could be responsible for the low biofilm-forming properties of RM1221. Therefore in this study, an attempt to investigate the possible effects of inactivation of *cje0256* on *C. jejuni* RM1221's biofilm forming ability was carried out. In addition, purification of Cje0256 was also attempted to assess its enzymatic properties in a similar fashion to the study conducted with Cj0979 discussed in section 3.2.3.

3.3.1 Investigation of biofilm formation ability of *C. jejuni* RM1221

Biofilm assays of *C. jejuni* strains 11168H and RM1221 were conducted using 96-well microtiter plates, under static conditions, for a period of four days under microaerobic conditions. Initial inoculum was set to OD₆₀₀ 0.5 in BHI broth, and biofilm CV staining was carried out on Days 3 and 4. Assays consisted of three biological and technical replicates. Figure 61 represents the results of biofilm stained on day 3 and 4. As seen, 11168H formed a stronger biofilm than RM1221, as indicated by the absorbance values. The formation of a ring-like structure at the air-liquid interface took place with RM1221, but it appeared fainter when stained, in comparison to 11168H tubes. The difference observed on the graph was also statistically significant, as denoted by the *p*-values. Therefore, it was confirmed that RM1221 was indeed a poor biofilm former when compared to 11168H, but the difference was marginal.

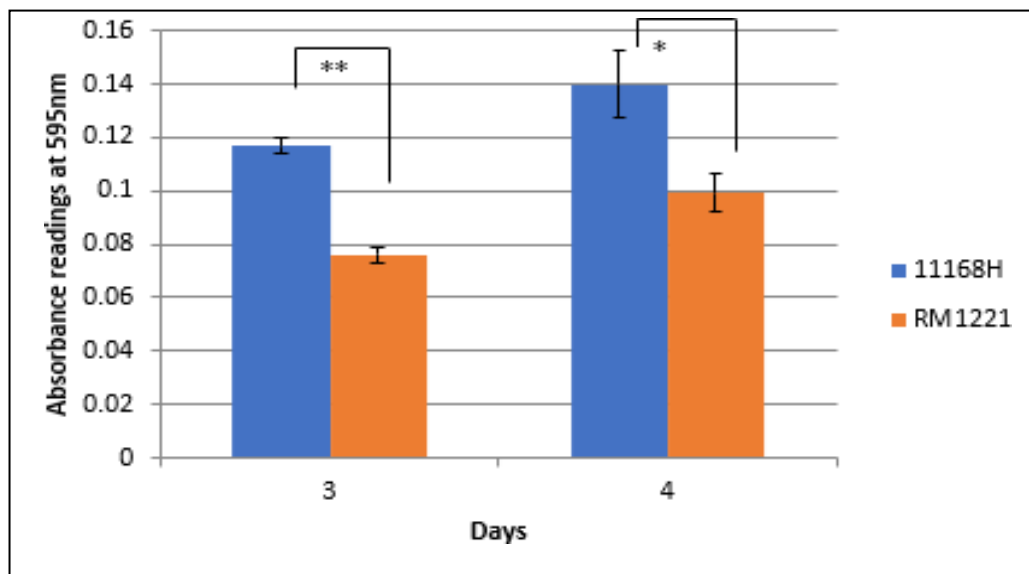


Figure 61. Biofilm assay of *C. jejuni* 11168H and RM1221. Absorbance of CV staining was measured at 595 nm on days 3 and 4. The graph is a representation of three independent experiments consisting of three technical replicates. Standard error of mean values was used to represent error bars. * $0.01 < p \leq 0.05$, ** $0.001 < p \leq 0.01$.

3.3.2 Construction of *C. jejuni* RM1221/*cje0256* mutant

Construction of *cje0256* knockout mutant in RM1221 using site-directed mutagenesis was attempted in this section, in order to study the biofilm forming properties of the resultant mutant. A *kan^r* gene cassette was used to disrupt the *cje0256* in *C. jejuni* RM1221 to create RM1221/*cje0256*. In order to achieve this, several strategies were employed to protect the DNA from the intracellular DNase activity present in strain RM1221.

3.3.2.1 Construction and verification of pUC19-*cje0256*-kanR construct

The schematic description of the construction of the pUC19-*cje0256*-kanR is illustrated in Figure S10 in the Appendix. Primers *cje0256f_mod* and *cje0256r_mod* were designed to amplify *cje0256* (\approx 2.2 kb) with flanking regions from *C. jejuni* RM1221 chromosomal DNA using Q5[®] High-Fidelity DNA Polymerase. The PCR fragment (Figure 62) contains EcoRI/XbaI sites in preparation for ligation with the pUC19 vector. The pUC19 vector was digested with EcoRI and XbaI and ligated with *cje0256* PCR fragment; the ligated product was then transformed into *E. coli* XL1 blue competent cells. The transformation mixture was plated on an ampicillin, IPTG, and X-gal plate for blue-white screening. The white transformants were selected and further screened with CloneChecker, and clones with a higher molecular weight band were chosen for further analysis with restriction analysis. Restriction enzymes EcoRI and Eco53KI were used to verify the intermediate pUC19-*cje0256* construct, as illustrated in Figure 63. Expected fragments of 3.5 kb and 1.3 kb were obtained on the gel. A *kan^r* resistance cassette was isolated from plasmid pJMK30. The Eco53KI site on the intermediate vector was utilized as the insertional site for the SmaI *kan^r* fragment (Figure 63a). The ligated product was transformed into *E. coli* XLI blue competent cells to produce pUC19-*cje0256*-kanR. The final recombinant construct was screened by CloneChecker once again, and clones with higher molecular weight band were selected for further restriction analysis with EcoRI. The digestion produced the expected fragments of sizes of 3.5 kb and 2.8 kb, confirming

that the inserted gene and the *kan^r* were in the same orientation (Figure 64).

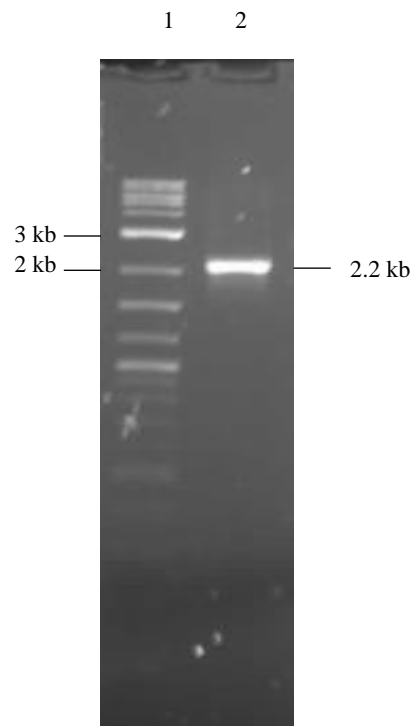


Figure 62. Amplification of *cje0256* gene with flanking regions from *C. jejuni* RM1221 chromosomal DNA using primers *cje0256f_mod* and *cje0256r_mod*. Q5[®] High-Fidelity DNA Polymerase was used. Expected PCR product size is 2.2 kb.

Samples: 1, 2-Log DNA ladder; 2, *cje0256* PCR product.

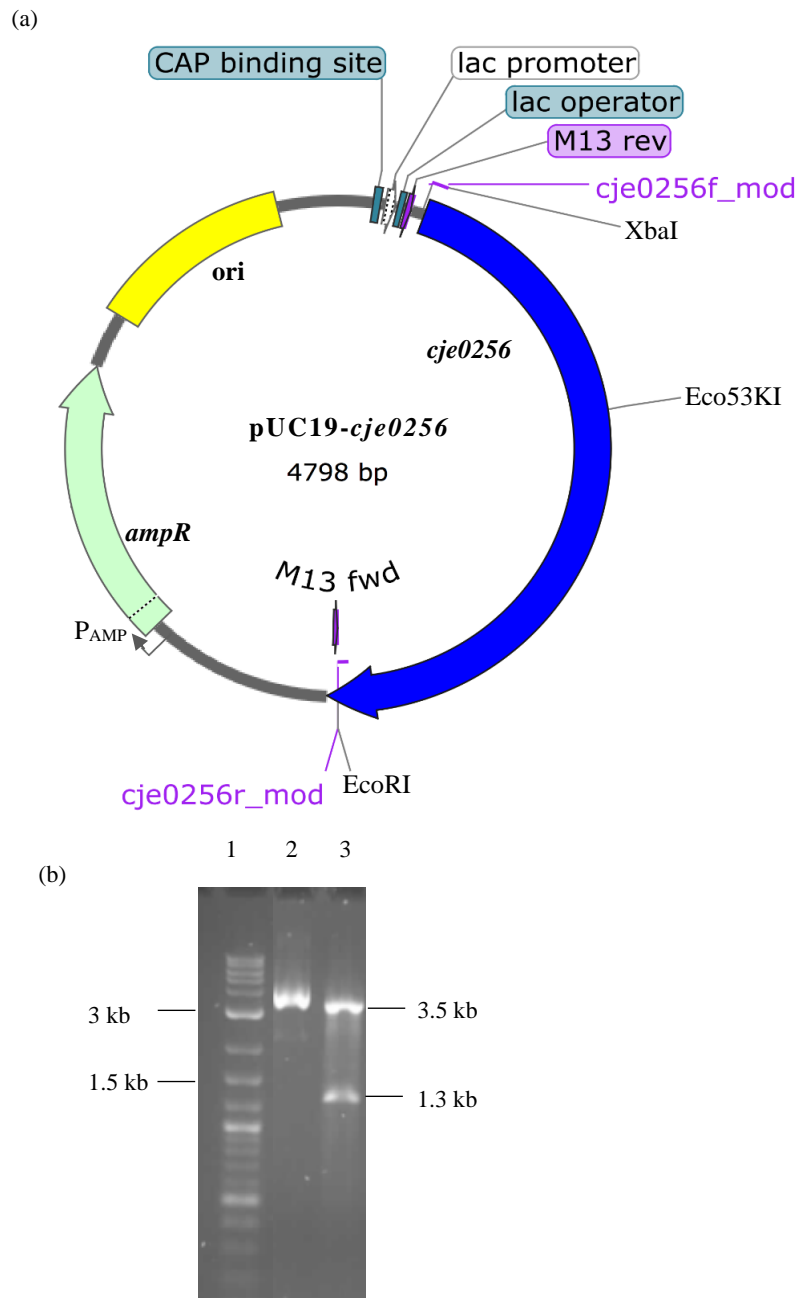


Figure 63. Verification of an intermediate construct pUC19-*cje0256* by restriction analysis.

(a) Restriction map of the plasmid indicating EcoRI and Eco53KI restriction sites used in restriction analysis, XbaI/EcoRI cloning sites and Eco53KI insertional site of *kan^r* cassette.

(b) Gel image showing uncut and digested pUC19-*cje0256* with EcoRI and Eco53KI. Expected sizes: 3.5 kb and 1.3 kb.

Samples: 1, 2-Log DNA ladder; 2, pUC19-*cje0256*; 3, pUC19-*cje0256* EcoRI/Eco53KI

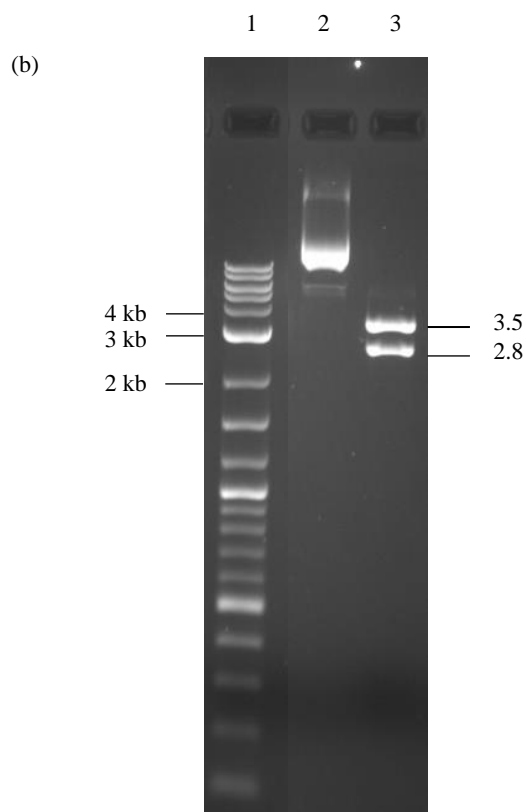
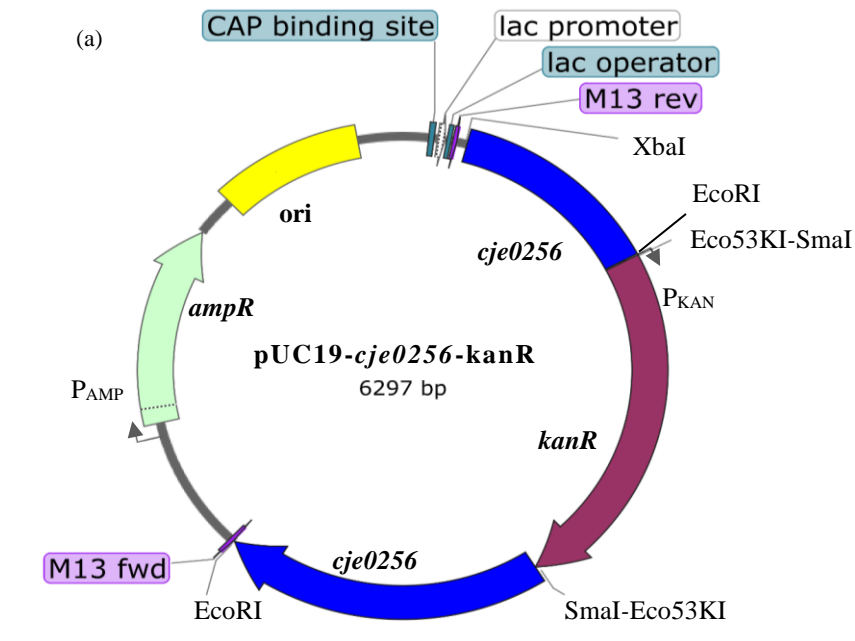


Figure 64. Verification of pUC19-*cje0256*-kanR by restriction analysis.

(a) Restriction map of the plasmid indicating EcoRI sites used in restriction analysis, and Eco53KI/SmaI cloning sites.

(b) Gel image showing uncut and digested pUC19-*cje0256*-kanR with EcoRI. Expected sizes: 3.5 kb and 2.8 kb.

Samples: 1, 2-Log DNA ladder; 2, pUC19-*cje0256*-kanR; 3, pUC19-*cje0256*-kanR EcoRI

3.3.2.2 Electroporation of pUC19-*cje0256*-kanR into *C. jejuni* RM1221 strain

C. jejuni RM1221 competent cells were prepared following the standard operating protocol with a minor modification. The new protocol included an initial incubation in ice for 1 h with chelating agent EDTA (10 μ M). This step was included to facilitate EDTA to hinder any DNase genes, which may otherwise cause degradation of the transformed DNA. Approximately 1 μ g of pUC19-*cje0256*-kanR and pRRC (control) were electroporated into the cells in parallel, with a time constant of 5.1 ms, using the standard electroporation conditions described in Section 2.24. Despite adding EDTA and using sufficient DNA, the electroporation experiments did not yield any colonies. The results remained the same even after several attempts. Another attempt with a higher electroporation resistance of 600 Ω was carried out, following the method by Gaasbeek *et al.* (2009), but this attempt also resulted in no transformants.

3.3.2.3 Methylation of DNA

Methylation of pUC19-*cje0256*-kanR plasmid was executed with the purpose of providing extra protection to the DNA before electroporation into RM1221 cells. This step was undertaken to circumvent the action of a restriction endonuclease and was carried out following a similar study conducted with *H. pylori* (Donahue *et al.*, 2000). NEB EcoGII methyltransferase was chosen to target all adenine residues. Methylation was carried out following the manufacturer's protocol, and an incubation time of 1–4 h was tested.

3.3.2.4 Restriction digestion of methylated DNA

Restriction enzyme RsaI was used to validate the DNA methylation procedure. After the methylation process, the DNA was purified following enzyme inactivation by heat. A small aliquot of methylated DNA was used for digestion with RsaI. Untreated pUC19-*cje0256*-kanR was employed as a control for the restriction analysis. The digestion results, as illustrated in Figure 65, indicated that some degree of methylation has certainly occurred, as a difference in

band patterns between the digested treated (lane 5) and untreated DNA (lane 3) were observed. Approximately 0.9 μg of methylated DNA was used for electroporation into *C. jejuni* RM1221 cells. As a control, methylated pRRC plasmid was used for electroporation. The electroporation experiments did not produce any colonies, even with methylated DNA.

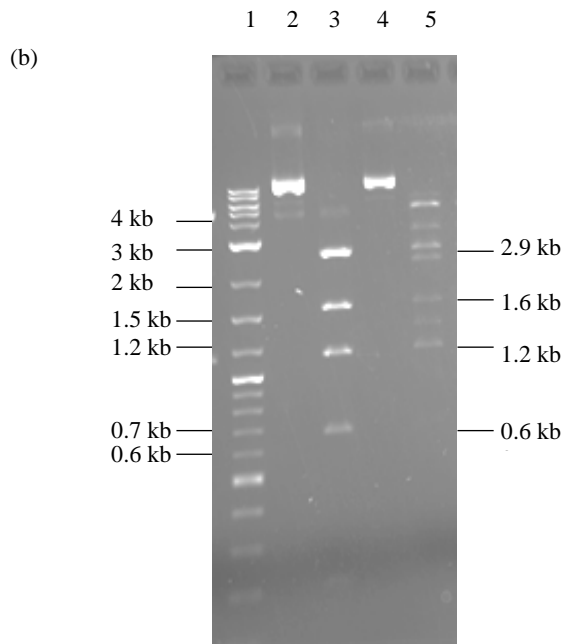
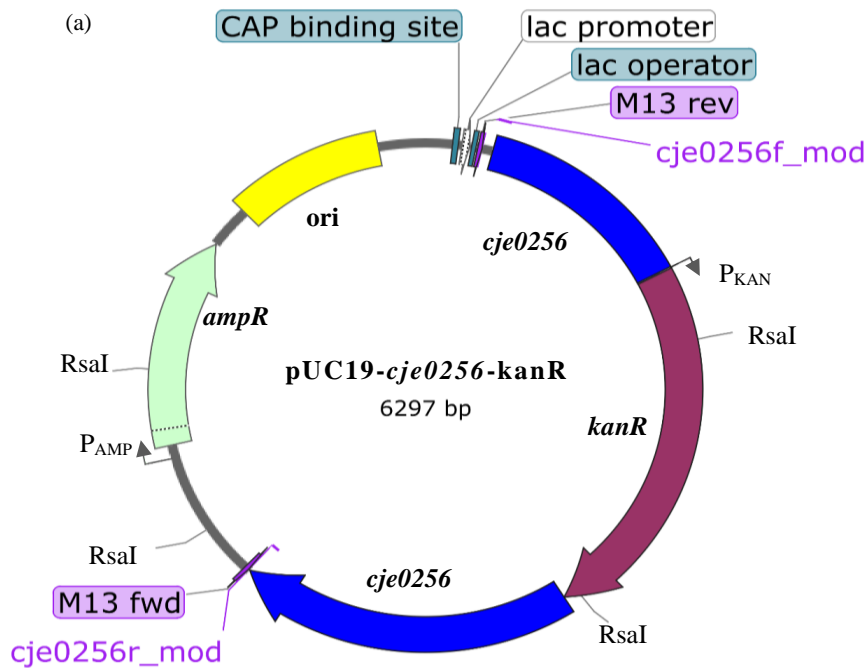


Figure 65. Restriction analysis of methylated pUC19-*cje0256*-kanR with *RsaI*
 (a) Restriction map of the plasmid indicating *RsaI* sites used in restriction analysis.

(b) Gel image showing untreated and methylated pUC19-*cje0256*-kanR with *RsaI*. Expected sizes with untreated DNA: 2.9 kb; 1.6 kb; 1.2 kb; and 0.68 kb. Samples: 1, 2-Log DNA ladder; 2, pUC19-*cje0256*-kanR; 3, pUC19-*cje0256*-kanR *RsaI*; 4, methylated DNA; 5, methylated DNA *RsaI*.

The methylated DNA was then re-methylated in an attempt to increase the percentage of methylated DNA for downstream electroporation experiments. Re-methylation was carried out, but restriction analysis with *RsaI* confirmed the lack of any drastic changes in the bands, excluding the presence or absence of some minor bands (Figure 66). The four major fragments expected with the untreated DNA digestion with *RsaI* were seen with methylated (lane 2) and re-methylated (lane 3) DNA samples as well. Approximately 0.8 μg of remethylated DNA was electroporated into RM1221 cells with 200 Ω and 600 Ω resistances, and kanamycin-resistant clones were not obtained with both electroporation experiments.

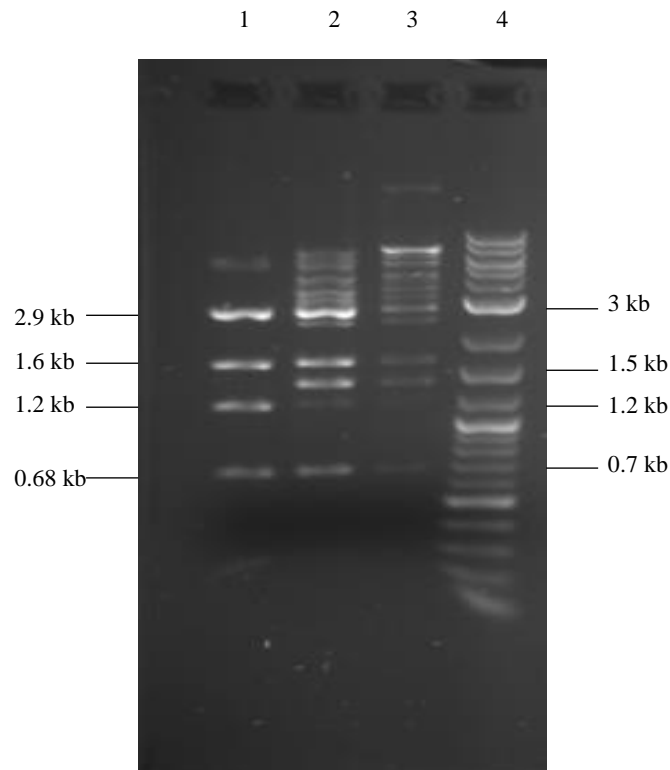


Figure 66. Restriction analysis of re-methylated pUC19-*cje0256-kanR* with *RsaI*. Expected sizes with untreated DNA: 2.9 kb; 1.6 kb; 1.2 kb; and 0.68 kb. Samples: 1, pUC19-*cje0256-kanR* *RsaI*; 2, methylated DNA *RsaI*; 3, remethylated DNA *RsaI*; 4, 2-Log DNA ladder.

3.3.3 Functional analysis of a putative nuclease Cje0256

An attempt to test the enzymatic properties of the purified Cje0256 was carried out in this section. Cje0256 with and without leader peptide was purified in this study. The arabinose-inducible pBAD33 expression vector was used for the expression of the His-tagged protein. The 6xHis tag was attached to the C-terminal of Cje0256/Cje0256LP, and purification was executed following manufacturer's protocol.

3.3.3.1 Construction of pBAD33-*cje0256* and pBAD33-*cje0256LP*

The identification of the sequence corresponding to the leader peptide in Cje0256 was determined using SignalP 3.0. The program predicted a most likely cleavage between LNA-KS. The first 51 bases corresponding to the leader peptide were removed and the resulting gene sequence was assigned as *cje0256LP* as shown in Figure S11 in the Appendix.

Expression constructs pBAD33-*cje0256* and pBAD33-*cje0256LP* were constructed to facilitate the purification of proteins Cje0256 and Cje0256LP. Primers *cje0256_for* and *cje0256_rev* were designed for the amplification of *cje0256* from *C. jejuni* RM1221 chromosomal DNA (Figure 67a). The expected *cje0256* PCR product is shown in Figure S12 in the Appendix. Primers *cje0256_LP_for_mod* and *cje0256_LP_rev_mod* were designed for the amplification of *cje0256LP* gene from RM1221 chromosomal DNA (Figure 68a). The expected *cje0256LP* PCR product is shown in Figure S13 in the Appendix. Q5[®] High-Fidelity DNA Polymerase was used for the PCR amplifications. The coding sequence used for the 6xHis tag in these constructs remained the same sequence as the pBAD33-*cj0979LP* construct. The pBAD33 and *cje0256/cje0256LP* were digested with XbaI and SphI. The resulting linear fragments were ligated and transformed into *E. coli* C2566L cells. Clones from both transformations were screened by CloneChecker for the presence of the inserts and subsequently confirmed by restriction analysis. Enzyme EcoRI was used for the restriction

analysis of both constructs, and the expected fragments were produced as illustrated in Figures 67 and 68. One clone from each construct was sent for Sanger sequencing to ensure that the insert and flanking regions contained no mutations. Sequencing from both directions of the insert was carried out using vector-related primers (pBAD_for and pBAD_rev). The sequencing results revealed a 100% identity for pBAD33-*cje0256* and pBAD33-*cje0256*LP, confirming no errors.

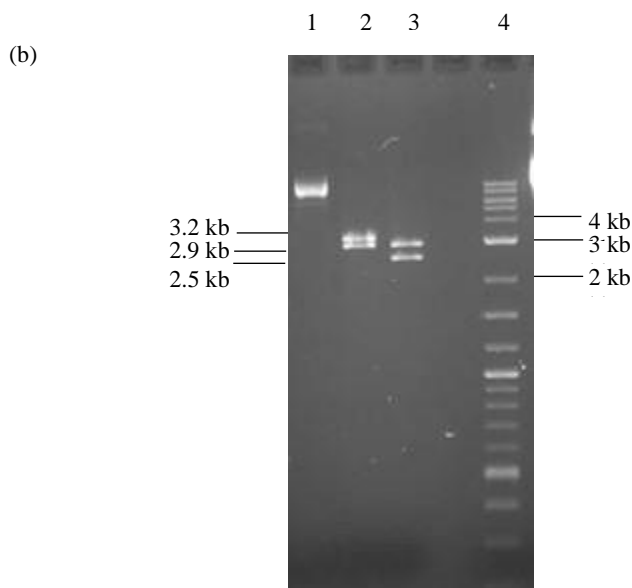
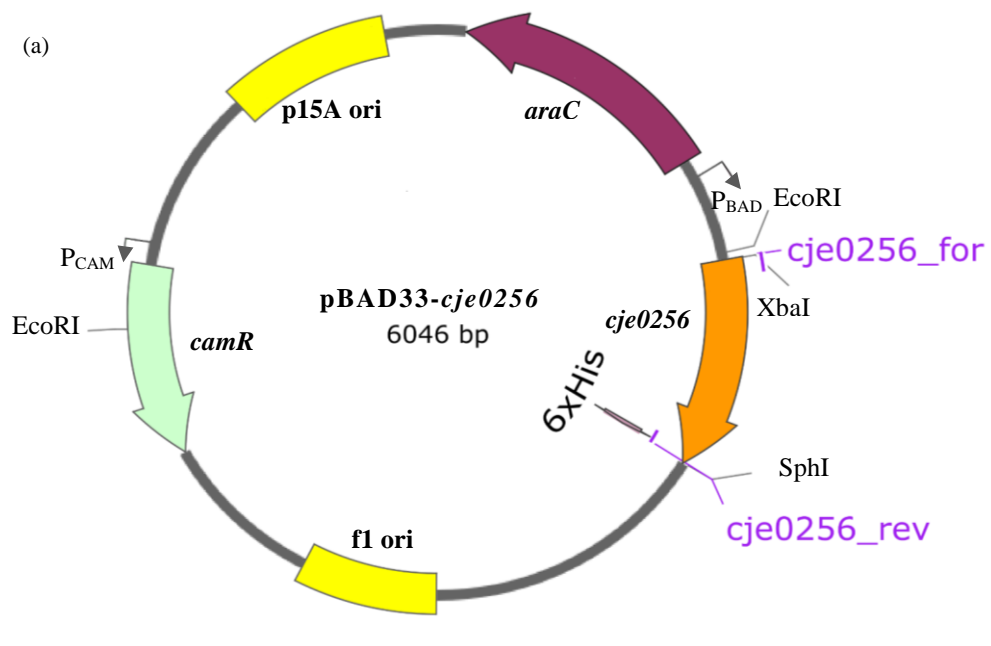


Figure 67. Verification of *pBAD33-cje0256* by restriction analysis.

(a) Restriction map of the plasmid indicating *EcoRI* sites used in restriction analysis, and *XbaI*/*SphI* cloning sites.

(b) Gel image showing uncut and digested *pBAD33-cje0256* with *EcoRI*.

Expected sizes: *pBAD33-cje0256*- 3.2 kb and 2.9 kb; *pBAD33*-2.9 kb and 2.5 kb.

Samples: 1, *pBAD33-cje0256*; 2, *pBAD33-cje0256* *EcoRI*; 3, *pBAD33* *EcoRI*; 4, 2-Log DNA ladder.

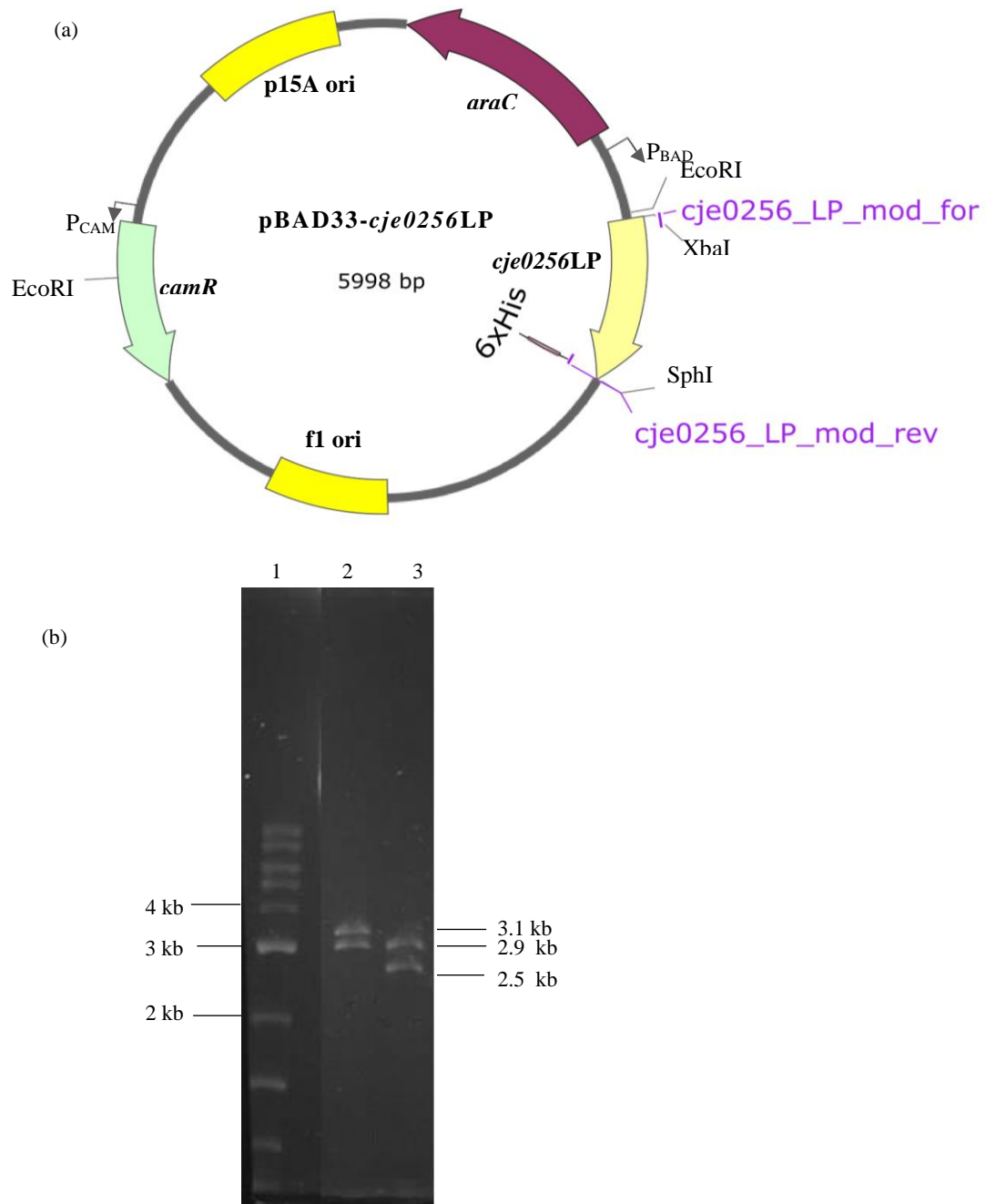


Figure 68. Verification of pBAD33-*cje0256LP* by restriction analysis.
 (a) Restriction map of the plasmid indicating EcoRI restriction sites used in restriction analysis, and XbaI/SphI cloning sites.
 (b) Gel image showing uncut and digested pBAD33-*cje0256LP* with EcoRI. Expected sizes: pBAD33-*cje0256*-3.1 kb and 2.9 kb; pBAD33-2.9 kb and 2.5 kb. Samples: 1, 2-Log DNA ladder; 2, pBAD33-*cje0256LP* EcoRI; 3, pBAD33 EcoRI

3.3.3.2 Purification of Cje0256 and Cje0256LP

The *E. coli* strains carrying the pBAD33-*cje0256* and pBAD33-*cje0256LP* plasmids were expressed in the presence of arabinose for the purification of their respective proteins. Strains were incubated in a shaker at 120 rpm and induced with 0.1% final concentration arabinose once the OD₆₀₀ of the culture reached 0.6. The cultures were induced for a further 2 h, after which they were collected for protein purification. At the end of the induction period, the OD₆₀₀ measurements of the cultures were as follows: *E. coli*/pBAD33-*cje0256* - OD₆₀₀ of the induced sample, 0.78 and OD₆₀₀ of the uninduced sample, 0.98; *E. coli*/pBAD33-*cje0256LP* - OD₆₀₀ of the induced sample, 0.83 and OD₆₀₀ of the uninduced sample, 0.85. The MagneHis protein purification kit was employed to conduct purification following the manufacturer's protocol. After the purification process, whole cell suspensions, lysates, wash fractions, and eluates were run on an SDS-PAGE gel. Equivalent amount of each fraction was run on the gel. Figures 69 and 70 represent the results, which revealed no expected protein products in any of the lanes. In Figure 69, several bands were obtained after Coomassie staining in lanes 1-6, but the expected protein band (27.23 kDa) was not seen in any of the fractions.

In Figure 70, the band patterns between the induced and uninduced whole cell suspensions and lysates fractions appeared similar, with no band obtained near the 25.4 kDa corresponding to the target protein's size. In this particular purification, the *E. coli*/pBAD33-*cj0979LP* strain was used as a control. The expected band for the Cj0979LP protein was obtained near 16.8 kDa. In summary, the lanes containing the eluates indicated no expected protein products in either of the gels. The successful purification of Cj0979LP protein confirmed that the purification process used was adequate, and the failure to detect Cje0256/Cje0256LP most likely occurred due to the instability of the proteins.

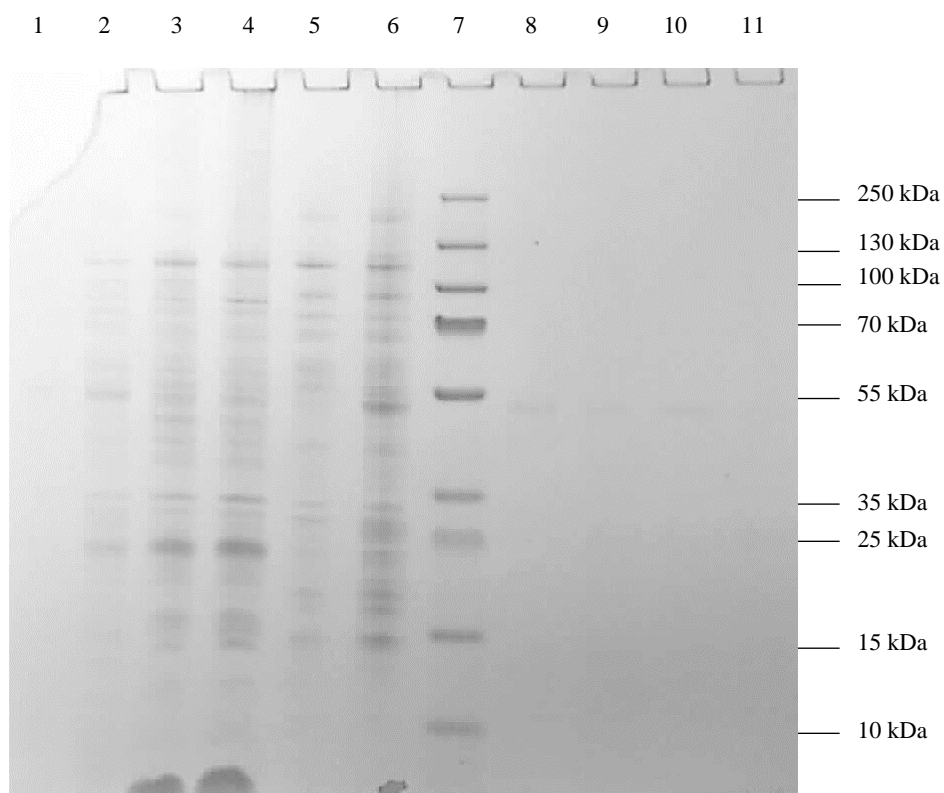


Figure 69. Analysis of fractions from *E. coli*/pBAD33-*cje0256* protein expression and purification experiment. Expected size of Cje0256-27.23 kDa.

Samples: 1, Uninduced whole cell suspension; 2, Induced whole cell suspension; 3, Uninduced lysate; 4, Induced lysate; 5, Uninduced wash fractions 1,2 and 3; 6, Induced wash fractions 1,2 and 3; 7, Pre-stained ladder; 8, Eluate from uninduced sample same day as purification; 9, Eluate from induced sample same day as purification; 10, Eluate from uninduced sample after two days storage at 4°C; 11, Eluate from induced sample after two days storage at 4°C.

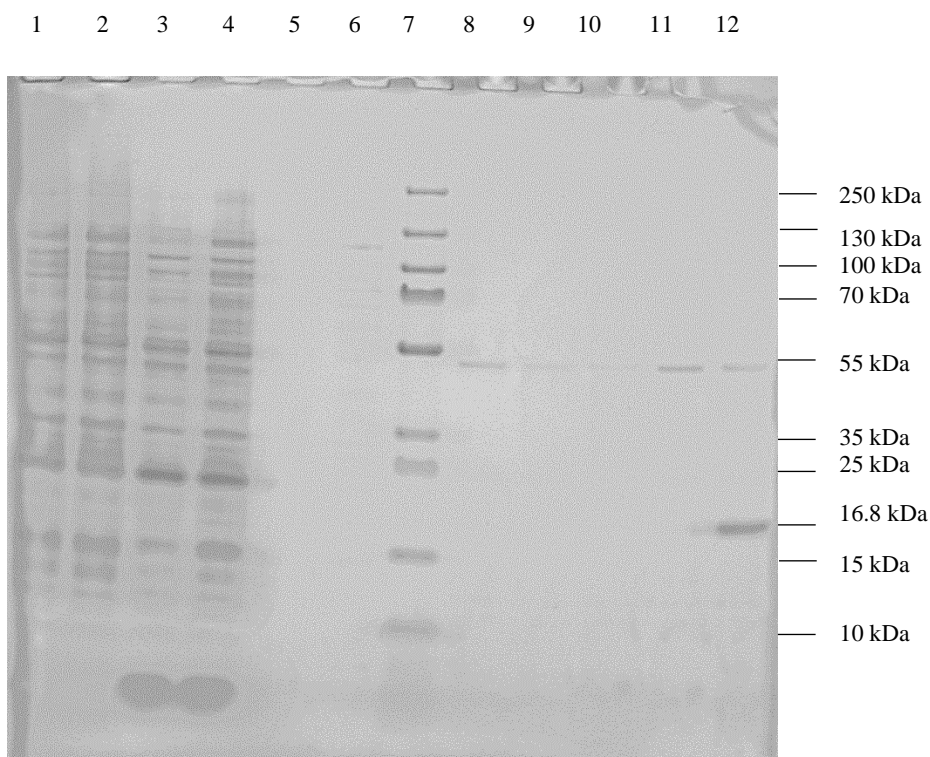


Figure 70. Analysis of fractions from *E. coli*/pBAD33-*cje0256*LP and *E. coli*/pBAD33-*cj0979*LP protein expression and purification experiment. Expected sizes: Cje0256LP- 25.4 kDa; Cj0979LP- 16.8 kDa.

Samples: 1, Uninduced whole cell suspension; 2, Induced whole cell suspension; 3, Uninduced lysate; 4, Induced lysate; 5, Uninduced wash fractions 1,2 and 3; 6, Induced wash fractions 1,2 and 3; 7, Pre-stained ladder; 8, Eluate from uninduced sample same day as purification; 9, Eluate from induced sample same day as purification; 10, Eluate from induced sample same day as purification; 11, Purified Cj0979LP protein from uninduced sample; 12, Purified Cj0979LP protein from induced sample

To troubleshoot, protease inhibitor was added to provide stability to the proteins in case they underwent degradation during lysis. The protein expression and purification processes were repeated with *E. coli* strains carrying the *cje0256* and *cje0256*LP. Three samples of each construct were tested on the SDS-PAGE gel. As a positive control strain, *E. coli*/pBAD33-*cj0979*LP was purified in parallel. At the end of 2 h, the OD₆₀₀ measurements of the three cultures were as follows: *E. coli*/pBAD33-*cje0256*-OD₆₀₀ of induced sample, 0.82 and OD₆₀₀ of uninduced sample, 0.95; *E. coli*/pBAD33-*cje0256*LP- OD₆₀₀ of induced sample, 0.89 and OD₆₀₀ of uninduced sample, 0.97; *E. coli*/pBAD33-*cj0979*LP- OD₆₀₀ of induced sample, 0.87

and OD₆₀₀ of uninduced sample, 0.95. All the purified samples were run on an SDS-PAGE gel with equivalent amounts and stained using Coomassie staining for protein detection. Figure 71 illustrates the image of the stained gel containing the eluate samples. Only the positive control lane corresponding to Cj0979LP revealed a band with the expected protein size (16.8 kDa), while the other lanes corresponding to the induced eluate samples of Cje0256 and Cje0256LP showed no protein products.

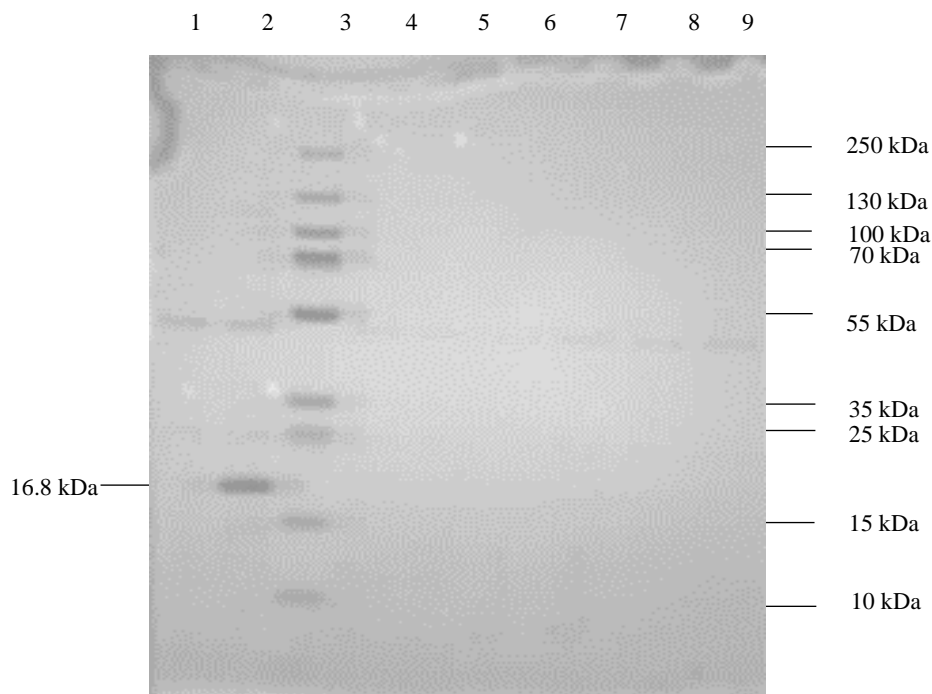


Figure 71. Analysis of fractions from *E. coli*/pBAD33-*cje0256*, *E. coli*/pBAD33-*cje0256*LP, and *E. coli*/pBAD33-*cj0979*LP expression and purification experiments. Purification of Cj0979LP was carried out as positive control. Expected sizes: Cje0256LP-25.4 kDa; Cje0256-27.23 kDa; Cj0979LP-16.8 kDa. Samples: 1, Purified Cj0979LP from uninduced sample; 2, Purified Cj0979LP from induced sample; 3, Pre-stained ladder; 4, Eluate from uninduced sample (Cje0256); 5, Eluate from induced sample with protease inhibitor (Cje0256); 6, Eluate from induced sample (Cje0256); 7, Eluate from uninduced sample (Cje0256LP); 8, Eluate from induced sample with protease inhibitor (Cje0256LP); 9, Eluate from induced sample (Cje0256LP).

3.3.3.3 Western blotting

The samples were analysed on an SDS-PAGE gel and tested by Western blotting since protein detection was not successful with Coomassie staining. This rerun was undertaken as blotting assays have better sensitivity for protein detection, as evidenced with Cj0979 protein in Section 3.2. The same primary and secondary antibodies against the 6xHis tag were used. Figure 72 illustrates the Western blotting result, and once again, only the control lane produced the expected protein band of 16.8 kDa. The bands for Cje0256 at 27.23 kDa and Cje0256LP at 25.4 kDa were not obtained even with better sensitivity testing.

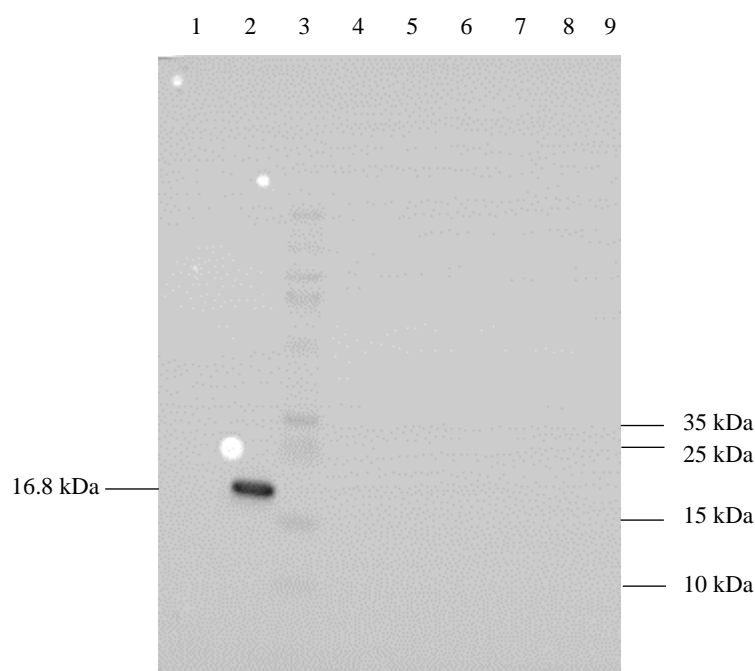


Figure 72. Western blotting of Cj0979LP and eluates from *E. coli*/pBAD33-*cje0256* and *E. coli*/pBAD33-*cje0256*LP purification experiments. Detection of Cj0979LP was carried out as positive control. Expected sizes: Cje0256LP-25.4 kDa; Cje0256-27.23 kDa; Cj0979LP-16.8 kDa.

Samples: 1, Purified Cj0979LP from uninduced sample; 2, Purified Cj0979LP from induced sample; 3, Pre-stained ladder; 4, Eluate from uninduced sample (Cje0256); 5, Eluate from induced sample with protease inhibitor (Cje0256); 6, Eluate from induced sample (Cje0256); 7, Eluate from uninduced sample (Cje0256LP); 8, Eluate from induced sample with protease inhibitor (Cje0256LP); 9, Eluate from induced sample (Cje0256LP).

Chapter 4: Discussion and future work

4.1 Construction and verification of systems for regulated gene expression in *C. jejuni*

In *E. coli*, the arabinose-inducible P_{BAD} promoter system allows the generation of conditionally lethal mutants where investigation of essential gene is required (Guzman *et al.*, 1995). The AraC regulator and P_{BAD} promoter are widely employed in other Gram-positive and Gram-negative bacteria that require tight control of gene regulation. Some studies have used the arabinose-inducible promoter system from *E. coli* for the expression of toxic genes in other bacterial species such as *Pseudomonas* (Qiu *et al.*, 2008). One study illustrated the induction mechanism in *Pseudomonas* differed from that of the model organism *E. coli*; expression was independent of CCR (Meisner and Goldberg, 2016). The authors attributed this variance to the difference in the function of CCR between the two bacteria; unlike *E. coli*, *Pseudomonas* prefers amino acids and organic acids for metabolism. Similarly, *Campylobacter* prefers amino acids and organic acids as metabolites. Studies have found the presence of the catabolite activator protein sequence upstream of the *fur* gene in *Campylobacter*, but details of the regulatory mechanism in these bacteria is still unclear (Chan *et al.*, 1995; van Vliet *et al.*, 2000). CCR occurs when multiple carbon sources are available in the medium, so bacteria consume the most preferred carbon source first for energy production, continuing sequentially until they reach the least preferred carbon source, which is consumed last (van der Stel *et al.*, 2018). Amino acids such as serine and aspartate, followed by glutamate and proline, represent the most preferred sources for catabolism in *Campylobacter*. In addition, *C. jejuni* also utilizes organic acids such as lactate, pyruvate, acetate, and other intermediates of TCA cycle for catabolism (Hofreuter, 2014). *Campylobacter* cannot metabolise glucose and other common sugars like *E. coli*, since they lack transporters and key enzymes involved in the glycolytic pathway. *C. jejuni* was regarded as non-saccharolytic bacteria until evidence of fucose utilization was recently demonstrated in *C. jejuni* NCTC 11168, which is the only exception (Hofreuter, 2014; Stahl *et*

al., 2011).

This study aimed to develop a gene regulation system under the control of the P_{BAD} promoter in *Campylobacter* for the investigation of essential genes such as *amiA*, which may be responsible for CFF. Initial difficulties were encountered in producing highly efficient competent cells of *Campylobacter*, mainly because commonly used shuttle vectors cannot be sustained in *C. jejuni* (Karlyshev and Wren, 2005a). To optimize electroporation, an altered procedure was performed to produce highly efficient cells. A reduction in the duration of the initial incubation on the non-selective plate (instead of overnight incubation) helped increase the electroporation efficiency. Reduced incubation time averts excessive growth, which may otherwise leave the cells competing for nutrients on selective plates. Also, shorter incubation periods provide sufficient time for expression of the newly acquired antibiotic-resistance gene while avoiding the growth of non-transformed cells. In addition, reduced incubation time decreases the chances of cell division, which may lead to plasmid loss and thus false-positive results. The genes *araE* and *lacYA177C* encoding arabinose transporters, which are not present within *C. jejuni*, were introduced into these bacteria by electroporation. These genes were placed under the control of a chloramphenicol promoter P_{CAM} for constitutive expression, along with the *gfp* gene under the control of the P_{BAD} promoter. Such an approach was undertaken following the study conducted by Khlebnikov *et al.* (2000). Constitutive expression from the P_{CAM} promoter has produced successful expression of many exogenous genes in *C. jejuni* (Karlyshev and Wren, 2005a).

Modified *lacY* gene was successfully introduced into *C. jejuni* 11168H, but the introduction of *araE* was initially not successful. The reason for this failure is not known, as the expression plasmids were constructed following the same principle (i.e., coupling the pRRC plasmid and the P_{BAD} regulatory region). In addition, the overall plasmid sizes were comparable. Both AraE

and LacY are sugar-proton symporters located in the inner membrane of the cells. Both genes were isolated from *E. coli* K12. In addition, both constructs possessed similar flanking regions for homologous recombination. The difference in the electroporation results cannot be explained at present.

To troubleshoot electroporation, a mutant 11168H/*cj1051* was constructed. The mutant possessed higher transformation efficiency than the wild-type and permitted integration of the gene cassette carrying the *araE* gene. Overall, knocking out the *cj1051* did increase the transformation efficiency marginally, as suggested by Holt *et al.* (2012). The study revealed that inactivation of this gene in *C. jejuni* led to a thousand-fold increase in transformation efficiency when plasmids from a heterologous *C. jejuni* host were used but only allowed weak transformation of plasmids from an *E. coli* host. In addition, the findings from the study of Holt *et al.* (2012) were consistent with another study by Zeng *et al.* (2015). The authors deduced that *cj1051* was a limiting factor contributing towards conjugation efficiency but was not the sole determinant. Genetic manipulation across *C. jejuni* strains has been challenging for many years, and it is possible that more than one restriction-modification system is present in *C. jejuni* 11168H, thus affecting the natural competence of these bacteria (Davis *et al.*, 2008).

Initial confirmation of the integration of gene cassettes carrying *araE/lacYA177C* was achieved using PCR verification using the GoTaq[®] Green Master Mix (Promega) with primers specific to the integration sites (ak233-235). A product obtained with these external primers would indicate the location of the integration site. The PCR testing of the 11168H/pRRBCD-*egfp-lacYA177C* derivative yielded the expected band, which revealed that the gene cassette was inserted into the integration site where the ak235 primer sequence was located (Figure 19). However, difficulties were encountered during the PCR analysis of the 11168H/*cj1051*/pRRBCD-*egfp-araE* transformants, as amplification was obtained only with

the internal primers pRR1 and ak237. The external primers (ak233-235) did not yield the same product as the 11168H/pRRBCD-*egfp-lacYA177C* transformants, despite using similar PCR conditions. However, genome sequencing of the derivative strains confirmed that the delivery gene cassettes were wholly integrated between the 16S rRNA and 28S rRNA gene clusters, as expected with both plasmids (Figure 29 and Figure 30). The flanking regions of the gene cassettes were designed to recombine with one of the three rRNA loci corresponding to the three ak233-235 primers. Attempts were therefore made to troubleshoot PCR issues with the 11168H/*cj1051*/pRRBCD-*egfp-araE* transformants. The more robust NEB Q5[®] High-Fidelity DNA Polymerase was used, and a PCR product corresponding to the expected fragment size was obtained, confirming that the gene cassette was inserted at the integration site where the primer ak235 sequence was located (Figure 31). This finding demonstrates that the initial problem with PCR verification occurred due to the type of polymerase employed. In conclusion, both of these gene cassettes carrying the transporter genes were successfully integrated into the *C. jejuni* 11168H genome, which was confirmed by PCR and genome sequencing.

The *C. jejuni* derivative strains were tested for *gfp* induction in the presence of arabinose to determine whether the inducible promoter can be regulated in *Campylobacter*. Solid agar plates failed to reveal any fluorescence with the *C. jejuni* derivative strains, under the same microscope settings as used for the control *E. coli*/pRRBCD-*egfp-lacYA177C* strain. Liquid cultures were tested because the sensitivity of fluorescence signal detection would be greater with a fluorimeter than with a fluorescence microscope. The fluorescence signals of the *C. jejuni* derivative strains in liquid cultures appeared very weak compared to the *E. coli* control strain. In this study, gene expression was tested by measuring fluorescence of the GFP protein; however, an alternative method involving monitoring gene expression at the mRNA level using reverse transcription PCR could be used in the future (Sharkey *et al.*, 2004). The fluorescence intensities obtained with *C. jejuni* cultures were insignificant compared to the *E.*

coli/pRRBCD-egfp-lacYA177C strain, even when twice the amount of arabinose was used (Figures 33 and 34). The lack of GFP induction in both strains implied that arabinose was not transported into the cells for the induction of the promoter, even when the gene responsible for transportation was under the control of a constitutive promoter. The P_{CAM} promoter is a part of the chloramphenicol resistance gene cassette, which was derived from plasmid pAV35 originating from *C. coli* (van Vliet *et al.*, 1998).

Conversely, the growth-rate assays revealed that addition of arabinose caused retardation in the rates, even with the wild-type 11168H strain that does not contain the transporters for arabinose (Figure 32). The molecular mechanism of growth inhibition caused by arabinose is unclear and requires further study. Alternatively, as future work, arabinose transport assays similar to the work by Khlebnikov *et al.* (2000) could be conducted in which ¹⁴C- labelled arabinose and scintillation counter were employed. In their study, the transporter genes were preinduced with IPTG, followed by incubation with 0.02% arabinose for 2 min and then the cells were analysed in a scintillation counter. A similar experiment could be conducted to check for the presence of arabinose transportation in the *C. jejuni* derivatives. In conclusion, the GFP expression results suggest that regardless of the presence of the arabinose transporter genes within the chromosome, *Campylobacter*, unlike *E. coli*, lacks the ability to transport arabinose into their cells. This indicates that some notable differences in the biology of these bacteria exist that require further study.

In the closely related bacteria *H. pylori*, a system harbouring the *lacI*-P_{TAC} region of *E. coli* was developed for conditional mutant generation for the study of two essential genes (*pbpI* and *ftsI*) (Boneca *et al.*, 2008). The system was validated in these bacteria in the presence of IPTG as the inducer. As an alternative to an arabinose-inducible gene expression system and other sugar-related systems, future studies could test another system harbouring the P_{TET}

promoter, since it does not require special transporter proteins for the tetracycline inducer in *Campylobacter*. Induction by P_{TET} has been widely studied in many bacteria, including *H. pylori* for gene regulation studies (McClain *et al.*, 2013; Debowski *et al.*, 2013). Furthermore, investigation of essential gene using the tetracycline promoter has been carried out in *Mycobacteria* with the generation of conditional lethal mutants (Carroll *et al.*, 2005). Utilization of the P_{TET} promoter coupled with the pRR plasmid system could therefore be a viable option in *Campylobacter* for the investigation of essential genes such as *amiA*.

Another strategy could be to test an *Lactococcus lactis* ZnP inducible promoter by coupling with the pRR delivery plasmid in *Campylobacter* (Lull and Poquet, 2004). The expression construct can be validated in the *L. lactis* strain first using the reporter gene *gfp*. If evidence exists for GFP induction, then the expression construct can then be tested with *C. jejuni* in the hope of constructing a regulatable expression system. This EDTA-inducible ZnP promoter has been successfully used by Trémillon *et al.* (2010) to study the *S. aureus* nuclease in *L. lactis*. Future studies could attempt to maintain this promoter in *C. jejuni*.

4.2 Investigation of molecular mechanism of biofilm formation and dispersal in *C. jejuni* 11168H

This study primarily aimed to identify the genetic determinant involved in the biofilm formation and dispersion of *C. jejuni* 11168H. The biofilm-formation pattern of *C. jejuni* 11168H was investigated due to this strains' identification as a high yielding biofilm-former as well as its use as a control strain for most biofilm studies involving *Campylobacter* (Brown *et al.*, 2015b). Previous studies revealed that dispersed cells possess greater colonizing properties than their planktonic or sessile cells (Guilhen *et al.*, 2017). *C. jejuni* species are able to form mono-species biofilms *in vitro* where growth conditions are more specific to the microorganism and preferably under static conditions, where better fixation is achieved (Rossi *et al.*, 2017; Teh *et*

al., 2019). In this present study, biofilm optimization experiments of *C. jejuni* 11168H under static conditions were conducted to determine the biofilm formation pattern. The results from this study revealed that strong biofilms formed after 4 days of incubation and continued growing until day 8, after which dispersal was observed (Figure 35). Dispersal was quantified by measuring the absorbance of CV stain. The formation trend obtained during the first 3 days compared favourably with results from previous studies by Reuter *et al.* (2010) and Brown *et al.* (2015b). However, the results after day 4 could not be compared with the literature, as longer incubation times of this particular strain have not been previously investigated.

As described in introduction, *Campylobacter* biofilms predominantly consist of eDNA. Brown *et al.* (2015a) demonstrated that addition of DNase I caused disintegration of eDNA, which in turn caused dispersion of *C. jejuni* biofilms. In another study by Brown *et al.* (2015b), the authors identified an extracellular nuclease gene responsible for biofilm dispersal in another *C. jejuni* strain. Similarly, the present study investigated the gene involved in regulating this process in *C. jejuni* 11168H. A decrease in biofilm formation of wild-type 11168H after day 8 implied that the dispersion might be a genetically regulated process in *C. jejuni*. In this study, the *cj0979* gene, which was proposed as a putative nuclease according to the GenBank sequence database, was inactivated in strain 11168H. The biofilm growth of the mutant (11168H/*cj0979*) was compared to that of the 11168H strain. The results indicated that although there was a slight increase in absorbance readings for the mutant, the difference was not significant, as reflected by the high *p*-values (Figure 48). Given that this gene is a DNase-encoding gene, an increase in biofilm mass was expected with the mutant, provided the eDNA remains undisturbed and does not undergo degradation. However, this expectation was not confirmed. Similar mutant studies involving bacteria such as *N. gonorrhoea* and *V. cholerae* resulted in stronger biofilm mass compared to their wild-types (Seper *et al.*, 2011; Steichen *et al.*, 2011). Comparing the results obtained from this present study to the literature, it can be

concluded that *cj0979* may not be the only nuclease gene in *C. jejuni* 11168H; there may be similar genes whose functions have not yet been detailed. This possibility is plausible, as there is evidence of another *C. jejuni* strain, RM1221, with such properties with more than one DNase-encoding gene (Brown *et al.*, 2015b). In another study, two thermonucleases have been identified in *S. aureus*, both possessing similar DNA-degrading enzymatic properties (Kiedrowski *et al.*, 2011; Kiedrowski *et al.*, 2014). Since biofilm studies of the mutant did not result in the expected findings, future studies should examine different levels of expression of *cj0979* and investigate their effects on *C. jejuni* biofilms, with the aid of a regulatable expression system.

This study also investigated the enzymatic properties of purified Cj0979LP protein. The purified Cj0979 could only be quantifiable using a high sensitivity assay such as Western blotting, which indicated the low yield of the protein. However, the initial obstacles with protein expression were overcome by conducting purification after removing the leader peptide and employing the same histidine coding sequence used in Atas *et al.* (2016). The purified Cj0979LP could be detected with Coomassie staining (Figure 58). Degradation of substrate DNA was obtained with purified Cj0979LP, establishing its DNA-degrading properties. This finding was further illustrated in tests with biofilms. Treatment of *C. jejuni* 11168H biofilms with the purified protein resulted in a reduction in biofilm formation (Figure 60). The results were consistent with the functions of similar thermonucleases discovered in *S. aureus* and *N. gonorrhoeae* (Steichen *et al.*, 2011; Kiedrowski *et al.*, 2014). In summary, this study was the first to investigate the role of *cj0979* in *Campylobacter* biofilms. This novel finding indicates that the *cj0979* gene is indeed an extracellular nuclease possessing DNase activities that can degrade DNA and play a role in biofilm dispersion. In future work, to further establish the properties of the nuclease in biofilm formation, the protein could be added to the initial inoculum to monitor its effects on the ability of *C. jejuni* 11168H to form new biofilms.

Supernatant samples from *C. jejuni* 11168H biofilms were checked for the presence of nuclease activity by using eDNA as substrate. Brown *et al.* (2015b) carried out experiments focused on detecting the nuclease activity in *C. jejuni* NCTC 11168 cell suspensions against self-DNA. Their results showed a lack of nuclease activity. In another study by Jung *et al.* (2017), a similar procedure testing *C. jejuni* NCTC 11168 cell suspensions was conducted, and only one sample exhibited (very weak) nuclease activity. In the present study, therefore, a slightly different approach was adopted. Experiments were set up to detect nuclease activity in the cell-free culture supernatant sample. The gel electrophoresis results did not provide convincing evidence regarding enzymatic activity of the nuclease. The samples containing the supernatant ran slower on the agarose gel than in the control DNA lane. Treatment of the supernatant with Proteinase K suggested the presence of binding proteins. In summary, detection of the activity of nuclease in the culture supernatant, using gel electrophoresis posed complications due to the slower migration of the DNA complex in the supernatant (Figure 39). Conversely, when the culture supernatant was added to *C. jejuni* 11168H biofilms in the presence of DNase buffer, a reduction in biofilm formation was observed, suggesting that some level of activity of the nuclease in the culture supernatant exists and reduces biofilm formation. The results confirmed that the purified protein and the secreted enzyme in the culture supernatant contained DNase activity and can reduce biofilm formation.

To further investigate the composition of the DNA-protein complex, the supernatant after media exchange was treated with trypsin and the flowthrough fraction containing smaller peptides was analysed using mass spectrometry. The total amount of proteins recovered from the trypsin-treated samples only represented 50% of the amount present in the initial protein sample. This estimation could be incorrect due to the limitations of the BCA assay. According to the manufacturer, the presence of substances such as sucrose (sugars) can interfere with the protein-concentration estimation. The very low A260/A230 ratio of the sample suggested the

presence of potential interfering substances such as mainly sugars and oligosaccharides, in the DNA complex sample.

Jowiya *et al.* (2015) identified dextran as one of the components of the EPM in *C. jejuni* biofilms. The dextran-digestion experiment in this study revealed a lack of dextran-like sugars present in the DNA complex, indicating that the low A260/A230 ratio could be a representation of the presence of free polysaccharides (most likely CPS). According to the mass spectrometry data, no known DNA-binding protein was identified, as most of the hits represented general housekeeping genes. Due to the limitation of the experiment, the uncharacterized protein Cj0449c that was listed in the mass spectrometry data may not represent a DNA-binding protein (Figure 41). This is because the flowthrough fraction would have contained not only bound proteins, but also non-bound proteins smaller than 10 kDa, which would have passed through the centrifugation step. To alter this experiment, it is necessary to first remove all the non-bound proteins and then proceed with trypsin treatment to cleave off bound proteins in order to identify the presence of DNA-binding proteins.

4.3 Investigation of the role of *cje0256* in the biofilm-forming ability of *C. jejuni* RM1221

This study investigated the biofilm-forming ability of *C. jejuni* RM1221. The results indicated that RM1221 has 70% of 11168H's capacity to form biofilms (Figure 61), which contradicts results from previous research, in which the strain exhibited only 30% of 11168H's capacity (Brown *et al.*, 2015b). In *C. jejuni* RM1221, three DNase-encoding genes (*cje0256*, *cje1441*, and *cje0566*) have been identified as extracellular nucleases and have been shown to play a role in the natural competence of this strain (Brown *et al.*, 2015b; Gaasbeek *et al.*, 2009; Gaasbeek *et al.*, 2010). In a study by Brown *et al.* (2015b), the authors emphasized the role of *cje1441* in biofilm formation and deduced that DNase activity inhibits biofilm formation in the

RM1221 strain. In addition, they demonstrated that, unlike the wild-type strain, the RM1221/*cje1441* mutant lacked the ability to degrade genomic DNA, further highlighting the enzymatic activity of Cje1441. In addition, the nuclease activities of Cje1441 and Cje0566 proteins were confirmed with DNA-hydrolysis assays (Gaasbeek *et al.*, 2010). Furthermore, Gaasbeek *et al.* (2009) tested extracts of *Campylobacter dns* (*cje0256*) positive and negative strains for the presence of nuclease activity using phage lambda DNA as substrate; the authors observed complete DNA degradation with the *dns* positive strain.

In this study, the attempt to investigate the role of the *cje0256* gene in *C. jejuni* RM1221 biofilm formation was not successful, as the pUC19-*cje0256*-kanR derivative could not be introduced into the *C. jejuni* RM1221 strain. The electroporation experiments were implemented using several batches of newly prepared cells. Initially, the protocol was unchanged. The cells were prepared using a freshly prepared buffer, and electroporation was carried out with untreated pUC19-*cje0256*-kanR and control plasmid pRRC, using standard conditions (as stated in Materials and Methods) and altered conditions (higher resistance of 600 Ω) (Gaasbeek *et al.*, 2009). Overall, neither of the electroporations produced any chloramphenicol-resistant colonies for RM1221/pRRC or kanamycin-resistant colonies for RM1221/pUC19-*cje0256*-kanR. In an attempt to troubleshoot, the protocol was slightly modified; 10 μ M EDTA was incorporated to check for its DNase-hindering effects as executed by Brown *et al.* (2015b), since the strain consists of three DNase enzymes. However, the modification did not improve the electroporation efficiency, which suggests that EDTA alone was not sufficient to counteract the intracellular nuclease activity.

In a further modification, DNA methylation was carried out to provide extra protection from potential DNA-degrading enzymes. A generic methyltransferase NEB EcoGII, which targets the adenine (A) residues of RM1221, was chosen. This enzyme was selected because the target

sequence of *Campylobacter* RM1221 was unknown. Beauchamp *et al.* (2017) identified the target sequence for methylation of *C. jejuni* 11168 as RAATTY. Given this study as a reference and the fact that *Campylobacter* has AT-rich genomes, the selection of EcoGII, which targets all adenine in any sequence context, was justifiable. Complete methylation was not achieved, which was acceptable, as only < 75% methylation of plasmid DNA was guaranteed by NEB (Figure 65). Re-methylation was attempted, but it did not produce a drastic change in the methylation pattern, which could be due to the steric hindrance created by the already methylated adenine residues. No transformants were produced with the methylated and re-methylated DNA when introduced into EDTA-treated and untreated RM1221 cells. Gaasbeek *et al.* (2009) listed RM1221 as a naturally non-transformable strain due to the presence of the same gene (*cje0256*) that inhibits the natural competence of the cells. Despite modifications to the DNA and competent cells, the construction of the knockout strain was unsuccessful. This failure may indicate that the strain is not just resistant to natural transformation, as demonstrated by Gaasbeek *et al.* (2009), but also resistant to electroporation procedures under normal conditions without incorporating any host-specific modifications, due to the cytoplasmic nuclease activity. No studies were found describing direct electroporation of exogenous DNA into RM1221 cells. However, a study by Miller *et al.* (2000) demonstrated electroporation of pMW10-based vectors, after modifying the vector according to the host-specific requirements. The vector was first introduced into an RM1221/*Str^r* derivative strain by triparental mating. This transformed vector was then used for direct electroporation with wild-type RM1221 cells. Since the strain produces more than one DNA-degrading enzyme but adenine methylation did not succeed, future work could consider other methylase targeting C/G-recognizing bases instead. As an alternative strategy, to determine the role of *cje0256* in biofilm, future work should examine the regulation of the expression of this gene and its effects on RM1221 biofilm-forming properties.

Furthermore, expression plasmids designed for protein purification were successfully constructed and verified by sequencing to be free of any mutations. Protein expression experiments with both pBAD33-*cje0256* and pBAD33-*cje0256LP* were carried out. The staining procedures used were similar to Cj0979 detection experiments. Neither Cje0256 nor Cje0256LP proteins were detectable using Coomassie staining or Western blotting techniques. Western blotting is a high sensitivity assay allowing detection in the pg level. Coomassie staining detects proteins up to 7 ng, and the dye binds to arginine, lysine, and histidine residues. Analysis of the amino acid sequences of Cj0979 and Cje0256, using ExPASy Bioinformatics research portal, revealed that there was no significant difference in the composition of arginine, lysine, and histidine residues between the two proteins. This indicates that there were no issues with the detection technique used. The OD₆₀₀ readings of the induced cultures of *E. coli*/pBAD33-*cje0256* and *E. coli*/pBAD33-*cje0256LP* were lower than their respective uninduced cultures, which indicates arabinose utilization by the cells. Lack of protein detection could be due to one of the following reasons: the protein is toxic to *E. coli*; the protein is not stable and rapidly degrades during the expression process; or the yield obtained was too low even for detection with Western blotting. Future research could focus on studying the optimum conditions required for protein stability by performing a time-course experiment or by purifying the protein at relatively lower temperatures. If 6xHis tag is inaccessible, then attaching the His tag to the start of the protein (i.e., N-terminus) could be considered as a strategy for purification. Alternatively, if protein toxicity is the issue, choosing another recipient strain that is more robust and built for the expression of difficult proteins could be considered.

Chapter 5: Conclusion

This study aimed to develop a regulatory gene expression system in *Campylobacter*, incorporating the widely used arabinose-inducible P_{BAD} promoter, to investigate the effects of essential genes and other genes whose functions are unknown. *Campylobacter* does not utilise glucose or other carbohydrates for metabolism, as it lacks the transporters and other vital enzymes within the glycolytic pathway (Stahl *et al.*, 2012). This study provided an early understanding of the introduction and the lack of expression of arabinose transporter genes in *C. jejuni*. Despite the successful introduction of *araE* and *lacYA177C* into these bacteria, the induction of the reporter gene *gfp* was not achieved when compared to *E. coli* strains.

This study was the first to examine the exogenous introduction of these two arabinose transporter genes into *C. jejuni*. Although the maintenance of the constructed regulated system in *Campylobacter* did not succeed, such a system remains important for the study of other vital genes in *Campylobacter*. Furthermore, the biofilm studies conducted in this research revealed that Cj0979 possesses enzymatic properties. Reduction in biofilm formation was obtained when tested with purified Cj0979. Neither this protein nor its properties have been studied elsewhere. Similar to this study, an attempt to study the role of the *cje0256* gene in *C. jejuni* RM1221 was undertaken since it was listed as a DNase encoding gene in a previous study (Gaasbeek *et al.*, 2009). This strain consists of two other DNase encoding genes and was found to be non-transformable (Gaasbeek *et al.*, 2010).

In conclusion, this study was undertaken to better understand the factors and mechanisms involved in CFF and biofilm dispersal of *C. jejuni*, since these bacteria are known to persist in the environment for longer periods and cause infections in humans. Identifying the key determinants in these processes will aid in the development of antimicrobials that will decrease the prevalence of these bacteria and thereby reduce the spread of campylobacteriosis.

Chapter 6: References

Allos, B. (2001) 'Campylobacter jejuni infections: Update on emerging issues and trends', *Clinical Infectious Diseases*, 32(8), pp. 1201-1206.

Amano, K. and Shibata, Y. (1992) 'Structural studies of peptidoglycans in *Campylobacter* species', *Microbiology and Immunology*, 36(9), pp. 961-967.

Armbruster, C. R. and Parsek, M. R. (2018) 'New insight into the early stages of biofilm formation', *Proceedings of the National Academy of Sciences of the United States of America*, 115(17), pp. 4317-4319.

Ashgar, S. S. A., Oldfield, N. J., Wooldridge, K. G., Jones, M. A., Irving, G. J., Turner, D. P. J. and Ala'Aldeen, D. A. A. (2007) 'CapA, an autotransporter protein of *Campylobacter jejuni*, mediates association with human epithelial cells and colonization of the chicken gut', *Journal of Bacteriology*, 189(5), pp. 1856-1865.

Atas, A., Seddon, A. M., Ford, D. C., Cooper, I. A., Wren, B. W., Oyston, P. C. F. and Karlyshev, A. V. (2016) 'YPTB3816 of *Yersinia pseudotuberculosis* strain IP32953 is a virulence-related metallo-oligopeptidase', *BMC Microbiology*, 16, pp. 1-9.

Baig, F., Fernando, L. P., Salazar, M. A., Powell, R. R., Bruce, T. F. and Harcum, S. W. (2014) 'Dynamic transcriptional response of *Escherichia coli* to inclusion body formation', *Biotechnology and Bioengineering*, 111(5), pp. 980-999.

Balogu, T.V., Nwaugo, V.O. and Onyeagba, R.A. (2014) 'Persistence and biofilm assessment of *Campylobacter jejuni* in poultry abattoir', *Nigerian Food Journal*, 32(1), pp. 54-61.

Baneyx, F. and Mujacic, M. (2004) 'Recombinant protein folding and misfolding in *Escherichia coli*', *Nature Biotechnology*, 22(11), pp. 1399-1408.

Beauchamp, J. M., Leveque, R. M., Dawid, S. and DiRita, V. J. (2017) 'Methylation-dependent DNA discrimination in natural transformation of *Campylobacter jejuni*', *Proceedings of the National Academy of Sciences of the United States of America*, 114(38), pp. E8053-E8061.

Beenken, K. E., Spencer, H., Griffin, L. M. and Smeltzer, M. S. (2012) 'Impact of extracellular nuclease production on the biofilm phenotype of *Staphylococcus aureus* under *in vitro* and *in vivo* conditions', *Infection and Immunity*, 80(5), pp. 1634-1638.

Beisel, C. L. and Afroz, T. (2016) 'Rethinking the hierarchy of sugar utilization in bacteria', *Journal of Bacteriology*, 198(3), pp. 374-376.

Berends, E. T. M., Horswill, A. R., Haste, N. M., Monestier, M., Nizet, V. and von Koeckritz-Blickwede, M. (2010) 'Nuclease expression by *Staphylococcus aureus* facilitates escape from neutrophil extracellular traps', *Journal of Innate Immunity*, 2(6), pp. 576-586.

Beumer, R., de Vries, J. and Rombouts, F. (1992) '*Campylobacter jejuni* non-culturable coccoid cells', *Int J Food Microbiol*, 15(1), pp. 153-63.

Binnenkade, L., Kreienbaum, M. and Thormann, K. M. (2018) 'Characterization of ExeM, an extracellular nuclease of *Shewanella oneidensis* MR-1', *Frontiers in Microbiology*, 9, pp 1-9.

Birk, T., Wik, M. T., Lametsch, R. and Knochel, S. (2012) 'Acid stress response and protein induction in *Campylobacter jejuni* isolates with different acid tolerance', *BMC Microbiology*, 12(174), pp. 1-13.

Black, R., Perlman, D., Clements, M., Levine, M. and Blaser, M. (1993) 'Human volunteer studies with *Campylobacter jejuni*', *Symp On Campylobacter jejuni: Current Status and Future Trends*, California, 10-13 March.

Bolton, D. J. (2015) '*Campylobacter* virulence and survival factors', *Food Microbiology*, 48, pp. 99-108.

Boneca, I. G., Ecobichon, C., Chaput, C., Mathieu, A., Guadagnini, S., Prevost, M., Colland, F., Labigne, A. and de Reuse, H. (2008) 'Development of inducible systems to engineer conditional mutants of essential genes of *Helicobacter pylori*', *Applied and Environmental Microbiology*, 74(7), pp. 2095-2102.

Bos, R., van der Mei, H. and Busscher, H. (1999) 'Physico-chemistry of initial microbial adhesive interactions - its mechanisms and methods for study', *FEMS Microbiology Reviews*, 23(2), pp. 179-230.

Bras, A., Chatterjee, S., Wren, B., Newell, D. and Ketley, J. (1999) 'A novel *Campylobacter jejuni* two-component regulatory system important for temperature-dependent growth and colonization', *Journal of Bacteriology*, 181(10), pp. 3298-3302.

Bridier, A., Sanchez-Vizueté, P., Guilbaud, M., Piard, J., Naitali, M. and Briandet, R. (2015) 'Biofilm-associated persistence of food-borne pathogens', *Food Microbiology*, 45, pp. 167-178.

Bronnec, V., Turonova, H., Bouju, A., Cruveiller, S., Rodrigues, R., Demnerova, K., Tresse, O., Haddad, N. and Zagorec, M. (2016) 'Adhesion, biofilm formation, and genomic features of *Campylobacter jejuni* Bf, an atypical strain able to grow under aerobic conditions', *Frontiers in Microbiology*, 7, pp. 1-14.

Bronowski, C., James, C. E. and Winstanley, C. (2014) 'Role of environmental survival in transmission of *Campylobacter jejuni*', *FEMS Microbiology Letters*, 356(1), pp. 8-19.

Brooks, L. R. K. and Mias, G. I. (2018) '*Streptococcus pneumoniae*'s virulence and host

immunity: Aging, diagnostics, and prevention', *Frontiers in Immunology*, 9, pp. 1-29.

Brosius, J., Erfle, M. and Storella, J. (1985) 'Spacing of the -10 and -35 regions in the tac promoter - effect on its *in vivo* activity', *Journal of Biological Chemistry*, 260(6), pp. 3539-3541.

Brown, H. L., Hanman, K., Reuter, M., Betts, R. P. and van Vliet, A. H. M. (2015a) '*Campylobacter jejuni* biofilms contain extracellular DNA and are sensitive to DNase I treatment', *Frontiers in Microbiology*, 6, pp. 1-11.

Brown, H. L., Reuter, M., Hanman, K., Betts, R. P. and van Vliet, A. H. M. (2015b) 'Prevention of biofilm formation and removal of existing biofilms by extracellular DNases of *Campylobacter jejuni*', *PLOS One*, 10(3), pp. 1-21.

Brown, H. L., Reuter, M., Salt, L. J., Cross, K. L., Betts, R. P. and van Vliet, A. H. M. (2014) 'Chicken juice enhances surface attachment and biofilm formation of *Campylobacter jejuni*', *Applied and Environmental Microbiology*, 80(22), pp. 7053-7060.

Buchanan, J., Simpson, A., Aziz, R., Liu, G., Kristian, S., Kotb, M., Feramisco, J. and Nizet, V. (2006) 'DNase expression allows the pathogen group A *Streptococcus* to escape killing in neutrophil extracellular traps', *Current Biology*, 16(4), pp. 396-400.

Cappelier, J., Magras, C., Jouve, J. and Federighi, M. (1999) 'Recovery of viable but non-culturable *Campylobacter jejuni* cells in two animal models', *Food Microbiology*, 16(4), pp. 375-383.

Cappelier, J., Rossero, A. and Federighi, M. (2000) 'Demonstration of a protein synthesis in starved *Campylobacter jejuni* cells', *International Journal of Food Microbiology*, 55(2000), pp. 63-67.

Carniello, V., Peterson, B. W., van der Mei, H. C. and Busscher, H. J. (2018) 'Physico-chemistry from initial bacterial adhesion to surface-programmed biofilm growth', *Advances in Colloid and Interface Science*, 261, pp. 1-14.

Carroll, P., Muttucumar, D. and Parish, T. (2005) 'Use of a tetracycline-inducible system for conditional expression in *Mycobacterium tuberculosis* and *Mycobacterium smegmatis*', *Applied and Environmental Microbiology*, 71(6), pp. 3077-3084.

Centers for Disease Control and Prevention (2017) *Campylobacter (Campylobacteriosis)*.

Available at: <https://www.cdc.gov/Campylobacter/index.html> (Accessed: 07 January 2019)

Champion, O. L., Gaunt, M., Gundogdu, O., Elmi, A., Witney, A., Hinds, J., Dorrell, N. and Wren, B. (2005) 'Comparative phylogenomics of the food-borne pathogen *Campylobacter jejuni* reveals genetic markers predictive of infection source', *Proceedings of the National Academy of Sciences of the United States of America*, 102(44), pp. 16043-16048.

Chan, V., Louie, H. and Bigham, H. (1995) 'Cloning and transcription regulation of the ferric uptake regulatory gene of *Campylobacter jejuni* Tgh9011', *Gene*, 164(1), pp. 25-31.

Chaput, C., Ecobichon, C., Cayet, N., Girardin, S. E., Werts, C., Guadagnini, S., Prevost, M.C., Mengin-Lecrux, D., Labigne, A. and Boneca, I. G. (2006) 'Role of AmiA in the morphological transition of *Helicobacter pylori* and in immune escape', *PLOS Pathogens*, 2(9), pp. 844-852.

Chaveerach, P., ter Huurne, A., Lipman, L. and van Knapen, F. (2003) 'Survival and resuscitation of ten strains of *Campylobacter jejuni* and *Campylobacter coli* under acid conditions', *Applied and Environmental Microbiology*, 69(1), pp. 711-714.

Cheng, Y., Feng, G. and Moraru, C. I. (2019) 'Micro- and nanotopography sensitive bacterial attachment mechanisms: A review', *Frontiers in Microbiology*, 10, pp. 1-17.

Chiang, W., Nilsson, M., Jensen, P. O., Hoiby, N., Nielsen, T. E., Givskov, M. and Tolker-Nielsen, T. (2013) 'Extracellular DNA shields against aminoglycosides in *Pseudomonas aeruginosa* biofilm', *Antimicrobial Agents and Chemotherapy*, 57(5), pp. 2352-2361.

Chua, S. L., Liu, Y., Yam, J. K. H., Chen, Y., Vejborg, R. M., Tan, B. G. C., Kjelleberg, S., Tolker-Nielsen, T., Givskov, M. and Yang, L. (2014) 'Dispersed cells represent a distinct stage in the transition from bacterial biofilm to planktonic lifestyles', *Nature Communications*, 5, pp.1-12.

Costa, K., Bacher, G., Allmaier, G., Dominguez-Bello, M., Engstrand, L., Falk, P., de Pedro, M.A. and Garcia-del Portillo, F. (1999) 'The morphological transition of *Helicobacter pylori* cells from spiral to coccoid is preceded by a substantial modification of the cell wall', *Journal of Bacteriology*, 181(12), pp. 3710-3715.

Costerton, J., Stewart, P. and Greenberg, E. (1999) 'Bacterial biofilms: A common cause of persistent infections', *Science*, 284(5418), pp. 1318-1322.

Culotti, A. and Packman, A. I. (2015) '*Pseudomonas aeruginosa* facilitates *Campylobacter jejuni* growth in biofilms under oxic flow conditions', *FEMS Microbiology Ecology*, 91(12), pp. 1-8.

Daruwalla, K., Paxton, A. and Henderson, P. (1981) 'Energization of the transport- systems for arabinose and comparison with galactose transport in *Escherichia coli*', *Biochemical Journal*, 200(3), pp. 611-627.

Dasti, J. I., Tareen, A. M., Lugert, R., Zautner, A. E. and Gross, U. (2010) '*Campylobacter*

jejuni: A brief overview on pathogenicity associated factors and disease mediating mechanisms', *International Journal of Medical Microbiology*, 300(4), pp. 205-211.

Davis, L., Young, K. and DiRita, V. (2008) 'Genetic manipulation of *Campylobacter jejuni*', *Curr Protoc Microbiol*, 8, pp.1-24.

Deboer, H., Comstock, L. and Vasser, M. (1983) 'The tac promoter - a functional hybrid derived from the *trp* and *lac* promoters', *Proceedings of the National Academy of Sciences of the United States of America-Biological Sciences*, 80(1), pp. 21-25.

Debowski, A. W., Verbrugghe, P., Sehnal, M., Marshall, B. J. and Benghezal, M. (2013) 'Development of a tetracycline-inducible gene expression system for the study of *Helicobacter pylori* pathogenesis', *Applied and Environmental Microbiology*, 79(23), pp. 7351-7359.

Donahue, J., Israel, D., Peek, R., Blaser, M. and Miller, G. (2000) 'Overcoming the restriction barrier to plasmid transformation of *Helicobacter pylori*', *Molecular Microbiology*, 37(5), pp. 1066-1074.

Doyle, L. P (1944) 'A *Vibrio* associated with swine dysentery', *Am. J. Vet. Res.*, 5, pp. 3-5.

Doyle, M. P. and Roman, D. J. (1981) 'Growth and survival of *Campylobacter fetus* subsp. *jejuni* as a function of temperature and pH', *Journal of Food Protection*, 44(8), pp. 596-601.

Dykes, G., Sampathkumar, B. and Korber, D. (2003) 'Planktonic or biofilm growth affects survival, hydrophobicity and protein expression patterns of a pathogenic *Campylobacter jejuni* strain', *International Journal of Food Microbiology*, 89(1), pp. 1-10.

Elvers, K. and Park, S. (2002) 'Quorum sensing in *Campylobacter jejuni*: Detection of a *luxS* encoded signalling molecule', *Microbiology Society*, 148(5), pp. 1475-1481.

Elvin, C., Thompson, P., Argall, M., Hendry, P., Stamford, N., Lilley, P. and Dixon, N. (1990) 'Modified bacteriophage-lambda promoter vectors for overproduction of proteins in *Escherichia coli*', *Gene*, 87(1), pp. 123-126.

Elwell, C. and Dreyfus, L. (2000) 'DNase I homologous residues in CdtB are critical for cytolethal distending toxin-mediated cell cycle arrest', *Molecular Microbiology*, 37(4), pp. 952-963.

Englesberg, E., Squires, C. and Meronk, F. (1969) 'The L-arabinose operon in *Escherichia coli* B/r: A genetic demonstration of two functional states of the product of a regulator gene', *Proceedings of the National Academy of Sciences of the United States of America*, 62(4), pp. 1100-1107.

Epps, S. V. R., Harvey, R. B., Hume, M. E., Phillips, T. D., Anderson, R. C. and Nisbet, D. J. (2013) 'Foodborne *Campylobacter*: Infections, metabolism, pathogenesis and reservoirs', *International Journal of Environmental Research and Public Health*, 10(12), pp. 6292-6304.

European Centre for Disease Prevention and Control (2017) *Campylobacteriosis-Annual epidemiological report for 2017*. Available at: <https://www.ecdc.europa.eu/en/publications-data/campylobacteriosis-annual-epidemiological-report-2017> (Accessed 10 April 2019)

Feng, J., Lamour, G., Xue, R., Mirvakliki, M. N., Hatzikiriakos, S. G., Xu, J., Li, H., Wang, S. and Lu, X. (2016) 'Chemical, physical and morphological properties of bacterial biofilms affect survival of encased *Campylobacter jejuni* F38011 under aerobic stress', *International Journal of Food Microbiology*, 238, pp. 172-182.

Freitag, C. M., Strijbis, K. and van Putten, J. P. M. (2017) 'Host cell binding of the flagellar tip protein of *Campylobacter jejuni*', *Cellular Microbiology*, 19(6), pp. 1-13.

Firdich, E., Biboy, J., Huynh, S., Parker, C. T., Vollmer, W. and Gaynor, E. C. (2017) 'Morphology heterogeneity within a *Campylobacter jejuni* helical population: The use of calcofluor white to generate rod-shaped *C. jejuni* 81-176 clones and the genetic determinants responsible for differences in morphology within 11168 strains', *Molecular Microbiology*, 104(6), pp. 948-971.

Fritz, G., Megerle, J. A., Westermayer, S. A., Brick, D., Heermann, R., Jung, K., Rädler, J.O. and Gerland, U. (2014) 'Single cell kinetics of phenotypic switching in the arabinose utilization system of *E. coli*', *PLOS One*, 9(2), pp. 1-13.

Fux, C., Costerton, J., Stewart, P. and Stoodley, P. (2005) 'Survival strategies of infectious biofilms', *Trends in Microbiology*, 13(1), pp. 34-40.

Gaasbeek, E. J., Wagenaar, J. A., Guilhabert, M. R., van Putten, J. P. M., Parker, C. T. and van der Wal, F. J. (2010) 'Nucleases encoded by the integrated elements CJIE2 and CJIE4 inhibit natural transformation of *Campylobacter jejuni*', *Journal of Bacteriology*, 192(4), pp. 936-941.

Gaasbeek, E. J., Wagenaar, J. A., Guilhabert, M. R., Wosten, M. M. S. M., van Putten, J. P. M., van der Graaf-van Bloois, L., Parker, C.T. and van der Wal, F. J. (2009) 'A DNase encoded by integrated element CJIE1 inhibits natural transformation of *Campylobacter jejuni*', *Journal of Bacteriology*, 191(7), pp. 2296-2306.

Garrett, T. R., Bhakoo, M. and Zhang, Z. (2008) 'Bacterial adhesion and biofilms on surfaces', *Progress in Natural Science-Materials International*, 18(9), pp. 1049-1056.

Gaynor, E., Cawthraw, S., Manning, G., MacKichan, J., Falkow, S. and Newell, D. (2004) 'The genome-sequenced variant of *Campylobacter jejuni* NCTC 11168 and the original clonal clinical isolate differ markedly in colonization, gene expression, and virulence-associated

phenotypes', *Journal of Bacteriology*, 186(2), pp. 503-517.

Giangaspero, M. (2018) 'A cosmopolitan one health issue: Campylobacteriosis', *Clinical Microbiology*, 7(1), pp. 1-5.

Gölz, G., Kittler, S., Malakauskas, M. and Alter, T. (2018) 'Survival of *Campylobacter* in the food chain and the environment', *Current Clinical Microbiology Reports*, 5(2), pp. 126-134.

Gölz, G., Sharbati S., Backert S. and Alter, T. (2012) 'Quorum sensing dependent phenotypes and their molecular mechanisms in *Campylobacterales*', *European Journal of Microbiology and Immunology* 2, 1, pp. 50-60.

Goulden, E.F., Høj, L. and Hall, M.R. (2013) *Microbial management for bacterial pathogen control in invertebrate aquaculture hatcheries*. Swaston: Woodhead Publishing Series in Food Science, Technology and Nutrition.

Grande, R., Di Giulio, M., Bessa, L. J., Di Campli, E., Baffoni, M., Guarnieri, S. and Cellini, L. (2011) 'Extracellular DNA in *Helicobacter pylori* biofilm: A backstairs rumour', *Journal of Applied Microbiology*, 110(2), pp. 490-498.

Guerry, P., Alm, R., Power, M. and Trust, T. (1992) 'Molecular and structural analysis of *Campylobacter* flagellin', *Symp On Campylobacter jejuni: Current Status and Future Trends*, California, 10-13 March.

Guilhen, C., Charbonnel, N., Parisot, N., Gueguen, N., Iltis, A., Forestier, C. and Balestrino, D. (2016) 'Transcriptional profiling of *Klebsiella pneumoniae* defines signatures for planktonic, sessile and biofilm-dispersed cells', *BMC Genomics*, 17, pp. 1-15.

Guilhen, C., Forestier, C. and Balestrino, D. (2017) 'Biofilm dispersal: Multiple elaborate

strategies for dissemination of bacteria with unique properties', *Molecular Microbiology*, 105(2), pp. 188-210.

Gunther, N.W. IV. and Chen, C. (2009) 'The biofilm forming potential of bacterial species in the genus *Campylobacter*', *Food Microbiology*, 26(1), pp. 44-51.

Guzman, L., Belin, D., Carson, M. and Beckwith, J. (1995) 'Tight regulation, modulation, and high-level expression by vectors containing the arabinose P_{BAD} promoter', *Journal of Bacteriology*, 177(14), pp. 4121-4130.

Haiko, J. and Westerlund-Wikström, B. (2013) 'The role of the bacterial flagellum in adhesion and virulence', *Biology*, 2(4), pp. 1242-1267.

Hamer, R., Chen, P., Armitage, J. P., Reinert, G. and Deane, C. M. (2010) 'Deciphering chemotaxis pathways using cross species comparisons', *BMC Systems Biology*, 4, pp. 1-19.

Hamilton, H., Dominguez, N., Schwartz, K., Hackett, K. and Dillard, J. (2005) '*Neisseria gonorrhoeae* secretes chromosomal DNA via a novel type IV secretion system', *Molecular Microbiology*, 55(6), pp. 1704-1721.

Hanning, I., Jarquin, R. and Slavik, M. (2008) '*Campylobacter jejuni* as a secondary colonizer of poultry biofilms', *Journal of Applied Microbiology*, 105(4), pp. 1199-1208.

Hansen, C. R., Khatiwara, A., Ziprin, R. and Kwon, Y. M. (2007) 'Rapid construction of *Campylobacter jejuni* deletion mutants', *Letters in Applied Microbiology*, 45(6), pp. 599-603.

Hao, H., Ren, N., Han, J., Foley, S. L., Iqbal, Z., Cheng, G., Xiuhua, K., Jie, Liu., Zhenli, L., Menghong, D., Yulian, W. and Yuan, Z. (2016) 'Virulence and genomic feature of multidrug resistant *Campylobacter jejuni* isolated from broiler chicken', *Frontiers in Microbiology*, 7,

pp. 1-14.

Hartley, D. and Kane, J. (1991) 'Properties of inclusion bodies from recombinant *Escherichia coli*', *Bioprocess Technology*, 16(2), p. 101-102.

Harvey, P. and Leach, S. (1998) 'Analysis of coccal cell formation by *Campylobacter jejuni* using continuous culture techniques, and the importance of oxidative stress', *Journal of Applied Microbiology*, 85(2), pp. 398-404.

Hazeleger, W., Wouters, J., Rombouts, F. and Abee, T. (1998) 'Physiological activity of *Campylobacter jejuni* far below the minimal growth temperature', *Applied and Environmental Microbiology*, 64(10), pp. 3917-3922.

Hendrixson, D. and DiRita, V. (2003) 'Transcription of σ^{54} dependent but not σ^{28} -dependent flagellar genes in *Campylobacter jejuni* is associated with formation of the flagellar secretory apparatus', *Molecular Microbiology*, 50(2), pp. 687-702.

Hermans, D., Van Deun, K., Martel, A., Van Immerseel, F., Messens, W., Heyndrickx, M., Haesebrouck, F. and Pasmans, F. (2011) 'Colonization factors of *Campylobacter jejuni* in the chicken gut', *Veterinary Research*, 42, pp. 1-14.

Hofreuter, D. (2014) 'Defining the metabolic requirements for the growth and colonization capacity of *Campylobacter jejuni*', *Frontiers in Cellular and Infection Microbiology*, 4, pp. 1-19.

Holt, J. P., Grant, A. J., Coward, C., Maskell, D. J. and Quinlan, J. J. (2012) 'Identification of Cj1051c as a major determinant for the restriction barrier of *Campylobacter jejuni* strain NCTC 11168', *Applied and Environmental Microbiology*, 78(22), pp. 7841-7848.

Houry, A., Briandet, R., Aymerich, S. and Gohar, M. (2010) 'Involvement of motility and flagella in *Bacillus cereus* biofilm formation', *Microbiology Society*, 156, pp. 1009-1018.

Howard, S. L., Jagannathan, A., Soo, E. C., Hui, J. P. M., Aubry, A. J., Ahmed, I., Karlyshev, A., Kelly, J.F., Jones, M.A., Stevens, M.P., Logan, S.M. and Wren, B. W. (2009) '*Campylobacter jejuni* glycosylation island important in cell charge, legionaminic acid biosynthesis, and colonization of chickens', *Infection and Immunity*, 77(6), pp. 2544-2556.

Huang, Y., Hu, R., Chiang, Y., Chung, T., Chung, T. and Yang, T. (2011) 'Establishment of an arabinose-inducible system in *Stenotrophomonas maltophilia*', *Folia Microbiologica*, 56(1), pp. 18-22.

Hudock, J., Borger, A. and Kaspar, C. (2005) 'Temperature-dependent genome degradation in the coccoid form of *Campylobacter jejuni*', *Current Microbiology*, 50(2), pp.110-113.

Humphrey, S., Chaloner, G., Kemmett, K., Davidson, N., Williams, N., Kipar, A., Humphrey, T. and Wigley, P. (2014) '*Campylobacter jejuni* is not merely a commensal in commercial broiler chickens and affects bird welfare', *mBio*, 5(4), pp. 1-7.

Humphrey, T. (1990) 'The synergistic inhibition of *Campylobacter jejuni* by rifampicin and hydrogen-peroxide', *Letters in Applied Microbiology*, 10(2), pp. 97-100.

Ibáñez de Aldecoa, A. L., Zafra, O. and Gonzalez-Pastor, J. E. (2017) 'Mechanisms and regulation of extracellular DNA release and its biological roles in microbial communities', *Frontiers in Microbiology*, 8, pp. 1-19.

Ica, T., Caner, V., Istanbulu, O., Nguyen, H.D., Ahmed, B., Call, D. R. and Beyenal, H. (2012) 'Characterization of mono- and mixed-culture *Campylobacter jejuni* biofilms', *Applied and Environmental Microbiology*, 78(4), pp. 1033-1038.

Ikeda, N. (2014) 'Molecular mechanisms of coccoid form formation in *Campylobacter jejuni*', *PhD Thesis*. Kingston University.

Ikeda, N. and Karlyshev, A. V. (2012) 'Putative mechanisms and biological role of coccoid form formation in *Campylobacter jejuni*', *European Journal of Microbiology and Immunology*, 2(1), pp. 41-49.

Jakubovics, N. S., Shields, R. C., Rajarajan, N. and Burgess, J. G. (2013) 'Life after death: The critical role of extracellular DNA in microbial biofilms', *Letters in Applied Microbiology*, 57(6), pp. 467-475.

Jamal, M., Ahmad, W., Andleeb, S., Jalil, F., Imran, M., Nawaz, M. A., Hussain, T., Ali, M., Rafiq, M. and Kamil, M. A. (2018) 'Bacterial biofilm and associated infections', *Journal of the Chinese Medical Association*, 81(1), pp. 7-11.

Janssen, R., Kroghelt, K. A., Cawthraw, S. A., van Pelt, W., Wagenaar, J. A. and Owen, R. J. (2008) 'Host-pathogen interactions in *Campylobacter* infections: The host perspective', *Clinical Microbiology Reviews*, 21(3), pp. 505-518.

Jefferson, K. (2004) 'What drives bacteria to produce a biofilm?', *FEMS Microbiology Letters*, 236(2), pp. 163-173.

Jeon, B., Itoh, K. and Ryu, S. (2005) 'Promoter analysis of cytolethal distending toxin genes (*cdtA*, *B*, and *C*) and effect of a *luxS* mutation on CDT production in *Campylobacter jejuni*', *Microbiology and Immunology*, 49(7), pp. 599-603.

Jin, S., Joe, A., Lynett, J., Hani, E., Sherman, P. and Chan, V. (2001) 'JlpA, a novel surface-exposed lipoprotein specific to *Campylobacter jejuni*, mediates adherence to host epithelial cells', *Molecular Microbiology*, 39(5), pp. 1225-1236.

Jones, D., Sutcliffe, E. and Curry, A. (1991) 'Recovery of viable but non-culturable *Campylobacter jejuni*', *Journal of General Microbiology*, 137(10), pp. 2477-2482.

Jones, M., Marston, K., Woodall, C., Maskell, D., Linton, D., Karlyshev, A. and Barrow, P. (2004) 'Adaptation of *Campylobacter jejuni* NCTC 11168 to high-level colonization of the avian gastrointestinal tract', *Infection and Immunity*, 72(7), pp. 3769-3776.

Joshua, G., Guthrie-Irons, C., Karlyshev, A. and Wren, B. (2006) 'Biofilm formation in *Campylobacter jejuni*', *Microbiology*, 152(1), pp. 387-396.

Jowiya, W., Brunner, K., Abouelhadid, S., Hussain, H. A., Nair, S. P., Sadiq, S., Williams, L.K., Trantham, E.K., Stephenson, H., Wren, B.W., Bajaj-Elliott, M., Cogan, T.A., Laws, A.P., Wade, J., Dorell, N. and Allan, E. (2015) 'Pancreatic amylase is an environmental signal for regulation of biofilm formation and host interaction in *Campylobacter jejuni*', *Infection and Immunity*, 83(12), pp. 4884-4895.

Jung, G. H., Lim, E. S., Woo, M., Lee, J. Y., Kim, J. and Paik, H. (2017) 'Inverse correlation between extracellular DNase activity and biofilm formation among chicken-derived *Campylobacter* strains', *Journal of Microbiology and Biotechnology*, 27(11), pp. 1942-1951.

Kaakoush, N. O., Castano-Rodriguez, N., Mitchell, H. M. and Man, S. I. M. (2015) 'Global epidemiology of *Campylobacter* infection', *Clinical Microbiology Reviews*, 28(3), pp. 687-720.

Kaiser, P., Poh, T., Rothwell, L., Avery, S., Balu, S., Pathania, U., Hughes, S., Goodchild, M., Morrell, S., Watson, M., Bumstead, N., Kaufman, J. and Young, J.R. (2005) 'A genomic analysis of chicken cytokines and chemokines', *Journal of Interferon and Cytokine Research*, 25(8), pp. 467-484.

Kalmokoff, M., Lanthier, P., Tremblay, T., Foss, M., Lau, P. C., Sanders, G., Austin, J., Kelly, J. and Szymanski, C. M. (2006) 'Proteomic analysis of *Campylobacter jejuni* 11168 biofilms reveals a role for the motility complex in biofilm formation', *Journal of Bacteriology*, 188(12), pp. 4312-4320.

Kaplan, J. and Fine, D. (2002) 'Biofilm dispersal of *Neisseria subflava* and other phylogenetically diverse oral bacteria', *Applied and Environmental Microbiology*, 68(10), pp. 4943-4950.

Karlyshev, A. and Wren, B. (2005a) 'Development and application of an insertional system for gene delivery and expression in *Campylobacter jejuni*', *Applied and Environmental Microbiology*, 71(7), pp. 4004-4013.

Karlyshev, A., Everest, P., Linton, D., Cawthraw, S., Newell, D. and Wren, B. (2004) 'The *Campylobacter jejuni* general glycosylation system is important for attachment to human epithelial cells and in the colonization of chicks', *Microbiology*, 150(6), pp. 1957-1964.

Karlyshev, A., Ketley, J. and Wren, B. (2005b) 'The *Campylobacter jejuni* glycome', *FEMS Microbiology Reviews*, 29(2), pp. 377-390.

Karlyshev, A., Linton, D., Gregson, N. and Wren, B. (2002) 'A novel paralogous gene family involved in phase-variable flagella-mediated motility in *Campylobacter jejuni*', *Microbiology*, 148(2), pp. 473-480.

Khlebnikov, A., Datsenko, K., Skaug, T., Wanner, B. and Keasling, J. (2001) 'Homogeneous expression of the PBAD promoter in *Escherichia coli* by constitutive expression of the low-affinity high-capacity AraE transporter', *Microbiology*, 147, pp. 3241- 3247.

Khlebnikov, A., Risa, O., Skaug, T., Carrier, T. and Keasling, J. (2000) 'Regulatable arabinose-

inducible gene expression system with consistent control in all cells of a culture', *Journal of Bacteriology*, 182(24), pp. 7029-7034.

Kiedrowski, M. R., Crosby, H. A., Hernandez, F. J., Malone, C. L., McNamara, J. O. and Horswill, A. R. (2014) '*Staphylococcus aureus* Nuc2 is a functional, surface- attached extracellular nuclease', *PLOS One*, 9(4), pp. 1-13.

Kiedrowski, M. R., Kavanaugh, J. S., Malone, C. L., Mootz, J. M., Voyich, J. M., Smeltzer, M. S., Bayles., K.W. and Horswill, A. R. (2011) 'Nuclease modulates biofilm formation in community-associated methicillin-resistant *Staphylococcus aureus*', *PLOS One*, 6(11), pp. 1-16.

Kim, J., Park, C. and Kim, Y. (2015) 'Role of *flgA* for flagellar biosynthesis and biofilm formation of *Campylobacter jejuni* NCTC 11168', *Journal of Microbiology and Biotechnology*, 25(11), pp. 1871-1879.

Klancnik, A., Botteldoorn, N., Herman, L. and Mozina, S. S. (2006) 'Survival and stress induced expression of *groEL* and *rpoD* of *Campylobacter jejuni* from different growth phases', *International Journal of Food Microbiology*, 112(3), pp. 200-207.

Klancnik, A., Guzej, B., Jamnik, P., Vuckovic, D., Abram, M. and Mozina, S. S. (2009) 'Stress response and pathogenic potential of *Campylobacter jejuni* cells exposed to starvation', *Research in Microbiology*, 160(5), pp. 345-352.

Koike Y, S. (1982) 'The coccoid form of *Campylobacter* spp: Fluctuation in cellular morphology', *Bulletin of the Nippon Veterinary and Animal Science University*, 31, pp. 136–142.

Konkel, M., Garvis, S., Tipton, S., Anderson, D. and Cieplak, W. (1997) 'Identification and

molecular cloning of a gene encoding a fibronectin-binding protein (CadF) from *Campylobacter jejuni*', *Molecular Microbiology*, 24(5), pp. 953-963.

Konkel, M., Klena, J., Rivera-Amill, V., Monteville, M., Biswas, D., Raphael, B. and Mickelson, J. (2004) 'Secretion of virulence proteins from *Campylobacter jejuni* is dependent on a functional flagellar export apparatus', *Journal of Bacteriology*, 186(11), pp. 3296-3303.

Kostakioti, M., Hadjifrangiskou, M. and Hultgren, S. J. (2013) 'Bacterial biofilms: Development, dispersal, and therapeutic strategies in the dawn of the post antibiotic era', *Cold Spring Harbor Perspectives in Medicine*, 3(4), pp. 1-23.

Kumar, A., Alam, A., Rani, M., Ehtesham, N. Z. and Hasnain, S. E. (2017) 'Biofilms: Survival and defense strategy for pathogens', *International Journal of Medical Microbiology*, 307(8), pp. 481-489.

Lamas, A., Regal, P., Vazquez, B., Miranda, J. M., Cepeda, A. and Franco, C. M. (2018) '*Salmonella* and *Campylobacter* biofilm formation: A comparative assessment from farm to fork', *Journal of the Science of Food and Agriculture*, 98(11), pp. 4014-4032.

Lara-Tejero, M. and Galan, J. (2000) 'A bacterial toxin that controls cell cycle progression as a deoxyribonuclease I-like protein', *Science*, 290(5490), pp. 354-357.

Lara-Tejero, M. and Galan, J. (2001) 'CdtA, CdtB, and CdtC form a tripartite complex that is required for cytolethal distending toxin activity', *Infection and Immunity*, 69(7), pp. 4358-4365.

Lee, J., Alzarban, S. and Wilcox, G. (1981) 'Genetic-characterization of the *araE* gene in *Salmonella typhimurium* lt2', *Journal of Bacteriology*, 146(1), pp. 298-304.

- Lee, Y., Moon, B., Choi, J., Chang, H., Noh, B. and Park, J. (2005) 'Isolation, identification, and characterization of aero-adaptive *Campylobacter jejuni*', *Journal of Microbiology and Biotechnology*, 15(5), pp. 992-1000.
- Lejeune, P. (2003) 'Contamination of abiotic surfaces: What a colonizing bacterium sees and how to blur it', *Trends in Microbiology*, 11(4), pp. 179-184.
- Lewis, K. (2001) 'Riddle of biofilm resistance', *Antimicrobial Agents and Chemotherapy*, 45(4), pp. 999-1007.
- Li, J., Feng, J., Ma, L., Nunez, C. D. L. F., Goelz, G. and Lu, X. (2017) 'Effects of meat juice on biofilm formation of *Campylobacter* and *Salmonella*', *International Journal of Food Microbiology*, 253, pp. 20-28.
- Liaqat, I., Mirza, S. A., Iqbal, R., Ali, N. M., Saleem, G., Majid, S. and Shahid, M. (2018) 'Flagellar motility plays important role in biofilm formation of *Bacillus cereus* and *Yersinia enterocolitica*', *Pakistan Journal of Pharmaceutical Sciences*, 31(5), pp. 2047-2052.
- Lim, E. S. and Kim, J. (2017) 'Role of *eptC* in biofilm formation by *Campylobacter jejuni* NCTC 11168 on polystyrene and glass surface', *Journal of Microbiology and Biotechnology*, 27(9), pp. 1609-1616.
- Line, J. E., Hiatt, K. L., Guard-Bouldin, J. and Seal, B. S. (2010) 'Differential carbon source utilization by *Campylobacter jejuni* 11168 in response to growth temperature variation', *Journal of Microbiological Methods*, 80(2), pp.198-202.
- Llull, D. and Poquet, I. (2004) 'New expression system tightly controlled by zinc availability in *Lactococcus lactis*', *Applied and Environmental Microbiology*, 70(9), pp. 5398-5406.

Louwen, R., Heikema, A., van Belkum, A., Ott, A., Gilbert, M., Ang, W., Endtz, H.P., Bergman, M.P. and Nieuwenhuis, E. E. (2008) 'The sialylated lipooligosaccharide outer core in *Campylobacter jejuni* is an important determinant for epithelial cell invasion', *Infection and Immunity*, 76(10), pp. 4431-4438.

Magajna, B. A. and Schraft, H. (2015) '*Campylobacter jejuni* biofilm cells become viable but non-culturable (VBNC) in low nutrient conditions at 4 °C more quickly than their planktonic counterparts', *Food Control*, 50, pp. 45-50.

Mann, E. E., Rice, K. C., Boles, B. R., Endres, J. L., Ranjit, D., Chandramohan, L., Tsang, L.H., Smeltzer, M.S., Horswill, A.R. and Bayles, K. W. (2009) 'Modulation of eDNA release and degradation affects *Staphylococcus aureus* biofilm maturation', *PLOS One*, 4(6), pp. 1-12.

Marchant, J., Wren, B. and Ketley, J. (2002) 'Exploiting genome sequence: Predictions for mechanisms of *Campylobacter* chemotaxis', *Trends in Microbiology*, 10(4), pp. 155-159.

Marks, L. R., Davidson, B. A., Knight, P. R. and Hakansson, A. P. (2013) 'Interkingdom signaling induces *Streptococcus pneumoniae* biofilm dispersion and transition from asymptomatic colonization to disease', *Mbio*, 4(4), pp. 1-13.

Marschall, L., Sagmeister, P. and Herwig, C. (2016) 'Tunable recombinant protein expression in *E. coli*: Enabler for continuous processing?', *Applied Microbiology and Biotechnology*, 100(13), pp. 5719-5728.

Mc Fadyean, J. and Stockman, S. (1913) *Report of the Departmental Committee appointed by the Board of Agriculture and Fisheries to inquire into epizootic abortion. Part III. Abortion in sheep* edn. London: HMSO.

McClain, M. S., Duncan, S. S., Gaddy, J. A. and Cover, T. L. (2013) 'Control of gene expression in *Helicobacter pylori* using the tet repressor', *Journal of Microbiological Methods*, 95(3), pp. 336-341.

McClaine, J. and Ford, R. (2002) 'Reversal of flagellar rotation is important in initial attachment of *Escherichia coli* to glass in a dynamic system with high- and low-ionic-strength buffers', *Applied and Environmental Microbiology*, 68(3), pp. 1280-1289.

Medema, G., Schets, F., Vandegiessen, A. and Havelaar, A. (1992) 'Lack of colonization of 1-day-old chicks by viable, non-culturable *Campylobacter jejuni*', *Journal of Applied Bacteriology*, 72(6), pp. 512-516.

Megerle, J. A., Fritz, G., Gerland, U., Jung, K. and Raedler, J. O. (2008) 'Timing and dynamics of single cell gene expression in the arabinose utilization system', *Biophysical Journal*, 95(4), pp. 2103-2115.

Meisner, J. and Goldberg, J. B. (2016) 'The *Escherichia coli* rhaSR-PrhaBAD inducible promoter system allows tightly controlled gene expression over a wide range in *Pseudomonas aeruginosa*', *Applied and Environmental Microbiology*, 82(22), pp. 6715-6727.

Melo, R. T., Mendonca, E. P., Monteiro, G. P., Siqueira, M. C., Pereira, C. B., Peres, P. A. B. M., Fernandez, H. and Rossi, D. A. (2017) 'Intrinsic and extrinsic aspects on *Campylobacter jejuni* biofilms', *Frontiers in Microbiology*, 8, pp. 1-15.

Miller, J., Dower, W. and Tompkins, L. (1988) 'High-voltage electroporation of bacteria - genetic-transformation of *Campylobacter jejuni* with plasmid DNA', *Proceedings of the National Academy of Sciences of the United States of America*, 85(3), pp. 856-860

Miller, W., Bates, A., Horn, S., Brandl, M., Wachtel, M. and Mandrell, R. (2000) 'Detection

on surfaces and in caco-2 cells of *Campylobacter jejuni* cells transformed with new *gfp*, *yfp*, and *cfp* marker plasmids', *Applied and Environmental Microbiology*, 66(12), pp. 5426-5436.

Moorhead, S. M. and Griffiths, M. W. (2011) 'Expression and characterization of cell-signalling molecules in *Campylobacter jejuni*', *Journal of Applied Microbiology*, 110(3), pp. 786-800.

Moran, A. and Upton, M. (1986) 'A comparative-study of the rod and coccoid forms of *Campylobacter jejuni* ATCC 29428', *Journal of Applied Bacteriology*, 60(2), pp. 103-110.

Morgan-Kiss, R., Wadler, C. and Cronan, J. (2002) 'Long-term and homogeneous regulation of the *Escherichia coli* araBAD promoter by use of a lactose transporter of relaxed specificity', *Proceedings of the National Academy of Sciences of the United States of America*, 99(11), pp. 7373-7377.

Mori, T., Hasegawa, N., Sugita, K., Shinjoh, M., Nakamoto, N., Shimizu, T., Hori, S., Iketani, O., Fujiwara, H., Takano, Y. and Iwata, S. (2014) 'Clinical features of bacteremia due to *Campylobacter jejuni*', *Internal Medicine*, 53(17), pp. 1941-1944.

Newman, J. and Fuqua, C. (1999) 'Broad-host-range expression vectors that carry the L-arabinose-inducible *Escherichia coli* araBAD promoter and the *araC* regulator', *Gene*, 227(2), pp. 197-203.

Ng, L., Sherburne, R., Taylor, D. and Stiles, M. (1985) 'Morphological forms and viability of *Campylobacter* species studied by electron-microscopy', *Journal of Bacteriology*, 164(1), pp. 338-343.

Nguyen, V. T., Fegan, N., Turner, M. S. and Dykes, G. A. (2012) 'Role of attachment to surfaces on the prevalence and survival of *Campylobacter* through food systems', *Journal of*

Food Protection, 75(1), pp. 195-206.

Nguyen, V. T., Turner, M. S. and Dykes, G. A. (2010) 'Effect of temperature and contact time on *Campylobacter jejuni* attachment to, and probability of detachment from, stainless steel', *Journal of Food Protection*, 73(5), pp. 832-838.

Nijland, R., Hall, M. J. and Burgess, J. G. (2010) 'Dispersal of biofilms by secreted, matrix degrading, bacterial DNase', *PLOS One*, 5(12), pp. 1-7.

Novick, A. and Weiner, M. (1957) 'Enzyme induction as all or none phenomenon', *Proceedings of the National Academy of Sciences of the United States of America*, 43(7), pp. 553-566.

Novotny, L. A., Amer, A. O., Brockson, M. E., Goodman, S. D. and Bakaletz, L. O. (2013) 'Structural stability of *Burkholderia cenocepacia* biofilms is reliant on eDNA structure and presence of a bacterial nucleic acid binding protein', *PLOS One*, 8(6), pp. 1-15.

Nyati, K. K. and Nyati, R. (2013) 'Role of *Campylobacter jejuni* infection in the pathogenesis of Guillain-Barre syndrome: An update', *Biomed Research International*, 2013, pp. 1-13.

Ogden, S., Haggerty, D., Stoner, C., Kolodrubetz, D. and Schleif, R. (1980) 'The *Escherichia coli* L-arabinose operon binding sites of the regulatory proteins and a mechanism of positive and negative regulation', *Proceedings of the National Academy of Sciences of the United States of America*, 77(6), pp. 3346-3350.

Oliver, J. (2005) 'The viable but non-culturable state in bacteria', *Journal of Microbiology*, 43(1), pp. 93-100.

On, S. (2001) 'Taxonomy of *Campylobacter*, *Arcobacter*, *Helicobacter* and related bacteria:

Current status, future prospects and immediate concerns', *Journal of Applied Microbiology*, 90, pp. 1S-15S.

Park, S. (2002) 'The physiology of *Campylobacter* species and its relevance to their role as foodborne pathogens', *International Journal of Food Microbiology*, 74(3), pp. 177-188.

Parkhill, J., Wren, B., Mungall, K., Ketley, J., Churcher, C., Basham, Chillingworth, T., Davies, R.M., Feltwell, T., Holroyd, S., Jagels, K., Karlyshev, A.V., Moule, S., Pallen, M.J., Penn, C.W., Quail, M.A., Rajendream, M.A., Rutherford, K.M., van Vliet, A.H.M., Whitehead, S. and Barrell, B. (2000) 'The genome sequence of the food-borne pathogen *Campylobacter jejuni* reveals hypervariable sequences', *Nature*, 403(6770), pp. 665-668.

Pearson, A., Greenwood, M., Healing, T., Rollins, D., Shahamat, M., Donaldson, J. and Colwell, R. (1993) 'Colonization of broiler-chickens by waterborne *Campylobacter jejuni*', *Applied and Environmental Microbiology*, 59(4), pp. 987-996.

Pei, Z. and Blaser, M. (1993) 'PEB1, the major cell-binding factor of *Campylobacter jejuni*, is a homolog of the binding-component in Gram-negative nutrient transport systems', *Journal of Biological Chemistry*, 268(25), pp. 18717-18725.

Pettigrew, M. M., Marks, L. R., Kong, Y., Gent, J. F., Roche-Hakansson, H. and Hakansson, A. P. (2014) 'Dynamic changes in the *Streptococcus pneumoniae* transcriptome during transition from biofilm formation to invasive disease upon influenza A virus infection', *Infection and Immunity*, 82(11), pp. 4607-4619.

Pickett, C. and Whitehouse, C. (1999) 'The cytolethal distending toxin family', *Trends in Microbiology*, 7(7), pp. 292-297.

Plummer, P. J. (2012) 'LuxS and quorum-sensing in *Campylobacter*', *Frontiers in Cellular*

and *Infection Microbiology*, 2(22), pp. 1-9.

Poelzler, T., Stueger, H. and Lassnig, H. (2018) 'Prevalence of most common human pathogenic *Campylobacter* spp. in dogs and cats in Styria, Austria', *Veterinary Medicine and Science*, 4(2), pp. 115-125.

Pratt, L. and Kolter, R. (1998) 'Genetic analysis of *Escherichia coli* biofilm formation: Roles of flagella, motility, chemotaxis and type I pili', *Molecular Microbiology*, 30(2), pp. 285-293.

Pruzzo, C., Tarsi, R., Lleo, M., Signoretto, C., Zampini, M., Colwell, R. and Canepari, P. (2002) 'In vitro adhesion to human cells by viable but non-culturable *Enterococcus faecalis*', *Current Microbiology*, 45(2), pp. 105-110.

Purdy, D., Buswell, C., Hodgson, A., McAlpine, K., Henderson, I. and Leach, S. (2000) 'Characterisation of cytolethal distending toxin (CDT) mutants of *Campylobacter jejuni*', *Journal of Medical Microbiology*, 49(5), pp. 473-479.

Qin, Z., Ou, Y., Yang, L., Zhu, Y., Tolker-Nielsen, T., Molin, S. and Qu, D. (2007) 'Role of autolysin-mediated DNA release in biofilm formation of *Staphylococcus epidermidis*', *Microbiology Society*, 153(7), pp. 2083-2092.

Qiu, D., Damron, F. H., Mima, T., Schweizer, H. P. and Yu, H. D. (2008) 'P_{BAD}-based shuttle vectors for functional analysis of toxic and highly regulated genes in *Pseudomonas* and *Burkholderia* spp. and other bacteria', *Applied and Environmental Microbiology*, 74(23), pp. 7422-7426.

Quinones, B., Miller, W. G., Bates, A. H. and Mandrell, R. E. (2009) 'Autoinducer-2 production in *Campylobacter jejuni* contributes to chicken colonization', *Applied and Environmental Microbiology*, 75(1), pp. 281-285.

Ramesh, A., Ikeda, N., Rubinchik, S. and Karlyshev, A. V. (2019) 'Expression of *Escherichia coli araE* and modified *lacY* genes in *Campylobacter jejuni* is not sufficient for arabinose transport', *Access Microbiology*, 1(5), pp. 1-8.

Rao, K., Yazaki, E., Evans, D. and Carbon, R. (2004) 'Objective evaluation of small bowel and colonic transit time using pH telemetry in athletes with gastrointestinal symptoms', *British Journal of Sports Medicine*, 38(4), pp. 482-487.

Reeder, T. and Schleif, R. (1991) 'Mapping, sequence, and apparent lack of function of *araI*, a gene of the *Escherichia coli* arabinose regulon', *Journal of Bacteriology*, 173(24), pp. 7765-7771.

Rees, J., Soudain, S., Gregson, N. and Hughes, R. (1995) '*Campylobacter jejuni* infection and Guillain-Barre syndrome', *New England Journal of Medicine*, 333(21), pp. 1374-1379.

Reeser, R. J., Medler, R. T., Billington, S. J., Jost, B. H. and Joens, L. A. (2007) 'Characterization of *Campylobacter jejuni* biofilms under defined growth conditions', *Applied and Environmental Microbiology*, 73(6), pp. 1908-1913.

Ren, F., Li, X., Tang, H., Jiang, Q., Yun, X., Fang, L., Huang, P.Y., Tang, Y.Y., Li, Q.C., Huang, J.L. and Jiao, X. (2018) 'Insights into the impact of *flhF* inactivation on *Campylobacter jejuni* colonization of chick and mice gut', *BMC Microbiology*, 18, pp. 1-11.

Reuter, M., Mallett, A., Pearson, B. M. and van Vliet, A. H. M. (2010) 'Biofilm formation by *Campylobacter jejuni* is increased under aerobic conditions', *Applied and Environmental Microbiology*, 76(7), pp. 2122-2128.

Robinson, D. (1981) 'Infective dose of *Campylobacter jejuni* in milk', *British Medical Journal*, 282(6276), pp.1584-1584.

Rollins, D. and Colwell, R. (1986) 'Viable but non-culturable stage of *Campylobacter jejuni* and its role in survival in the natural aquatic environment', *Applied and Environmental Microbiology*, 52(3), pp. 531-538.

Rossi, D. A., Melo, R. T., Mendonça, E.P. and Monteiro, G.P. (2017) *Biofilms of Salmonella and Campylobacter in the poultry industry*. London: Poultry science, IntechOpen.

Roy, R., Tiwari, M., Donelli, G. and Tiwari, V. (2018) 'Strategies for combating bacterial biofilms: A focus on anti-biofilm agents and their mechanisms of action', *Virulence*, 9(1), pp. 522-554.

Rubinchik, S. (2014) 'The development and application of an *in vitro* model of *Campylobacter* interactions with host cell receptors'. *PhD Thesis*. Kingston University.

Sanders, S. Q., Boothe, D. H., Frank, J. F. and Arnold, J. W. (2007) 'Culture and detection of *Campylobacter jejuni* within mixed microbial populations of biofilms on stainless steel', *Journal of Food Protection*, 70(6), pp. 1379-1385.

Satpathy, S., Sen, S. K., Pattanaik, S. and Raut, S. (2016) 'Review on bacterial biofilm: An universal cause of contamination', *Biocatalysis and Agricultural Biotechnology*, 7, pp. 56-66.

Sauer, K., Cullen, M., Rickard, A., Zeef, L., Davies, D. and Gilbert, P. (2004) 'Characterization of nutrient-induced dispersion in *Pseudomonas aeruginosa* PAO1 biofilm', *Journal of Bacteriology*, 186(21), pp. 7312-7326.

Schleif, R. (2010) 'AraC protein, regulation of the L-arabinose operon in *Escherichia coli*, and the light switch mechanism of AraC action', *FEMS Microbiology Reviews*, 34(5), pp. 779-796.

Schleifer, K. and Kandler, O. (1972) 'Peptidoglycan types of bacterial cell-walls and their

taxonomic implications', *Bacteriological Reviews*, 36(4), pp. 407-477.

Schnee, A. E. and Petri, W. A. (2017) 'Campylobacter jejuni and associated immune mechanisms: Short-term effects and long-term implications for infants in low-income countries', *Current Opinion in Infectious Diseases*, 30(3), pp. 322-328.

Sebald, M. and Veron, M. (1963) 'Teneur en bases de l'ADN et classification des *Vibrions* (base dna content and classification of *Vibrions*)', *Inst. Pasteur*, 105, pp. 897-910.

Seper, A., Fengler, V. H. I., Roier, S., Wolinski, H., Kohlwein, S. D., Bishop, A. L., Camilli, A., Reidl, J. and Schild, S. (2011) 'Extracellular nucleases and extracellular DNA play important roles in *Vibrio cholerae* biofilm formation', *Molecular Microbiology*, 82(4), pp. 1015-1037.

Seper, A., Hosseinzadeh, A., Gorkiewicz, G., Lichtenegger, S., Roier, S., Leitner, D. R., Grutsch, A., Reidl, J., Urban, C.D. and Schild, S. (2013) '*Vibrio cholerae* evades neutrophil extracellular traps by the activity of two extracellular nucleases', *PLOS Pathogens*, 9(9), pp. 1-15.

Sharkey, F., Banat, I. and Marchant, R. (2004) 'Detection and quantification of gene expression in environmental bacteriology', *Applied and Environmental Microbiology*, 70(7), pp. 3795-3806.

Siegele, D. and Hu, J. (1997) 'Gene expression from plasmids containing the araBAD promoter at subsaturating inducer concentrations represents mixed populations', *Proceedings of the National Academy of Sciences of the United States of America*, 94(15), pp. 8168-8172.

Silva, J., Leite, D., Fernandes, M., Mena, C., Gibbs, P. A. and Teixeira, P. (2011) '*Campylobacter* spp. as a foodborne pathogen: A review', *Frontiers in Microbiology*, 2, pp. 1-

12.

Siringan, P., Connerton, P. L., Payne, R. J. H. and Connerton, I. F. (2011) 'Bacteriophage-mediated dispersal of *Campylobacter jejuni* biofilms', *Applied and Environmental Microbiology*, 77(10), pp. 3320-3326.

Skarp, C. P. A., Hanninen, M. and Rautelini, H. I. K. (2016) 'Campylobacteriosis: The role of poultry meat', *Clinical Microbiology and Infection*, 22(2), pp. 103-109.

Skirrow, M. (1977) '*Campylobacter* enteritis: A "new" disease', *British medical journal*, 2, pp. 9-11.

Smith, C. K., Abuoun, M., Cawthraw, S. A., Humphrey, T. J., Rothwell, L., Kaiser, P., Barrow, P.A. and Jones, M. A. (2008) '*Campylobacter* colonization of the chicken induces a proinflammatory response in mucosal tissues', *FEMS Immunology and Medical Microbiology*, 54(1), pp. 114-121.

Smith, T. and Orcutt, M.L. (1927) '*Vibrios* from calves and their serological relation to *Vibrio fetus*', *Journal of Experimental Medicine*, 45(2), 391-397.

Snelling, W., Matsuda, M., Moore, J. and Dooley, J. (2005) 'Under the microscope – *Campylobacter jejuni*', *Letters in Applied Microbiology*, 41(4), pp. 297-302.

Srey, S., Jahid, I. K. and Ha, S. (2013) 'Biofilm formation in food industries: A food safety concern', *Food Control*, 31(2), pp. 572-585.

Stahl, M., Butcher, J. and Stintzi, A. (2012) 'Nutrient acquisition and metabolism by *Campylobacter jejuni*', *Frontiers in Cellular and Infection Microbiology*, 2, pp. 1-10.

Stahl, M., Friis, L. M., Nothhaft, H., Liu, X., Li, J., Szymanski, C. M. and Stintzi, A. (2011) 'L-

fucose utilization provides *Campylobacter jejuni* with a competitive advantage', *Proceedings of the National Academy of Sciences of the United States of America*, 108(17), pp. 7194-7199.

Steichen, C. T., Cho, C., Shao, J. Q. and Apicella, M. A. (2011) 'The *Neisseria gonorrhoeae* biofilm matrix contains DNA, and an endogenous nuclease controls its incorporation', *Infection and Immunity*, 79(4), pp. 1504-1511.

Stern, N., Bailey, J., Blankenship, L., Cox, N. and Mchan, F. (1988) 'Colonization characteristics of *Campylobacter jejuni* in chick ceca', *Avian Diseases*, 32(2), pp. 330-334.

Stern, N., Jones, D., Wesley, I. and Rollins, D. (1994) 'Colonization of chicks by non-culturable *Campylobacter spp*', *Letters in Applied Microbiology*, 18(6), pp. 333-336.

Suchanek, Verena. (2017) 'Role of Motility and its Regulation in *Escherichia coli* Biofilm formation'. *PhD Thesis*. Ruperto-Carola University of Heidelberg.

Sukchawalit, R., Vattanaviboon, P., Sallabhan, R. and Mongkolsuk, S. (1999) 'Construction and characterization of regulated L-arabinose-inducible broad host range expression vectors in *Xanthomonas*', *FEMS Microbiology Letters*, 181(2), pp. 217-223.

Sulaeman, S., Le Bihan, G., Rossero, A., Federighi, M., De, E. and Tresse, O. (2010) 'Comparison between the biofilm initiation of *Campylobacter jejuni* and *Campylobacter coli* strains to an inert surface using BioFilm ring test (R)', *Journal of Applied Microbiology*, 108(4), pp. 1303-1312.

Svensson, S. L., Pryjma, M. and Gaynor, E. C. (2014) 'Flagella-mediated adhesion and extracellular DNA release contribute to biofilm formation and stress tolerance of *Campylobacter jejuni*', *PLOS One*, 9(8), pp. 1-13.

Tang, J., Zhou, R., Shi, X., Kang, M., Wang, H. and Chen, H. (2008) 'Two thermostable nucleases coexisted in *Staphylococcus aureus*: Evidence from mutagenesis and *in vitro* expression', *FEMS Microbiology Letters*, 284(2), pp. 176-183.

Tangwacharin, P., Chanthachum, S., Khopaibool, P. and Griffiths, M. W. (2006) 'Morphological and physiological responses of *Campylobacter jejuni* to stress', *Journal of Food Protection*, 69(11), pp. 2747-2753.

Teh, A. H. T., Lee, S. M. and Dykes, G. A. (2019) 'Association of some *Campylobacter jejuni* with *Pseudomonas aeruginosa* biofilms increases attachment under conditions mimicking those in the environment', *PLOS One*, 14(4), pp. 1-15.

Teh, A., Lee, S. and Dykes, G. (2014) 'Does *Campylobacter jejuni* form biofilms in food-related environments?', *Applied and Environmental Microbiology*, 80(17), pp. 5154– 5160.

Tetz, G. V., Artemenko, N. K. and Tetz, V. V. (2009) 'Effect of DNase and antibiotics on biofilm characteristics', *Antimicrobial Agents and Chemotherapy*, 53(3), pp. 1204-1209.

Thomas, V. C., Thurlow, L. R., Boyle, D. and Hancock, L. E. (2008) 'Regulation of autolysis-dependent extracellular DNA release by *Enterococcus faecalis* extracellular proteases influences biofilm development', *Journal of Bacteriology*, 190(16), pp. 5690-5698.

Trachoo, N., Frank, J. and Stern, N. (2002) 'Survival of *Campylobacter jejuni* in biofilms isolated from chicken houses', *Journal of Food Protection*, 65(7), pp. 1110-1116.

Trémillon, N., Issaly, N., Mozo, J., Duvignau, T., Ginisty, H., Devic, E. and Poquet, I. (2010) 'Research production and purification of *Staphylococcal* nuclease in *Lactococcus lactis* using a new expression-secretion system and a pH-regulated mini-reactor', *Microbial Cell Factories*, 9, pp. 1-12.

- Trieu-Cuot, P., Gerbaud, G., Lambert, T. and Courvalin, P. (1985) 'In vivo transfer of genetic information between Gram-positive and Gram-negative bacteria', *EMBO J*, 4(13A), pp. 3583-3587.
- Tuson, H. H. and Weibel, D. B. (2013) 'Bacteria-surface interactions', *Soft Matter*, 9(17), pp. 4368-4380.
- van der Stel, A., van de Lest, C. H. A., Huynh, S., Parker, C. T., van Putten, J. P. M. and Woesten, M. M. S. M. (2018) 'Catabolite repression in *Campylobacter jejuni* correlates with intracellular succinate levels', *Environmental Microbiology*, 20(4), pp. 1374-1388.
- van Vliet, A., Rock, J., Madeleine, L. and Ketley, J. (2000) 'The iron-responsive regulator fur of *Campylobacter jejuni* is expressed from two separate promoters', *FEMS Microbiology Letters*, 188(2), pp. 115-118.
- van Vliet, A., Wooldridge, K. and Ketley, J. (1998) 'Iron-responsive gene regulation in a *Campylobacter jejuni* fur mutant', *Journal of Bacteriology*, 180(20), pp. 5291-5298.
- Vandamme, P. and Deley, J. (1991) 'Proposal for a new family, *Campylobacteraceae*', *International Journal of Systematic Bacteriology*, 41(3), pp. 451-455.
- Vegge, C. S., Brondsted, L., Li, Y., Bang, D. D. and Ingmer, H. (2009) 'Energy taxis drives *Campylobacter jejuni* toward the most favorable conditions for growth', *Applied and Environmental Microbiology*, 75(16), pp. 5308-5314.
- Vendeville, A., Winzer, K., Heurlier, K., Tang, C. and Hardie, K. (2005) 'Making 'sense' of metabolism: Autoinducer-2, LuxS and pathogenic bacteria', *Nature Reviews Microbiology*, 3(5), pp. 383-396.

Véron, M. and Chatelain, R. (1973) 'Taxonomic study of the genus *Campylobacter* Sebald and Véron and designation of the neotype strain for the type species, *Campylobacter fetus* (Smith and Taylor) Sebald and Véron', *International journal of systematic bacteriology*, 23(2), pp. 122-134.

Wagenaar, J. A., French, N. P. and Havelaar, A. H. (2013) 'Preventing *Campylobacter* at the source: Why is it so difficult?', *Clinical Infectious Diseases*, 57(11), pp. 1600-1606.

Weingarten, R. A., Taveirne, M. E. and Olson, J. W. (2009) 'The dual-functioning fumarate reductase is the sole succinate: Quinone reductase in *Campylobacter jejuni* and is required for full host colonization', *Journal of Bacteriology*, 191(16), pp. 5293-5300.

Whitchurch, C., Tolker-Nielsen, T., Ragas, P. and Mattick, J. (2002) 'Extracellular DNA required for bacterial biofilm formation', *Science*, 295(5559), pp. 1487-1487.

Whiteley, M., Gita Banger, M., Bumgarner, R.E., Parsek, M.R., Teitzel, G.M., Lory, S. and Greenberg, E.P. (2001) 'Gene expression in *Pseudomonas aeruginosa* biofilms', *Nature*, 413, pp. 860-864.

Wolf, P. and Oliver, J. (1992) 'Temperature effects on the viable but non-culturable state of *Vibrio vulnificus*', *FEMS Microbiology Ecology*, 101(1), pp. 33-39.

World Health Organization (2018) *Campylobacter*. Available at: <http://www.who.int/news-room/fact-sheets/detail/Campylobacter> (Accessed: 17 January 2019)

Wu, J. and Xi, C. (2009) 'Evaluation of different methods for extracting extracellular DNA from the biofilm matrix', *Applied and Environmental Microbiology*, 75(16), pp. 5390- 5395.

Yanisch-Perron, C., Vieira, J. and Messing, J. (1985) 'Improved M13 phage cloning vectors

and host strains - nucleotide-sequences of the M13mp18 and Puc19 vectors', *Gene*, 33(1), pp. 103-119.

Yao, R., Burr, D., Doig, P., Trust, T., Niu, H. and Guerry, P. (1994) 'Isolation of motile and non-motile insertional mutants of *Campylobacter jejuni* - the role of motility in adherence and invasion of eukaryotic cells', *Molecular Microbiology*, 14(5), pp. 883-893.

Young, K. T., Davis, L. M. and DiRita, V. J. (2007) '*Campylobacter jejuni*: Molecular biology and pathogenesis', *Nature Reviews Microbiology*, 5(9), pp. 665-679.

Zeng, X., Ardeshna, D. and Lin, J. (2015) 'Heat shock-enhanced conjugation efficiency in standard *Campylobacter jejuni* strains,' *Applied and Environmental Microbiology*, 81(13), pp. 4546-4552.

Zhang, J., Liu, Y., Cui, G. and Cui, Q. (2015) 'A novel arabinose-inducible genetic operation system developed for *Clostridium cellulolyticum*', *Biotechnology for Biofuels*, 8, pp. 1-13.

Zhang, Y., Shang, X., Lai, S., Zhang, G., Liang, Y. and Wen, T. (2012) 'Development and application of an arabinose-inducible expression system by facilitating inducer uptake in *Corynebacterium glutamicum*', *Applied and Environmental Microbiology*, 78(16), pp. 5831-5838.

Zhao, J., Wang, Q., Li, M., Heijstra, B. D., Wang, S., Liang, Q. and Qi, Q. (2013) '*Escherichia coli* toxin gene *hipA* affects biofilm formation and DNA release', *Microbiology*, 159, pp. 633-640.

Ziprin, R., Young, C., Stanker, L., Hume, M. and Konkel, M. (1999) 'The absence of cecal colonization of chicks by a mutant of *Campylobacter jejuni* not expressing bacterial fibronectin-binding protein', *Avian Diseases*, 43(3), pp. 586-589

Appendix

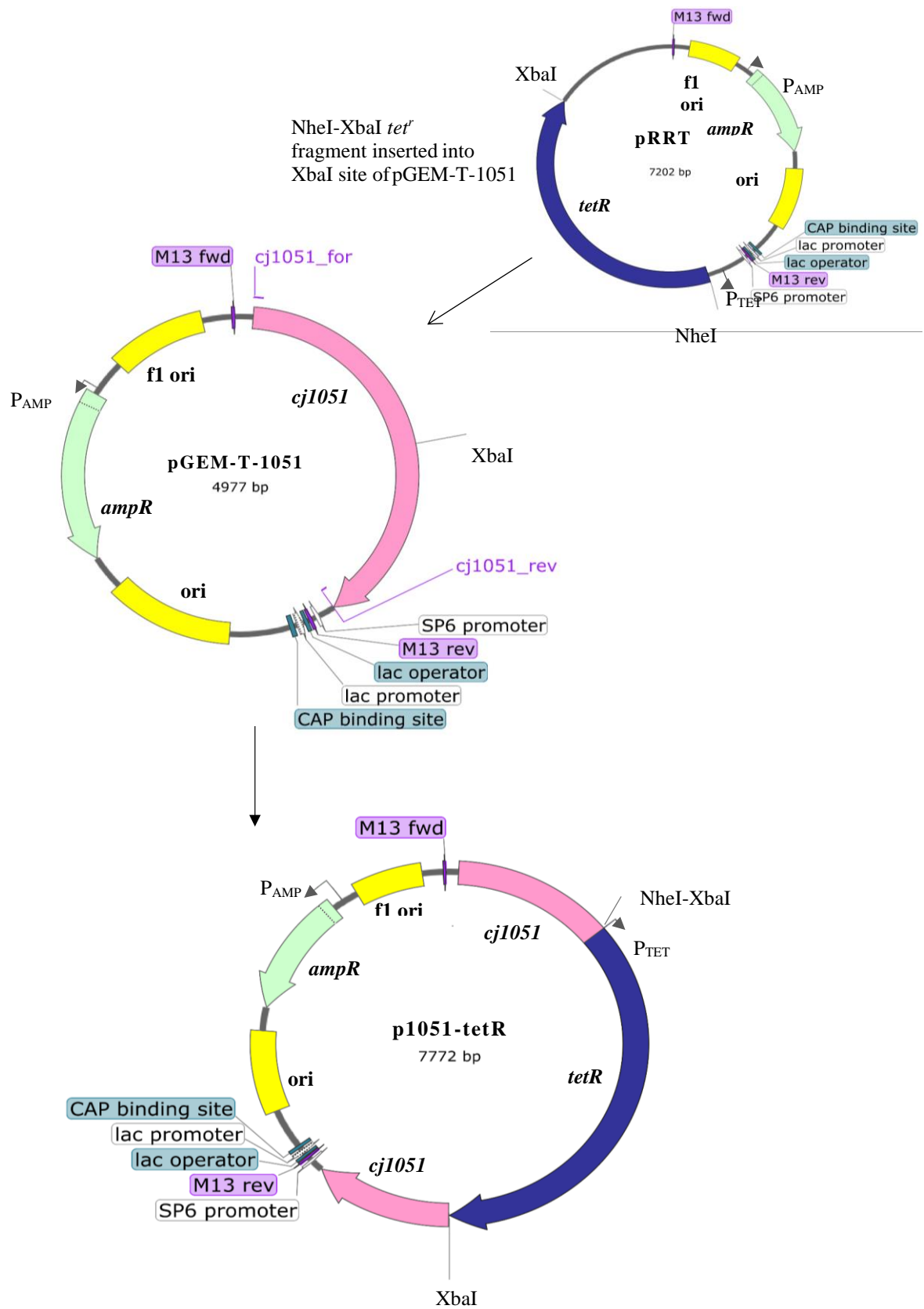


Figure S1. Scheme of construction of plasmid p1051-tetR. Not in scale.

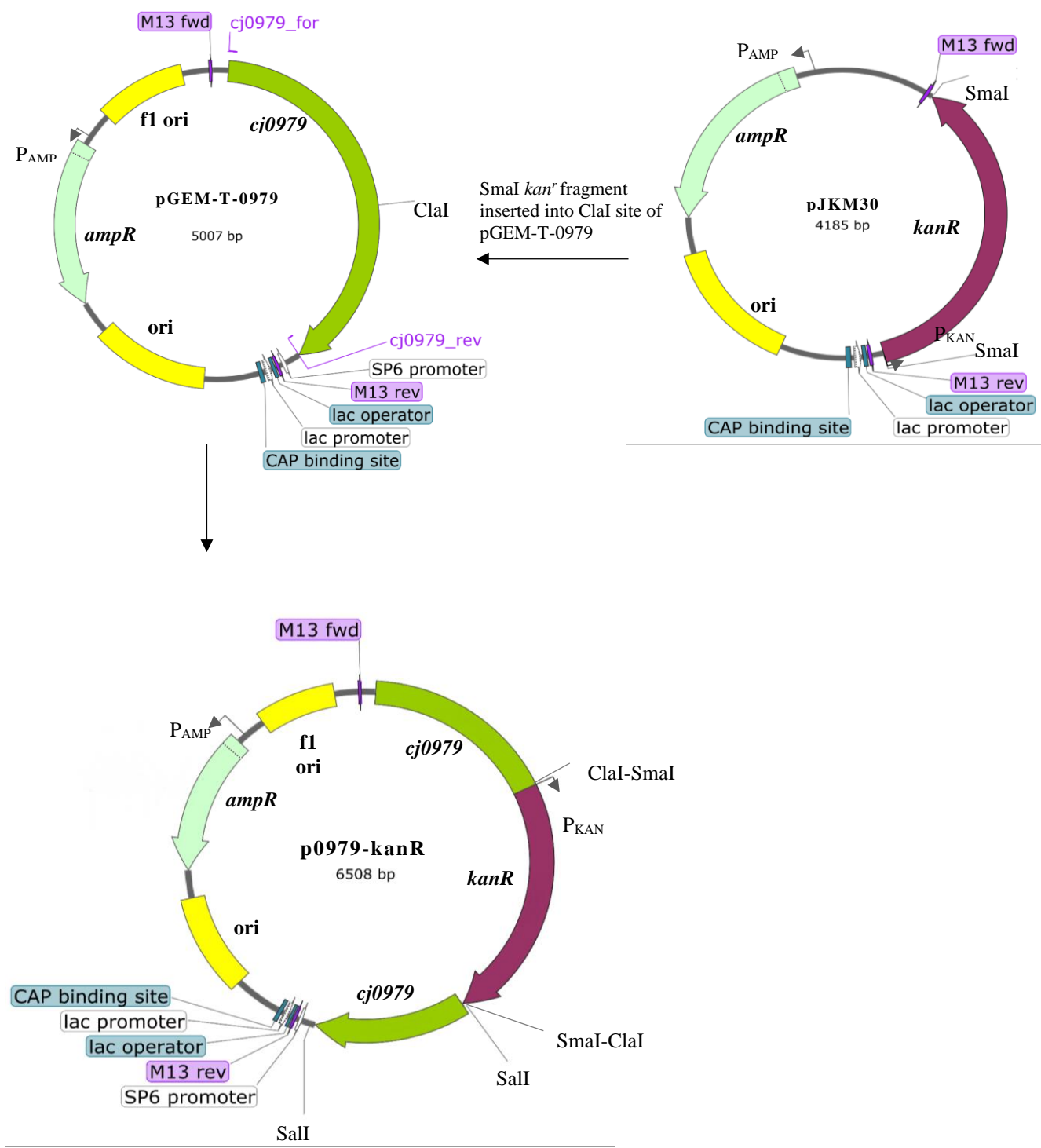


Figure S2. Scheme of construction of plasmid p0979-kanR. Not in scale.

>cj0979_PCR_product

AAAATCTAGAAGGAGGTATACCATGAGAAATAAATTATAAAAAAATATTTAATCTGAGAAAATTACTAAGTGATCCAAAAAACTTTT
TTCTGTATTAATCTTCACTCTTGTAGTTGTTTTTATCCAGAACTATATTGCCAAAATTTCTAGTTTTGAAGGAAAAGTAGTTAGAAT
TATGTGATGGAGATACTATAGAAGTAAATCATGAAAACAACTCGCTAGAATAAGATTTTTTCGGTATAGATGCACCAGAAGCTAAACA
AAGTTTTGGAAAGCAGTCAAAGAAGCTTTAAGTAGAATTTAAGTGGCAAACAAGTTGAAATTTATATAAAAAATAAGATACTTA
TGGTAGAATTGTTGCTATTGTAAGCTTAATGATGTTGATATTAATCGATTTTTGGTAAGCAAAGGCTATGCTTGGGCTGATACTTA
CTATAGTAACGCTTATACCAAAGAACAAGAAAATGCTAAGAAAAATCATTTAGGCTTTTGGAAAGAGAGTAATCCATAGAGCCTTA
TAAATGGAGAAAACAATAAATTCATCACCATCACCATCAC TAAGCATGCGGAA

Figure S3. cj0979 region amplified with primers cj0979_expr_for and cj0979_expr_rev. Highlighted in yellow- coding sequence for 6xHis tag.

>cj0979N_PCR_product

AAAATCTAGAAGGAGGTATACCATGACCATCACCATCACCATAGAATAAATTATAAAAAAATATTTAATCTGAGAAAATTACTAA
GTGATCCAAAAAACTTTTTTCTGTATTAATCTTCACTCTTGTAGTTGTTTTTATCCAGAACTATATTGCCAAAATTTCTAGTTTTG
AAGGAAAAGTAGTTAGAATTTATTGATGGAGATACTATAGAAGTTAATCATGAAAACAACTCGCTAGAATAAGATTTTTTCGGTATAG
ATGCACCAGAAGCTAAACAAGTTTTGGAAAGCAGTCAAAGAAGCTTTAAGTAGAATTTAAGTGGCAAACAAGTTGAAATTTATTT
ATAAAAAATAAGATACTTATGGTAGAATTGTTGCTATTGTAAGCTTAATGATGTTGATATTAATCGATTTTTGGTAAGCAAAGGCT
ATGCTTGGGCTGATACTTACTATAGTAACGCTTATACCAAAGAACAAGAAAATGCTAAGAAAAATCATTTAGGCTTTTGGAAAGAGA
GTAATCCTATAGAGCCTTATAAATGGAGAAAACAATAAATTTAAGCATGCAAGCGGAA

Figure S4. cj0979N region amplified with primers cj0979_N_expr_for and cj0979_N_expr_rev. Highlighted in yellow- coding sequence for 6xHis tag.

>Cj0979

MRINYKKIFNLRKLLSDPKKLFVSVLIFTLVVVF IQNYIAQNSSFEGKVVR
IIDGDTIEVNHENKLARIRFFGIDAPELQKQSFQKQSKAALSRI LSGKQVE
IIYKNKDTYGRIVAIVKLNVDINRFLVSKGYAWADTYYSNAYTKEQENA
KKNHLGLWKESNPIEPYKWRKHNKF

>Nuc (Thermonuclease, Staphylococcus aureus)

MTEYLLSAGICMAIVSILLIGMAISNVSKGYAKRFFFATSCVLVTLVVVSSLSSSANAQTNDNGVNR
GSEDP TVYSATSTKKLHKEPATLIKAIDGDTVKLMYKQPMTFRLLLVDPETKHPKKGVEKYGPEASAF
TKKMVENAKKIEVEFDKGQRTDKYGRGLAYIYADGKMNVEALVRQGLAKVAVYKPNNTHEQLLRKSEA
QAKKEKLNIEWSNADSGQ

Colour code: Red-leader peptide; Green- pro-protein upstream region

>Nuc2 (Thermonuclease, Staphylococcus aureus)

MKSNKSLAMIVVAIIIVGVLAQFMNHTGPFKKGTNHETVQDLNGKDKVHVQRVVDGDTFIAN
QNGKEIK VRLIGVDTPEVTKPNTVPQPFQKQKASNYSKKTLTNQDVYLEYDKEKQDRYGRTLA
YVWISKD

Alignment of amino acid sequences generated by Clustal Omega

```

Cj0979      -----MRINYKKIFNLRKLLSDPKKLFVSVLIFTLVVVF
Nuc         MTEYLLSAGICMAIVSILLIGMAISNVSKGYAKRFFF----FA----TSCLVTLVVVVS
Nuc2       ---MKSNKSLAMIVVAIIIVGV-----

Cj0979      IQN-----YIAQNSSFEGKVVR IIDGDTIEVNHENKLAR
Nuc         SLSSSANAQTNDNGVNRSGSEDP TVYSATSTKKLHKEPATLIKAIDGDTVKLMYKQPMT
Nuc2       -LAF---QFMNHTGPFKKGTNHETVQDLN-----GKDKVHVQRVVDGDTFIANQNGKEIK
                .      : : :****.      : :

Cj0979      IRFFGIDAPELKQS-----FGKQSKAALSRI LSGKQVEI IY---KNKDTYGRIVAIVK
Nuc         FRLLLVDPETKHPKKGVEKYGPEASAF TKKMVENAKKIEVEFDKGQRTDKYGRGLAYIY
Nuc2       VRLIGVDTPEVTKPNTVPQPFQKQKASNYSKKTLTNQD-VYLEYDK-EKQDRYGRTLAYVW
                . * : : * : * : : * : : : * : * * * : * :

Cj0979      LNDVDINRFLVSKGYAWADTYYSNAY-----TKEQENAKKNHLGLWKESNPIEPYKWRK
Nuc         ADGKMNVEALVRQGLAKVAVYKPNNTHEQLLRKSEAQAKKEKLNIEWSNADSGQ----
Nuc2       ISKD-----

Cj0979      HNKF
Nuc         ----
Nuc2       ----

```

Just with Nuc:

```

Cj0979  -----MRINYKKIFNLRKLLSD-----PKKLF----SVLIFTLVVVFIQNYIAQ-
Nuc     MTEYLLSAGICMAIVSILLIGMAISNVSKGQYAKRFFFATSCLVLTLLVVSSLSSSANA
          : : .*: : :*: *:* * *::***** . *:

Cj0979  -----NSSFEGKVVRIIDGDTIEVNHENKLARIRFFGIDA
Nuc     SQTDNGVNRSGSEDPTVYSATSTKKLHKEPATLIKAIDGDTVKLMYKGPMTFRLLLVDT
          . . .::: *****::: .::: :*: :*:

Cj0979  PELKQSF-----GKQSKEALSRI-LSGKQVEI IY---KNKDTYGRIVAVIKLNDVDINR
Nuc     PETKHPKKGVEKYGPEASAFTKKMVENAKKIEVEFDKGQRTDKYGRGLAYIYADGKMVNE
          ** *: * :. .::: ..*:*: : :..*.*** :* : . . :*.

Cj0979  FLVSKGYAWADTYYSNA-----YTKEQENAKKNHLGLWKESNPIEPYKWRKHNF
Nuc     ALVNRQGLAKVAYVYKPNNTHEQLLRKSEAQAKKEKLNWSEDNADSGQ-----
          **:* * . * . * :.*****:* * . . :*.

```

Figure S5. Clustal Omega comparison of Cj0979, Nuc and Nuc 2. Start of pro-protein (green), start of mature proteins/catalytic domains (purple)

Prediction for Cj0979:

Leader peptide (39 aa) in read:

A

>Cj0979

MRINYKKIFNLRKLLSDPKKLF**SVLIFTLVVVFIQNYIA**QNSSFEGKVVRIIDGDTIEV
 NHENKLARIRFFGIDAPELKQSFQKQSKEALSRI LSGKQVEI IYKNKDTYGRIVAVIKL
 NDVDINRFLVSKGYAWADTYYSNAYTKEQENAKKNHLGLWKESNPIEPYKWRKHNF

B

>cj0979

ATGAGAATAAATTATAAAAAAATATTTAATCTGAGAAAATTACTAAGTGATCCAAAAA
ACTTTTTCTGTATTAATCTTCACTCTTGTAGTTGTTTTATCCAGAACTATATTGCC

CAAAATTCAGTTTTGAAGGAAAAGTAGTTAGAATTATTGATGGAGATACTATAGAAGT
 TAATCATGAAAACAACTCGCTAGAATAAGATTTTTCGGTATAGATGCACCAGAACTTA
 AACAAAGTTTTGGAAAGCAGTCAAAGAAGCTTTAAGTAGAATTTAAGTGGCAAACAA
 GTTGAATTTATTAATAAAATAAAGATACTTATGGTAGAATTGTTGCTATTGTAAAGCT
 TAATGATGTTGATATTAATCGATTTTGGTAAGCAAAGGCTATGCTTGGGCTGATACTT
 ACTATAGT AACGCTTATACCAAGAACAAGAAAATGCTAAGAAAATCATTTAGGTCT
 TTGGAAAGAG AGTAATCCTATAGAGCCTTATAAATGGAGAAAACACAATAAATCTAA

C

>cj0979LP

CAAAATTCAGTTTTGAAGGAAAAGTAGTTAGAATTATTGATGGAGATACTATAGAAGT
 TAATCATGAAAACAACTCGCTAGAATAAGATTTTTCGGTATAGATGACCAGAACTTAA
 ACAAGTTTTGGAAAGCAGTCAAAGAAGCTTTAAGTAGAATTTAAGTGGCAAACAAG
 TTGAAATTTATTAATAAAATAAAGATACTTATGGTAGAATTGTTGCTATTGTAAAGCTT
 AATGATGTTGATATTAATCGATTTTGGTAAGCAAAGGCTATGCTTGGGCTGATACTTA
 CTATAGTAACGCTTATACCAAGAACAAGAAAATGCTAAGAAAATCATTTAGGTCTTT
 GGAAAGAGAGTAATCCTATAGAGCCTTATAAATGGAGAAAACACAATAAATCTAA

Figure S6. Sequence of *cj0979LP*. Font in red - sequence corresponding to leader peptide. A- amino acid sequence of Cj0979, B- nucleotide sequence of gene *cj0979*, C-nucleotide sequence of gene *cj0979LP* without leader peptide.

>cj0979LP_PCR_product

AAAATCTAGAAAGAAGGAGATATACCATGCAAAATTCAGTTTTGAAGGAAAAGTAGTTAGAATTATTGATGGAGATACTATAGAAG
 TTAATCATGAAAACAACTCGCTAGAATAAGATTTTTCGGTATAGATGCACCAGAACTTAAACAAGTTTTGGAAAGCAGTCAAAG
 AAGCTTTAAGTAGAATTTAAGTGGCAAACAAGTTGAAATTTATTAATAAAATAAAGATACTTATGGTAGAATTGTTGCTATTGTAA
 AGCTTAATGATGTTGATATTAATCGATTTTGGTAAGCAAAGGCTATGCTTGGGCTGATACTTACTATAGTAACGCTTATACCAAG
 AACAAAGAAAATGCTAAGAAAATCATTTAGGTCTTTGGAAAGAGAGTAATCCTATAGAGCCTTATAAATGGAGAAAACACAATAAAT
 TC**CATCATCATCATCATCAC**TAAGCATGCGGAA

Figure S7. *cj0979LP* region amplified with primers *cj0979LP_for* and *cj0979LP_rev*. Highlighted in yellow- coding sequence for 6xHis tag.

>Cje1441

MKKLIILSLSTLAFADYTYKPKSEDFAKYFTKQNCQVLDKFFYYINCYDYSLKGTAKAVAYRLEADNLKG
 EQIKRPRFEDDNIIPKKYRTTWSDYKNSGYDRGHTLSNASMRKTTQAQRSTFLMSNITPQNPNQINQRVW
 NKIEKRERQVALKLGSLVNLVNYDNNPQRIKNNIAIPSSYTKILKGDNFKECYQVPNHVDVENENLRIY
 KVKCDNF

BLASTp result:

DNA/RNA non-specific endonuclease [*Campylobacter*]

Identity: 66%, Coverage percentage: 100%

```
Query 1 MKKLIIILSLLSTLAFADYTQYKPSSEDFAKYFTKQNCQVLDKFFYYINCYDYSKLGTKAVA 60
      MK I L +S FA YKPS DF+ YF NCSQ+LDKF+Y+NCYDY LKGTKAVA
Sbjct 1 MKIFIFLLTISLNIFA-LEPYKPSADFSYFNNINCSQILDKFFYLNCYDYKLGTKAVA 59

Query 61 YRLEADNLKGEQIKKRPRFEDDTNIPKKYRTTWSYKNSGYDRGHTLSNASMRKTTQAQR 120
      Y++EA NLK QIKKRPRFEDDTNIPKKYRTTWS+YKNSGY RGHT NAS + AQ
Sbjct 60 YKVEASNLDKDRQIKKRPRFEDDTNIPKKYRTTWSNYKNSGYTRGHTAPNASFSFSKAAQN 119

Query 121 STFLMSNITPQNPNQINQRVWNKIEKRERQVASKLGSLEVLNLVNVDNNPQRIKNNIAIPS 180
      S FLMSNITPQN QIN ++WN+IE+RER +AL+ S+EVLNLV YD PQ IKN IAIPS
Sbjct 120 SVFLMSNITPQNAQINNKIWNEIEQRERNLALEFQSIIEVLNVLVYDKEPQYIKNRIAIPS 179

Query 181 SYTKILKGDNFKECYQVPNHVDVENENLRIYKVKCDNF 217
      Y KI+K FKECYQ PNH+V +EN++ Y++ CD F
Sbjct 180 FVVKIIKTPKFKECYQAPNHEVDENIKQYQINCDKF 216
```

>Cje0566

```
MKKLIIILSLLSTLAFADYTQYKPSSEDFAKYFTKQSCSQVLDKFFYYLNCYDYNLKGTKAVAYKLEVDNLKG
EQIKKRPRFEDDTNIPKKYRTTWSYKNSGYDRGHTLSNASMRKTTQAQRSTFLMSNITPQNPNQINQRVW
NKIEKRERQVASKLGSLEVLNLVNVDNNPQRIKNNIAIPSSYIKILKGENFKECYQVPNHEVEDENIRKY
KIDCDKI
```

BLASTp result:

DNA/RNA non-specific endonuclease [*Campylobacter*]

Identity: 66%, Coverage percentage: 100%

```
Query 1 MKKLIIILSLLSTLAFADYTQYKPSSEDFAKYFTKQSCSQVLDKFFYYLNCYDYNLKGTKAVA 60
      MK I L +S FA YKPS +F+ YF +CSQ+LDKF+YLNCYDY LKGTKAVA
Sbjct 1 MKIFIFLLTISLNIFA-LEPYKPSADFSYFNNINCSQILDKFFYLNCYDYKLGTKAVA 59

Query 61 YKLEVDNLKGEQIKKRPRFEDDTNIPKKYRTTWSYKNSGYDRGHTLSNASMRKTTQAQR 120
      YK+E NLK QIKKRPRFEDDTNIPKKYRTTWS+YKNSGY RGHT NAS + AQ
Sbjct 60 YKVEASNLDKDRQIKKRPRFEDDTNIPKKYRTTWSNYKNSGYTRGHTAPNASFSFSKAAQN 119

Query 121 STFLMSNITPQNPNQINQRVWNKIEKRERQVASKLGSLEVLNLVNVDNNPQRIKNNIAIPS 180
      S FLMSNITPQN QIN ++WN+IE+RER +A + S+EVLNLV YD PQ I+N+IAIPS
Sbjct 120 SVFLMSNITPQNAQINNKIWNEIEQRERNLALEFQSIIEVLNVLVYDKEPQYIKNRIAIPS 179

Query 181 SYIKILKGENFKECYQVPNHEVEDENIRKYKIDCDKI 217
      Y+KI+K FKECYQ PNHEV DENI++Y+I+CDK
Sbjct 180 FVVKIIKTPKFKECYQAPNHEVDENIKQYQINCDKF 216
```

Figure S8. Homologues of *C. jejuni* RM1221 DNases checked against *C. jejuni* NCTC 11168 genome using non-redundant protein database. Amino acid sequences of Cje1441, Cje0566 and Cje0256 were used as the query sequence for BLASTp analysis.

Cje0256/Cj0979

Coverage percentage-38%, Identity-50%

```
Query 19 KKLFSVLIFTLVVV 32
      KK+ SVLI L ++
Sbjct 2 KKIISVLIILALSLL 15

Query 154 HLGLWKES 161
      HL WKE
Sbjct 100 HLPCWKEG 107

Query 129 SKGY-AWADTYYSNAYTKEQENAKKNHLGLWKESNP 165
      SKG+ A + Y S Y + ++ + W + P++
Sbjct 176 SKGWIARSYLYMSKTYNIRLSQERKLM EAWDRQYPM 213

Query 80 QSFGKQ 85
      Q+FGK
Sbjct 95 QNFGKH 100

Query 141 NAYTKE 146
      N YTK+
```

```

Sbjct 71 NEYTKK 76
Query 153 NHLG--LWKESNPIEPYKWRKHNF 175
          N LG W + P+K K K+
Sbjct 32 NDLGSSYWYDFYCQAPFKVNKKGKY 56

```

Cje0566/Cj0979

Coverage percentage-34%, Identity-27%

```

Query 20 KLFSVLIFTLV-----VVFIQNYIAQNSSFEGKVVRIIDGDTIE-----VNHENKLARIR 69
          KL S+ + LV I+N IA SS+ ++I+ G+ + NHE + IR
Sbjct 153 KLGSLVNLVNYDNNPQRIRNQIAIPSSY----IKILKGENFKECYQVPNHEVEDENIR 208

```

```

Query 70 FFGIDAPEL 78
          + ID ++
Sbjct 209 KYKIDCDKI 217

```

```

Query 138 YYSNAY 143
          YY N Y
Sbjct 44 YYLNCY 49

```

Cje1441/Cj0979

Coverage percentage-34%, Identity-27%

```

Query 20 KLFSVLIFTLV-----VVFIQNYIAQNSSFEGKVVRIIDGDTIE-----VNHENKLARIR 69
          KL S+ + LV I+N IA SS+ +I+ GD + NH+ + +R
Sbjct 153 KLGSLVNLVNYDNNPQRIRKNNIAIPSSY----TKILKGDNFKECYQVPNHDEVENENLR 208

```

```

Query 70 FFGI 73
          + +
Sbjct 209 IYKV 212

```

```

Query 138 YYSNAY 143
          YY N Y
Sbjct 44 YYINCY 49

```

Figure S9. Amino acid sequence similarity of *C. jejuni* 11168 Cj0979 and *C. jejuni* RM1221 DNases. Amino acid sequences were used as the query sequence for BLASTp analysis

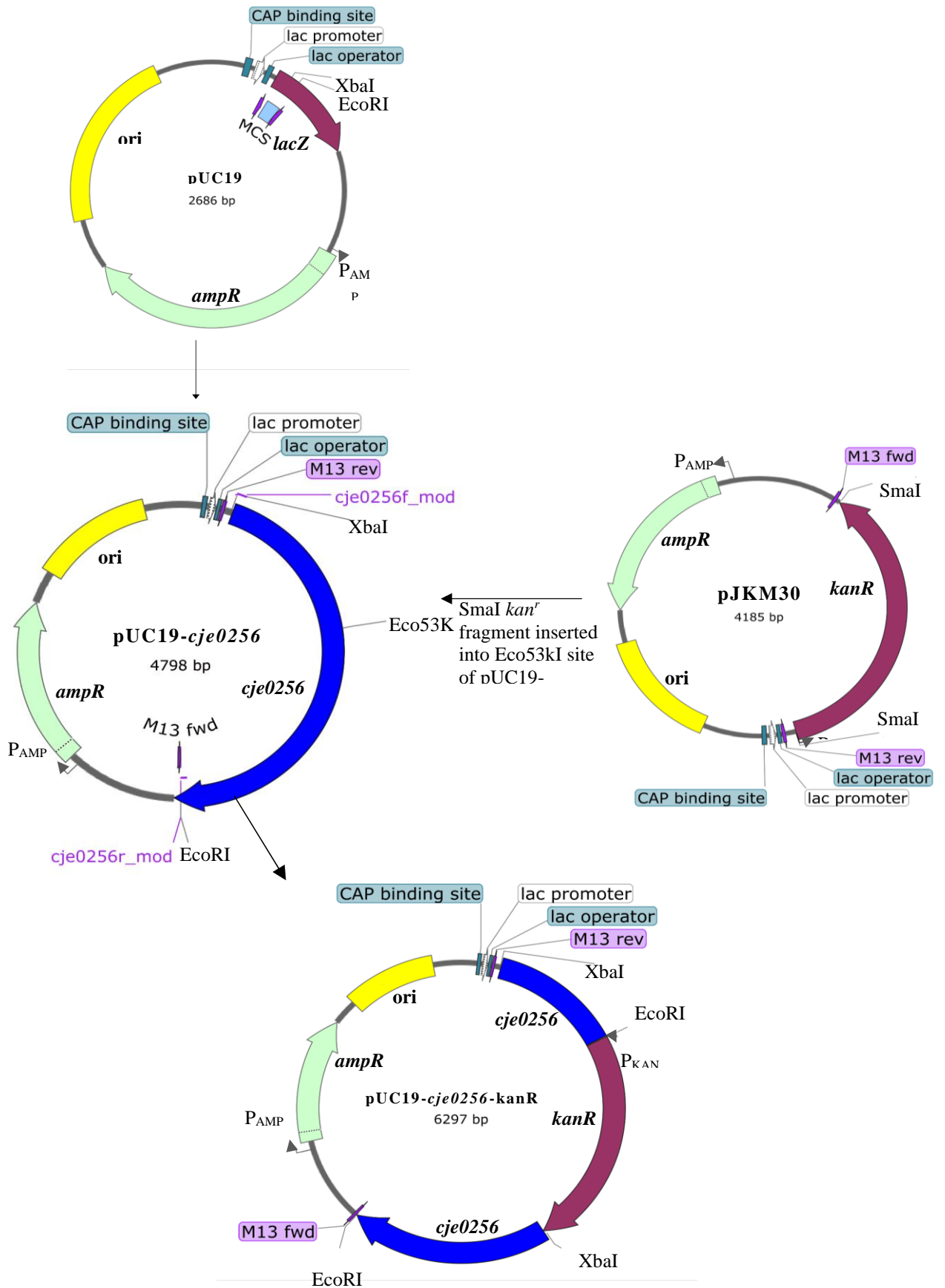


Figure S10. Scheme of construction of plasmid pUC19-*cje0256*-kanR. Not in scale.

A

>cje0256

MKKIISVLLILALSLLNAKSFEESKELVKFYNDLGSSYWDYFCQAPFKVNNKKGKYSISFE
VIKSDLYAPRNEYTKKGINQRIKRIEWEHIMPAQNFQKHLPCWKEGGRKACKNDPFAK
MEADKQNLVPAIGEINGDRSNFRYAEAPTNLKYTQYGNCKVYTDFAKAKRFYPANYSKGWI
ARSYLMSKTYNIRLSDQERKLMEAWDKQYPMDEKEKRIRALL

B

>cje0256

ATGAAAAAATAATAAGCGTTTTAATACTTGCTTTAAGCTTATTAATGCT

AAAAGTTTTGAAGAAAGCAAAAAAGAATTAGTAAAATTTTATAATGATCTAGGGAGCTC
TTACTGGTATGATTTTTATGTCAAGCACCTTTTAAAGTTAATAAAAAAGGAAAAATATA
TTAGTTTTGAAGTGATTAAGTGTATTTATATGCTCCTAGAAACGAATACACCAAAAAA
GGAAAAATTAACCAAGAATCAAACGCATAGAATGGGAGCATATTATGCCCGCCAAAA
CTTTGGAAAGCATTTACCTTGCTGGAAAGAAGGTGGCAGAAAAGCTTGTAATAATGATC
CAACTTTTGCAAAAATGGAAGCCGATAAACAAAACCTAGTTCAGCCATAGGAGAGATA
AATGGGGATAGAACAATTTAGATATGCTGAGGCTCCTACTAATTTAAAATATACTCA
ATATGGAAATGTAAGGTTTATACTGATTTTAAAGCAAAAAGATTTTATCCTGCAAAAT
ATTCTAAAGGCTGGATTGCAAGAAGCTATTTATATATGAGCAAAACTTATAATATCAGA
TTATCCGACCAAGAAAGAAAACCTTATGGAGGCTTGGGATAAACCAATACCCTATGGATGA
GAAAGAAAAAGAATTAGAGCATTACTCTAA

C

>cje0256LP

AAAAGTTTTGAAGAAAGCAAAAAAGAATTAGTAAAATTTTATAATGATCTAGGGAGCTC
TACTGGTATGATTTTTATGTCAAGCACCTTTTAAAGTTAATAAAAAAGGAAAAATATAT
AGTTTTGAAGTGATTAAGTGTATTTATATGCTCCTAGAAACGAATACACCAAAAAAGGA
AAAATTAACCAAGAATCAAACGCATAGAATGGGAGCATATTATGCCCGCCAAAACTTT
GGAAAGCATTTACCTTGCTGGAAAGAAGGTGGCAGAAAAGCTTGTAATAATGATCCAAC
TTTGCAAAAATGGAAGCCGATAAACAAAACCTAGTTCAGCCATAGGAGAGATAAATGGG
GATAGAAGCAATTTAGATATGCTGAGGCTCCTACTAATTTAAAATATACTCAATATGGA
AATGTAAGGTTTATACTGATTTTAAAGCAAAAAGATTTTATCCTGCAAAATATTCTAAA
GGCTGGATTGCAAGAAGCTATTTATATATGAGCAAAACTTATAATATCAGATTATCCGAC
CAAGAAAGAAAACCTTATGGAGGCTTGGGATAAACCAATACCCTATGGATGAGAAAGAAAA
AGAATTAGAGCATTACTCTAA

Figure S11. Sequence of *cje0256*LP. Font in red - sequence corresponding to leader peptide. A- amino acid sequence of Cje0256, B- nucleotide sequence of gene *cje0256*, C- nucleotide sequence of gene *cje0256*LP without leader peptide.

>cje0256_PCR product

ATAATCTAGAAAGAAGGAGATATACCATGAAAAAATAATAAGCGTTTTAATACTTGCTTTAAGCTTATTAATGCTAAAAAGTTTTG
AAGAAAGCAAAAAAGAATTAGTAAAATTTTATAATGATCTAGGGAGCTCTTACTGGTATGATTTTTATTGTCAAGCACCTTTAAG
TTAATAAAAAAGGAAAAATATATTAGTTTTGAAGTGATTAAAAGTGATTTTATATGCTCCTAGAAACGAATACACCAAAAAAGGAAAA
TTAACCAAGAATCAAACGCATAGAATGGGAGCATATTATGCCCGCCAAAACTTTGGAAAGCATTTACCTTGCTGGAAAGAAGGTG
GCAGAAAAGCTTGTAATAATGATCCAACCTTTTGCAAAAATGGAAGCCGATAAACAAAACCTAGTTCAGCCATAGGAGAGATAAATG
GGGATAGAAGCAATTTAGATATGCTGAGGCTCCTACTAATTTAAAATATACTCAATATGGAATTTGAAGGTTTATACTGATTTTA
AAGCAAAAAGATTTTATCCTGCAAAATATTCTAAAGGCTGGATTGCAAGAAGCTATTTATATATGAGCAAAACTTATAATATCAGAT
TATCCGACCAAGAAAGAAAACCTTATGGAGGCTTGGGATAAACCAATACCCTATGGATGAGAAAGAAAAAGAATTAGAGCATTACTC
ATCATCATCATCATCACTAAGCATGCTTCT

Figure S12. *cje0256* region amplified with primers *cje0256_for* and *cje0256_rev*. Highlighted in yellow-coding sequence for 6xHis tag.

>cje0256LP_PCR product

ATAATCTAGAAAGAAGGAGATATACCATGAAAAGTTTTGAAGAAAGCAAAAAAGAATTAGTAAAATTTTATAATGATCTAGGGAGCT
CTTACTGGTATGATTTTTATGTCAAGCACCTTTTAAAGTTAATAAAAAAGGAAAAATATATTAGTTTTGAAGTGATTAAGTGTAT
TATATGCTCCTAGAAACGAATACACCAAAAAAGGAAAAATTAACCAAGAATCAAACGCATAGAATGGGAGCATATTATGCCCGCC
AAAACCTTTGGAAAGCATTTACCTTGCTGGAAAGAAGGTGGCAGAAAAGCTTGTAATAATGATCCAACCTTTTGCAAAAATGGAAGCCG
ATAAACAAAACCTAGTTCAGCCATAGGAGAGATAAATGGGGATAGAAGCAATTTTAGATATGCTGAGGCTCCTACTAATTTAAAAT
ATACTCAATATGGAATTTGAAGGTTTATACTGATTTTAAAGCAAAAAGATTTTATCCTGCAAAATATTCTAAAGGCTGGATTGCAA
GAAGCTATTTATATATGAGCAAAACTTATAATATCAGATTATCCGACCAAGAAAGAAAACCTTATGGAGGCTTGGGATAAACCAATACC
CTATGGATGAGAAAGAAAAAGAATTAGAGCATTACTCATCATCATCATCATCACTAAGCATGCTTCT

Figure S13. *cje0256*LP region amplified with primers *cje0256_LP_for_mod* and *cje0256_LP_rev_mod*. Highlighted in yellow- coding sequence for 6xHis tag.